TRANSPORT PHENOMENA

Lecture notes

FLUID DYNAMICS

HEAT & MASS TRANSFER

D.W.F. Brilman
M.A. van der Hoef

University of Twente
Faculty of Science and Technology

PREFACE

In the course Transport Phenomena the fundamentals of transport of momentum, mass and energy are introduced and applied, aiming to understand and describe phenomena in situations encountered in industrial (engineering) practice and in daily life. Formulating the appropriate microscopic and macroscopic balances is thereby the basis for all activities and has proven to be a very powerful concept, which can be successfully applied in many (chemical) engineering disciplines.

To arrive at a good level of understanding of Transport Phenomena, careful study of the presented theory in this reader is required. Probably even more important is working on the problems provided in the corresponding exercise bundle. Trying to analyze and solve the problem statements yourself and discussion of your findings with colleagues is an effective way to educate yourself in Transport Phenomena.

In the module Transport Phenomena of the Chemical Engineering education at the University of Twente, this course is integrated with a course on (numerical) modeling, in which modeling skills are developed and applied to above mentioned situations derived from physical technology. Altogether, transport phenomena theory and numerical modeling skills, they should enable students to analyze and understand the basics of transport phenomena and develop the competence to model and/or design novel systems, based on sound fundamentals. With experiments (in the form of a practicum and as part of the final project) the link between theory and practice is further enforced. In the project, skills of problem analysis, systematic approach, recognizing the appropriate transport phenomena, formulating and solving (modeling) the correct balances and reporting are further integrated.

Prof.dr.ir. D.W.F. Brilman

Dr.ir. M.A. van der Hoef

Table of Contents

1 PHYSICAL TRANSPORT PHENOMENA

1.1 Introduction

In practice, both qualitative and quantitative ways of approach play a significant role in the design of process apparatus. In qualitative approaches, designs that are considered economically viable from experience are selected by means of qualitative considerations. However, to come to a final choice, a quantitative approach by means of mathematical models is essential. The quantitative considerations are (also) based on the conservation laws for mass, momentum[1)] and energy. In the field of transport phenomena, these laws are used extensively in dealing with problems.

In the design of process apparatus, one is confronted with systems that are not in thermodynamic equilibrium; there is exchange of mass, momentum and energy. Classical thermodynamics only predicts to which state of equilibrium the system strives and not the rate with which this equilibrium is reached. The field of physical transport phenomena occupies itself with the prediction of the velocity with which thermodynamic equilibrium is reached within a system. One is specifically interested in the velocity of transport processes in order to come to the design (determination of the main dimensions) of process apparatus.

1.2 Laws of Conservation

Before we go over to the formulation of conservation laws, it is of great importance that we ask the following questions:

a) <u>What is transported?</u>
Is there only transport of material, momentum or energy, or does combined transport occur? In process apparatuses there is often combined transport of mass, momentum and energy.

b) <u>Which transport mechanisms play a role?</u>
A provisional differentiation can be made between convective and molecular transport[2)]. Convective transport is transport by carrying along (convection); a fluid transports mass (fluid or eventually a substance dissolved in a fluid), momentum or energy by displacing itself.

[1)] Because momentum is a vector, one can generally formulate 3 momentum balances (x-momentum balance, y-momentum balance and z-momentum balance in Cartesian co-ordinates).

[2)] At a later stage, we will also encounter radiation.

c) Which variables are involved?

It is important to get an overview of the variables with which the considered system can be described unambiguously. If n variables play a role, one would generally also have to formulate n equations (conservation laws).

d) On which scale does the process occur?

In the formulation of conservation laws, the scale on which the process occurs plays an important role.

Physical technology is based on three empirical laws: the law of the conservation of mass (Lavoisier), momentum (Newton) and energy (Joule). An account should be set up for the three physical quantities concerning a chosen volume (the so-called control volume) that results in the mass balance, momentum balance and energy balance, respectively. For the choice of a suitable (according to form and size) control volume, a good physical intuition is essential. Considering the dimensions of the control volume, one can differentiate between macroscopic balances and microscopic balances.

1.3 Macroscopic balances

If we are interested in the macroscopic characteristics of the system, such as the mean value of a quantity in a chosen control volume, we set up a balance for the specific unit over the whole control volume. Balances over an apparatus (distillation column, chemical reactor) or a factory belong to this category.

The conservation laws can be generally formulated in words as follows (also see Fig. 1.1):

increase in quantity X in V per time unit = ingoing stream of X – outgoing stream of X
+ production of X in V per time unit

For the formulation of the balance, X is expressed as a quantity per unit of volume:

- Transport of mass : $X = \rho$ (kg/m^3)
- Transport of component *i* : $X = c_i$ (kmol/ m$^{3)}$
- Transport of thermal energy : $X = \rho u$ (J/ m^3)
- Transport of momentum : $X = \rho v$ (N.s/ m^3=kg/(m^2.s))

The advantage of this approach is that we only have to formulate one balance that is valid for different transport processes.

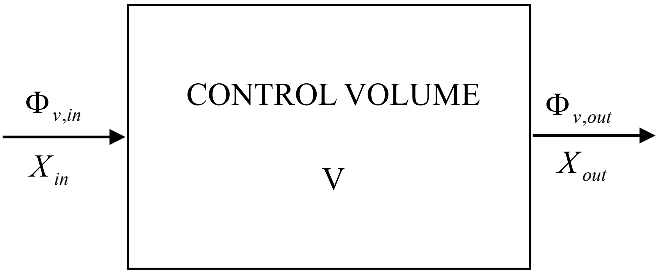

Fig. 1.1. An open system with simultaneous input, output and production of X.

Definitions:

$\Phi_{v,in}, \Phi_{v,out}$: Respective In and outgoing volume streams in m^3/s.
V : Volume (m^3).
r : Quantity of X produced per volume unit and per time unit.
X_{in}, X_{out} : Respective in and outgoing quantities of X per volume unit.

In formula form, the general balance reads:

$$\frac{d}{dt}(XV) = \Phi_{v,in}X_{in} - \Phi_{v,out}X_{out} + rV \tag{1.1}$$

As an explanation of this general balance formulation, the following two specific examples will be shown:

- A macroscopic heat balance for a well-stirred tank supplied with a heating spiral.
- A macroscopic momentum balance for the streaming of a fluid through a pipe with a hooked bend.

Example of a macroscopic heat balance for a well stirred, streamed through tank supplied with a heating spiral.

As a first example we will set-up a macroscopic heat balance for a well stirred, closed tank that was initially completely filled with cold water of a uniform temperature T_0 (see Fig. 1.2.). From t=0, warm water of a constant temperature T_{in} is added with a volume flow of $\Phi_{v,in}$, while water is drained from the tank with a flow of $\Phi_{v,out}$. The water drainage is such that the tank remains completely filled. In addition, an electrical heating element through which a power of Φ_w (W) is supplied to the liquid, is connected at a time, t=0. The tank is stirred very well, so that no differences in temperature exist. The density of the water ρ and the heat capacity C_p are supposed to be constant.

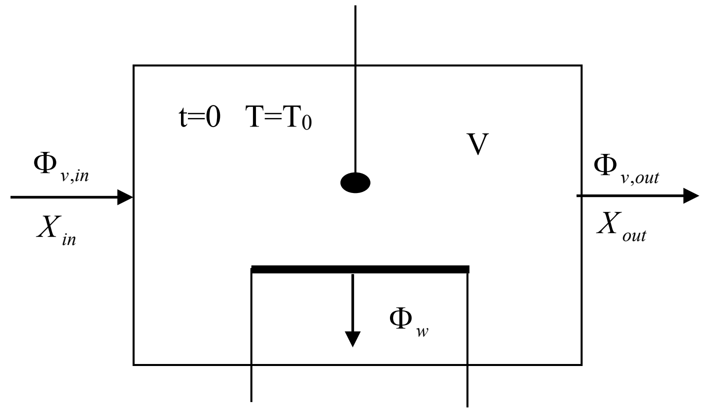

Fig. 1.2. A well stirred tank supplied with a heating spiral with power▯▯$_\mathrm{w}$

A heat balance over the tank V results in (with constant ρC_p):

$$\rho C_p \left(\frac{d\overline{T}}{dt} \right) V = \Phi_{v,in} \left(\rho C_p T_{in} \right) - \Phi_{v,out} \left(\rho C_p T_{out} \right) + \Phi_w \tag{1.2}$$

Note that the power ▯$_\mathrm{w}$, supplied by the heating spiral, appears as a production term in the heat balance (1.2). If it is assumed that the content of the tank is ideally mixed, the mean fluid temperature T in the tank is equal to the outgoing temperature T_{out} of the fluid:

$$\overline{T} = T_{out} \tag{1.3}$$

Furthermore, for a tank that is completely filled with liquid, it is valid, according to the law of the conservation of mass, that the ingoing and outgoing mass streams are equal (check this yourself by setting up a mass balance over the tank):

$$\rho \Phi_{\mathrm{v,in}} = \rho \Phi_{\mathrm{v,out}} \tag{1.4}$$

which for constant density implies that the in- and outgoing volume streams are equal. Under this and the previous assumptions, equation (1.2) is reduced to the following simple first order differential equation:

$$\frac{\mathrm{d}}{\mathrm{dt}} \left(\mathrm{T_{out}} \right) = \frac{\Phi_\mathrm{v}}{\mathrm{V}} \left(\mathrm{T_{in}} - \mathrm{T_{out}} \right) + \frac{\Phi_\mathrm{w}}{\rho \mathrm{C_p V}} \tag{1.5}$$

with the initial boundary condition:

$$t = 0: \quad T_{out} = T_0 \tag{1.6}$$

The solution of (1.5) with initial boundary condition (1.6) gives:

$$\frac{T_{in}+\dfrac{\Phi_w}{\rho C_p \Phi_v}-T_{out}}{T_{in}+\dfrac{\Phi_w}{\rho C_p \Phi_v}-T_0}=\exp\left(-\frac{\Phi_v}{V}t\right) \qquad (1.7a)$$

Note that the effect of the electrical heating spiral is equivalent to an increase of the ingoing temperature ΔT_{in} with:

$$\Delta T_{in}=\frac{\Phi_w}{\rho C_p \Phi_v} \qquad (1.7b)$$

Check by yourself what the outgoing temperature of the water T becomes after a very long time. Does the result correspond to your expectation?

Example of a macroscopic momentum balance for the streaming of a fluid through a pipe with a hooked bend.

As a second example we consider the streaming of a fluid through a pipe with a hooked bend (See Fig 1.3). We want to calculate the force (size and direction) $\overline{R}_{f\to w}$ that the streaming fluid exerts on the bend. We assume the diameter of the pipe to be constant. Besides, we neglect the friction between the streaming fluid and the (inside) wall of the pipe. We furthermore assume that no velocity differences exist over the diameter of the pipe at the entrance “1” and the exit “2”.

In the previous example, the choice of the control volume was obvious: the tank with volume V. Here a suitable choice for the control volume would be the fluid volume that finds itself between the points of reference “1” and “2” in the pipe. Apart from the specification of the control volume, a system of axes must be chosen; one possible choice is given in the following figure.

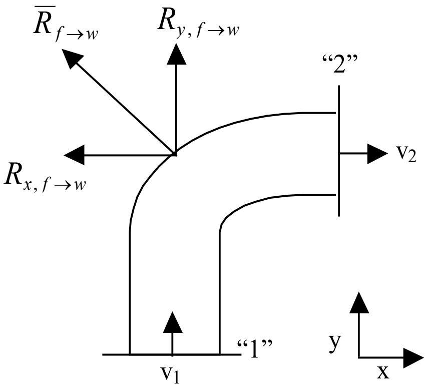

Fig. 1.3. Streaming of a fluid through a conduit with a hooked bend.

The force $\overline{R}_{f\to w}$ can be separated into $R_{x,f\to w}$ and $R_{y,f\to w}$, being the respective forces that the fluid exerts on the bend in the x and y directions. If these two components of $\overline{R}_{f\to w}$ are known, then we know the size and direction of $\overline{R}_{f\to w}$. The starting point for the calculation of $R_{x,f\to w}$ and $R_{y,f\to w}$ is a momentum balance for the x and y directions, respectively.

Momentum balance for the x direction:

$$\frac{d}{dt}(\rho v_x V) = \Phi_{v,in}(\rho v_x)_{in} - \Phi_{v,out}(\rho v_x)_{out} - R_{x,f\to w} \qquad (1.8)$$

Momentum balance for the y direction:

$$\frac{d}{dt}(\rho v_y V) = \Phi_{v,in}(\rho v_y)_{in} - \Phi_{v,out}(\rho v_y)_{out} - R_{y,f\to w} \qquad (1.9)$$

Note that $R_{x,f\to w}$ and $R_{y,f\to w}$ appear with a minus sign in (1.8) and (1.9) respectively, as they are to be regarded as negative momentum production terms. Filling the quantities defined in Fig. 1.3 into equations (1.8) and (1.9) after combination with the mass balance (check this yourself) gives, in the steady-state, the following reduced momentum equations:

$$0 = 0 - \Phi_m v_2 - R_{x,f\to w} \qquad (1.10a)$$

$$0 = \Phi_m v_1 - 0 - R_{y,f\to w} \qquad (1.10b)$$

With the help of equations (1.10a) and (1.10b) the respective x and y components of the asked force can be calculated. For the size of the resulting force $\left|\overline{R}_{f\to w}\right|$, it is simple to derive:

$$\left|\overline{R}_{f\to w}\right| = \Phi_m \sqrt{v_1^2 + v_2^2} \qquad (1.11)$$

As a last example of a macrobalance, a general energy balance will be derived that is actually a generalisation of the first law of the thermodynamics. According to this first law of thermodynamics:

the increase of the internal energy of a system per time unit = the heat added to the system per time unit + the external work done one the system per time unit

Or in formula form:

$$\frac{dU}{dt} = Q + W \tag{1.12}$$

where Q is the heat added to the system per time unit and W is the external work done on the system per time unit. For a streaming medium or a system that is streamed through, the internal energy U and the work done must be extended. It is furthermore meaningful to add the internal energy per mass or volume unit. We define u as the internal energy per mass unit (dimension of u: J/kg). For the internal energy of a streaming medium, the kinetic energy and the potential energy must be added to get the total energy content. Expressed as total energy per mass unit e (dimension of e: J/kg), it thus gives:

$$\mathrm{e} = \mathrm{u} + \frac{1}{2}\mathrm{v}^2 + \mathrm{gh} \tag{1.13}$$

or expressed as total energy per volume unit ρe (dimension of ρe: J/m^3):

$$\rho\mathrm{e} = \rho\mathrm{u} + \frac{1}{2}\rho\mathrm{v}^2 + \rho\mathrm{gh} \tag{1.14}$$

The heat added to the system per time unit will be indicated by Φ_w. With this adaptation, we can formulate the following general balance for total (internal + kinetic + potential) energy:

$$\begin{aligned}\frac{\mathrm{d}}{\mathrm{dt}}(\rho\mathrm{eV}) = \frac{\mathrm{d}}{\mathrm{dt}}\left(\rho\left(\mathrm{u} + \frac{1}{2}\mathrm{v}^2 + \mathrm{gh}\right)\mathrm{V}\right) &= \Phi_{\mathrm{v,in}}\left(\rho\left(\mathrm{u} + \frac{1}{2}\mathrm{v}^2 + \mathrm{gh}\right)\right)_{\mathrm{in}} \\ &- \Phi_{\mathrm{v,out}}\left(\rho\left(\mathrm{u} + \frac{1}{2}\mathrm{v}^2 + \mathrm{gh}\right)\right)_{\mathrm{out}} + \mathrm{W} + \Phi_{\mathrm{w}}\end{aligned} \tag{1.15a}$$

The pressure work done on the system is often split from the work term W in piping systems, so that (1.15a) can also be written as:

$$\begin{aligned}\frac{d}{dt}(\rho e V) = \frac{d}{dt}\left(\rho\left(u+\frac{1}{2}v^2+gh\right)V\right) = \Phi_{v,in}\left(\rho\left(u+\frac{1}{2}v^2+gh\right)\right)_{in} \\ -\Phi_{v,out}\left(\rho\left(u+\frac{1}{2}v^2+gh\right)\right)_{out} + \Phi_{v,in}p_{in} - \Phi_{v,out}p_{out} + W_e + \Phi_w\end{aligned} \qquad (1.15b)$$

where W_e is the external work done on the system per time unit with the exception of the pressure work. It will be clear that the quantity ρe on the left of equations (1.15a) and (1.15b) represents the mean value of the system volume V. The first two terms on the right of this equation represent the in and outgoing convective transport of total energy, respectively.

1.4 Rate of molecular transport processes

In paragraph 1.2. it has already been indicated that, apart from the convective transport of mass, momentum and (thermal) energy (heat), we can also differentiate molecular transport of these quantities. The Brown movement of molecules is primarily responsible for this type of transport and is therefore called molecular transport. Molecular transport can be differentiated into diffusion (mass transport), internal friction (momentum transport) and conduction (heat transport), which are respectively caused by concentration or density gradients, velocity gradients and temperature gradients1). Often both convective and molecular transport occurs simultaneously. For pipe surfaces, however, convective transport is generally more dominant than molecular transport. Molecular transport becomes important in non-streamed through media, in the direct environment of non-streamed through borders (walls) of a system or perpendicular to the main streaming direction of the medium. Subsequently, molecular mass transport (diffusion), molecular heat transport (conduction) and molecular momentum transport (internal friction) will be looked at more closely.

Molecular transport of mass (diffusion).

Consider a long tube containing a non-streaming fluid with a dissolved substance i. The concentration of i is high at the beginning of the tube and low at the end of the tube. If one waits long enough, this initial differences in concentration in the axial or x direction will disappear as a result of diffusion, even when there in total absence of streaming in the fluid. Molecular transport of material is described by Fick's law that states that the flow of material per unit area or mole flux2) of a component i, $\Phi''_{\mathrm{mole,i}}$ (kmole/(m^2.s)) in the x direction is given by (see Fig. 1.4):

$$\Phi''_{\mathrm{mole,i}} = -\mathrm{D_i}\frac{\mathrm{dc_i}}{\mathrm{dx}} \qquad (1.16)$$

where c_i is the concentration of component i (kmole/m^3) and D_i is the diffusion coefficient of component i in the considered medium (m^2/s). The mole flux of component i is proportional to the concentration gradient of component i, which is the driving force for molecular transport of material.

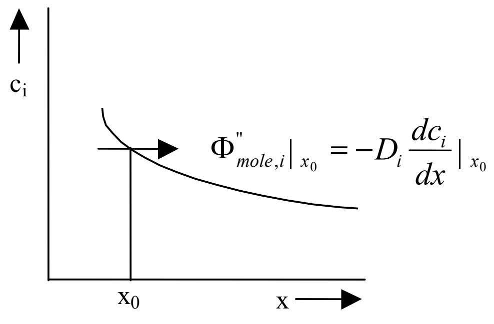

Fig. 1.4. Illustration of Fick's law. Molecular transport of component i occurs as a result of a concentration gradient in the x direction.

---

1) A gradient represents the change of a quantity (e.g. temperature) per unit length.

2) The concept "flux" refers to a quantity (e.g. material, momentum or heat) that is transported per time unit per surface unit. Here the meant surface is perpendicular to the direction of transport.

If concentration gradients exist in the x, y and z directions, molecular transport occurs in all three co-ordination directions. Equation (1.16) then becomes the following vector equation for the mole flux:

$$\overline{\Phi}''_{\text{mole},i} = -D_i\left(\frac{\partial c_i}{\partial x},\frac{\partial c_i}{\partial y},\frac{\partial c_i}{\partial z}\right) = -D_i \text{grad } c_i = -D_i \nabla c_i \tag{1.17a}$$

Here grad or ∇ is the gradient operator that is defined as follows in Cartesian co-ordinates:

$$\text{grad} = \nabla = \overline{\delta}_x \frac{\partial}{\partial x} + \overline{\delta}_y \frac{\partial}{\partial y} + \overline{\delta}_z \frac{\partial}{\partial z} \tag{1.17b}$$

where $\overline{\delta}_x, \overline{\delta}_y$, and $\overline{\delta}_z$ are the unit vectors in the x, y and z directions, respectively.

Molecular heat transport (conduction)

Consider a long metal rod that is perfectly isolated on the mantel side (outside). One end of the rod is submerged in boiling water, while the other end is subjected to the atmosphere. If one would wait long enough, the initial temperature differences in the axial or x direction will be completely disappear as a result of conduction and the temperature at the end of the rod will be equal to the temperature at the beginning of the rod. Heat exchange between the end of the rod and the atmosphere is neglected here. Molecular heat transport is described by the law of Fourier, which states that the heat flow per unit area or heat flux Φ''_h (W/m^2) in the x direction is given by (see Fig. 1.5):

$$\Phi''_h = -\lambda \frac{\partial T}{\partial x} \tag{1.18}$$

where T is the temperature (K) and λ is the heat conduction coefficient of the medium (W/(m.K)). The heat flux is proportional to the temperature gradient, which is the driving force for molecular heat transport. If temperature gradients are present in the x, y and z directions, molecular heat transport occurs in all three co-ordination directions. Equation (1.18) then becomes the following vector equation for heat flux:

$$\overline{\Phi}''_h = -\lambda\left(\frac{\partial T}{\partial x},\frac{\partial T}{\partial y},\frac{\partial T}{\partial z}\right) = -\lambda \text{ grad } T = -\lambda \nabla T \tag{1.19}$$

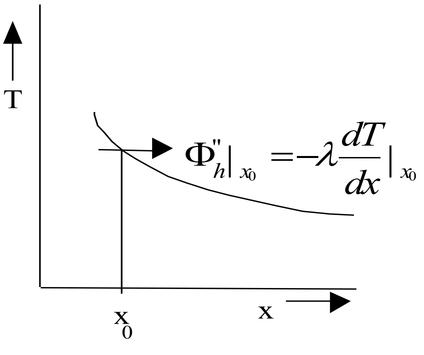

Fig. 1.5. Illustration of Fourier's law. Molecular heat transport occurs as a result of a temperature gradient in the x direction.

Fick's law and Fourier's law are practically analogous, which is even more clear if the last equation is rewritten in the following form, which is valid for constant density ρ and constant heat capacity C_p:

$$\Phi_h'' = -a \frac{d}{dx}\left(\rho C_p T\right) \tag{1.20}$$

where a is the thermal diffusivity, which has the same unit than the diffusion coefficient D_i (m^2/s), and is defined as follows:

$$a = \frac{\lambda}{\rho C_p} \tag{1.21}$$

The quantity $\rho C_p T$ represents the heat content per volume unit ("heat concentration" in J/m^3), which is analogous to the quantity c_i, the quantity of i (expressed in kmole) per volume unit.

Molecular momentum transport (internal friction)

The description of molecular momentum transport is essentially analogous to the description of molecular and heat transport. The analogy is, however, not complete as momentum is a vector quantity; along with size, direction is also of importance. Furthermore, two complimentary viewpoints exist for the interpretation of molecular momentum transport that respectively connects to the field of physical transport properties and the field of mechanics.

Molecular momentum transport will be treated here by means of a steady-state one-dimensional stream. Consider therefore the streaming of a fluid in the positive x direction, where a velocity gradient is present in the y direction (see Fig. 1.6). We naturally have convective momentum transport in the x direction in this situation. However, we accept that v_x is an exclusive function of the y co-ordinate, so that there is no x dependency.

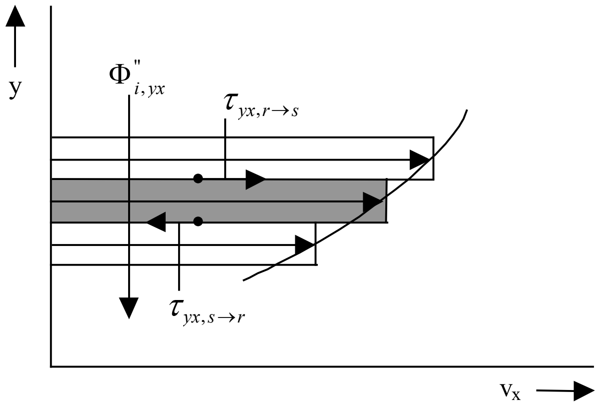

Fig. 1.6. Molecular momentum transport in a streaming fluid. Streaming is stationary and occurs only in the positive x direction. The subscript “s” means “slow” and ”r” means “rapid”.

In this situation, layers of fluid slide over one another, which will result in internal friction as a result of molecular interactions (Van der Waal’s forces and polar forces). Apart from that, molecules can also exchange momentum through collisions, which is of dominant importance for gases. The fluid layers exert forces on another in the x direction, which implies x momentum exchange between layers, i.e. molecular transport of x momentum in the y direction and therefore perpendicular to the stream direction. Fluid layers with a high velocity (high momentum concentration) will yield momentum to fluid layers with low velocity (low momentum concentration).

The shaded fluid layer will get momentum from the more rapid upper layer on the one hand, but will also give momentum to the slower flowing bottom layer. In the above figure, $\tau_{yx,r\to s}$ and $\tau_{yx,s\to r}$ represent forces per surface unit (respectively working in the positive and negative directions), that are respectively exerted by the more rapid upper layer and the slower bottom layer on the shaded layer. Because steady state streaming is mentioned here, there is no net momentum accumulation by these or any other fluid layers because no acceleration or deceleration can occur, and therefore it must be that $\tau_{yx,r\to s} = -\tau_{yx,s\to r}$.

Molecular momentum transport is described by the law of Newton, which states that the momentum flux $\Phi''_{i,yx}$ (Pa=N/m^2) in the y direction is given by (see Fig 1.7):

$$\Phi''_{i,yx} = -\eta \frac{dv_x}{dy} \tag{1.22}$$

where η is the dynamic viscosity (kg/m.s) of the fluid. The momentum flux is proportional to the velocity gradient, which is the driving force for molecular momentum transport. The first subscript indicates that the transport occurs in the y direction and the second subscript indicates that x momentum is transported. Check for yourself that for the velocity profile represented in Fig. 1.6, the momentum flux is indeed negative. The analogy with the other molecular transport processes becomes clearer when the law of Newton is rewritten in the following form, which is valid for constant density ρ:

$$\Phi''_{i,yx} = -\nu \frac{d}{dy}\left(\rho v_x\right) \tag{1.23}$$

where ν is the kinematic viscosity, which has the same unit as the diffusion coefficient D_i (m^2/s) and is defined as follows:

$$\nu = \frac{\eta}{\rho} \tag{1.24}$$

The kinematic viscosity ν can be regarded as a diffusion coefficient for momentum.

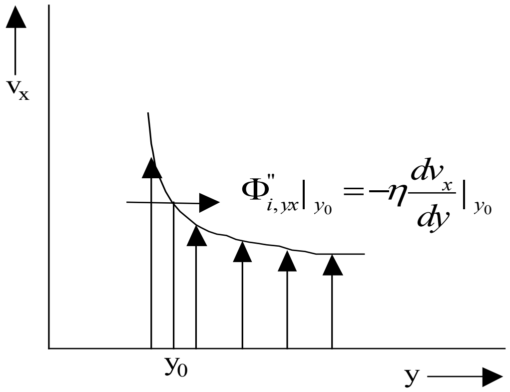

Fig. 1.7. Molecular momentum transport (internal friction) in terms of momentum flux.

Apart from the formulation in terms of the momentum flux, which links closely to the formulations of substance and heat transport, the formulation in terms of shear stress τ_{yx} is also used. For equation (1.22) we can write in terms of shear stress[1] (see fig. 1.8):

$$\tau_{yx} = -\eta \frac{dv_x}{dy} \tag{1.25}$$

---

[1] Stress expresses the force per surface unit, therefore the dimension of a stress is the same as that of a pressure, i.e. Pa=N/m^2

The shear stress τ_{yx} lies on the level where y = constant and points in the x direction and is defined as follows: τ_{yx} on $y=y_0$ is the force per surface unit that the fluid with y values smaller than y_0 exerts on the fluid with y values larger than y_0. Check for yourself that the shear stress τ_{yx} on $y=y_0$ for the velocity profile represented in Fig. 1.8 is indeed positive.

Transport coefficients

The laws of Fick, Fourier and Newton can be seen as the definition equations of the transport coefficients (D_i, a, λ, ν and η). These quantities are dependent on the pressure and temperature in principal, but practically independent of the gradient of the quantity that is the driving force for the transport. For making estimates it is important to have an impression of the order of D_i, λ, and η in gases, liquids and solids.

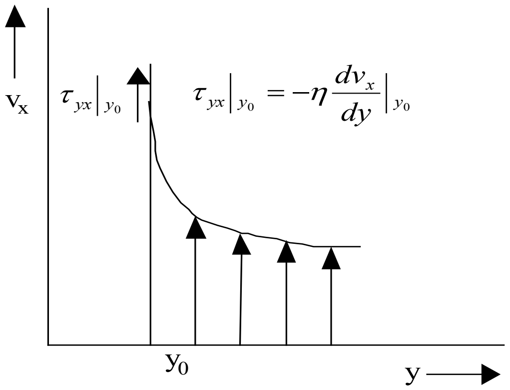

Fig. 1.8. Molecular momentum transport (internal friction) in terms of shear stress.

Gases:

At normal pressure and temperature, D_i, a and ⍰ for gases are in the order of $0.5.10^{-5}$ to 2.10^{-5} m^2/s. That these transport coefficients are of the same order for gases has to do with the fact that material, heat and momentum are “bodily” transported, i.e. as a result of their own movement. According to the kinetic gas theory1) the following is respectively valid for the dynamic viscosity η and the heat conduction coefficient λ:

$$\eta = \frac{2}{3\pi^{3/2}} \frac{\sqrt{mkT}}{d^2} \tag{1.26}$$

and

$$\lambda = \frac{1}{\pi^{3/2}} \frac{\sqrt{k^3\,T/m}}{d^2} \tag{1.27}$$

---

1) Equation 1.27 is strictly speaking valid for a single atom gas.

where m represents the mass of the molecule, k the constant of Boltzmann and d the collision diameter, which should be determined by means of an experimentally known value of η or λ. Note that this theory predicts that η and λ increase with the root from the absolute temperature T, and that both quantities are independent of pressure, which corresponds with experimental data for pressures to about 10 atm. A more refined kinetic theory has been developed by Chapman and Enskog¹⁾.

The kinetic theories for the prediction of transport coefficients in liquids are far less developed than those for gases, with the result that knowledge about these quantities is mainly empirical in nature. For diffusion coefficients in liquids at room temperature, one finds values in the order of 10^{-8} to 10^{-9} m^2/s. For liquids one often uses the equation of Einstein-Nernst-Eyring, which gives a relation between the diffusion coefficient of a specific component i in a solvent D_i, the dynamic viscosity of the solvent η and the absolute temperature T:

$$\frac{D_i \eta}{T} = \text{constant} \tag{1.28}$$

The dynamic viscosity of liquids is strongly variable: η=0.001 kg/(m.s) for water and η=1.5 kg/(m.s) for glycerine (both at 20°C). The viscosity of a liquid is generally strongly temperature dependent:

$$\eta(T) = \eta(T_0)\exp\left[\frac{E_a}{R}\left(\frac{1}{T} - \frac{1}{T_0}\right)\right] \tag{1.29}$$

where T is the absolute temperature, T_0 is a reference temperature (in K), E_a is the “activation energy” (in J/mole) and R the gas constant. Note that the viscosity of liquids, in contrast to that of gases, decreases with increasing temperature. This fact means that the mechanism for momentum transport in liquids differs fundamentally from that in gases. The heat conduction coefficient λ of most liquids lies between 0.1 W/(m.K) (organic compounds) and 0.6 W/(m.K) (water).

Solids:

The diffusion coefficients in solids are relatively small in relation to that in liquids and gases, due to the bad mobility: 10^{-11} to 10^{-13} m^2/s. For the heat conduction coefficient, one should differentiate between amorphic substances, crystalline substances and metals. λ is about 1 W/(m.K) for amorphic substances, somewhat higher for crystalline substances, while it is

---

1) For a comprehensive description of this theory, see the book “Molecular Theory of Gases and Liquids” by J.O. Hirschfelder, C.F. Curtiss and R.B. Bird.

highest for metals due to the (considerable) heat transport by free electrons: λ varies between 10 and 500 W/(m.K) for metals. According to the law of Wiedemann, Franz and Lorenz, a relation exists between the heat conduction coefficient λ and the electrical conduction coefficient λ_e for metals:

$$\frac{\lambda}{\lambda_e T} = L \tag{1.30}$$

with L the Lorenz number. The Lorenz number L varies for pure metals from about 22 to 29.10^{-9} Volt^2/K^2 and is practically independent of the temperature. This equation is not suitable for non-metals, because then the transport processes of heat and electric charge are not dominated by the free electrons any more.

Under normal conditions, no flow occurs in solids, so that the concept of viscosity is not looked at for the study of the deformation of solids. The study of the deformation of solids and the connected phenomena belong to the field of mechanics, and will not receive any further attention here.

2. MICROSCOPIC MASS BALANCE

In the previous chapter, we have encountered the macroscopic balances. In this chapter, a microscopic balance will come up for discussion, specifically the microscopic mass balance, also called the continuity equation. As mentioned before, a microscopic balance gives information on the microscopic system characteristics such as the distribution of a quantity (e.g. mass) over a specific chosen volume.

We start with a system where flow of a compressible medium, i.e. a medium of which the density is not constant, occurs is all three co-ordination directions (x, y and z direction). The three components of the flow velocity, v_x, v_y and v_z, are position dependent, i.e. a function of x, y and z, and furthermore time dependent. For the derivation of the continuity equation, we consider a non-moving, differential[1] volume element in the flowing medium, where the measurements of the element amount to dx, dy and dz in the x, y and z directions, respectively (see fig. 2.1).

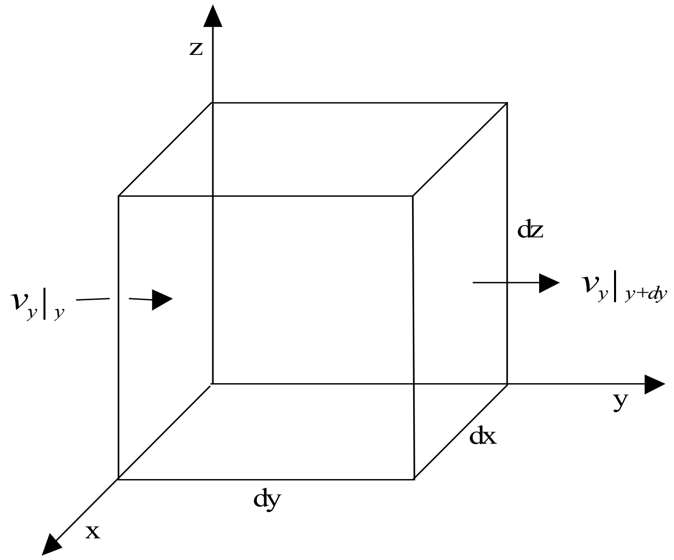

Fig. 2.1. A non-moving, differential volume element with volume dV=dxdydz, with flow of a compressible medium in the three co-ordination directions x, y and z.

The law for the conservation of mass for a volume element dV=dxdydz reads in words:

the increase of mass in dV=dxdydz per time unit = net inflow of mass per time unit in the x direction + net inflow of mass per time unit in the y direction + net inflow of mass per time unit in the z direction + production of mass per time unit in dV=dxdydz

---

[1] By a differential element is meant that the measurements dx, dy en dz are chosen infinite (arbitrary) small. This choice is essential as the system quantities (density and velocity components) vary continuously (gradually) with the position.

Inflow of mass in the y direction per time unit through surface dxdz (kg/s):

$$\rho v_y\Big|_y dxdz$$

Outflow of mass in the y direction per time unit through surface dxdz (kg/s):

$$\rho v_y\Big|_{y+dy} dxdz$$

Net inflow of mass in the y direction per time unit (kg/s):

$$\left(\rho v_y\Big|_y - \rho v_y\Big|_{y+dy}\right)dxdz = \left(\rho v_y\Big|_y - \left(\rho v_y\Big|_y + dy\frac{\partial(\rho v_y)}{\partial y}\right)\right)dxdz$$

$$= -\frac{\partial(\rho v_y)}{\partial y} dxdydz \qquad (2.1)$$

Inflow of mass in the x direction per time unit through surface dydz (kg.s):

$$\rho v_x\Big|_x dydz$$

Outflow of mass in the x direction per time unit through surface dydz (kg/s):

$$\rho v_x\Big|_{x+dx} dydz$$

Net inflow of mass in the x direction per time unit (kg/s):

$$\left(\rho v_x\Big|_x - \rho v_x\Big|_{x+dx}\right)dydz = \left(\rho v_x\Big|_x - \left(\rho v_x\Big|_x + dx\frac{\partial(\rho v_x)}{\partial x}\right)\right)dydz$$

$$= -\frac{\partial(\rho v_x)}{\partial x} dxdydz \qquad (2.2)$$

Inflow of mass in the z direction per time unit through surface dxdy (kg.s):

$$\rho v_z\Big|_z dxdy$$

Outflow of mass in the z direction per time unit through surface dxdy (kg/s):

$$\rho v_z\Big|_{z+dz} dxdy$$

Net inflow of mass in the x direction per time unit (kg/s):

$$\left(\rho v_z\Big|_z - \rho v_z\Big|_{z+dz}\right)dxdy = \left(\rho v_z\Big|_z - \left(\rho v_z\Big|_z + dz\frac{\partial(\rho v_z)}{\partial z}\right)\right)dxdy$$

$$= -\frac{\partial(\rho v_z)}{\partial z} dxdydz \qquad (2.3)$$

The increase in mass per time unit in the considered differential volume element dV=dxdydz amounts to (kg/s):

$$\frac{\partial}{\partial t}(\rho dV)=\frac{\partial\rho}{\partial t}dV=\frac{\partial\rho}{\partial t}dxdydz \qquad (2.4)$$

As we are formulating the law for the conservation of (total) mass, the mass produced per time unit in dV is zero[1]. Filling in of the equations (2.1), (2.2), (2.3) and (2.4) into the law of conservation of mass that is formulated in words, gives, after division by dV=dxdydz, the microscopic mass balance, or continuity equation:

$$\frac{\partial\rho}{\partial t}=-\frac{\partial(\rho v_x)}{\partial x}-\frac{\partial(\rho v_y)}{\partial y}-\frac{\partial(\rho v_z)}{\partial z}=-div(\rho\overline{v})=-(\nabla.\rho\overline{v}) \qquad (2.5)$$

The physical interpretation of the above equation is as follows: on the left stands the accumulation of mass per volume unit, while the net inflow of mass per volume unit and per time unit stands on the right. In equation (2.5), div or ∇ is the divergence operator. With the notation $(\nabla.\rho v)$, it is shown that the internal product between the vector differential operator ∇ and the vector $\rho\overline{v}$ has to be formed, with a scalar quantity as the result:

$$(\nabla.\rho\overline{v})=\left(\overline{\delta}_x\frac{\partial}{\partial x}+\overline{\delta}_y\frac{\partial}{\partial y}+\overline{\delta}_z\frac{\partial}{\partial z}\right).\left(\overline{\delta}_x(\rho v_x)+\overline{\delta}_y(\rho v_y)+\overline{\delta}_z(\rho v_z)\right)$$

$$=\frac{\partial(\rho v_x)}{\partial x}+\frac{\partial(\rho v_y)}{\partial y}+\frac{\partial(\rho v_z)}{\partial z} \qquad (2.6)$$

If density is constant, which is a good approximation for liquids under normal conditions, then the continuity equation is reduced to:

$$div(\overline{v})=(\nabla.\overline{v})=\frac{\partial v_x}{\partial x}+\frac{\partial v_y}{\partial y}+\frac{\partial v_z}{\partial z}=0 \qquad (2.7)$$

The quantity $-(\Delta.\overline{v})$ can (analogous to the term $-(\nabla.\rho\overline{v})$) be taken as the net inflow of volume per volume unit and per time unit, or the relative change in volume per time unit. In many books on physical transport phenomena, one finds an alternative form of the continuity equation, where the concept “derivative following the motion” is used. As this concept is also of importance for the formulation of the microscopic momentum balances, it will be introduced here by means of a simple example. The continuity equation will then be newly formulated with the help of this concept. Consider therefore a river in which the

---

[1] If chemical reactions occur in the medium, the total (net) mass production is also zero according to the law of Lavoisier.

concentration of fish is c, where c represents the number of fish per volume unit. As the fish are moving, c will be a function of the position, i.e. the x, y and z co-ordinates, and the time t. We are interested in the change in concentration per time unit c_t that is registered by three observers A, B and C. Observer A is is in rest on the riverbank, observer B moves in a rowing boat at velocity $\bar{u}$, while observer C is in a boat that floats with the stream and thus has the same velocity as the stream.

Observer A is in a stationary position and will therefore register a concentration change per time unit that corresponds with the partial derivative of c according to time ∂c/∂t, therefore:

$$c_t = \frac{\partial c}{\partial t} \tag{2.8}$$

The position of observer B (x, y and z co-ordinates) is a function of time, and therefore the registered concentration change in this case will be caused by the concentration change in the time t that is registered on a stationary position on the one hand, and on the other hand by the concentration change registered as a result of the movement of observer B. Observer B will register a change in concentration that corresponds to the total derivative of c according to time dc/dt, thus:

$$\begin{aligned} c_t &= \frac{dc}{dt} = \frac{d}{dt}\left(c\left(t, x(t), y(t), z(t)\right)\right) = \frac{\partial c}{\partial t} + \frac{\partial c}{\partial x}\frac{dx}{dt} + \frac{\partial c}{\partial y}\frac{dy}{dt} + \frac{\partial c}{\partial z}\frac{dz}{dt} \\ &= \frac{\partial c}{\partial t} + \frac{\partial c}{\partial x}u_x + \frac{\partial c}{\partial y}u_y + \frac{\partial c}{\partial z}u_z \end{aligned} \tag{2.9}$$

where u_x, u_y and u_z are the respective x, y and z components of the velocity $\bar{u}$ with which the observer moves in the rowing boat.

As observer C moves with the (momentary and local) water velocity $\bar{v}$, we can replace the u_x, u_y and u_z of (2.9) by v_x, v_y and v_z, respectively. Observer C will register a change in concentration that (per definition) corresponds to the substantial derivative of c according to time Dc/Dt, thus:

$$\begin{aligned} c_t &= \frac{Dc}{Dt} = \frac{D}{Dt}\left(c\left(t, x(t), y(t), z(t)\right)\right) = \frac{\partial c}{\partial t} + \frac{\partial c}{\partial x}\frac{dx}{dt} + \frac{\partial c}{\partial y}\frac{dy}{dt} + \frac{\partial c}{\partial z}\frac{dz}{dt} \\ &= \frac{\partial c}{\partial t} + \frac{\partial c}{\partial x}v_x + \frac{\partial c}{\partial y}v_y + \frac{\partial c}{\partial z}v_z \end{aligned} \tag{2.10}$$

For the substantial derivative of the density ρ according to time, it is valid according to equation (2.10) that:

$$\frac{D\rho}{Dt} = \frac{\partial \rho}{\partial t} + v_x \frac{\partial \rho}{\partial x} + v_y \frac{\partial \rho}{\partial y} + v_z \frac{\partial \rho}{\partial z} = \frac{\partial \rho}{\partial t} + (\overline{v}.\nabla)\rho \tag{2.11}$$

while according to the continuity equation (2.5) it is valid that:

$$\begin{aligned} \frac{\partial \rho}{\partial t} + \frac{\partial(\rho v_x)}{\partial x} + \frac{\partial(\rho v_y)}{\partial y} + \frac{\partial(\rho v_z)}{\partial z} &= \frac{\partial \rho}{\partial t} + \rho \frac{\partial v_x}{\partial x} + v_x \frac{\partial \rho}{\partial x} \\ + \rho \frac{\partial v_y}{\partial y} + v_y \frac{\partial \rho}{\partial y} + \rho \frac{\partial v_z}{\partial z} + v_z \frac{\partial \rho}{\partial z} &= \frac{\partial \rho}{\partial t} + \rho(\nabla.\overline{v}) + (\overline{v}.\nabla)\rho \end{aligned} \tag{2.12}$$

which, with the help of equation (2.11), can be written as:

$$\frac{D\rho}{Dt} + \rho(\nabla.\overline{v}) = 0 \tag{2.13}$$

For an incompressible medium, the second term on the left in (2.13) is zero (on the grounds of (2.7)), so that the continuity equation reduces to:

$$\frac{D\rho}{Dt} = 0 \tag{2.14}$$

3 MICROSCOPIC MOMENTUM BALANCE

In this chapter, attention will be focused on the analysis of a number of flow problems on the one hand, and on the other on the derivation of the microscopic momentum balance, or the Navier-Stokes equations. The Navier-Stokes equations are of extreme importance in both theoretical and practical flow studies as all laminar¹⁾ single-phase flows can be described by these equations. These equations are, however, very complicated and only in relatively simple cases analytical (approximate) solutions can be reached. Quantitative analysis of complex flow phenomena recently became possible through the development of efficient numerical techniques on the one hand, and on the other through the availability of fast computers. In this context, the development of this "young" field can be called "computational fluid dynamics (CFD)", a field that concentrates on the development and application of numerical techniques for the solution of the Navier-Stokes equations.

3.1 Simple flow problems

With "simple flow problems" is meant that all considered flows comply with the following characteristics:

- flow is in steady-state and laminar
- flow only occurs in one direction
- the medium acts as a Newtonian fluid²⁾ and is not compressible.

In all cases, we are interested in the spatial distribution of the velocity component (in the main flow direction) within a considered system volume so that a microscopic momentum balance (momentum balance for a differential volume element dV) can be formulated each time. The method handled in the following examples is not suitable for curved streamlines. For the analysis of these systems, one should use the (general) Navier-Stokes equations for the relevant co-ordination system.
Considering the velocity distribution it can be noted that one is often not interested in the distribution itself, but more in the quantities such as the maximum velocity, the average velocity and the shear stress on the system walls that can be derived from it.

The law for the conservation of momentum can be formulated as follows for a differential volume element dV:

the increase of momentum in dV per time unit = ingoing momentum quantity per time unit – outgoing momentum quantity per time unit + sum of the forces acting on dV

---

(1) Flows can be divided into laminar and turbulent flow. In a liquid with laminar (layered) flow, the stream lines (layers of fluid particles) do not cross each other, while it happens continuously in a turbulent (with whirls) flowing fluid.

(2) This means that the relationship between the momentum flux or shear stress and the velocity gradient is given according to the law of Newton (see paragraph 1.3).

The calculation of this balance formulation results in a differential equation for the velocity component in the main direction. Integration of this equation gives, after application of the boundary conditions, the expression for the velocity profile. Considering the formulation of these boundary conditions, one distinguishes between types of boundary layers (G = gas, L = liquid, S = solid[3)]):

L – S boundary layer or G – S boundary layer: For this type of boundary layer it is valid that the fluid velocity is equal to the velocity with which the solid wall moves. This type of boundary condition is called the “no-slip” boundary condition. On non-moving solid walls, the fluid velocity is therefore equal to zero.

L – G boundary layer: On this type of boundary layer the momentum flux (and thus the velocity gradient) in the fluid is very small and can be considered to be zero for practical calculations. This type of boundary condition is called the “free-slip” boundary condition.

L – L boundary layer[1)]: On this type of boundary layer, both the momentum flux perpendicular to the boundary layer and the velocity are continuous, i.e. these quantities have the same value on both sides of the boundary layer.

We describe the molecular momentum transport in terms of a momentum flux for which we will, according to the convention in the literature, in future use the symbol τ.

3.1.1 Steady-state flow between plates

An incompressible Newtonian fluid flows in the steady-state, under the influence of an applied pressure gradient, laminar between two endlessly stretched out, flat plates (see Fig. 3.1). For the analysis of the flow between the flat plates, the axis system is chosen centrally between the plates where the positive x-co-ordinate is in the flow direction of the liquid. Furthermore, a differential volume element dV = bdxdy is taken as starting point[2)] for the formulation of the x-momentum balance, where b is the width of the plates perpendicular to the xy-plane. The different transport terms of the x-momentum are given in Fig. 3.1.

[3)] Under “solid” a solid system wall such as the (inside) wall of a pipe is also understood.

[1)] It is assumed that the two liquids that are in contact with one another are immiscible.

[2)] The measurements in the volume element in both the x-direction and y-direction are chosen infinite small because v_x can essentially vary continuously with both co-ordinates.

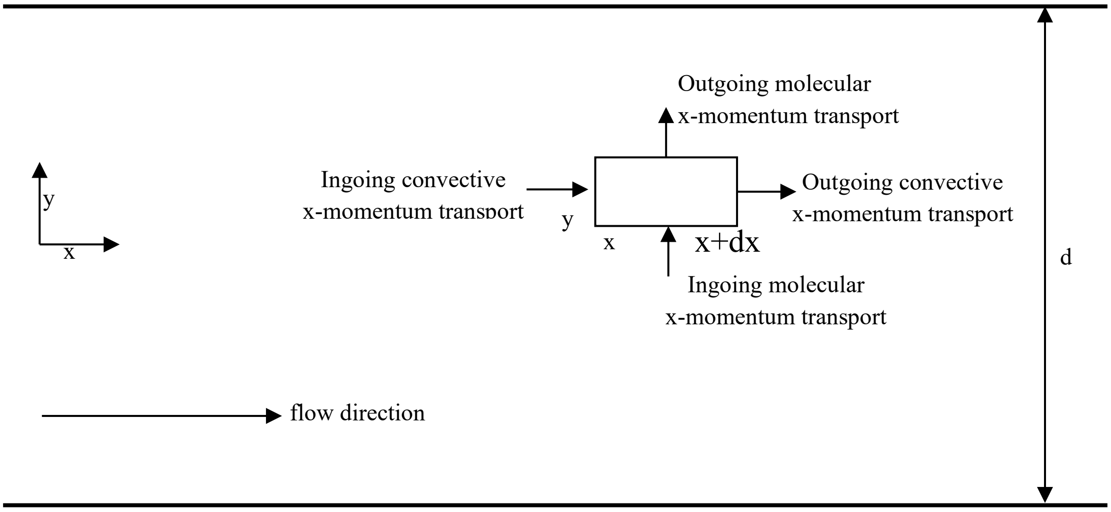

Fig. 3.1. Flow between two endlessly outstretched flat plates. In this figure the different transport terms from the x-momentum balance are given.

In this situation, convective transport of x-momentum occurs in the x-direction, and molecular transport of x-momentum occurs in the y-direction, thus perpendicular to the flow direction. A velocity gradient[3)], which is the driving force for the molecular transport, is present in the y-direction. In this case, apart from the transport terms, we also have to do with the net pressure forces that are exerted on the control volume: the pressure force $p.bdy|_x$ exerts on the "left side" of the control volume in the positive x-direction, while the pressure force $p.bdy|_{x+dx}$ is exerted on the "right side" of the control volume in the negative x-direction. The microscopic balance for x-momentum reads as follows:

$$\begin{aligned}\frac{\partial}{\partial t}(\rho v_x bdxdy) = 0 = (\rho v_x)v_x bdy\big|_x - (\rho v_x)v_x bdy\big|_{x+dx} \\ + \tau_{yx} bdx\big|_y - \tau_{yx} bdx\big|_{y+dy} + pbdy\big|_x - pbdy\big|_{x+dx}\end{aligned} \qquad (3.1)$$

In the steady-state situation, there is no accumulation of x-momentum in the considered control volume, and therefore the left hand side of (3.1) is zero. The first two terms in the right hand side of (3.1) represent the in and outgoing convective x-momentum transport respectively. The following two give the respective in and outgoing molecular x-momentum transport, while the last two terms represent the net pressure force that acts on the control volume (check for yourself that all terms in (3.1) have the dimension of a force). The convective transport terms are formulated as the product of x-momentum per volume unit ρv_x(N.s/m^3) and a volume stream $v_x bdy$(m^3/s). The molecular transport terms are

---

[3)] On the walls (y=±d/2), v_x will have a value of zero because of the 'no-slip" condition, while v_x will have a certain (positive) value elsewhere.

formulated as the product of an x-momentum flux in the y direction (quantity of x-momentum per surface unit transported per time unit in the y direction)τ_{yx}((N.s)/m^2.s)=N/m^2=Pa) and the size of the surface bdx through which transport is realised.

Concerning the signs in (3.1) the following should be noted. An ingoing momentum stream showing in the positive axis direction is positive, while an ingoing momentum stream is negative if it is showing in the negative axis direction. An outgoing momentum stream showing in the positive axis direction is negative, while an outgoing momentum stream is positive if it shows in the negative axis direction. These rules are summarised again in the following table 3.1.

Table 3.1. The sign of the momentum stream in different situations.

Momentum stream	Showing in positive axis direction	Showing in negative axis direction
Ingoing momentum stream	positive	negative
Outgoing momentum stream	negative	positive

Equation (3.1) is divided by dV=bdxdy, and consequently the limit[1] dx→0 and dy→0 is taken so that it results in the following equation:

$$0 = -\frac{\partial}{\partial x}\left(\rho v_x^2\right) - \frac{\partial p}{\partial x} - \frac{\partial \tau_{yx}}{\partial y} \qquad (3.2)$$

On the grounds of the continuity equation, the first term in the right member of (3.2) is zero for an incompressible medium. If, apart from that, it is assumed that the pressure gradient $\partial p / \partial x$ is independent of y, then the following simple first order differential equation follows (Check this yourself!):

$$\frac{d\tau_{yx}}{dy} = -\frac{dp}{dx} \qquad (3.3)$$

which, with the boundary condition τ_{yx}=0 for y=0, can be integrated to:

---

[1] As an alternative, a truncated Taylor series can be used, as done for the deduction of the continuity equation.

$$\tau_{yx} = -\eta \frac{dv_x}{dy} = \left(-\frac{dp}{dx} \right) y \tag{3.4}$$

whereby the (Newtonian) relationship between the momentum flux and the velocity gradient is also substituted at the same time. Note that the momentum flux τ_{yx} varies linear to the y-co-ordinate. Because the pressure gradient dp/dx is negative, the momentum flux is positive for y>0 and negative for y<0. The boundary condition that is applied for the integration of (3.3) implicates that the velocity profile is symmetrical with regard to the line y=0, which corresponds to our physical intuition. Integration of (3.4) with the boundary condition v_x=0 for y=-d/2 or y=+d/2 ("no-slip" boundary condition) gives the following expression for the velocity profile:

$$v_x = \frac{1}{2\eta} \left(-\frac{dp}{dx} \right) \left(\left(\frac{d}{2} \right)^2 - y^2 \right) \tag{3.5}$$

The streaming fluid evidently has a parabolic velocity profile with a maximum for y=0:

$$\left(v_x \right)_{\max} = \frac{d^2}{8\eta} \left(-\frac{dp}{dx} \right) \tag{3.6}$$

The average velocity $<v_x>$ follows from:

$$< v_x >= \frac{\int_{-\frac{d}{2}}^{\frac{d}{2}} v_x(y) dy}{\int_{-\frac{d}{2}}^{\frac{d}{2}} dy} = \frac{d^2}{12\eta} \left(-\frac{dp}{dx} \right) = \frac{2}{3} \left(v_x \right)_{\max} \tag{3.7}$$

The profile of the momentum flux τ_{yx} and velocity v_x is represented qualitatively in Fig. 3.2.

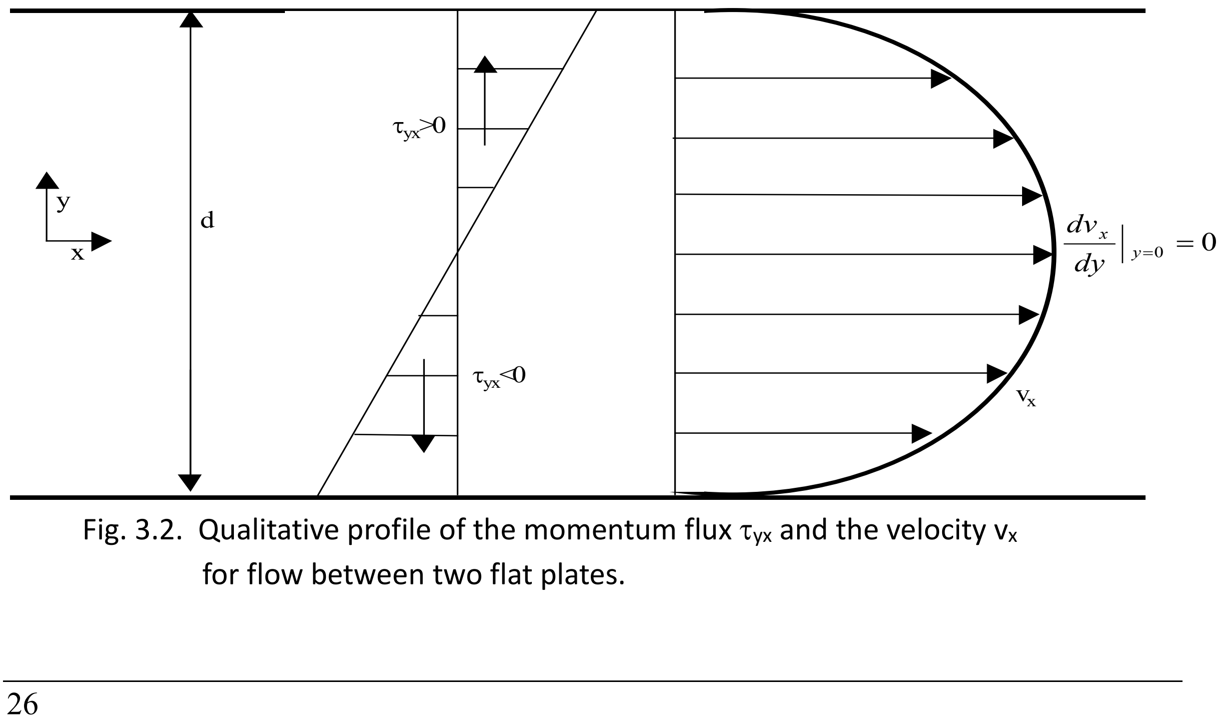

Fig. 3.2. Qualitative profile of the momentum flux τ_{yx} and the velocity v_x for flow between two flat plates.

3.1.2 Steady-state flow through a round tube

We will now consider the steady-state flow of an incompressible Newtonian fluid that streams through a round tube under influence of an applied pressure gradient (see Fig. 3.3). For the analysis of this tube flow, we use cylindrical co-ordinates, whereby we assume at the same time that flow is rotation symmetric. The positive z-co-ordinate shows in the flow direction of the fluid. In this case a cylindrical shell with the volume dV=2πrdrdz is taken as starting point for the formulation of the differential z-momentum balance. The different transport terms of z-momentum are given in Fig. 3.3.

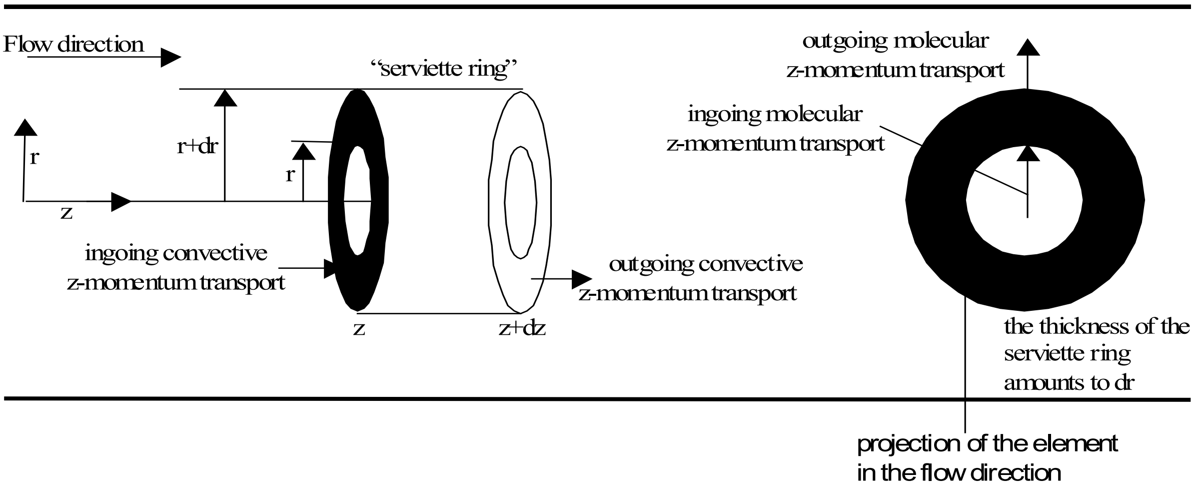

Fig. 3.3 Flow through a round tube. The different transport terms from the z-momentum balance are given in this figure.

Analogous to the situation for flat plates, convective transport of z-momentum occurs in the z-direction and molecular transport of z-momentum occurs in the r-direction, thus perpendicular to the flow direction. Apart from the transport terms, we again have to do with net pressure forces that are exerted on the control volume. The pressure force $p.2\pi rdr|_z$ is exerted on the dark shaded "left side" of the cylindrical shell in the positive z-direction, while the pressure force $p.2\pi rdr|_{z+dz}$ is exerted in a negative direction on the light shaded "right side" of the cylindrical shell. The microscopic balance for z-momentum reads as follows:

$$\begin{aligned}\frac{\partial}{\partial t}(\rho v_z 2\pi r dr dz) = 0 = (\rho v_z)v_z 2\pi r dr\big|_z - (\rho v_z)v_z 2\pi r dr\big|_{z+dz} \\ + \tau_{rz} 2\pi r dz\big|_r - \tau_{rz} 2\pi r dz\big|_{r+dr} + p 2\pi r dr\big|_z - p 2\pi r dr\big|_{z+dz}\end{aligned} \tag{3.8}$$

In the steady-state situation, there is no accumulation of z-momentum in the control volume and therefore the left hand side of (3.8) equals zero. The terms in this equation can be interpreted in an analogous way to those in the x-momentum balance for the flat plates. Equation (3.8) is divided by $dV=2\pi rdrdz$, and subsequently the limit $dr\rightarrow 0$ and $dz\rightarrow 0$ is taken, resulting in the following equation:

$$0=-\frac{\partial}{\partial z}\left(\rho v_z^2\right)-\frac{\partial p}{\partial z}-\frac{1}{r}\frac{\partial}{\partial r}\left(r\tau_{rz}\right) \tag{3.9}$$

Note that (3.9) is very similar to (3.2), the only principal difference being in the last term, which represents the net increase of z-momentum per unit of volume and time as a result of molecular z-momentum transport. The presence of the so-called scale factor r in this term takes into account the effect of the with radial co-ordinate increasing surface through which the molecular transport is realised.

For an incompressible medium on the other hand, the first term in the right member of (3.9) equals zero, on the grounds of the continuity equation. If it is also assumed that the pressure gradient $\partial p/\partial z$ is independent of r, the following simple first order differential equation follows (check this for yourself!):

$$\frac{1}{r}\frac{d}{dr}\left(r\tau_{rz}\right)=-\frac{dp}{dz} \tag{3.10}$$

which can be integrated to:

$$\tau_{rz}=-\eta\frac{dv_z}{dr}=\left(-\frac{dp}{dz}\right)\frac{r}{2}+\frac{C}{r} \tag{3.11}$$

In equation (3.11), C is the integration constant and the Newtonian relation between the momentum flux and the velocity gradient is completed. Because τ_{rz} is limited for all r-values, C=0 has to be chosen. From equation (3.11) we can then read that the momentum flux varies linear to r and is a maximum for r=R, i.e. on the tube wall. Integration of equation (3.11) with the “no-slip” boundary condition $v_z=0$ for r=R (R is the radius of the tube), gives the following expression for the velocity profile:

$$v_z=\frac{1}{4\eta}\left(-\frac{dp}{dz}\right)\left(R^2-r^2\right) \tag{3.12}$$

The streaming medium evidently also shows a parabolic velocity profile in this case, with a maximum for r=0:

$$(v_z)_{\max} = \frac{R^2}{4\eta}\left(-\frac{dp}{dz}\right) \tag{3.13}$$

The average velocity follows from:

$$< v_z >= \frac{\int_0^R v_z(r)2\pi r dr}{\int_0^R 2\pi r dr} = \frac{R^2}{8\eta}\left(-\frac{dp}{dz}\right) = \frac{1}{2}(v_z)_{\max} \tag{3.14}$$

Thus $<v_z>/(v_z)_{\max}$ is smaller for the tubular pipe than for the corresponding quotient for the flat plates. Although both geometry's show a parabolic velocity profile, the relatively slow flowing fluid layer near the tube wall weighs heavier in the calculation of the average velocity because (for constant "layer thickness" dr), there the surface ($2\pi rdr$) is larger. For constant axial pressure gradient dp/dz it is valid that $dp/dz=(p_0-p_L)/(0-L)=-(p_0-p_L)/L$, where p_0 and p_L are the respective pressures at the beginning and end of the tube, and L is the tube length. For the volume stream Φ_v, it is valid in this situation:

$$\Phi_v = \pi R^2 < v_z >= \frac{\pi(p_0 - p_L)R^4}{8\eta L} \tag{3.15}$$

This relation is known as the law of Hagen-Poiseuille and gives the relation between the volume stream through the tube Φ_v and the pressure drop (p_0-p_L) applied over the tube, which is the driving force for flow. The profile of the momentum flux τ_{rz} and the velocity v_z is qualitatively represented in Fig. 3.4.

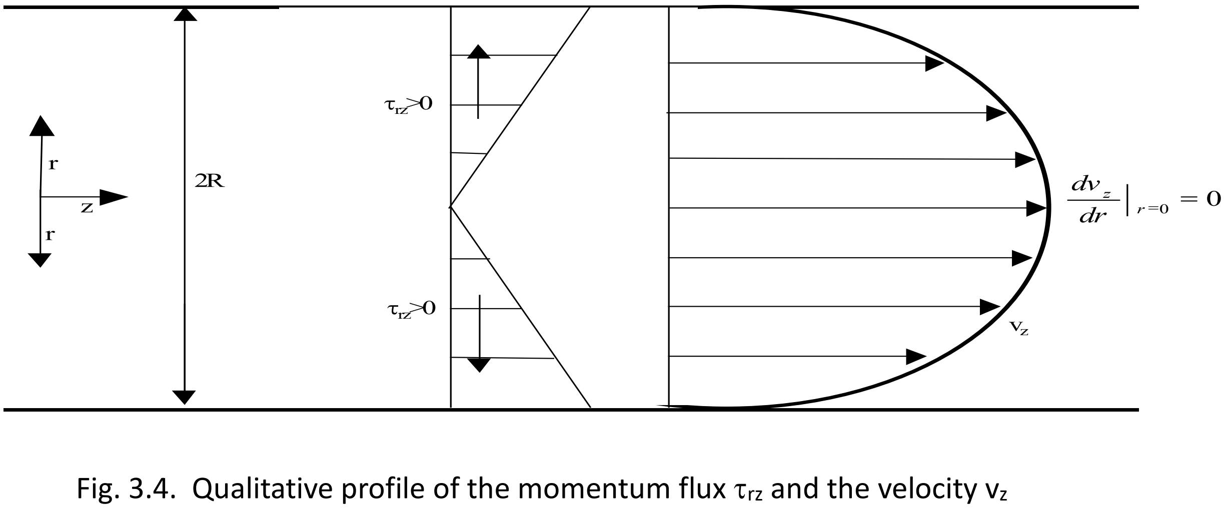

Fig. 3.4. Qualitative profile of the momentum flux τ_{rz} and the velocity v_z for flow through a round tube.

For the z-component of the (viscous) force that the fluid exerts on the tube wall, it is valid that:

$$\begin{aligned} F_z &= \tau_{rz}\big|_{r=R}\left(2\pi RL\right) = -\eta\frac{dv_z}{dr}\Big|_{r=R}\left(2\pi RL\right) \\ &= \pi R^2\left(p_0 - p_L\right) = 8\pi\eta < v_z > L \end{aligned} \qquad (3.16)$$

From the above equation it seems that the viscous force F_z is proportional to the product $\eta<v_z>L$. When we look at the law of Stokes, which gives an expression for the friction force exerted for flow around a sphere in the regime of creeping flow[1], we will again encounter this characteristic form[2].

3.1.3 Steady-state flow through an annulus

In a number of situations there is no known boundary condition for momentum flux, but only boundary conditions for velocity are available. As an example of such a system we will consider the steady-state flow of an incompressible Newtonian fluid that flows through the annular space between two concentric cylinders under the influence of an applied pressure gradient (see Fig. 3.5). The radius of the inner cylinder amounts to ‘a’ and that of the outer cylinder to ‘b'. The choice of the co-ordination system is identical to that of the previous example.

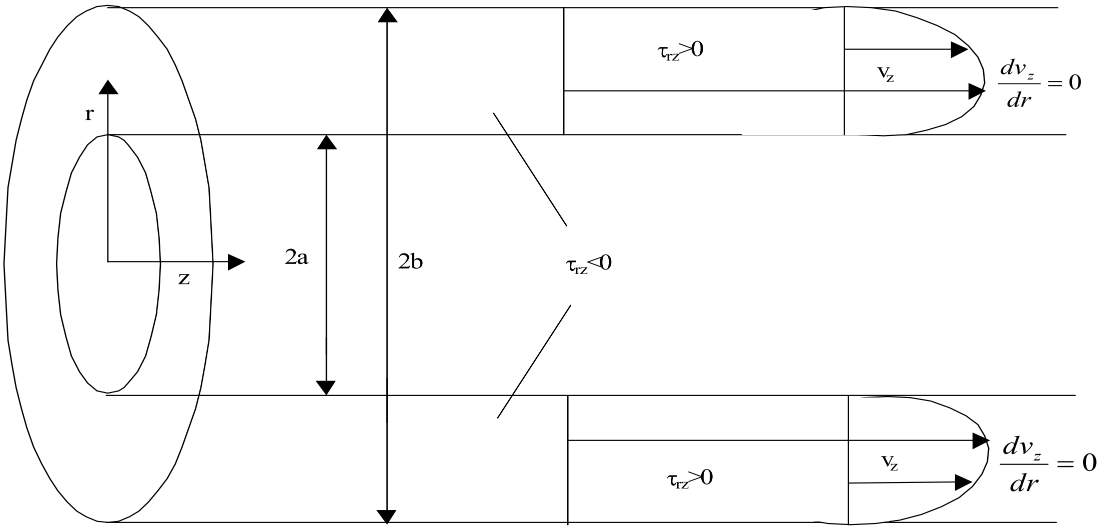

---

[1] In the regime of creeping flow, the streamlines completely adapt to the form of the sphere.

[2] By characteristic form is meant the product of dynamic viscosity, characteristic velocity and characteristic dimension.

Fig. 3.5. Flow through an annular space between two concentric cylinders with radius a (inner cylinder) and b (outer cylinder).

For the analysis of this flow problem, we use equation (3.11) as starting point, where C is replaced by C_1. Because this equation is valid here for a≤r≤b, the boundary condition for r=0 used in the previous example (that τ_{rz} is limited for all r-values, thus also for r=0) can of coarse not be used here.

$$\tau_{rz} = -\eta \frac{dv_z}{dr} = \left(-\frac{dp}{dz} \right) \frac{r}{2} + \frac{C_1}{r} \tag{3.17}$$

Integration of (3.17) gives:

$$-\eta v_z = \left(-\frac{dp}{dz} \right) \frac{r^2}{4} + C_1 \ln(r) + C_2 \tag{3.18}$$

Here we thus have two integration constants C_1 and C_2 that could be determined by means of the two known boundary conditions for the velocity on r=a and r=b. After application of these boundary conditions, the following two equations for the two unknowns C_1 and C_2 result:

$$0 = \left(-\frac{dp}{dz} \right) \frac{a^2}{4} + C_1 \ln(a) + C_2 \tag{3.19a}$$

$$0 = \left(-\frac{dp}{dz} \right) \frac{b^2}{4} + C_1 \ln(b) + C_2 \tag{3.19b}$$

Solution of the system (3.19) and filling C_1 and C_2 in (3.18) gives the following expression for the velocity profile in the annular space (for constant axial pressure gradient):

$$v_z = \frac{(p_0 - p_L) b^2}{4 \eta L} \left\{ 1 - \left(\frac{r}{b} \right)^2 + \frac{\left(1 - \left(\frac{a}{b} \right)^2 \right)}{\ln\left(\frac{b}{a} \right)} \ln\left(\frac{r}{b} \right) \right\} \tag{3.20}$$

For the average velocity $<v_z>$, the following definition equation is valid:

$$< v_z > = \frac{\int_a^b v_z(r) 2\pi r dr}{\int_a^b 2\pi r dr} = \frac{\Phi_v}{\pi \left(b^2 - a^2 \right)} \tag{3.21}$$

which gives the following expression for $<v_z>$ after solution:

$$< v_z > = \frac{(p_0 - p_L) b^2}{8 \eta L} \left[1 + \left(\frac{a}{b} \right)^2 - \frac{\left(1 - \left(\frac{a}{b} \right)^2 \right)}{\ln\left(\frac{b}{a} \right)} \right] \tag{3.22}$$

We can subsequently also determine the expression for momentum flux τ_{rz} with the law of Newton:

$$\tau_{rz} = -\eta \frac{dv_z}{dr} = \frac{(p_0 - p_L)}{2L} \left\{ r - \frac{1 - \left(\frac{a}{b} \right)^2}{2 \ln\left(\frac{b}{a} \right)} \frac{b^2}{r} \right\} \tag{3.23}$$

In contrast with the previous two examples, the result is dependent on the (assumed) relation between the momentum flux (shear stress) and the velocity gradient. For the z-component of the (viscous) force that the flowing fluid exerts on the walls of the annular space, it is valid that:

$$F_z = -\tau_{rz}\big|_{r=a} (2\pi a L) + \tau_{rz}\big|_{r=b} (2\pi b L) = \pi (b^2 - a^2)(p_0 - p_L) \tag{3.24}$$

Check that $\tau_{rz}=0$ and $v_z=(v_z)_{max}$ for $r=r_{max}$, where it is valid for r_{max}:

$$r_{\max}^2 = \frac{b^2 - a^2}{2 \ln\left(\frac{b}{a} \right)} \tag{3.25}$$

Corresponding to our expectations, the equations for the streamed through annular space go over into those for the round tubular conduit for a→0, while for a>>(b-a), these equations reduce to the equations that are valid for flow between flat plates (check this for yourself!).

3.2 Navier-Stokes equations

In the previous paragraph we have formulated and calculated the microscopic momentum balances for a number of relatively simple flow problems. It is, however, not necessary that we follow this procedure every time for the analysis of a new flow problem. As an alternative we can also start from the general microscopic balances for mass and momentum that we will subsequently simplify in a “suitable way”. We automatically get a list of assumptions, which we have made during the simplification, as by-product of this procedure. Besides, it is safer to go out from the general microscopic balances in the relevant co-ordinate systems for the analysis of complex flow problems (two and three dimensional flows with curved streamlines). These general microscopic balances for momentum are known as Navier-Stokes[1] equations. The derivation of the Navier-Stokes equations can essentially be done analogous to the derivation of the continuity equation by setting up microscopic balances for x-momentum, y-momentum and z-momentum. In this introductory subject, however, the derivation will be left out and these equations will be postulated. Those who are interested are referred to more detailed courses in the field of "advanced physical transport phenomena".

For constant density and constant dynamic viscosity, the Navier-Stokes equations read as follows in vector notation[1]:

$$\rho \frac{D\overline{v}}{Dt} = \rho\left[\frac{\partial \overline{v}}{\partial t} + (\overline{v}.\nabla)\overline{v}\right] = -\nabla p + \eta\nabla^2\overline{v} + \rho\overline{g} \tag{3.26}$$

where $(\overline{v}.\nabla)$ is the following differential operator:

$$(\overline{v}.\nabla) = v_x\frac{\partial}{\partial x} + v_y\frac{\partial}{\partial y} + v_z\frac{\partial}{\partial z} \tag{3.27}$$

while ∇^2 is the Laplace operator of which the Cartesian co-ordinates are given by:

$$\nabla^2 = \frac{\partial^2}{\partial x^2} + \frac{\partial^2}{\partial y^2} + \frac{\partial^2}{\partial z^2} \tag{3.28}$$

For frictionless media (η=0) there is no viscous momentum transport and the law of Euler[2] is valid:

$$\rho \frac{D\overline{v}}{Dt} = \rho\left[\frac{\partial \overline{v}}{\partial t} + (\overline{v}.\nabla)\overline{v}\right] = -\nabla p + \rho\overline{g} \tag{3.29}$$

This equation is often used to describe flowing gases as gases generally have a low (dynamic) viscosity (for air at atmospheric conditions, η=2.10^{-5} kg/(m.s)).

All terms in equation (3.26) have the dimension of a force per volume unit (N/m^3). In fact, the Navier-Stokes equations represent the second law of Newton (mass x acceleration = sum of forces) that is applied here to an infinitesimally small volume element that moves

---

[1] This method of notation is only valid for Cartesian co-ordinates.

[2] These equations were first deducted by Euler in 1755.

everywhere with the flowing medium. In the left hand side of (3.26) stands the momentum change per volume unit of the element, while in the right hand side stands the sum of the forces exerted on the element (per volume unit). In the following table the Navier-Stokes equations (for constant ρ and η) are given in Cartesian co-ordinates. We will use these equations in the following paragraph as starting point for the analysis of a simple flow problem.

Table 1: Navier-Stokes equations (constant ρ and η) in Cartesian co-ordinates.

---

x-component:

$$\rho\left[\frac{\partial v_x}{\partial t}+v_x\frac{\partial v_x}{\partial x}+v_y\frac{\partial v_x}{\partial y}+v_z\frac{\partial v_x}{\partial z}\right]=-\frac{\partial p}{\partial x}+\eta\left[\frac{\partial^2 v_x}{\partial x^2}+\frac{\partial^2 v_x}{\partial y^2}+\frac{\partial^2 v_x}{\partial z^2}\right]+\rho g_x$$

y-component:

$$\rho\left[\frac{\partial v_y}{\partial t}+v_x\frac{\partial v_y}{\partial x}+v_y\frac{\partial v_y}{\partial y}+v_z\frac{\partial v_y}{\partial z}\right]=-\frac{\partial p}{\partial y}+\eta\left[\frac{\partial^2 v_y}{\partial x^2}+\frac{\partial^2 v_y}{\partial y^2}+\frac{\partial^2 v_y}{\partial z^2}\right]+\rho g_y$$

z-component:

$$\rho\left[\frac{\partial v_z}{\partial t}+v_x\frac{\partial v_z}{\partial x}+v_y\frac{\partial v_z}{\partial y}+v_z\frac{\partial v_z}{\partial z}\right]=-\frac{\partial p}{\partial z}+\eta\left[\frac{\partial^2 v_z}{\partial x^2}+\frac{\partial^2 v_z}{\partial y^2}+\frac{\partial^2 v_z}{\partial z^2}\right]+\rho g_z$$

3.3 Working with the Navier-Stokes equations

As already stated in the introduction, all laminar single-phase flows can essentially be described by the Navier-Stokes equations. As an example, a simple laminar flow problem will be analysed on the basis of these equations.

Flow along a vertically positioned wall.

As an example we consider the steady-state flow of an incompressible Newtonian fluid (with dynamic viscosity η) along a vertically wall. In and outflowing effects can be ignored. An expression for the velocity profile $v_x(y)$ is asked.

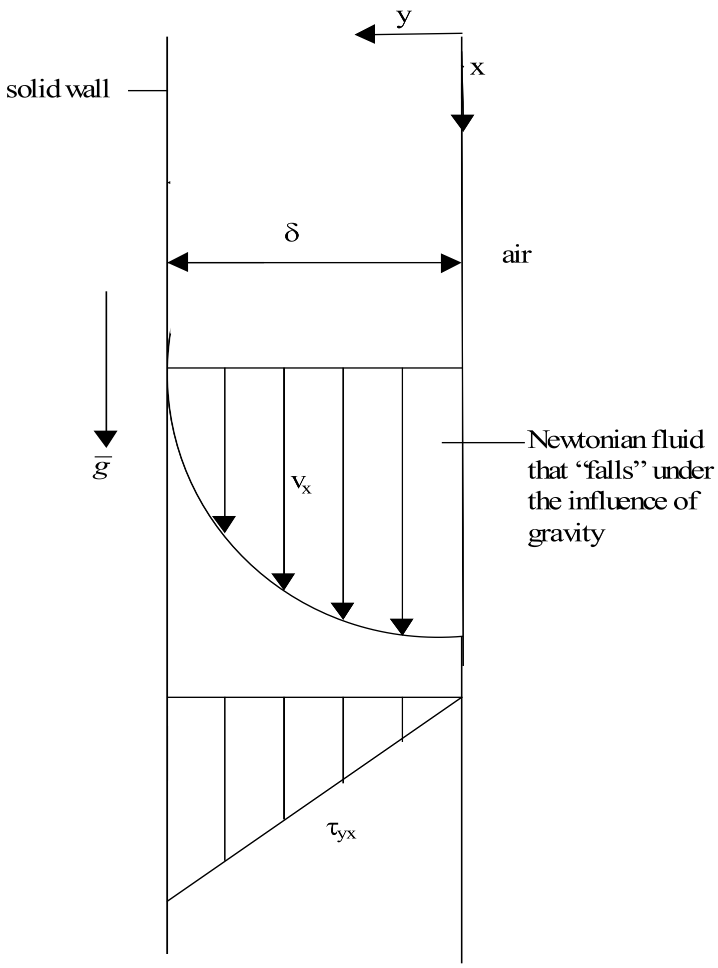

Fig. 3.6. Flow of a fluid along a vertically set up wall.

This problem can be described in Cartesian co-ordinates and as flow occurs in the x-direction, the microscopic balance for x-momentum is chosen as starting point. There is steady-state flow ($\partial v_x/\partial t=0$) and flow only occurs in the x-direction ($v_y=0$ and $v_z=0$) whereby, on the grounds of the continuity equation, v_x (for constant y) is independent of x ($\partial v_x/\partial x=0$).

The left hand side of the microscopic balance for x-momentum is therefore equal to zero. There is no pressure gradient in the x-direction so that: $\partial p/\partial x=0$. Molecular momentum transport occurs in the y-direction as v_x is dependent on y (but independent of x and z so that: $\partial^2 v_x/\partial x^2=0$ and $\partial^2 v_x/\partial z^2=0$). Gravity acts in the positive x-direction so that $g_x=g$, with g the gravity constant. The (general) microscopic balance for x-momentum thus reduces to:

$$0=\eta\frac{d^2v_x}{dy^2}+\rho g \tag{3.30}$$

The following two boundary conditions are valid for (3.30):

$$v_x=0 \quad \text{for } y=\delta \qquad \text{and} \qquad \tau_{yx}=-\eta\frac{dv_x}{dy}=0 \quad \text{for } y=0 \tag{3.31}$$

Integration of (3.30) with the boundary conditions (3.31) results in the following expression for the velocity profile (check this for yourself):

$$v_x=\frac{\rho g\delta^2}{2\eta}\left(1-\left(\frac{y}{\delta}\right)^2\right) \tag{3.32}$$

Note that the fluid falls with a “half parabolic” velocity profile along the vertical wall and that the maximum velocity $(v_x)_{max}$ is reached for y=0, i.e. at the fluid-air boundary layer. From (3.32) it can be read that it is valid for $(v_x)_{max}$ that:

$$(v_x)_{\max}=\frac{\rho g\delta^2}{2\eta} \tag{3.33}$$

For the average velocity $\langle v_x\rangle$, it is simple to derive that this amounts to 2/3 of the maximum velocity $(v_x)_{max}$ (check this yourself).

4 BERNOULLI'S LAW FOR FRICTIONLESS FLOW

For the description of a number of flow phenomena, additional equations to the mass and momentum balances are required. The mechanical energy balance, or the law of Bernoulli, is an often occurring and important example and will be looked at more closely in this chapter. The mechanical energy balance that we formulate in this chapter is valid for ideal fluids, i.e. for fluids without internal friction. In Chapter 6, we will encounter the extended law of Bernoulli, which is valid for flows with internal friction.

The law of Bernoulli for frictionless flows is essentially a conservation rule for the different forms of mechanical energy. In a flowing fluid, pressure, kinetic energy and potential energy can be seen as forms of mechanical energy. For frictionless flows, these different forms of mechanical energy can be converted into one another; whereby it is worth noting that no mechanical energy can be lost hereby. For flows with internal friction, on the other hand, a loss1) of mechanical energy can occur.

4.1 Derivation of the Law of Bernoulli

For the derivation of the law of Bernoulli (for frictionless flow), the equation of Euler is taken as starting point:

$$\rho \frac{D\overline{v}}{Dt} = -\nabla p + \rho \overline{g} \tag{4.1}$$

This equation describes the momentum change of a volume element, which moves with the flowing medium as a result of the forces acting on that element. On the left hand side of (4.1) stands the momentum change per volume unit, on the right hand side the sum of the forces (per volume unit) that act on the element. If (4.1) is internally multiplied2) with the velocity $\overline{v}$, it results in the following scalar equation, which gives the substantial derivative for the time of the kinetic energy per mass unit:

$$\rho \frac{D}{Dt}\left(\frac{1}{2}v^2\right) = -\left(\overline{v}.\nabla p\right) + \rho\left(\overline{v}.\overline{g}\right) \tag{4.2}$$

If equation (4.2) is divided by the density ρ, the following equation results:

---

1) In such systems a conversion of mechanical energy into internal energy occurs, which results in a temperature increase of the fluid. This temperature increase is important only in extreme cases.

2) The x-, y- and z-component of (4.1) are respectively multiplied by v_x, v_y and v_z.

$$\frac{D}{Dt}\left(\frac{1}{2}v^2\right)=-\left(\bar{v}.\frac{\nabla p}{\rho}\right)+\left(\bar{v}.\bar{g}\right) \tag{4.3}$$

The first term in the right member of (4.3) can be written as the following according to the definition of the substantial derivative of time (check this yourself!):

$$\left(\bar{v}.\frac{\nabla p}{\rho}\right)=\frac{D}{Dt}\left(\int_{p_0}^{p}\frac{dp}{\rho}\right)-\frac{\partial}{\partial t}\left(\int_{p_0}^{p}\frac{dp}{\rho}\right) \tag{4.4a}$$

where p₀ is an arbitrarily chosen reference pressure. In the steady state, the last term in (4.4a) is equal to zero, so that equation (4.4a) reduces to:

$$\left(\bar{v}.\frac{\nabla p}{\rho}\right)=\frac{D}{Dt}\left(\int_{p_0}^{p}\frac{dp}{\rho}\right) \tag{4.4b}$$

The gravitation force per mass unit $\bar{g}$ can be expressed as the gradient of a potential Ψ, which represents the potential energy[1] per mass unit: $\bar{g}=-\nabla\Psi$. According to the definition of the substantial derivative for $D\Psi/Dt$ and the definition of the potential Ψ, it is valid that:

$$\frac{D\Psi}{Dt}=\frac{\partial\Psi}{\partial t}+\left(\bar{v}.\nabla\Psi\right)=\frac{\partial\Psi}{\partial t}-\left(\bar{v}.\bar{g}\right) \tag{4.5a}$$

As Ψ is independent of time, it is valid that $\partial\Psi/\partial t=0$, so that equation (4.5a) can be written as:

$$\frac{D\Psi}{Dt}=-\left(\bar{v}.\bar{g}\right) \tag{4.5b}$$

substitution of the simplified expressions (4.4b) and (4.5b) into the right member of equation (4.3) gives, after union of the terms:

$$\frac{D}{Dt}\left\{\frac{1}{2}v^2+\Psi+\int_{p_0}^{p}\frac{dp}{\rho}\right\}=0 \tag{4.6}$$

---

[1] The minus sign indicates that the potential energy (per mass unit) Ψ increases in the opposite direction of the vector $\bar{g}$.

The potential energy per mass unit ψ can be expressed as ψ=gh, where h is the height with regard to a specific reference level. Integration of equation (4.6) between point 1 and point 2 gives the law of Bernoulli for a frictionless fluid:

$$\frac{1}{2}v_2^2 - \frac{1}{2}v_1^2 + gh_2 - gh_1 + \int_{p_1}^{p_2} \frac{dp}{\rho} = 0 \tag{4.7}$$

The above equation can also be expressed in the alternative, so-called "Δ-formulation":

$$\Delta\left(\frac{1}{2}v^2\right) + \Delta(gh) + \int_{p_1}^{p_2} \frac{dp}{\rho} = 0 \tag{4.8}$$

whereby Δ is defined as: Δ = "2" – "1". With the integration of the differential equation (4.6), which is formulated in terms of a substantial differential quotient, we essentially follow a differential volume element along its streamline. Equation (4.8) shows that the sum[2)] of the kinetic energy, the potential energy and the pressure energy is constant. As a result of the flow conversion of e.g. pressure energy into potential and/or kinetic energy can occur. The sum of these forms of energy does, however, remain constant. If the fluid is incompressible, the density ρ may be removed from the integral sign in the last term of (4.8), so that the following results after multiplication with ρ:

$$\Delta\left(\frac{1}{2}\rho v^2\right) + \Delta(\rho gh) + \Delta p = 0 \tag{4.9}$$

The terms in this equation have the dimension of a pressure and can be seen as forms of mechanical energy per volume unit.

Summing up, the law of Bernoulli, equation (4.8), is valid:

- along a streamline for a differential volume element,
- for ideal, i.e. frictionless fluids,
- for compressible fluids,
- in cases where no work is applied to the fluid,
- in the steady or quasi-steady state.

If equation (4.9) is divided by ρg, the mechanical energy forms are expressed as a measure of height:

[2)] All terms in the law of Bernoulli have the dimension J/kg and all represent the amount of mechanical energy per mass unit.

$$\Delta\left(\frac{v^2}{2g}\right)+\Delta h+\Delta\left(\frac{p}{\rho g}\right)=0 \tag{4.10}$$

In Fig. 4.1 an illustration of the above form of the law of Bernoulli is given, where the physical meaning of the different terms is clarified. A frictionless fluid flows with a uniform velocity from a tank with a constant liquid level, through a horizontal tube.

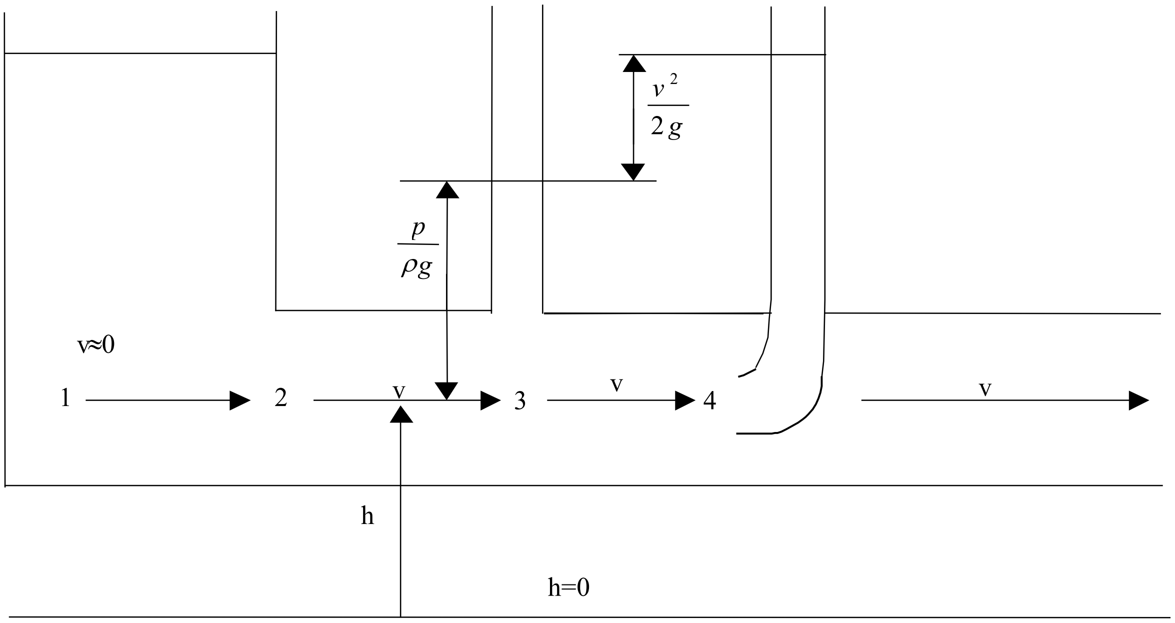

Fig. 4.1. Illustration of the law of Bernoulli for flow through a horizontal tube.

At point 1, the fluid has no velocity, at points 2 and 3 the velocity is equal to each other. At point 1 the height (as a measure of the mechanical energy) with regard to a fictitious zero level consists of h (“position height”) and p/ρg (“pressure height”). At point 3, a part of the pressure height p/ρg is converted to “velocity height” $v^2/2g$, whereby the pressure on point 3 is lower than on point 1. At point 4, the fluid is slowed down by the obstacle that is directed to the front, whereby the velocity decreases to zero just in front of this obstacle. As a result of the slowing of the fluid, the “velocity height” is converted to “pressure height” so that the pressure at point 4 is again equal to that at point 1.

The velocity of the flow in the tube can be measured by measurement of the height difference between points 3 and 4. The so-called Pitot tube is based on this measurement principle (see paragraph 4.2.).

The law of Bernoulli is valid for a differential volume element that moves along a streamline. In flows that we encounter in practice, the fluid elements follow different streamlines so that, strictly speaking, Bernoulli's law is not applicable. Particularly for low flow velocities, v will vary over the pipe diameter so that the expression for the kinetic energy per mass unit $e_{kin}=v^2/2$ should (for constant density ρ) be replaced by:

$$e_{kin} = \frac{1}{2}\frac{< v^3 >}{< v >} \tag{4.11}$$

The slanting parentheses (< >) indicate that the relevant quantity should be averaged over the pipe diameter. In these situations, the law of Bernoulli reads:

$$\Delta\left(\frac{1}{2}\frac{< v^3 >}{< v >}\right) + \Delta(gh) + \frac{\Delta p}{\rho} = 0 \tag{4.12}$$

4.2 Applications

Although no frictionless fluids exist, internal friction play a minor role for a number of flow phenomena, so that the law of Bernoulli can be used for the description of these phenomena. The following applications for Bernoulli's law will be treated successively:

- streaming of a liquid through a hole in the bottom of a tank.
- measurement of the velocity with a Pitot tube.
- flow through a pipe with a sudden widening.

As first application of the law of Bernoulli, we consider the flow of a liquid through a narrow opening in the bottom of a tank (see Fig. 4.2.). The diameter of the opening is given as A_g, where A_g is much smaller than the diameter of the tank A_v. The fluid height in the tank is given as h. The point 2, situated on the centre-line through the opening, and the point 1 of the liquid level, situated vertically above point 2, are two points of the same streamline. Point 2 is chosen so that the pressure in the outflowing liquid is there equal to the pressure at point 1, i.e. the atmospheric pressure p_0. Application of the law of Bernoulli (equation (4.9)) between the points 1 and 2 gives:

$$\frac{1}{2}\rho v_2^2 - \frac{1}{2}\rho v_1^2 + \rho g h_2 - \rho g h_1 + p_2 - p_1 = 0 \tag{4.13}$$

As $p_1=p_2=p_0$ and (on the grounds of the continuity equation) $v_1<<v_2$, and it is moreover laid down that $h_2-h_1=-h$, equation (4.13) reduces to:

$$v_2 = \sqrt{2gh} \qquad (4.14)$$

The outflow velocity v_2 is therefore proportional to the root of the fluid height. The outflowing volume stream Φ_v is the product of the outflow velocity v_2 and the area of the opening, A. The question, however, is which area should be used, as the outflowing fluid stream shows a contraction. Strictly speaking, the with p_0 corresponding surface A* should be used, but as this surface is unknown, A* is expressed by means of an empirically determined coefficient C_c, the so-called contraction coefficient, in the surface of the outflow opening A_g:

$$A^* = C_c A_g \qquad (4.15)$$

The following (empirical) expression is then valid for the outflowing volume debit Φ_v:

$$\Phi_v = C_c A_g \sqrt{2gh} \qquad (4.16)$$

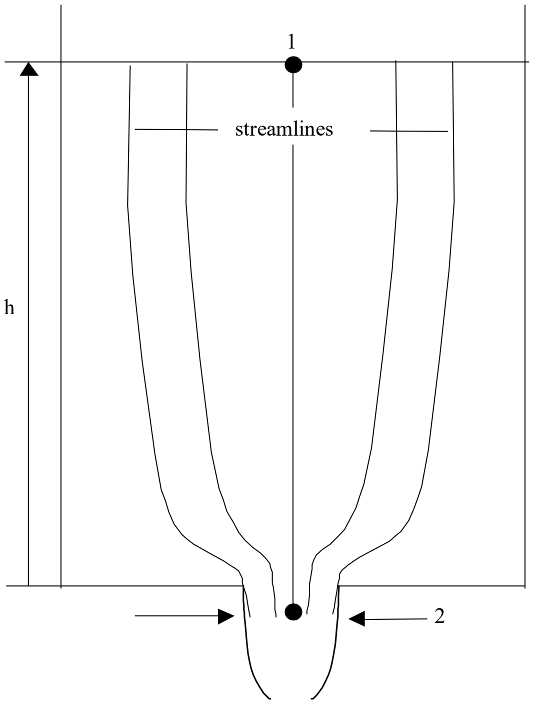

Fig. 4.2. Outflow of a liquid through a hole in the bottom of a tank.

The time t*, which is needed for the tank to empty, can be calculated by combining the expression for the outflowing volume stream with the macroscopic mass balance for the tank:

$$\frac{d}{dt}(\rho A_v h) = -\Phi_m = -\rho\Phi_v = -\rho C_c A_g \sqrt{2gh} \tag{4.17}$$

As the density ρ and the diameter of the tank A_v are constant, (4.17) can be written as:

$$\frac{dh}{dt} = -C_c \frac{A_g}{A_v}\sqrt{2gh} \tag{4.18}$$

Integration of (4.18) with the starting condition t=0: h=h_0, gives the following expression for the fluid height in the tank as function of the time:

$$\sqrt{h(t)} = \sqrt{h_0} - \left(C_c \frac{A_g}{A_v}\sqrt{\frac{g}{2}} \right) t \tag{4.19}$$

The expression for the time can be obtained by equalling the left member to zero:

$$t^* = \frac{\sqrt{h_0}}{C_c \frac{A_g}{A_v}\sqrt{\frac{g}{2}}} \tag{4.20}$$

The most important application of Bernoulli's law lies therein that one can derive the velocity of a flow by measuring pressures. As an example hereof, the measuring principle of the Pitot tube will be discussed more closely. A torpedo-shaped object is placed in a homogenous fluid flow1) with the axis of the object lying in the flow direction, while the round head of the object is turned towards the flow direction (see Fig. 4.3). In this situation, the streamlines will distribute symmetrically with regard to the centre-line AS. The velocity of the fluid elements will gradually decrease along the line AS and become zero at point S, the so-called stagnation point. Along the curved surface the velocity will gradually increase to a maximum value that is higher than the velocity of the undisturbed flow v, and will subsequently decrease again. On the curved surface, there must therefore be a point B somewhere where the velocity is equal to the velocity of the undisturbed flow. The application of Bernoulli's law between point A (p=p_1), where flow is undisturbed, and point S (p=p_2), the stagnation point, gives:

---

1) In a homogenous flow, the velocity is the same in every point as far as direction and size go.

$$p_1 + \frac{1}{2}\rho v^2 = p_2 \tag{4.21}$$

The pressure in the stagnation point S is therefore higher than the pressure p_1 in the undisturbed flow (the so-called static pressure) by an amount of $(1/2)\rho v^2$. This pressure that is built up in the stagnation point S by the kinetic energy being freed is called the stagnation pressure. The measuring principle of the Pitot tube follows immediately from (4.21): the velocity v (at known density ρ) can be determined by measuring the pressure difference p_2-p_1.

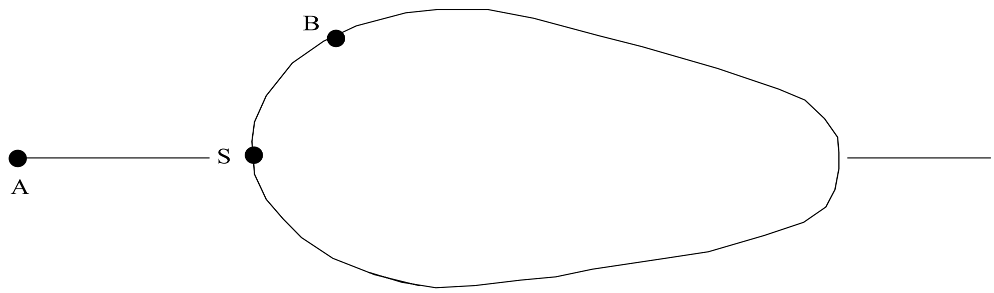

Fig. 4.3. Flow around a torpedo-shaped object. (point A: undisturbed flow conditions, point B: velocity equal to that at point A, point S: stagnation point)

As explanation, the measuring principle is given in more detail in the following figure (figure 4.4). The static pressure p_1 is measured in chamber K_1, the static pressure p_1 plus the stagnation pressure $(1/2)pv^2$ are measured in chamber 2 K_2. From the difference in pressure, which can be measured with a fluid manometer, the flow velocity in the tube can be calculated. If the fluid of which the flow velocity should be measured is the same as the manometer fluid, the fluid velocity follows from the read height difference as follows:

$$\frac{1}{2}v^2 = g\Delta h \tag{4.22}$$

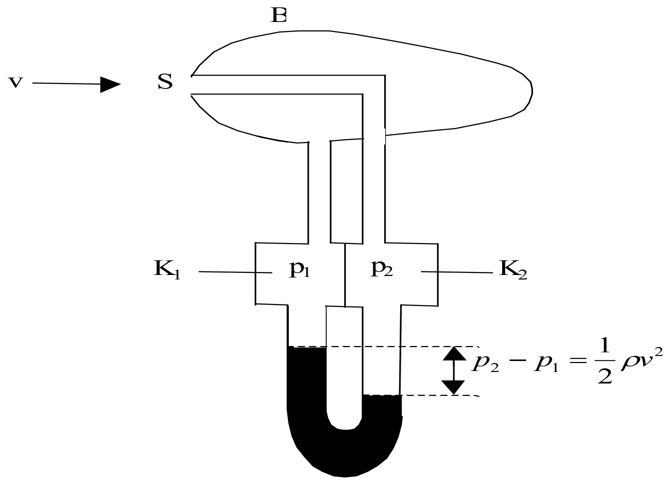

Fig. 4.4. Measurement of flow velocity by means of a Pitot tube.

Naturally, other instruments can also be used for measuring pressure differences, such as (difference) pressure gauges. Other instruments such as venturi meters, orifice meters and rotameters are also used to measure velocities of fluids. For venturi meters and orifice meters the measuring principle rests on pressure differences occurring as a result of velocity changes, while the principle of the rotameter is based on the rising height of a float in a weakly conical, vertically set up tube.

As a last application of Bernoulli's law, we will analyse flow through a pipe with a sudden widening. A frictionless fluid flows in the steady-state in plug flow through a horizontal pipe with diameter S_1 (see fig. 4.5.). The pipe with diameter S_1 suddenly goes over in a second, also horizontally placed, pipe with a larger diameter S_2. We are interested here in the force $F_{z,f\rightarrow w}$, which the fluid exerts on the walls of the piping system, whereby the (positive) z-co-ordinate shows in the main flow direction.

This force should be expressed in the density ρ, the pressure p_1 and the velocity v_1 for the widening and the diameters S_1 and S_2. The pressures p_1 and p_2 and the velocities v_1 and v_2 are average values over the conduit surfaces.

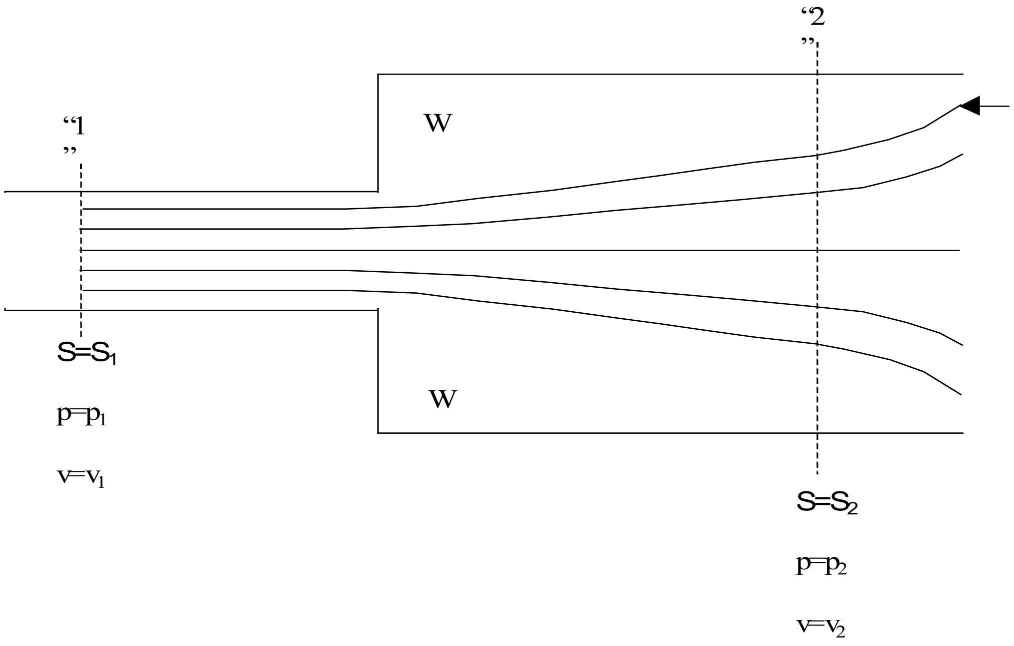

Fig. 4.5. Flow through a horizontal conduit with a sudden widening.

For the description of the system, we use the mass balance, momentum balance and mechanical energy balance. According to the (integral) mass balance it is valid that:

$$0 = \rho v_1 S_1 - \rho v_2 S_2 \tag{4.23}$$

According to the (integral) momentum balance in the main flow direction, it is valid that[1]:

$$0 = (\rho v_1) v_1 S_1 - (\rho v_2) v_2 S_2 + p_1 S_1 - p_2 S_2 - F_{z,f \to w} \tag{4.24}$$

According to the law of conservation of mechanical energy, which is applied here between the levels “1” and “2”, it is valid that:

$$0 = \frac{1}{2}\rho v_2^2 - \frac{1}{2}\rho v_1^2 + p_2 - p_1 \tag{4.25}$$

because there is no change in potential energy in this situation. As it is valid, according to (4.23), that:

$$v_2 = v_1 \left(\frac{S_1}{S_2} \right) \tag{4.26}$$

---

[1] the control volume here consists of the fluid volume between levels “1” and “2”.

v_2 in (4.25) can be expressed in the chosen quantities, so that (4.25) can be rewritten as:

$$p_2 = p_1 + \frac{1}{2}\rho v_1^2\left[1-\left(\frac{S_1}{S_2}\right)^2\right] \tag{4.27}$$

From (4.27), we can read that after the widening a pressure increase occurs, which is caused by the released kinetic energy. Substitution of (4.26) and (4.27) into (4.24) gives the following expression for $F_{z,f\rightarrow w}$ in terms of the chosen quantities:

$$F_{z,f\rightarrow w} = -\left\{\frac{1}{2}\rho v_1^2\left[1-\frac{S_1}{S_2}\right]^2 + p_1\left[1-\frac{S_1}{S_2}\right]\right\}S_2 \tag{4.28}$$

Note that the force that the (frictionless) fluid exerts on the wall is always opposite to the main flow direction. For a real fluid, i.e. with internal friction, viscous forces would act on the walls of the pipe and (4.28) should be modified. In practice, eddies will occur just behind the widening (given by W in Fig. 4.5) wherein part of the mechanical energy will be converted into internal or thermal energy ("eddy dissipation").

5 LAMINAR AND TURBULENT FLOW; BOUNDARY LAYERS

5.1 Laminar and turbulent flow

In the previous chapters, we did not make a specific discrimination regarding the character of the flow. Flows can generally be divided into laminar and turbulent flows.

i) Laminar flow ("layered flow"): In laminar flow, streamlines do not cross each other. This type of flow is associated with "low" flow velocities[1] and seldom occurs in process apparatus.

ii) Turbulent flow ("flow with eddies"): In turbulent flow, streamlines continuously cross each other. Displacement of fluid elements occurs superimposed on the main flow direction, where there is "chaotic movement" of these elements. This type of flow is associated with "high" flow velocities and frequently occurs in process apparatus.

The concept turbulent flow should not be associated too strongly with the presence of eddies. Laminar flow also knows eddies, e.g. behind obstacles placed in the stream (see Fig. 5.1.). These eddies do, however, straighten out in continuing flow. In this figure, the eddies that originate behind a cylinder ("obstacle") carried in a fluid stream are visualised. The quantity R is the Reynolds number Re, defined according to:

$$R = \mathrm{Re} = \frac{\rho v_\infty D}{\eta} \tag{5.1}$$

where ρ and η are the density and the dynamic viscosity of the fluid, respectively, v_∞ the oncoming flow velocity and D the diameter of the cylinder. Check for yourself, by means of a dimension analysis, that Re is dimensionless.

The occurrence of turbulence in a flowing fluid can be related to the (in)stability of the flow. (Small) disturbances are always present in a flow, even in the absence of obstacles. These disturbances can essentially cause the local instability (start of turbulence) in the flow, dependent on their being damped out (laminar flow) or strengthened (turbulent flow). Whether a disturbance is damped out or strengthened is determined by the viscous and inertial forces acting in the fluid. For laminar flow, viscous forces dominate, and for turbulent flow the inertial forces dominate.

The relation between the inertial forces and viscous forces that are active in the fluid is given by the (dimensionless) Reynolds number Re:

---

[1] Quantification of "low" and "high" flow velocities follows later by means of the Reynolds number, abbreviated as Re or R.

Re = inertial forces/ viscous forces (dimensionless) (5.2)

The Reynolds number plays a very important role in fluid dynamics for the characterisation of the flow regime (laminar or turbulent) and appears as one of the parameters in the dimensionless Navier-Stokes equations. These equations read in vector form[1] (for constant density and constant dynamic viscosity):

$$\rho\left[\frac{\partial \bar{v}}{\partial t}+(\bar{v}.\nabla)\bar{v}\right]=-\nabla p+\eta\nabla^2\bar{v}+\rho\bar{g} \qquad (5.3)$$

wherein $(\bar{v}.\nabla)$ is the following differential operator:

$$(\bar{v}.\nabla)=v_x\frac{\partial}{\partial x}+v_y\frac{\partial}{\partial_y}+v_z\frac{\partial}{\partial_z} \qquad (5.4)$$

while ∇^2 is the Laplace operator that is given in Cartesian co-ordinates as:

$$\nabla^2=\frac{\partial^2}{\partial x^2}+\frac{\partial^2}{\partial y^2}+\frac{\partial^2}{\partial z^2} \qquad (5.5)$$

R = 32

R = 55

R = 65

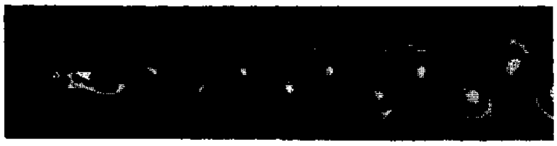

R = 71

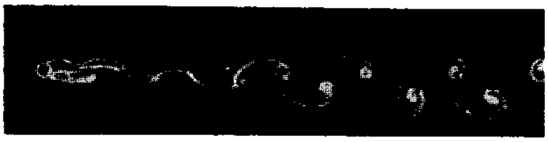

R = 102

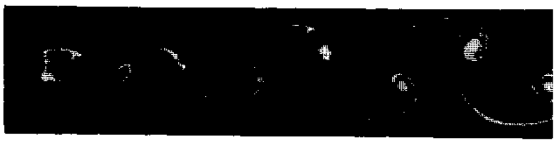

R = 161

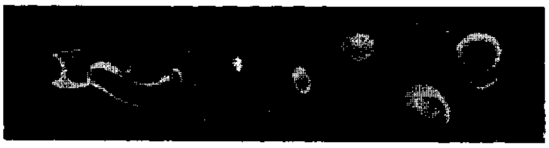

R = 225

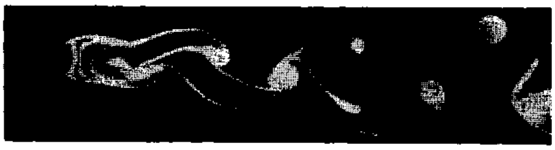

R = 281

---

[1] This way of notation is only valid for Cartesian co-ordinates.

Fig. 5.1. Formation of eddies behind a carried-along cylinder at different values of the Reynolds number R (=Re).

We make the above equation dimensionless with the help of a characteristic length measure d and the average velocity <v>:

- dimensionless co-ordinates x*, y* and z*:

$$x^* = \frac{x}{d} \qquad y^* = \frac{y}{d} \qquad z^* = \frac{z}{d} \tag{5.6}$$

- dimensionless time t*:

$$t^* = \frac{t < v >}{d} \tag{5.7}$$

- dimensionless velocity $\overline{v}\,^*$:

$$\overline{v}^* = \left(v_x^*, v_y^*, v_z^*\right) = \left(\frac{v_x}{< v >}, \frac{v_y}{< v >}, \frac{v_z}{< v >}\right) = \frac{\overline{v}}{< v >} \tag{5.8}$$

- dimensionless pressure p*:

$$p^* = \frac{p}{\rho\left(< v >\right)^2} \tag{5.9}$$

If these dimensionless quantities are substituted into equation (5.3), we get the following rewritten dimensionless Navier-Stokes equations:

$$\frac{\partial \overline{v}^*}{\partial t^*} + \left(\overline{v}^* . \nabla^*\right)\overline{v}^* = -\nabla^* p^* + \frac{\eta}{p < v >}\left(\nabla^*\right)^2 \overline{v}^* + \frac{gd}{\left(< v >\right)^2}\frac{\overline{g}}{g} \tag{5.10}$$

In (5.10) the Reynolds number Re and the Froude number Fr appear as parameters and are respectively defined as:

$$\mathrm{Re} = \frac{\rho < v > d}{\eta} \text{ = inertial forces/viscous forces} \tag{5.11}$$

and

$$Fr = \frac{\left(< v >\right)^2}{gd} \text{ = inertial forces/gravity forces} \tag{5.12}$$

On the grounds of the definition of the Reynolds number Re, we can already qualitatively state that low Re-values correspond to laminar flow and that high Re-values correspond to turbulent flow. For pipe flow, Reynolds determined experimentally by means of visualisation of the flow by a colour agent, that for Re<2000, flow is laminar and for Re>2300, flow is turbulent. In these experiments, a colour agent is injected in the flow direction. For Re<2000, the injected stain was visible as a thin "thread" and hardly[1] any radial distribution of the stain occurred. For Re>2300 (thus a relatively small increase of the average flow velocity), a considerable radial distribution of the stain by arising eddies occurred "suddenly" (see Fig. 5.2).

Fig. 5.2. Visualisation of the flow in a round tube by means of a stain injected in the flow direction.

Generally, no clear (instability) criterion for the change from laminar to turbulent flow can be formulated in terms of Re-values. Only a Re-range can be given within which flow can change from laminar to turbulent.

For tube flow the diameter D is taken for the characteristic length measure d in the Re-number:

$$\mathrm{Re} = \frac{\rho < v_z > D}{\eta} \tag{5.13}$$

It will be clear that the eddies that are present have a big influence on the radial velocity profile. During turbulent flow, in contrast to laminar flow, a considerable convective transport occurs perpendicular to the main flow direction as a result of the eddies. As this transport mechanism is a lot more effective than the molecular transport mechanism, the radial velocity profile for turbulent flow is considerably flatter than for laminar tube flow. For laminar flow, we have derived in Chapter 3 that:

$$\frac{v_z}{(v_z)_{\max}} = 1 - \left(\frac{r}{R}\right)^2 \qquad \text{and} \qquad \frac{< v_z >}{(v_z)_{\max}} = \frac{1}{2} \tag{5.14}$$

It has been experimentally determined for turbulent flow that the radial velocity profile and the average velocity approximately satisfy (valid for 10^4<Re10^5):

---

[1] As a result of radial concentration differences, molecular transport of the stain occurs. This effect can, however, be neglected.

$$\frac{v_z}{(v_z)_{\max}} = \left(1 - \frac{r}{R}\right)^{1/7} \quad \text{and} \quad \frac{< v_z >}{(v_z)_{\max}} = \frac{4}{5} \tag{5.15}$$

Both velocity profiles (in dimensionless form) are given in the following figure:

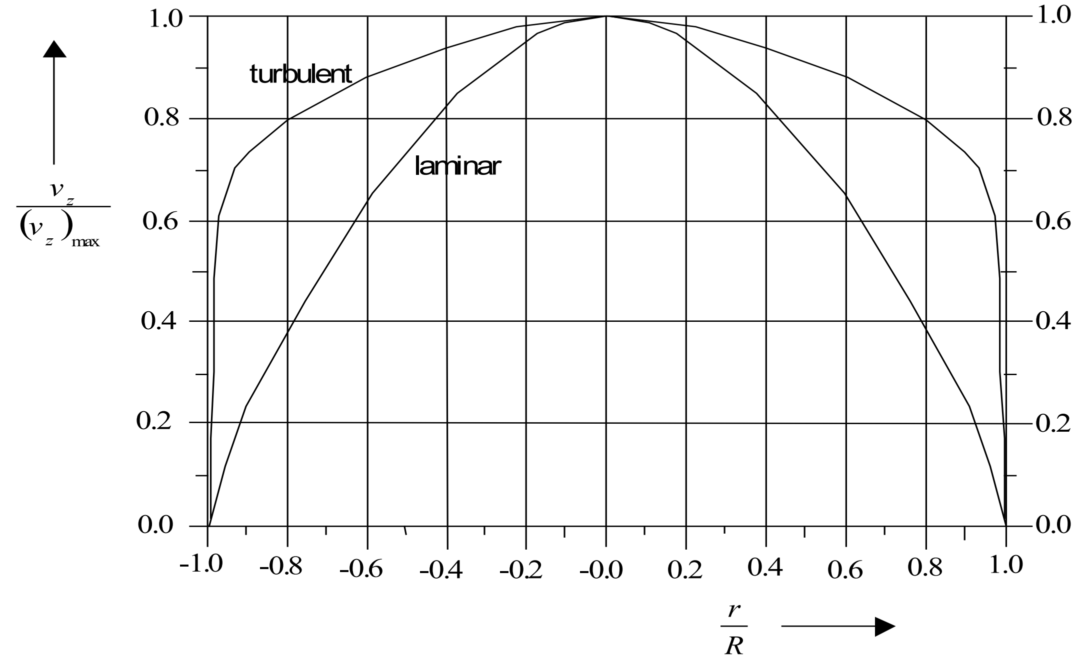

Fig. 5.3. Radial velocity profiles for laminar and turbulent tube flow.

From Fig. 5.3. it seems clear that the eddy transport has a considerable influence on the form of the radial velocity profile. For turbulent flow, the velocity profile in the centre of the tube is considerably flatter than for laminar flow. In the literature, a large number of semi-empirical models are proposed for the description of eddy transport. Only the models of Boussinesq and Prandtl are discussed here.

Boussinesq model:

In this model, it is assumed that the (radial) eddy transport can be described analogously to the molecular momentum transport. For the (radial) momentum flux as a result of the eddy transport it is valid that:

$$\tau_{rz}^{(t)} = -\eta^{(t)} \frac{dv_z}{dr} \tag{5.16}$$

where $\eta^{(t)}$ is the so-called Eddy viscosity which, in contrast to the dynamic viscosity η, is not a material constant, but a quantity that is dependent on local flow conditions. In the direct surroundings of the wall, eddy transport is not important and molecular momentum transport dominates.

Prandtl model:

On the basis of the assumption that movement of eddies in a fluid is analogous to the movement of molecules in a gas, Prandtl formulated the following expression for (radial) eddy transport wherein the so-called mixing length "l" plays an analogous role to that of the mean free path gas kinetic theory:

$$\tau_{rz}^{(t)} = \rho l^2 \left\{ \frac{dv_z}{dr} \right\}^2 \tag{5.17}$$

The mixing length l is dependent on the position and is supposed by Prandtl to be proportional to the distance from the solid wall that borders the turbulent flowing fluid ($l=\kappa(R-r)$ for tube flow, with κ a proportional constant ($\kappa \approx 0.36$)).

The occurrence of eddies also has important consequences for the relation between the applied pressure gradient (-dp/dz) and the resulting volume flow Φ_V. In the laminar flow regime, Φ_V is proportional to (-dp/dz), while being on approximate proportional to $(-dp/dz)^{4/7}$ in the turbulent flow regime.

At the beginning of this paragraph, it was stated that turbulent flow corresponds to a "more or less chaotic movement of the fluid elements". This is, however, a strongly simplified version of reality. For turbulent tube flow, e.g., there is a practically random movement of the fluid elements in the centre of the tube (the velocity fluctuations in the radial and axial directions are practically equal). However, closer to the tube wall, the fluctuations in the velocity in the axial velocity component are greater than the fluctuations in the radial velocity component, whereby both fluctuations approach zero on the tube wall. The physical behaviour of this turbulent flow is, in contrast to laminar flow behaviour, strongly dependent on the radial position. Although there is a continuous change in behaviour in reality, we can differentiate with increasing distance to the tube wall between the viscous sub-layer where molecular momentum transport dominates, the buffer zone where both molecular and turbulent momentum transport occur and the area with completely developed turbulence where turbulent momentum transport dominates (see Fig. 5.4).

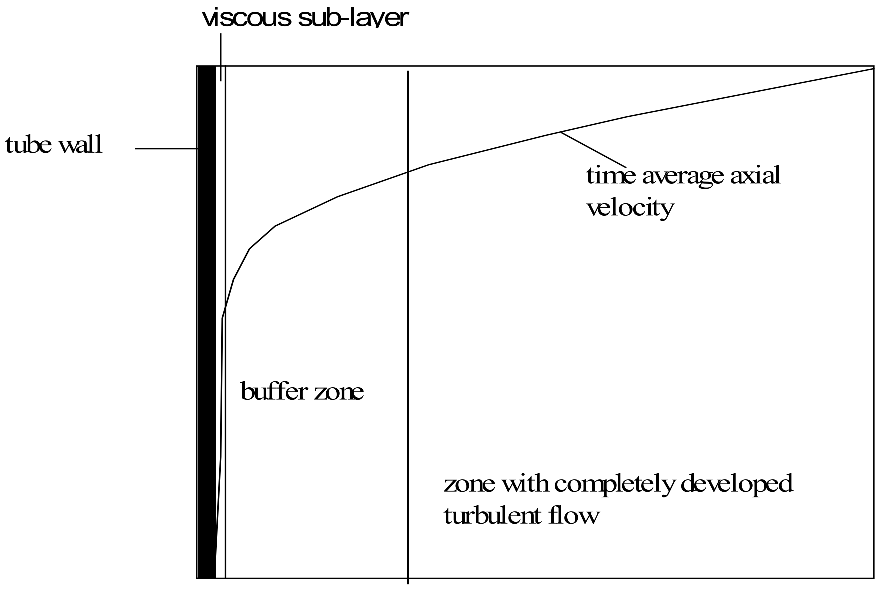

Fig. 5.4. Schematic representation of the structure of a turbulent flow in the surroundings of the tube wall.

5.2 Boundary layers

In practice we are often confronted with flowing fluids where there is a combined transport of mass, energy and momentum in the direct surroundings of solid walls. For an accurate quantification of these transport processes, information regarding the velocity profile in the direct surroundings of the wall is essential. The major part of the velocity change is often situated in a thin fluid layer, the so-called boundary layer, which is in contact with the wall on the one side, and on the other with the bulk of the fluid. The thickness of this boundary layer, given by δ, can be dependent on position and time. In this paragraph, we will look at a number of simple examples of similar boundary layer flows. The first example concerns the boundary layer development as a function of time ($\delta=\delta(t)$), the second example concerns the boundary layer development as a function of position ($\delta=\delta(x)$ with x the flow direction). Finally, we will consider the boundary layer development for flow around a cylinder and a sphere.

5.2.1 Non steady-state flow along a flat plate

As first acquaintance with the concept of boundary layers, we study the non steady-state flow of a Newtonian fluid along an infinitely long flat plate. The fluid is flowing in laminar flow mode and with a uniform velocity of v_∞ parallel to the plate. Initially the plate moves at the same velocity as the fluid. At time t=0, however, the velocity of the plate is suddenly brought back to v_p, so that a velocity difference originates between the bulk of the fluid and the plate. As a result of this velocity difference, the fluid will be slowed down by the plate and a disturbance of the velocity profile will occur as is shown qualitatively in the following figure. This figure shows the velocity of the fluid with regard to the plate. Further away from the plate the relative fluid velocity is $v_\infty - v_p$.

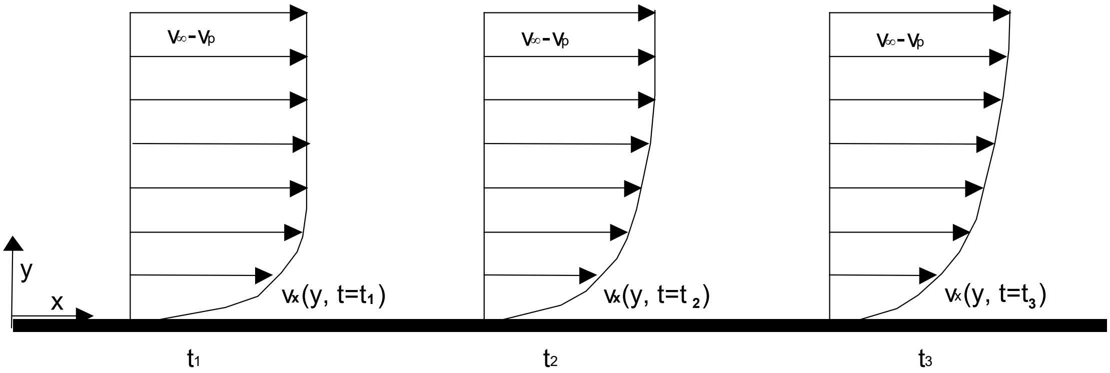

Fig. 5.5. Non-stationary fluid flow along a flat plate and the qualitative development of the velocity profile in the time t ($t_1<t_2<t_3$).

It is evident from the above figure that with increasing time t, the initially uniform velocity profile is increasingly disturbed. The velocity v_x is dependent on y and t, but independent of x. Because differences in v_x arise in the y-direction, molecular transport of x-momentum will occur in the y-direction, i.e. perpendicular to the flow direction. The non steady-state problem can be described by means of the following simplified form of the Navier-Stokes equations[1]:

$$\frac{\partial v_x}{\partial t} = \nu \frac{\partial^2 v_x}{\partial y^2} \tag{5.18}$$

For the solution of this parabolic partial differential equation, we have to specify one starting condition and two boundary conditions that are respectively given by:

$$t = 0: \quad v = v_\infty \tag{5.19a}$$

And $$y = 0 \quad v_x = v_p \tag{5.19b}$$

$$y = \infty \quad v_x = v_\infty \tag{5.19c}$$

The solution of (5.18) under the conditions (5.19) can be obtained by means of the method of combination of independent variables[2] and reads:

---

[1] Check for yourself which assumptions have been made for the reduction of the x-component of the Navier-Stokes equations to the simplified microscopic balance for x-momentum (equation (5.18)). Argue why the assumption of one-dimensional flow is principally incorrect.

[2] With the method of combination of independent variables, a partial differential equation can be transformed to an ordinary differential equation by means of a "suitable choice" of a "new" variable that is a function of the "old" independent variables. Check for yourself that by means of the choice of:

$$\omega = \frac{y}{\sqrt{4\nu t}},$$

the partial differential equation (5.18) transforms to the following ordinary differential equation:

$$\frac{v_x - v_p}{v_\infty - v_p} = erf\left(\frac{y}{\sqrt{4\nu t}}\right) \tag{5.20}$$

Where “erf” represents the so-called error function or “error integral”, which is defined according to:

$$erf(z) = \frac{2}{\sqrt{\pi}} \int_0^z e^{-\beta^2} d\beta \tag{5.21}$$

For the error function, which is of great importance for mathematical physics, tables are available that give the value of erf(z) as a function of z (see Table 5.1).

$$\frac{d^2 v_x}{d\omega^2} + 2\omega \frac{dv_x}{d\omega} = 0$$

Table 5.1. Values of the error function erf(z).

$\frac{y}{\sqrt{4\nu t}}$	$erf\left(\frac{y}{\sqrt{4\nu t}}\right)$	$\frac{y}{\sqrt{4\nu t}}$	$erf\left(\frac{y}{\sqrt{4\nu t}}\right)$
0.00	0.0000	1.10	0.8802
0.05	0.0564	1.20	0.9103
0.10	0.1125	1.30	0.9340
0.15	0.1680	1.40	0.9523
0.20	0.2227	1.50	0.9661
0.25	0.2763	1.60	0.9763
0.30	0.3286	1.70	0.9838
0.35	0.3794	1.80	0.9890
0.40	0.4284	1.90	0.9928
0.45	0.4755	2.00	0.9953
0.50	0.5205	2.10	0.9976
0.55	0.5633	2.20	0.9981
0.60	0.6039	2.30	0.9989
0.65	0.6420	2.40	0.9993
0.70	0.6778	2.50	0.9996
0.75	0.7112	2.60	0.9998
0.80	0.7421	2.70	0.9999
0.85	0.7707	2.80	0.9999
0.90	0.7969	2.90	0.9999
0.95	0.8209	3.00	0.9999
1.00	0.8427		

For more clarity, the error function erf(z) is graphically represented again in Fig. 5.6. The expression for the shear stress on the wall of the plate τ_w can be derived by means of Newton's law, with the result:

$$\tau_w = -\eta \frac{\partial v_x}{\partial y}\Big|_{y=0} = -\eta\left(\frac{\left(v_\infty - v_p\right)}{\sqrt{\pi \nu t}}\right) \qquad (<0) \qquad (5.22)$$

It follows from the above equation that the momentum flux on y=0 is negative, which can also be expected on the grounds of the velocity profile given in Fig. 5.5. From equation (5.22) we can read that the velocity profile on y=0, i.e. on the wall of the plate, is given by:

$$\frac{\partial v_x}{\partial y}\bigg|_{y=0} = \frac{\left(v_\infty - v_p\right)}{\sqrt{\pi \nu t}} \tag{5.23}$$

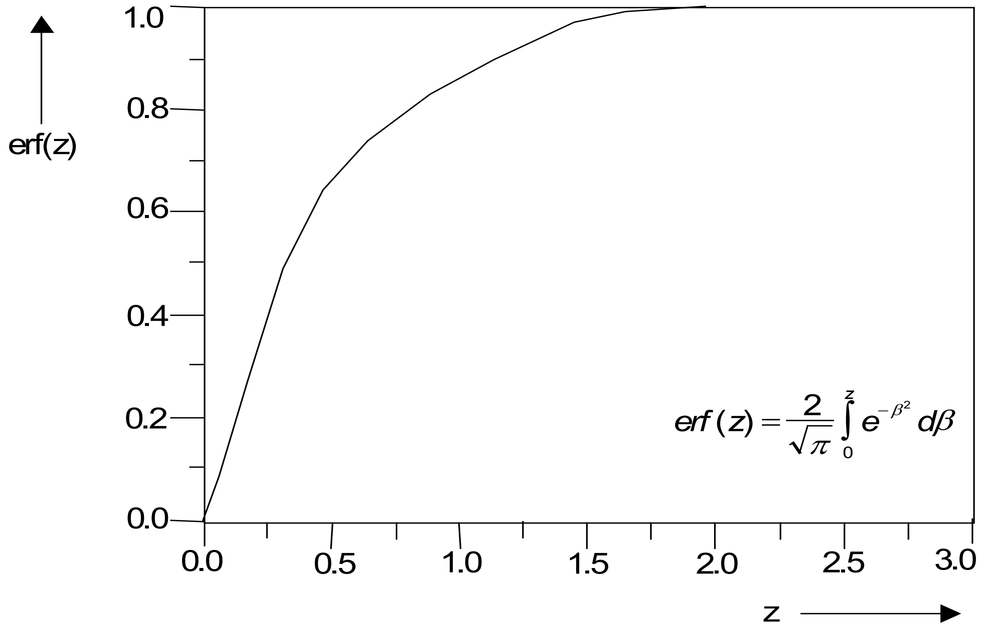

Fig. 5.6. The function erf(z), defined by equation (5.21), as a function of z.

It follows from equation (5.23) that, by bridging the velocity difference (v_∞-v_p), the tangent on the velocity profile on y=0 crosses the y-axis at a distance δ_*, given by:

$$\delta_* = \sqrt{\pi \nu t} \tag{5.24}$$

The result in dimensionless form is given in the following figure (Figure 5.7). From this figure (and table 5.1), we can read that for $z=z_* \approx 0.886$, which corresponds with δ_*, the actual relative velocity difference between the fluid and the plate $\left(v_x(\delta_*,t) - v_p\right)/\left(v_\infty - v_p\right)$ amounts to about 0.79. For $z = 2z_* = 1.772$, the relative velocity difference amounts to about 0.99, so that on $y = 2\delta_*$, the change of the relative velocity difference amounts to about 1-0.99=0.01. This means that the fundamental change of the fluid velocity is situated in a layer with thickness $2\delta_*$, measured from the plate. This layer, of which the thickness increases by the root of the time, we define as the boundary layer. We can also associate the quantity $2\delta_*$ with the penetration depth for molecular momentum transport, which we will give as δ_i. For the penetration depth for molecular momentum transport δ_i, the following is thus valid:

$$\delta_i = 2\sqrt{\pi \nu t} \tag{5.25}$$

For the analogous heat and mass transport, a similar equation is valid for the penetration depth for heat and mass, respectively. In equation (5.25), the kinematic viscosity *v* should then be replaced by the thermal diffusivity “a” and the diffusion coefficient “D”, respectively.

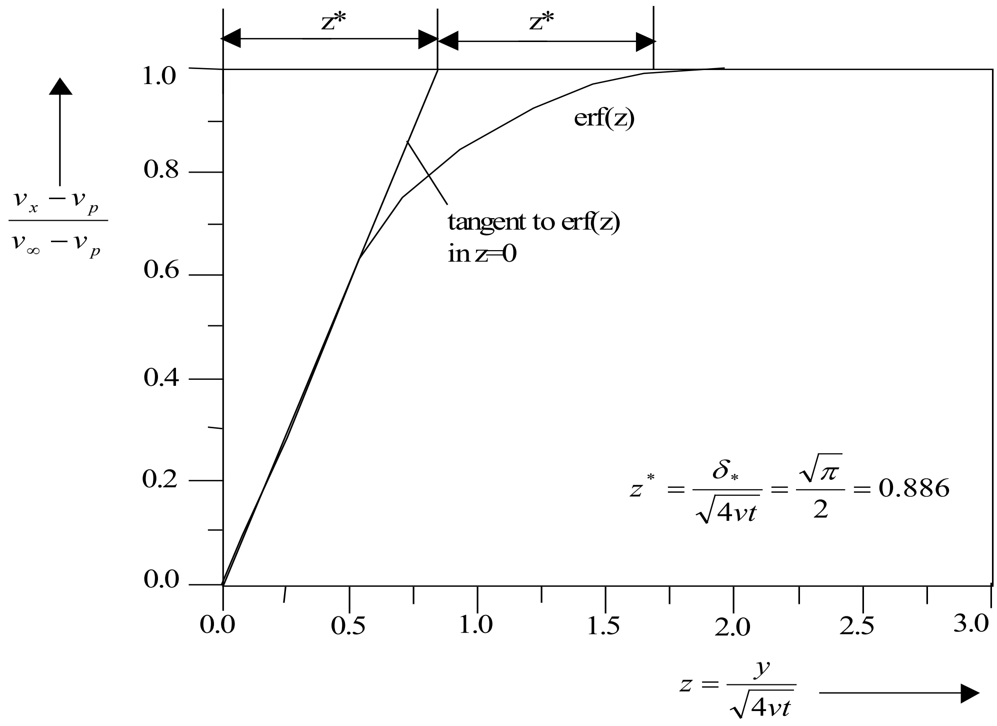

Fig. 5.7. Meaning of the quantity δ*, defined by equation (6.59).

In conclusion, for clarity, the meaning of the quantity δ*, defined in equation (5.24), is given again in relation to the velocity profile developing in time.

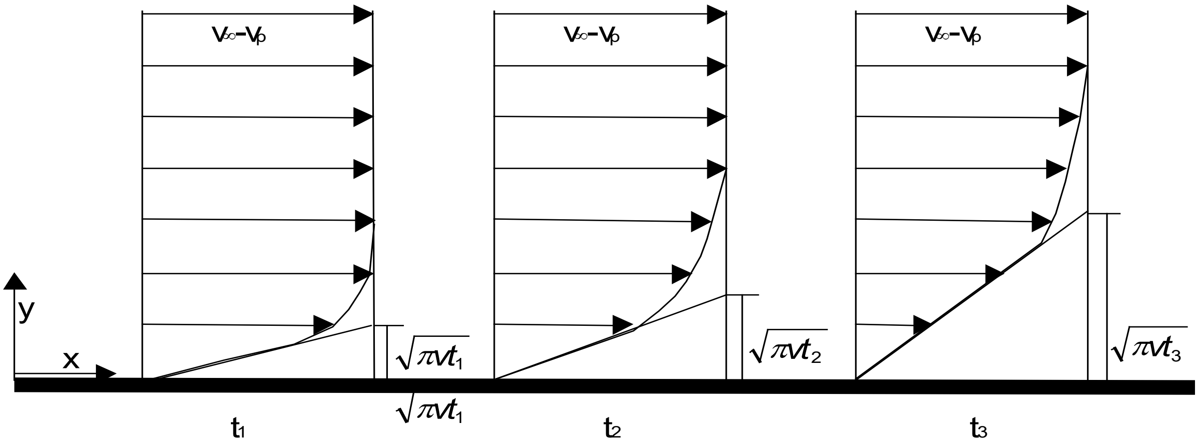

Fig. 5.8. Physical meaning of the quantity δ*, defined in equation (5.24), for non steady-state fluid flow along a flat plate ($t_1<t_2<t_3$).

5.2.2 Steady-state flow along a flat plate

We will now consider the steady-state, non-compressible flow of a Newtonian fluid along a non-moving, thin, flat plate. We firstly assume that the flow is laminar and that the fluid flows to the plate with a uniform velocity profile. As a result of the plate, a disturbance of the uniform velocity profile of the (two-sided) on-flowing fluid will occur, as is qualitatively shown in Fig. 5.9.

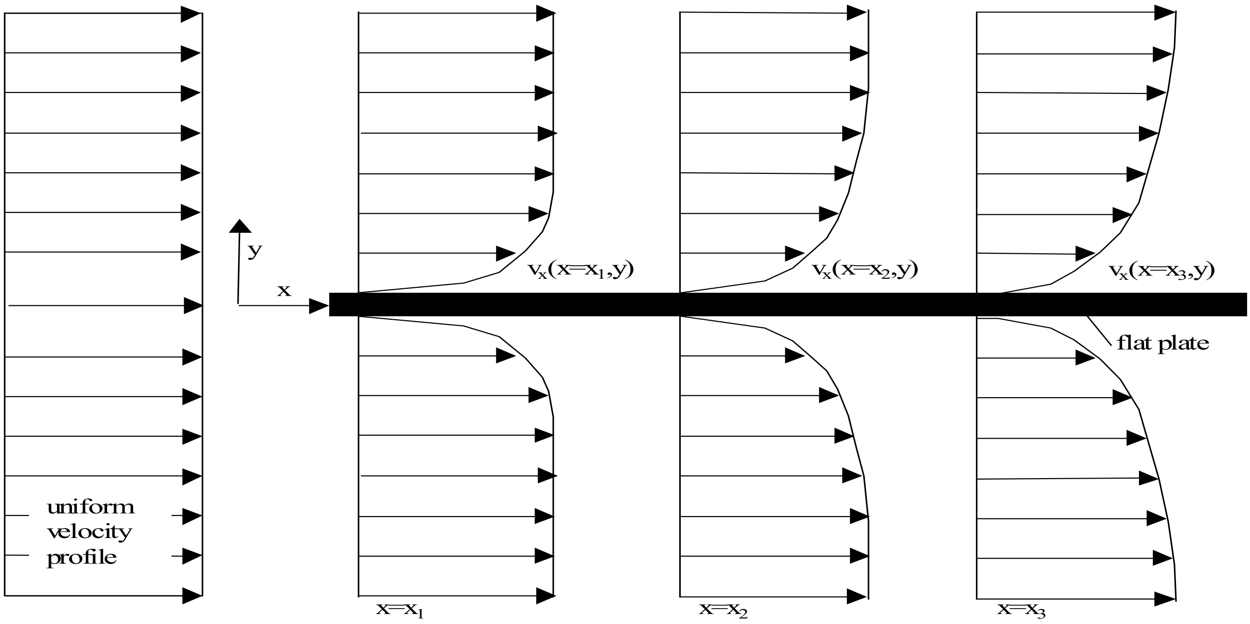

Fig. 5.9. Steady-state fluid flow along a thin, flat plate and the qualitative development of the velocity profile with increasing x-values.

Fluid particles closely located to the plate slow down the further located fluid elements via molecular momentum transfer. This slowing-down activity continues further into the fluid, so that the disturbance of the uniform velocity profile of the on-flowing fluid penetrates deeper into the fluid with increasing x. The layer in which this disturbance can be noticed is also called a boundary layer. Contrary to the previous example, we have here a boundary layer of which the thickness δ increases with increasing x. By means of the boundary layer theory[1], it can be derived that, for the (laminar) boundary layer thickness δ, it is (approximately) valid that:

$$\delta(x) = 4.64\sqrt{\frac{\nu x}{v_\infty}} \qquad (5.26)$$

---

[1] For an introduction into the boundary layer theory, you are referred to the book "Transport Phenomena" by R.B. Bird, W.E. Stewart and E.N. Lightfoot. For further study you are referred to the book "Boundary Layer Theory" by H. Schlichting.

Note that the boundary layer thickness δ increases with the root of x, which is analogous to the result of the non steady-state problem that we have studied in the previous paragraph. In our minds we can replace the time t from the non steady-state problem by the "travel time" x/v$_\infty$ for the present stationary problem. As example we calculate the thickness of the boundary layer for a flat plate (x=0.25m) which is drifted along by water (⍰=10^{-6} m^2/s) with a velocity v$_\infty$=1m/s[2)]. Substitution of this data into (5.26) gives:

$$\delta(x) = 0.00464\sqrt{x} \tag{5.27}$$

For x=0.25m, the boundary layer thickness is therefore δ=2.32mm, which makes it clear that the velocity gradient is situated in a very thin layer near the solid wall. By means of the boundary layer theory, one can also get an (approximate) expression for the velocity profile in the boundary layer, with the result:

$$\frac{v_x}{v_\infty} = \frac{3}{2}\left(\frac{y}{4.64\sqrt{\nu x/v_\infty}}\right) - \frac{1}{2}\left(\frac{y}{4.64\sqrt{\nu x/v_\infty}}\right)^3 \tag{5.28}$$

For the force F$_x$, which is exerted by the fluid on the plate towards which it is flowing from both sides (with width B and length L) it is the valid that:

$$F_x = 2\int_0^B\int_0^L \left(-\tau_{yx}\big|_{y=0}\right)dxdz = 2\int_0^B\int_0^L \left(\eta\frac{\partial v_x}{\partial y}\right)\bigg|_{y=0} dxdz = 1.292\sqrt{\rho\eta L B^2 v_\infty^3} \tag{5.29}$$

Blasius obtained an "exact" numerical solution for the (laminar) flowed on plate, and the force exerted by the fluid on the plate in the x-direction F$_x$ was subsequently calculated from this solution. The result of this calculation is an equation of the same form as (5.29), but the constant is 1.328 instead of 1.292. With this adapted constant, we rewrite equation (5.29) in a form that connects to the formulation of friction factor for submerged objects (see Chapter 6):

$$F_x = 1.328\left(\mathrm{Re}_L\right)^{-0.5}\left(2BL\right)\frac{1}{2}\rho v_\infty^2 \tag{5.30}$$

where Re$_L$ is the Reynolds number concerned with the length L of the plate:

$$\mathrm{Re}_L = \frac{\rho v_\infty L}{\eta} = \frac{v_\infty L}{\nu} \tag{5.31}$$

The "exact" expression for the shear stress τ_w, which is exerted by the fluid on the wall of the plate, reads:

$$\tau_w = 0.664\left(\mathrm{Re}_x\right)^{-0.5}\frac{1}{2}\rho v_\infty^2 \tag{5.32}$$

where Re$_x$ is the local Reynolds number, defined according to:

[2)] For these conditions, there is laminar flow of the water.

$$\mathrm{Re}_x = \frac{\rho v_\infty x}{\eta} = \frac{v_\infty x}{\nu} \tag{5.33}$$

It is stressed here that the equations given thus far are valid for laminar flow conditions. It is known from experiments that there are laminar flow conditions if the Reynolds number based on the length of the plate, Re_L, is smaller than $3.2.10^5$. If $\mathrm{Re}_L > 3.2.10^5$, the laminar boundary layer flow can turn into turbulent boundary layer flow. The exact Reynolds number where the boundary layer flow changes from laminar to turbulent is called the critical Reynolds number Re_c and is dependent on the experimental conditions such as the turbulence intensity of the undisturbed flow. Therefore, a range rather than an exact value is often given in literature for the Re_c: $3.10^5 < \mathrm{Re}_c < 3.10^6$.

We will subsequently consider the situation where the flat plate is flowed along by a turbulent flowing fluid. Analogous to the laminar flow situation, a laminar boundary layer will be formed[1] from x=0, of which the thickness δ increases with increasing x. Because of the higher velocity v_∞, the boundary layer will be formed over a shorter length x. As a result of the slowing down of the fluid elements, the inertial forces are dominated by the viscous forces in the direct vicinity of the plate. The with x increasing boundary layer thickness has as result that with increasing x, the inertial forces will gradually dominate the viscous forces so that flow becomes unstable. A change from laminar to turbulent flow can therefore occur in a relatively small area, the so-called transformation-area. Whether this change really occurs depends on the length of the plate L; with a short plate the change may not occur, while with a very long plate the laminar part at the beginning of the plate is of minor importance. Eddies originate in the area of change, whereby no further development of the laminar boundary layer occurs. These eddies quickly extend to the plate and result in a turbulent boundary layer with little further change. Analogous to the situation for turbulent tubular flow, we can differentiate between the viscous sub-layer, the buffer layer and the turbulent (undisturbed) bulk behind the area of change in increasing distance from the plate (see Fig. 5.10).

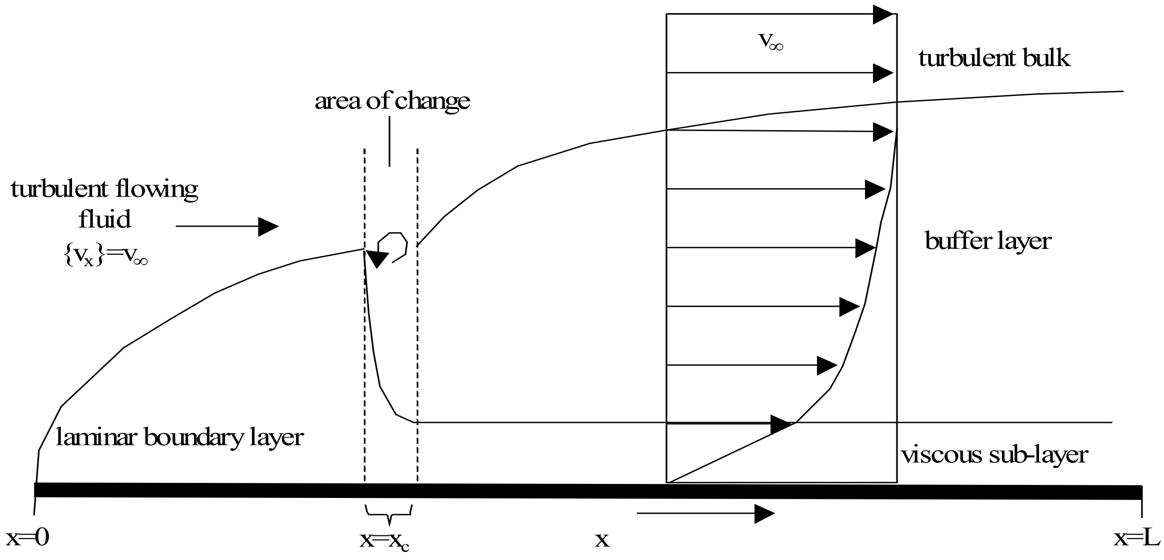

---

[1] Despite the fact that there is turbulent on-flow conditions in the fluid, a laminar boundary layer is formed at the beginning of the plate.

Fig. 5.10. The change from a laminar to a turbulent boundary layer for a flat plate, towards which a turbulent fluid flows[2]*.*

The turbulent boundary layer thus consists of the viscous sub-layer in which the momentum transport perpendicular to the x-direction is completely dominated by molecular transport, while there is combined molecular and turbulent momentum transport in the buffer layer. The following expression for the local shear stress on the wall of the plate τ_w in the turbulent boundary layer was found empirically:

$$\tau_w = 0.059\left(\mathrm{Re}_x\right)^{-0.2}\frac{1}{2}\rho v_\infty^2 \tag{5.34}$$

For the calculation of the force acting on the plate, we can differentiate between two situations:

A) There is a turbulent boundary layer flow over practically the whole plate. For the force F_x, which is exerted in the x-direction on the plate, it is valid for double-sided on-flow that:

$$F_x = 2\int_0^B\int_0^L\left(\tau_w\right)_{turbulent} dxdz = 0.074\left(\mathrm{Re}_L\right)^{-0.2}\left(2BL\right)\frac{1}{2}\rho v_\infty^2 \tag{5.35}$$

B) There is a laminar boundary layer flow over the beginning of the plate and turbulent boundary layer flow over the end of the plate. In this case it is valid for the force F_x, which is exerted on the plate for double-sided on-flow that:

$$F_x = 2\int_0^B\int_0^{x_c}\left(\tau_w\right)_{la\min ar} dxdz + 2\int_0^B\int_{x_c}^L\left(\tau_w\right)_{turbulent} dxdz \tag{5.36}$$

Substitution of equations (5.32) and (5.34), which respectively give the shear stress on the wall of the plate for the laminar beginning and the turbulent end, into (5.36), gives after integration:

$$F_x = \left\{1.328\left(\mathrm{Re}_c\right)^{-0.5}\left(2Bx_c\right) + 0.074\left\{\left(\mathrm{Re}_L\right)^{-0.2}\left(2BL\right) - \left(\mathrm{Re}_c\right)^{-0.2}\left(2Bx_c\right)\right\}\right\}\frac{1}{2}\rho v_\infty^2 \tag{5.37}$$

Considering the differentiation made in this paragraph, it should be noted here that the laminar part (at the beginning) is always present, but if $x_c \ll L$, the contribution of the beginning may be neglected for the calculation of F_x.

---

[2] By $\{v_x\}$, the average time value of the on-flow velocity is meant. For turbulent flow, the pressure and velocity vary in time around a given average value.

5.2.3 Steady-state flow around cylinder and sphere

We will now consider the steady-state, non-compressible, flow of a Newtonian fluid around a cylinder and a sphere. In contrast to the situation for flow along a flat plate, which was looked at in the previous paragraph, it is possible that with flow around a cylinder and around a sphere, release of the boundary layer can occur. This boundary layer release has important consequences for the size of the force exerted by the fluid on the object and will be analysed more closely for flow around a sphere.

As boundary layer release is closely connected to the pressure distribution in the boundary layer, we will concentrate on that. For simplification, we assume an ideal, i.e. frictionless, fluid. According to the law of Bernoulli for frictionless flow, it is valid along one streamline that:

$$p + \frac{1}{2}\rho v^2 = p_\infty + \frac{1}{2}\rho v_\infty^2 \tag{5.38}$$

Here p_∞ and v_∞ are the pressure and velocity at a great distance from the sphere, respectively. According to the law of Bernoulli the sum of the static pressure p and the kinetic energy per volume unit is constant in this situation. On the basis of the law of Bernoulli, the qualitative distribution of the pressure, shown in the following figure, will be clear. At the front and back of the sphere, the flow velocity v is low, and therefore the pressure p will be high[1]. On both top and bottom side of the sphere, the flow velocity v is high and the pressure p low, and a part of the static pressure is thus converted to kinetic energy. These changes in pressure and velocity around the sphere are primarily a result of the geometry.

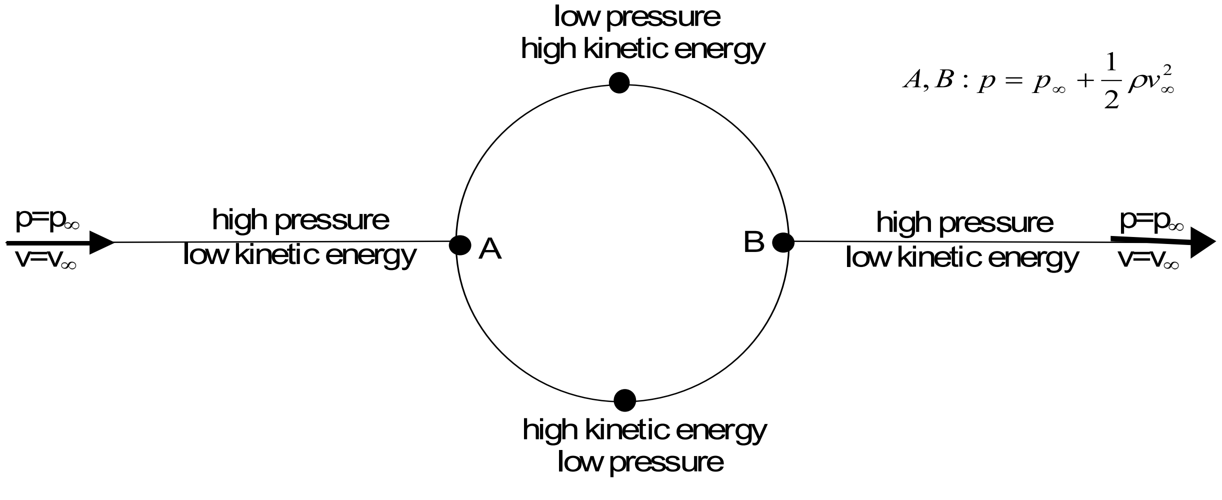

Fig. 5.11. Qualitative course of the static pressure and the kinetic energy (velocity) for the flow of a frictionless fluid around a sphere.

---

[1] The points A and B are called the stagnation points.

This pressure distribution around the sphere means that there is a negative pressure gradient and a positive pressure gradient present at the front and back, respectively(1). Therefore, an acceleration of the fluid elements will occur at the front and a deceleration at the back. If there is no friction, then the fluid at the ends of the low pressure has enough kinetic energy to build the high pressure that is prevalent at the front up again at the back. Regarding the vertical centre-line through the sphere, there is a symmetrical flow situation. As a result of this symmetry, a (hypothetical) frictionless fluid will thus not exert a net force on the sphere. This result is known in hydrodynamics as the *paradox of d'Alembert*. In reality, a resulting force is exerted on the sphere because of the friction.

We will subsequently consider the flow of a real fluid, i.e. a fluid with internal friction, around a sphere at different values of the Reynolds number Re. For the submerged sphere (and cylinder), the diameter D is taken as the characteristic measure of length in the Reynolds number Re:

$$\mathrm{Re} = \frac{\rho v_\infty D}{\eta} = \frac{v_\infty D}{\nu} \tag{5.39}$$

Dependent on the value of the Reynolds number Re, we can differentiate between different flow regimes. For Re<0.1, the streamlines seem to completely conform to the shape of the sphere (see Fig. 5.12), and the inertial forces have no influence on the momentum exchange between the fluid and the sphere. If the flow direction is reversed, the position of the streamlines does not change, which again means that there is symmetry with regard to the vertical centre-line through the sphere. This type of flow is called creeping flow and for the force F, which the sphere experiences in the flow direction, the law of Stokes is then valid:

$$F = 3\pi\eta v_\infty D \tag{5.40}$$

Stokes derived equation (5.40) in the nineteenth century on the basis of the Navier-Stokes equations. Note that the form of this equation is completely analogous to equation (3.16) for the viscous force exerted on the wall of a laminar round tubular pipe. The law of Stokes is applied, among others, to describe the movement of colloidal particles under the influence of an electric field, for the theoretical description of sedimentation phenomena and for the study of the behaviour of particles in aerosols.

For Re>0.1, the symmetry regarding the vertical centre-line through the sphere is lost and the law of Stokes is no longer valid(1). From experiments where the flow in the direct vicinity of the sphere was visualised, it seems that a release of boundary layers occur, for Re≥4. The streamlines are not running smoothly around the sphere anymore, and a wake, i.e. an area with an internal circulation(2), originates behind the sphere. The point of boundary layer release, the so-called separation point S, is dependent on the Reynolds number(3). With

---

(1) If the pressure gradient is negative, the pressure decreases in the flow direction, if the pressure gradient is positive, the pressure increases in the flow direction.

(1) For Re=1 the law of Stokes predicts a value for the force F which is about 10% too low.

(2) In this area the fluid flows around and an eddy is thus formed.

(3) Boundary layer release actually occurs for points on a circle of which the centre point lies on the horizontal (i.e. lying in the main flow direction) centre-line through the sphere.

increasing Re-value, the separation point S moves towards the front of the sphere. From these experiments it also seems that back-flow of the fluid occurs behind the separation point S. We will now aim to explain this seemingly strange behaviour of the fluid.

Where a real fluid flows around a sphere, a (thin) boundary layer will form in the direct vicinity of the wall of the sphere, in which the fundamental velocity gradient is localised (see Fig. 5.13).

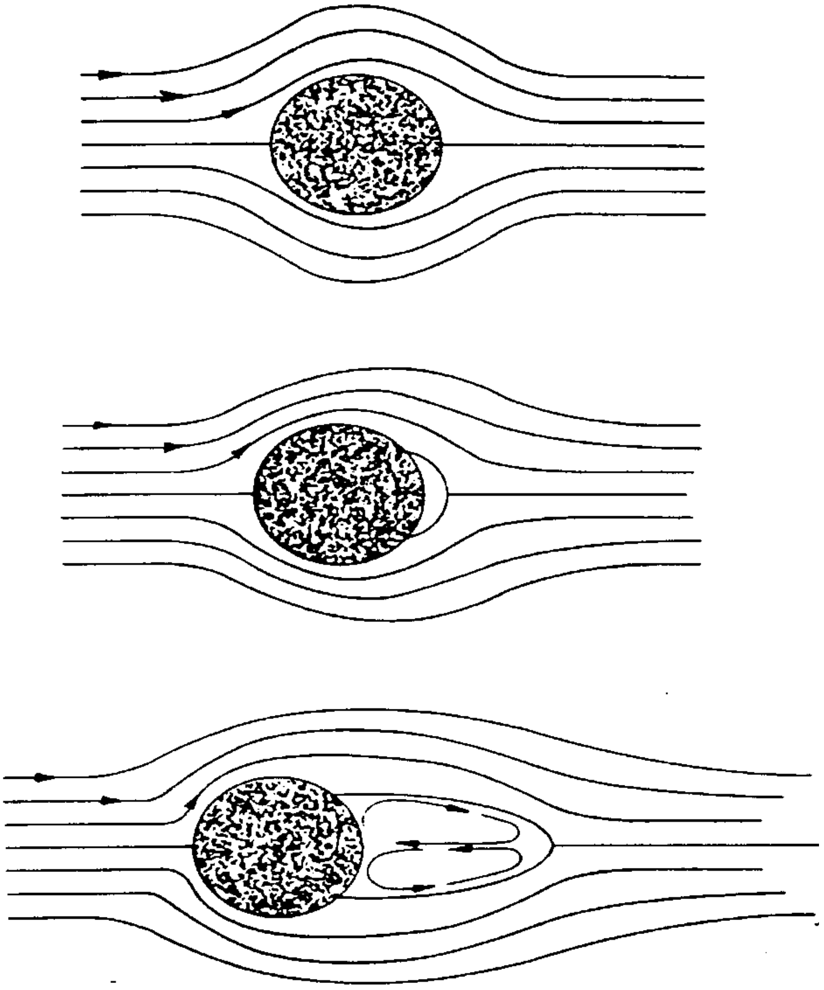

Fig. 5.12. The qualitative course of the streamlines for increasing values of the Reynolds number Re (Re=1, 4, 40).

Apart from the boundary layer, a conversion of pressure energy to kinetic energy occurs during the flow from D to E, while the reverse process occurs during the flow from E to F. Fluid particles that move around the sphere outside of the boundary layer will have the same velocity at points D and F, as no internal friction occurs outside of the boundary layer. However, fluid particles moving in the direct vicinity of the sphere, i.e. inside the boundary layer, will lose an (important) part of their energy as a result of the great (viscous) friction forces. Therefore, not enough kinetic energy can be built up at point E to overcome the externally applied positive pressure gradient that the particles experience along the trajectory from E to F. This means that after point S, the so-called separation point where all the kinetic energy built up at point E is fully consumed, the positive pressure gradient forces the fluid particles to flow back, which causes the release of the boundary layer at point S. It is useful to note here that the local pressure outside the boundary layer is "passed on" to the boundary layer.

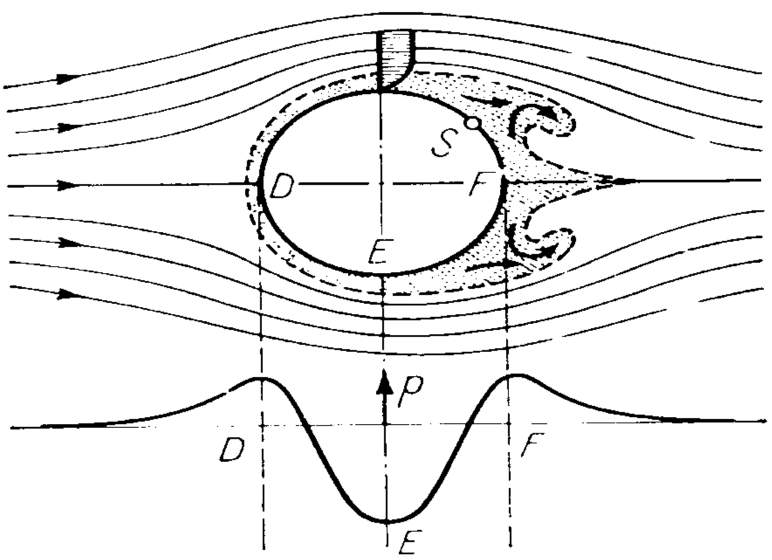

Fig. 5.13. Qualitative representation of the boundary layer release on the surface of a submerged sphere. Point S represents the separation point.

Analogous processes occur for flow around a cylinder and therefore this geometry will not be discussed separately. Instead, as illustration, a few photos are given in the following figure, which illustrate the development of the flow pattern around a cylinder as a function of time[1]. The experiment has been carried out so that the fluid is set into motion from a resting condition. The velocity with which the cylinder is approached increases from top left to bottom right. As seems from the first photo, there is a symmetrical course of the streamlines during the initial phase (low flow velocity), and no boundary layer release occurs. In the second photo, however, we see that boundary layer begins to let go at the back of the cylinder, i.e. close to the back stagnation point. In the third photo, boundary layer release occurs sooner, i.e. in front of a point situated more upstream. In the rest of the photos, the formation of eddies in the wake of the cylinder can be seen clearly.

---

[1] In the pictures given in Figure 5.14, the streamlines are made visible by means of tracer particles.

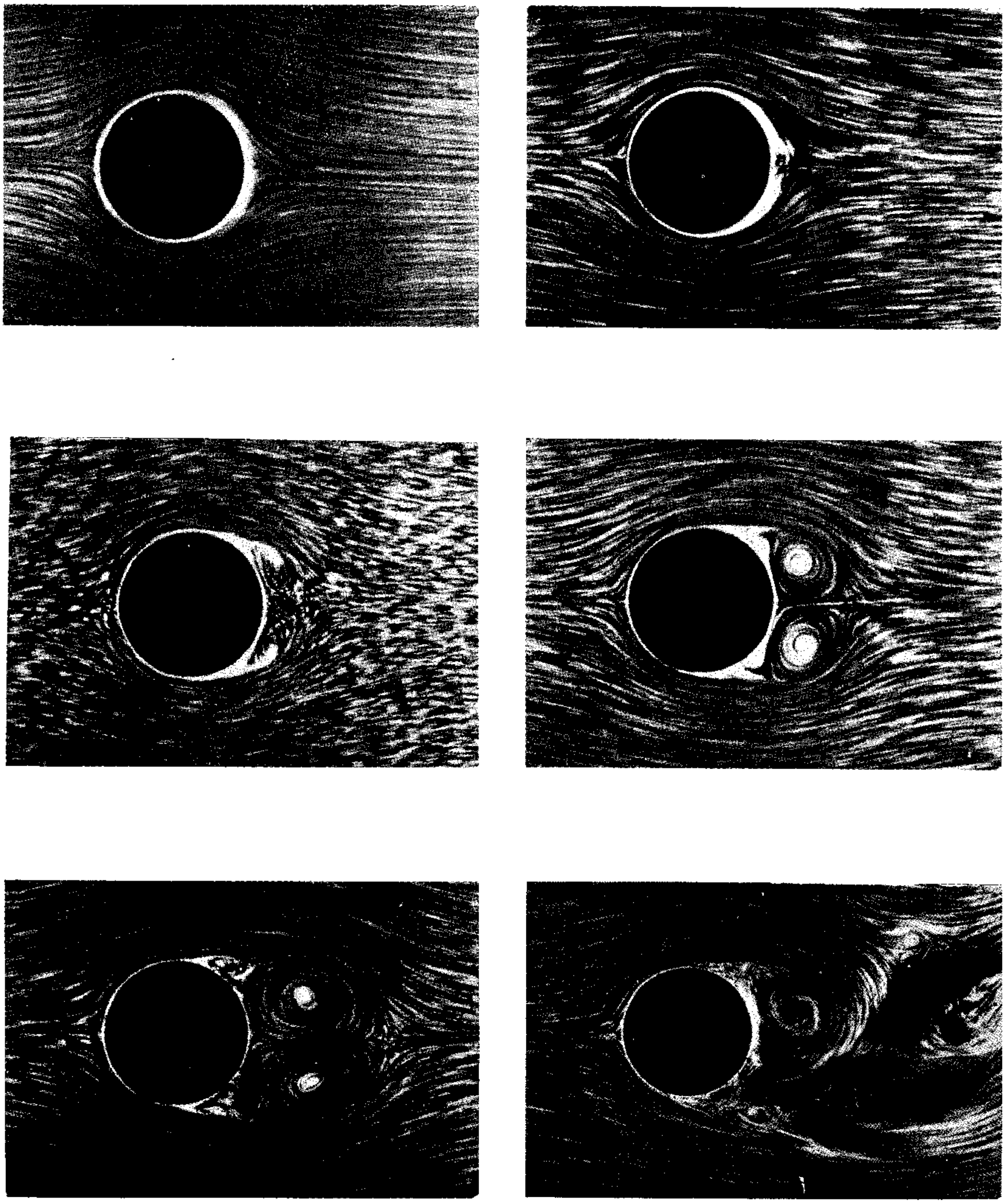

Fig. 5.14. Boundary layer release and formation of eddies behind cylinder.

An important (disadvantageous) result of the occurrence of boundary layer release and the formation of eddies connected therewith, is that the kinetic energy released through the geometry is partly dissipated and is therefore not available for the pressure increase any more. The net effect of this eddy dissipation is therefore a loss of pressure, i.e. a loss of mechanical energy. Through this, flow around objects have, apart from the already introduced friction drag, a so-called form drag. The form drag of flow around an object can be defined as the irreversible conversion of kinetic energy to internal energy as a result of eddy dissipation. The occurrence of boundary layer release and the form drag associated with it, is very much dependent on the shape of the object. As the shape change of the surface on the back side of a object occurs more gradually, the streamlines can adapt to the form more easily and boundary layer release will occur more slowly, which is advantageous for the friction factor of the object.

We will now still discuss the friction factors of the objects represented in the following figure: object A: a sphere with diameter D, object B: a drop with diameter D, object C: a sphere with diameter (1/2)D and object D: a round disc with diameter D.

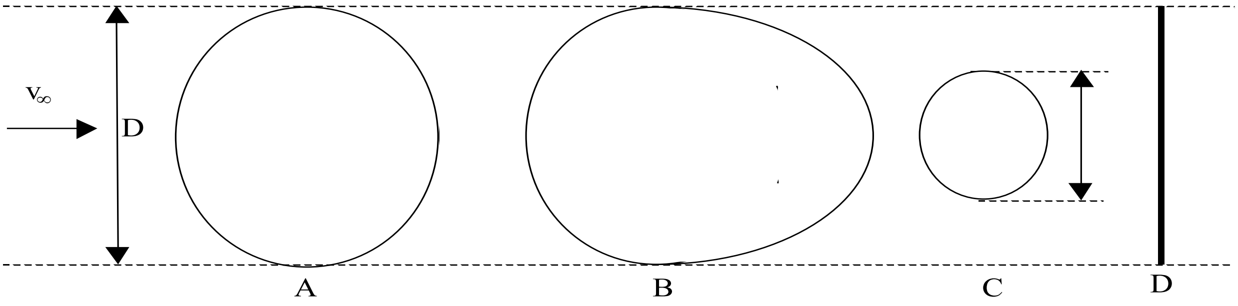

Fig. 5.15. flow around objects: A: a sphere with diameter D, B: a drop with diameter D, C: a sphere with diameter D/2 and D: a round disc with diameter D.

For low flow velocities, object A will have a lower friction factor than object B, because the friction drag, which is determining for low flow velocities, acts on a smaller surface. For high flow velocities, however, the situation is reversed and object A (despite the smaller wetting surface) has a higher friction factor than object B because the form drag of object A, which is determining for high flow velocities, is higher than that of object B. For very high flow velocities, object C (despite the smaller diameter) can have an even higher friction factor than object B. Object D has the highest form drag and, for sufficiently high flow velocities it is valid for the force F, which is exerted perpendicular to the plate, that:

$$F = \frac{1}{4}\pi D^2\left(\frac{1}{2}\rho v_\infty^2\right) \tag{5.41}$$

In the following chapter, we will look at the quantification of the friction factors of flow around cylinder and sphere more closely.

6 BERNOULLI'S LAW FOR FLOW WITH FRICTION; FRICTION FACTORS

We have already encountered Bernoulli's law for frictionless flow in chapter 4. We have subsequently analysed a few flow problems where friction is of secondary importance, on the basis of this law. However, in many process apparatus we are confronted with flow where friction plays an important role. This friction causes a loss of mechanical energy. There can also be exchange of work between the flowing medium and the process apparatus through which it flows. Here, the medium can basically both experience a net uptake (pump) or loss (turbine) of mechanical energy. It will be clear that, for a quantitative description of these processes, Bernoulli's law should be extended. This extended law of Bernoulli is of essential importance for the technical flow studies (pressure drop calculations) and will be discussed in the following paragraph.

6.1 Extended Law of Bernoulli

In Chapter 4, we have already encountered the law of Bernoulli for frictionless flow:

$$\Delta\left(\frac{1}{2}\frac{<v^3>}{<v>}\right)+\int_1^2\frac{dp}{\rho}+\Delta(gh)=0 \tag{6.1}$$

This equation is the expression of the rule of conservation of mechanical energy for steady-state (frictionless) flow: the change (Δ="2" − "1") of the sum of all forms of mechanical energy is zero, i.e. the sum of all forms of mechanical energy remains constant for the flow between two points "1" and "2" in the flow field. For the adaptation of (6.1) to the extended law of Bernoulli, we define:

e_f: the amount of mechanical energy lost per mass unit fluid between points "1" and "2" (J/kg).

a_u: the net amount of mechanical energy (work) supplied per mass unit between "1" and "2" (J/kg).

After modifying (6.1), the following expression for the macroscopic mechanical energy balance, i.e. the Bernoulli's law for flow with internal friction, results:

$$\Delta\left(\frac{1}{2}\frac{\langle v^3\rangle}{v}\right)+\int_1^2\frac{dp}{\rho}+\Delta(gh)=a_u-e_f \tag{6.2}$$

According to this law, the change (Δ= "2" − "1") of the sum of the different forms of mechanical energy (per mass unit) equals the work supplied between "1" and "2", minus the amount of mechanical energy (per mass unit) that is lost between "1" and "2". All terms in (6.2) have the dimension J/kg (amount of mechanical energy per mass unit). The quantity

a_u can be positive or negative. If $a_u>0$, net work is done on the fluid between "1" and "2". However, if $a_u<0$, net work is extracted from the fluid between "1" and "2". The quantity e_f is always positive for a Newtonian fluid$^{1)}$. We get an alternative formulation of (6.2), which is useful for pipes, by multiplying (6.2) with the mass flow Φ_m (kg/s):

$$\varphi_m\left(\frac{1}{2}\frac{\langle \mathrm{v}^3\rangle}{\mathrm{v}}-\frac{1}{2}\frac{\langle \mathrm{v}_1^3\rangle}{\langle \mathrm{v}_1\ \rangle}\right)+\int_1^2\frac{d\mathrm{p}}{\rho}+(gh_2-gh_1)=\varphi_m\left(a_u-e_f\right)\quad =A_u-E_f \qquad (6.3)$$

where the "Δ-formulation" has been worked out. The quantity A_u represents the net amount of work done on the fluid between "1" and "2":

$$A_u=\Phi_m a_u=(\rho<v>S)a_u \qquad (6.4a)$$

$$E_w=\Phi_m e_f=(\rho\ \langle \mathrm{v}\rangle\ S)\ e_f \qquad (6.4b)$$

In equation (6.3), the term e_f (or E_f) should be specified more closely in terms of the macroscopic system variables such as the average flow velocity <v>, which comes under discussion in the following paragraphs. As we do not have detailed information on the velocity profiles for such complex systems, the term e_f has to be determined empirically in these situations.

Concerning equation (6.3), we can summarise that it is valid for:

- **for laminar and turbulent flow,**
- **for a macroscopic system,**
- **for non-ideal fluids,**
- **for compressible fluids,**
- **situations where net work is done on or by the fluid.**

6.2 Friction factors

In the previous chapters, we concentrated on the analysis of relatively simple flow problems. As described in Chapter 3, we can basically describe all laminar single-phase flows with the Navier-Stokes equations. If these equations can be solved under the specification of "suitable" conditions (analytical or numerical), the flow friction can be calculated on the basis of the calculated pressure and velocity profiles. In Chapter 3, we have seen a few examples of this, such as the tubular pipe and the flow in an annular space. An analogous method is possible for turbulent single-phase flow, on the understanding that (approximate) semi-empirical models are needed.

---

1) For proof you are referred to the book "Transport Phenomena" by R.B. Bird, W.E. Stewart and E.N. Lightfoot.

In practice, we are often confronted with turbulent flows in systems with very complex geometry, so that, even with the very advanced computer models available nowadays, it becomes practically impossible to calculate the detailed pattern of the pressure and velocity. As we can then also not calculate the flow resistance, we will have to call on experimental data for the quantification of the flow resistance of these systems. In order to be able to use the experimental data efficiently, we will handle "correlations" that describe geometrically similar systems in terms of a number of characteristic dimensionless quantities.

Regarding the geometry, it can be noted that in very complex systems in practice, we only encounter two types of flow situations: flow through pipes and flow around objects. Here "pipes" should be interpreted widely. Examples of this category are: flow through a tube, flow through a rectangular canal that is open at he top, and flow through a filter. Examples of flow around objects are: flow around an aeroplane, flow around a bundle of pipes of a heat exchanger, and flow around a particle in a packed bed. For flow through pipes, one is often interested in the relation between the pressure drop over the pipe and the resulting volume flow. For flow around objects, one is only interested in the relation between the velocity with which the object is approached by a specific fluid and the force that the object experiences as a result. For both pipes and flow around objects, a flow resistance manifests itself in the form of an occurring pressure drop Δp. This pressure drop (loss of an amount of mechanical energy per volume unit) corresponds to the term ρe_w from the macroscopic mechanical energy balance (equation (6.3))$^{1)}$.

However, pressure change in flowing systems can have several causes. Apart from friction, a velocity change, a height change or supplied or removed work can cause pressure changes. The pressure change mentioned here is, however, determined completely by the flow resistance. Regarding flow resistance, we can differentiate between the following types: friction drag and form drag. For pipes with a constant diameter, flow resistance is determined completely by the friction drag, while for flow around obstacles, both friction drag and form drag generally play a role.

6.2.1 Friction factors for flow around objects

A force F, of which the resultant F is in the same direction as the flow velocity v_∞ is exerted by the fluid on the surface when the fluid flow around the object. The force F, which is experienced by the object, is expressed (for the whole Re-area) as a product of the characteristic surface A, the kinetic energy per volume unit of the approaching fluid and a dimensionless quantity C_D, the so-called drag coefficient:

---

1) We can write all terms in equation (6.3) as the product of the volume stream $\Phi_v(m^3/s)$ and a quantity that has the dimension of an amount of energy per volume unit (J/m^3)($\Phi_m e_w = \Phi_v(\rho e_w)$).

$$F = C_D A \left(\frac{1}{2}\rho v_\infty^2\right) \qquad (6.5)$$

The drag coefficient C_w is dependent on the geometry and the flow conditions (Re-number). It generally has to be determined on the basis of experimental data. We will subsequently give the Re-dependency of C_w[1)] for flow along a flat plate and flow around a cylinder and a sphere.

Flow along a flat plate:

For flow along a flat plate approached on both sides by laminar flow, it is valid for the force F exerted on the plate in the flow direction that:

$$F = 1.328(Re_L)^{-0.5}(2BL)\left(\frac{1}{2}\rho v_\infty^2\right) \qquad (6.6a)$$

The surface 2BL is taken as characteristic surface for the flat plate, so that, after comparison with the general expression (6.5), we can conclude that it is valid for the drag coefficient C_w that:

$$C_D = 1.328(Re_L)^{-0.5} \qquad (6.6b)$$

In the case of a flow along a flat plate on both sides, where the laminar beginning plays a secondary role, it is valid for the force F, exerted on the plate in the flow direction, that:

$$F = 0.074(\mathrm{Re}_L)^{-0.2}(2BL)\frac{1}{2}\rho v_\infty^2 \qquad (6.7a)$$

Comparison of (6.7a) to (6.5) gives, with the choice A=2BL, the following expression for C_D in the turbulent flow regime:

$$C_D = 0.074(Re_L)^{-0.2} \qquad (6.7b)$$

Comparison of (6.6b) to (6.7b) shows that the drag coefficient C_D is less strongly dependent on the Reynolds number Re_L in the turbulent flow regime than in the laminar flow regime. If both the laminar beginning and the turbulent end are of importance for the force action on the plate, it is valid for C_D that (check this for yourself!):

$$C_D = 1.328(Re_c)^{-0.5}\left(\frac{x_c}{L}\right) + 0.074\left\{(Re_L)^{-0.2} - (Re_L)^{-0.2}\left(\frac{x_c}{L}\right)\right\} \qquad (6.8)$$

The term (x_c/L) gives the length of the laminar beginning with regard to the total length of the plate. If this term is very small, (6.8) reduces to (6.7b) according to our expectations.

[1)] The correlations for C_D presented here are valid for non-compressible fluids. If the approaching fluid is compressible, Re is also, apart from C_D dependent on the Mach-number M. The Mach-number is defined as the relation between the flow velocity v_∞ and the sound velocity c: $M=v_\infty/c$. It seems that the effect of compressibility becomes of importance at $M \approx 0.3$.

Flow around a cylinder:

For perpendicularly flow around a cylinder, the surface projected in the flow direction is taken for the characteristic surface A: A=DL. In the following figure, the drag coefficient C_D for the perpendicularly approached cylinder is given as function of the Reynolds number.

From this figure, it seems that C_D is inversely proportional to Re for low Re-values, while C_D reaches a more or less constant value for high values of Re. Note that the value of C_D suddenly decreases for Re≈5.10^5. This phenomenon, which also occurs at flow around a sphere (in this case Re≈3.10^5), is connected with the change of a laminar boundary layer into a turbulent boundary layer before boundary layer release occurs. As a result of this change, boundary layer release occurs more at the back of the cylinder (sphere) and the form drag, and thus C_D, decreases.

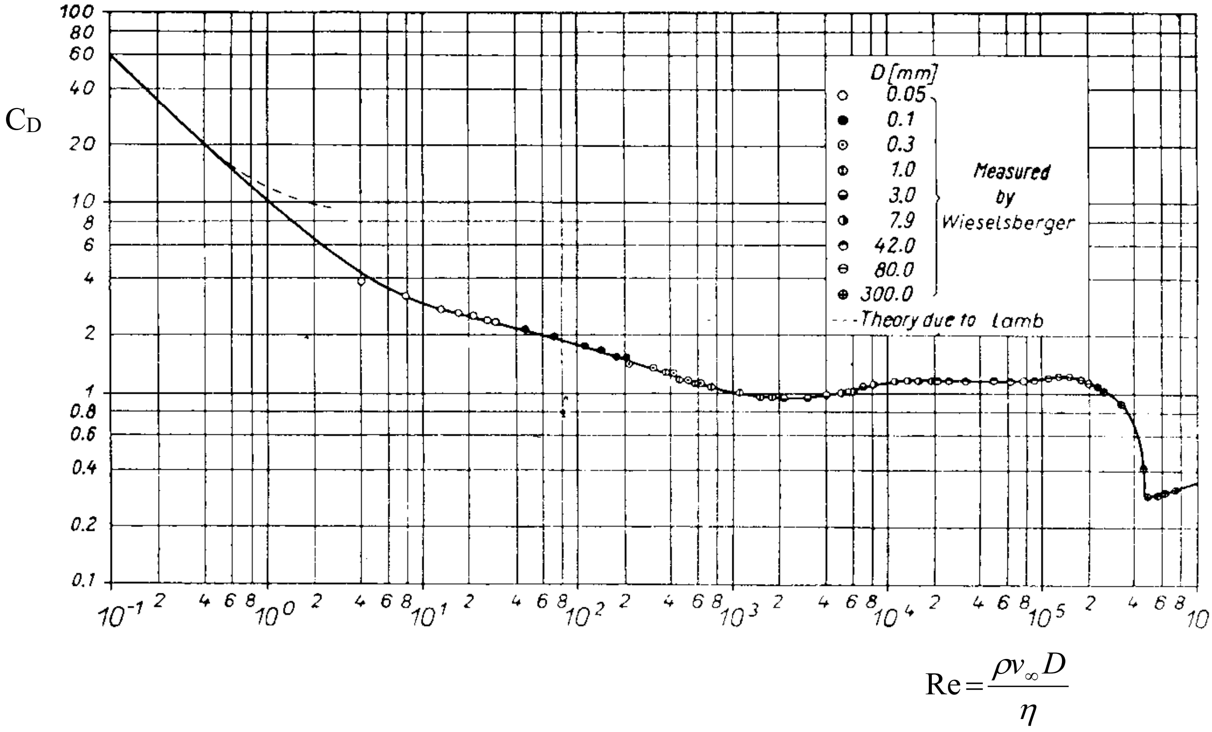

Fig. 6.1. The drag coefficient C_D as a function of the Reynolds number Re for perpendicular flow around a cylinder.

Flow around a sphere:

For flow around a sphere, the surface projected in the flow direction is taken as the characteristic surface: A=(1/4)πD^2. In the creeping flow regime, it is valid (according to the law of Stokes) for the force F, exerted on the sphere, that:

$$F = 3\pi\eta v_\infty D \tag{6.9a}$$

Comparison of (6.9a) to (6.5) gives the following expression for the drag coefficient C_D in the creeping flow regime (Re<0.1):

$$C_D = \frac{24}{\text{Re}} \tag{6.9b}$$

An often used empirical correlation, which, in contrast to (6.9b), is valid for the whole Reynolds range, reads[1]:

$$C_D = \frac{24}{\text{Re}}\left(1 + 0.15(\text{Re})^{0.687}\right) \quad \text{if: Re<1000} \tag{6.9c}$$

$$C_D = 0.44 \quad \text{if: Re}\geq 1000 \tag{6.9d}$$

Note that (6.9c) reduces to (6.9b) for low Re-values. In Fig. 6.2, C_D is given graphically as a function of Re.

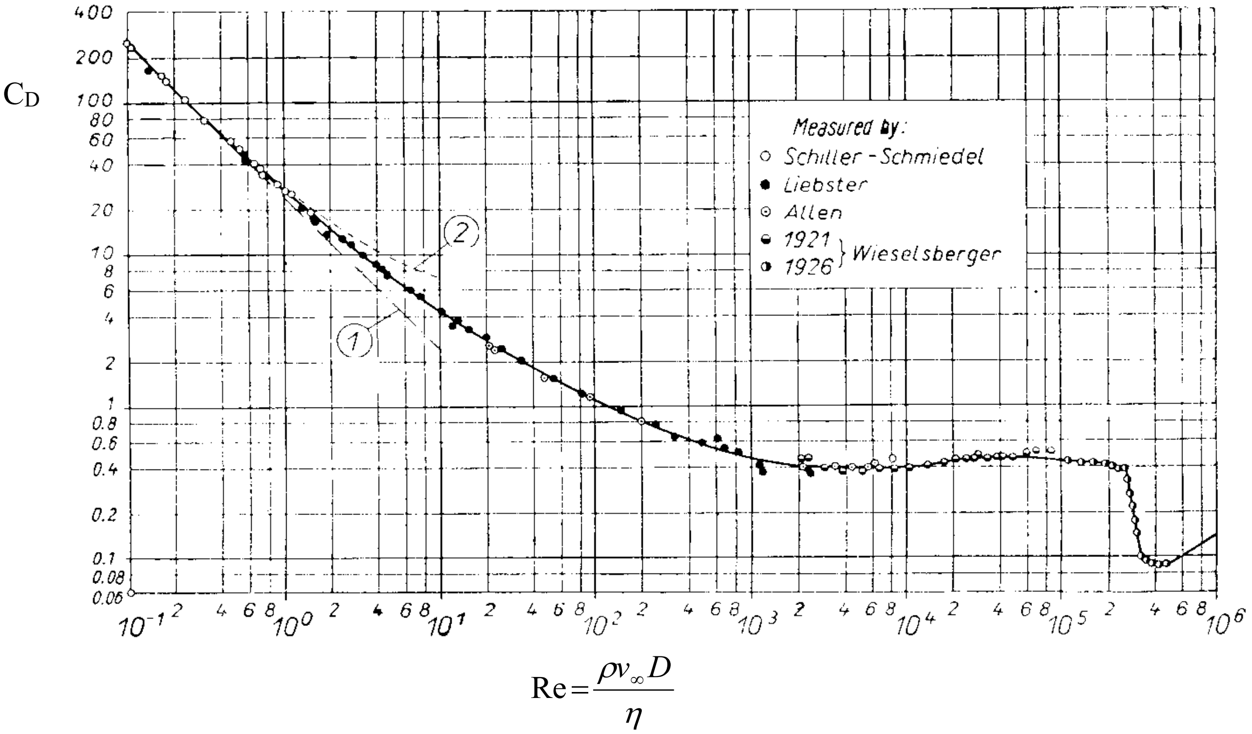

Fig. 6.2. Drag coefficient C_D as function of the Reynolds number Re for a submerged sphere.

The values of C_D and the dependence on Re are of special importance for the description of the movement of particles in a fluid, and will be examined more closely here on the basis of free falling spherical particles. We consider a spherical particle with diameter d_p, falling in the steady-state (in the positive z-direction) in a fluid (gas or liquid) with the velocity difference v_p. This velocity is measured according to a non-moving co-ordinate system where the z-co-ordinate shows in the direction of v_p. According to the second law of Newton, it is valid that:

---

[1] If Re>3.10^5, the laminar boundary layer changes to a turbulent boundary layer and C_D ("suddenly") takes on a considerably lower value (see Fig. 6.2).

$$m_p \frac{dv_p}{dt} = \sum F = F_z - F_o - F_w \tag{6.10}$$

where m_p is the mass of the sphere. In the right hand side of (6.10) the sum of the forces acting on the particle is given. Gravity F_z, the upward force F_o and the force as a result of friction F_w act on the sphere. Gravity is in the direction of v_p, while the upward force and the friction force are in the opposite direction. Substitution of all the forces in (6.10) gives:

$$\frac{1}{6}\pi d_p^3 \rho_p \frac{dv_p}{dt} = \frac{1}{6}\pi d_p^3 (\rho_p - \rho_f) g - C_D \left(\frac{1}{4}\pi d_p^2\right) \left(\frac{1}{2}\rho_f v_p^2\right) \tag{6.11}$$

In (6.11), ρ_p is the density of the particle and ρ_f the density of the fluid. For a steady-state falling sphere (falling at its terminal velocity), $dv_p/dt=0$, so that the general equation of motion for the sphere reduces to:

$$\frac{1}{6}\pi d_p^3 (\rho_p - \rho_f) g = C_D \left(\frac{1}{4}\pi d_p^2\right) \left(\frac{1}{2}\rho_f v_p^2\right) \tag{6.12}$$

In the above equation, C_D is dependent on the Reynolds number and thereby dependent on the velocity v_p. We will subsequently discuss two limit cases of (6.12), whereby an analytical expression for the velocity difference can be obtained.

Limit case a): The law of Stokes is valid ($Re<0.1$):
If Re ($=\rho_f v_p d_p/\eta$) is smaller than 0.1, equation (6.9b) is valid for C_D. Substitution of (6.9b) into (6.12) gives, after calculation:

$$v_p = \frac{(\rho_p - \rho_f) g d_p^2}{18\eta} \tag{6.13}$$

After calculation of v_p, we should naturally check whether the condition $Re<0.1$ was indeed complied with. It can qualitatively be stated that this situation occurs for "small' values of the particle diameter d_p and for "high" values of the dynamic viscosity η of the fluid.

Limit case b): C_D is a constant: C_D =0.44 (10^3<Re<10^5):
If 10^3<Re<$10^{5,}$ valid by good approximation that C_D=0.44. If C_D is a (known) constant, (6.12) can be written as:

$$v_p=\sqrt{\frac{4d_p(\rho_p-\rho_f)g}{3C_D\rho_f}} \tag{6.14}$$

After calculation of the velocity difference v_p, we will here also have to check whether the condition 10^3<Re<10^5 was indeed complied with.

In the Reynolds range 1<Re<1000, the velocity difference can be determined graphically. For this, equation (6.12) is rewritten in the following dimensionless form:

$$C_D Re^2=\frac{8}{6}\frac{\rho_f\left(\rho_p-\rho_f\right)g\,d_p^3}{\eta^2}=\frac{8}{6}Ar \tag{6.15}$$

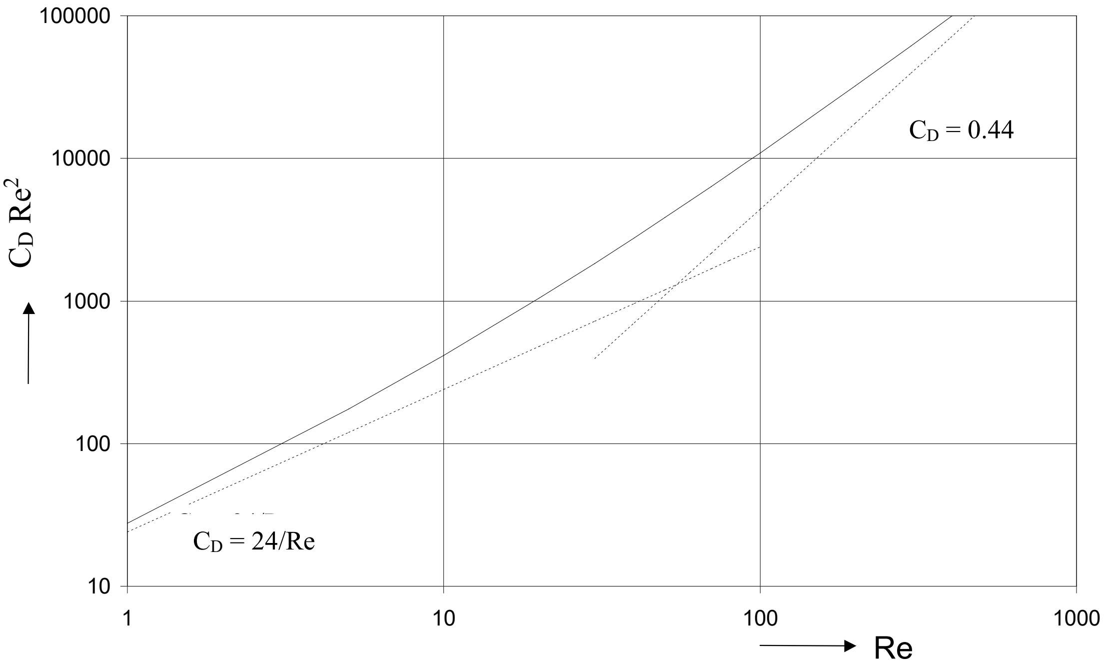

Fig. 6.3. The quantity C_DRe^2=(8/6)Ar as a function of the Re-number for spherical particles. The discussed limit situations are also given in this figure

Here Ar is the (dimensionless) number of Archimedes. The right hand side of (6.15) is a known quantity for a given fluid-particles-system. By means of the following figure, the value of Re and therewith the value of v_p can be determined by calculation C_DRe^2=(8/6)Ar. For more clarity, the discussed limit cases are also given in figure 6.3.

As a conclusion of this paragraph, we will still concentrate on the quantification of the amount of mechanical energy per time unit being changed into internal energy for a submerged object. We thus actually consider the term $\Phi_m e_w=E_f$ from the macroscopic energy balance. The amount of mechanical energy dissipated per time unit E_f is equal to the product of the force F, which is exerted on the object and the distance v_∞ travelled by the fluid per time unit:

$$E_f = \Phi_m e_f = F v_\infty = C_D A \left(\frac{1}{2}\rho v_\infty^3\right) \tag{6.16}$$

If the value of the drag coefficient is known, the value of E_w can be calculated by means of (6.16). On the other hand, in certain situations, such as for flow around a sphere in the creeping flow regime, the term E_w can be calculated analytically. The force F, which the fluid exerts on the object, can then be determined by means of (6.16) from the amount of mechanical energy dissipated per time unit.

6.2.2 Friction factors for tubular pipes

For a pipe, the fluid will exert a force F on the wetted surface (the inside wall of the pipe), of which the resultant F shows in the same direction as the average velocity <v>. Analogous to flow around objects, F (for the complete Re-range) is expressed as the product of a characteristic surface A, the average kinetic energy per volume unit of the fluid flowing through the pipe and a dimensionless quantity f, the so-called friction coefficient:

$$F = fA\left(\frac{1}{2}\rho < v >^2\right) \tag{6.17}$$

For flow through systems, we take the wetted surface as the characteristic surface A. The friction coefficient f is dependent on the geometry of the tube and the flow conditions (Re-number) and must generally be determined on the basis of experimental data. For flow through systems, we are often interested in the relation between the pressure drop over the tube Δp and the resulting average flow velocity <v>. It is therefore suitable to express the force F, exerted on the wetted surface, in pressure drop Δp in the definition equation of the friction coefficient f.

We therefore consider the steady-state flow of a fluid through a tube with length L. The surface S of the tube is constant and the wetted circumference amounts to Z (see Fig. 6.4). According to an integral or macroscopic momentum balance for the control volume V=SL, it is valid in steady-state condition that:

$$0 = \sum F = p_0 S - p_L S - \tau_w Z L = (\Delta p) S - F \tag{6.18}$$

Here τ_w is the average shear stress over the wetted surface (=Z.L), which the fluid exerts on the surface. The force F, exerted on the wetted surface is a product of τ_w and (Z.L). After combination of (6.17) and (6.18), the following equation results, known as the equation of Fanning:

$$\Delta p = f\left(\frac{ZL}{S}\right)\left(\frac{1}{2}\rho < v >^2\right) = 4f\left(\frac{ZL}{4S}\right)\left(\frac{1}{2}\rho < v >^2\right) \tag{6.19}$$

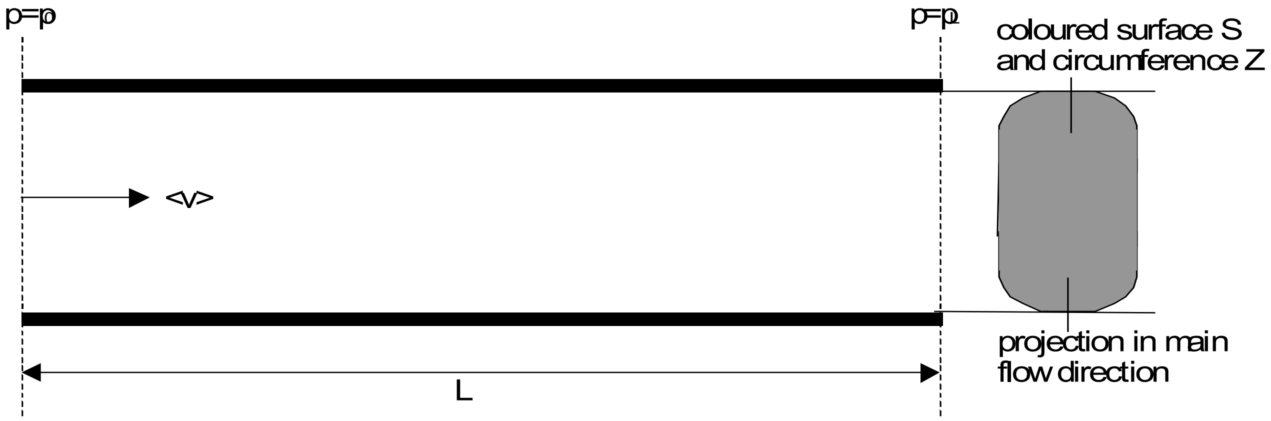

Fig. 6.4. Flow through a tube with constant diameter S, wetted surface Z and length L.

The quantity (4S/Z) is called the hydraulic diameter d_h, which, by addition of the factor 4 to equation (6.19), equals the tube diameter D for the round, tubular conduit:

$$d_h = \frac{4S}{Z} = 4\frac{\textit{surface through which the fluid flows}}{\textit{wetted circumference}} = 4\ \frac{\frac{1}{4}\pi D^2}{\pi D} = D \quad \text{(for a round tube)} \tag{6.20}$$

By means of the hydraulic diameter d_h, we can write the equation of Fanning as:

$$\Delta p = 4f\frac{L}{d_h}\left(\frac{1}{2}\rho < v >^2\right) \tag{6.21}$$

As we have not made any assumption concerning the geometry of the surface S for the derivation of the equation of Fanning, (6.21) is valid for a tube with an arbitrary diameter. In the following figure (figure 6.5), the definition of the hydraulic diameter is given for a number of flow situations. The friction coefficient f is dependent on the geometry and the flow conditions (Re-number) and must generally be determined on the basis of experimental data. However, in the laminar flow regime, an analytical expression can be obtained for f on the basis of the Hagen-Poiseuille equation derived in Chapter 3. For the relation between the pressure drop $\Delta p = p_0 - p_L$ and the average velocity <v>, it is then valid (Re<2000):

$$\Delta p = \frac{32\eta < v > L}{D^2} \tag{6.22}$$

Comparison of (6.22) to (6.21) gives, with $d_h = D$, the following expression for the friction coefficient f in the laminar flow regime (Re<2000):

$$4f = \frac{64}{\text{Re}} \tag{6.23}$$

In the turbulent flow regime, the empirical relation of Blasius is valid for f for smooth streamed through tubes:

$$4f = 0.316(\text{Re})^{-0.25} \qquad \text{for:} \quad 4.10^3 < \text{Re} < 10^5 \tag{6.24}$$

Note that in the turbulent flow regime for $4.10^3<Re<10^5$, the pressure drop Δp is proportional to $\langle v\rangle^{1.75}$, while Δp is proportional to <v> in the laminar flow regime. For pressure drop calculation in practice one frequently uses graphs giving f as function of the Re-number (see Fig. 6.6).

Flow situation		Hydraulic diameter $D_A = 4A / S$	A
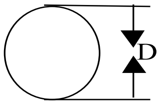	Circular pipe	D	$\frac{\pi}{4}D^2$
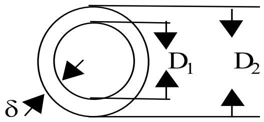	Concentric pipe or	D_2-D_1=2δ	$\frac{\pi}{4}\left(D_2^2-D_1^2\right)$
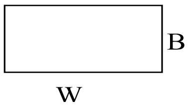	Rectangular pipe	$\frac{2WB}{W+B}$	WB
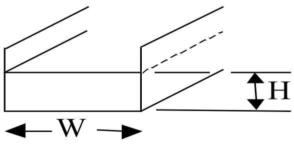	Open channel	$\frac{4WH}{W+2H}$	WH
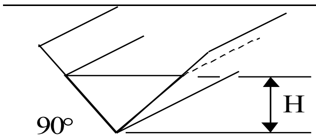	Open channel	$\frac{2H}{\sqrt{2}}$	H^2
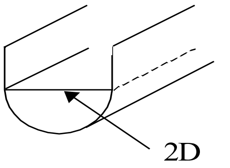	Half-filled	D	$\frac{\pi}{8}D^2$
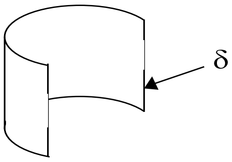	Liquid film	4δ	$\delta\pi D$

Hydraulic diameter of various channels

Fig. 6.5. The hydraulic diameter d_h for a number of flow situations.

Through the introduction of the hydraulic diameter, this graph is also applicable for flow through pipes and channels that have a different geometry than the streamed through round tube (see Fig. 6.5). Here one uses the hydraulic diameter d_h instead of the tube diameter D for the characteristic length measure in the Re-number:

$$\mathrm{Re} = \frac{\rho < v > d_h}{\eta} = \frac{< v > d_h}{\nu} \tag{6.25}$$

This approximation is only well valid for strong turbulent flow, i.e. for high Re-values. In Fig. 6.6, a number of (dashed) lines for tubes with rough inside walls are given next to the line for smooth tubes in the turbulent range. It follows from this figure that, for rough pipes, the friction coefficient f is dependent on Re and on the dimensionless quantity x/d_h. The quantity x is the average roughness of the inside tube surface. From Fig. 6.6 it seems that the roughness of the wall results in an increase of f and thus an increase in the pressure drop. Apart from this, for a specific value of x/d_h, the influence thereof on f, regarding the smooth wall, increases by Re up to an Re-number where the curves will run parallel to the horizontal axis.

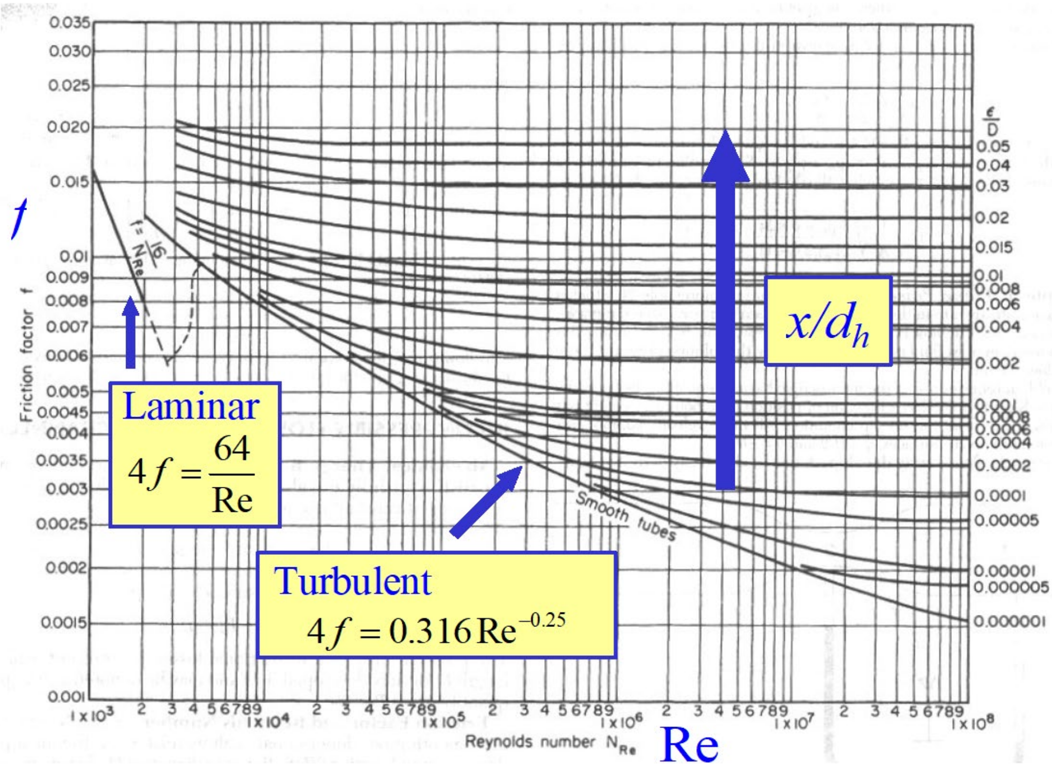

Fig. 6.6. The friction factor f as function of the Re-number. The parameter x/d_h represents the relative roughness of the tube wall.

This behaviour can be explained as follows. For "low" Re-values, the thickness of the viscous sub-layer is larger than the average roughness of the tube surface, so that the roughness does not stick through the sub-layer. In this situation, the effect of the roughness is limited to an increase of the wetted surface, so that f is (slightly) higher compared to a smooth-walled tube. If the flow becomes stronger turbulent, the thickness of the viscous sub-layer decreases so that the roughness partially protrudes through the viscous sub-layer. We then actually have an “obstacle” placed partially in the turbulent bulk of the flow. For sufficiently high Re-numbers, the friction factor of an obstacle is completely determined by the form drag, and is then purely proportional to (1/2)ρ<v>, and not dependent on Re any more. As the roughness increases, this situation occurs more readily and f takes on a constant value for lower Re-values.

The pressure drop Δp, according to equation (6.21), actually represents the amount of mechanical energy converted to internal energy per volume unit, so that we can write the following for the term $\Phi_m e_f = E_f$ in the macroscopic energy balance (equation (6.3)):

$$E_f = \Phi_m e_f = \Phi_\mathrm{v} \rho e_f = \Phi_\mathrm{v} (\Delta p)_{friction} = \Phi_\mathrm{v} \left(4f \, \frac{L}{d_h} \left(\frac{1}{2} \rho \langle \mathrm{v} \rangle^2 \right) \right) \qquad (6.26)$$

From the above equation then follows for the amount of mechanical energy being converted to internal energy (=e_f) per mass unit:

$$e_f = 4f \, \frac{L}{d_h} \left(\frac{1}{2} \rho \langle \mathrm{v} \rangle^2 \right) \quad \text{(J/kg)} \qquad (6.27)$$

Up to now we have limited ourselves in this paragraph to flow through tubes or pipes. In practice, we often encounter systems where, apart from straight parts, bends, turns, constrictions or widenings, stop-valves etc. occur, which cause extra flow resistance. The friction factor for high Re-values, which we are often confronted with in practice, is especially determined by the form drag, so that occurring pressure drop can be written as:

$$\Delta p = k_f \left(\frac{1}{2} \rho \langle \mathrm{v} \rangle^2 \right) \qquad e_f = k_f \left(\frac{1}{2} \langle \mathrm{v} \rangle^2 \right) \qquad (6.28)$$

Here k_f is a resistance coefficient that should be determined empirically (pressure drop measurement). Fig. 6.7. gives an overview of k_f-values for a number of different pieces of equipment. With the use of k_f-values, one should always check which (average) velocity is involved. It makes a difference for constrictions and widenings, and therefore one should mention the velocity to be used when giving k_f-values.

Naturally, we can also give the friction factor in the form of equation (6.28). Check for yourself that, for flow through a tube, the relation between the resistance coefficient k_f and the (more up to date) friction coefficient f is given by:

$$k_f = 4f \, \frac{L}{d_h} \qquad (6.29)$$

For a complete piping system, consisting of N straight pieces and M other types of equipment, it is valid for the total mechanical energy converted to internal energy per mass unit, that:

$$e_f = \sum_{i=1}^{i=N} 4f_i \, \frac{L_i}{(d_h)_i} \left(\frac{1}{2} \langle \mathrm{v} \rangle^2 \right) + \sum_{j=1}^{j=M} \left(k_f \right)_j \left(\frac{1}{2} \langle \mathrm{v} \rangle^2 \right) \text{(J/kg)} \qquad (6.30)$$

	Re					
Flow situation	50	100	200	400	1000	Turbulent
Diameter change:*)						0.05
Entering pipe, rounded						0.5
ditto, not rounded						
sudden constriction						0.45(1-m)
sudden widening						(1/m-1)(1/m-1)
measuring disk						2.7(1-m)(1-m^2)
Elbows:						
180° short						1.7-2.2
180° long						1.2
90° short						0.7-0.9
90° half-long	17	7	2.5	1.2	0.85	0.6-0.8
90° long						0.4-0.6
90° sharp corner						1.3-1.9
45°						0.3-0.4
T-connection	9	4.8	3.0	2.0	1.4	1.0
Throttle-valves:						
Spherical throttle-valve open	28	22	17	14	10	6-10
ditto, half-open						9.5
Sliding throttle valve open						1.17
ditto, half-open						4.5
Controlling throttle valve	55	17	9	5.8	3.2	2.0
ditto, with needle						to 70
Water meter						6-12
Cyclone						10-20

*) Regarding velocity below stream; m= diameter ratio (<1).

Fig. 6.7. Overview of k_f-values involved with the average in-flow velocity for systems with diameter changes, bends, throttle valves and other fittings. For a number of systems the Re-dependency is given.

6.2.3 Friction factors of packed beds

At the end of this chapter, we will look at the quantification of the friction factor in beds of solid particles (so-called packed or fixed beds). These systems are frequently used in the physical and chemical technology if a fluid (gas or liquid) has to be brought in contact with a (finely distributed) solid. The fluid and solid can undergo both a physical and chemical process. One can think of drying and coating as physical processes, while heterogeneously catalysed reactions are examples of chemical processes. In this last category of processes, one or more components present in the fluid are converted on the surface of the solid particles.

Beds with solid particles can roughly be divided into packed beds and fluidised beds. Both types of bed consist of a tube with a separator for the fluid. Above the separator is the bed with solid particles that are in a resting phase for a packed bed. In a fluid column, however, movement of the bed particles occurs because of the bubbles that are present. The system would therefore behave like a boiling "liquid" in many regards.

We will limit ourselves to the quantification of the friction factor of packed beds for which the following two approaches are possible:

A) The packed bed is regarded as a collection of particles whereby the friction factor is described on the basis of the friction factors of the individual particles.
B) The packed bed is regarded as a collection of "tubes" whereby the friction factor is described on the basis of the friction factors of the individual tubes.

We will follow approach B. For the quantification of the friction factor of packed beds, we will first define two quantities by which the packed bed can be characterised. These are the porosity ε of the packed bed and the specific surface a of the packing material.

- the porosity or volume fraction fluid (void fraction) of the packed bed:

$$\varepsilon = \frac{\text{volume between bed particles (m}^3\text{)}}{\text{volume of the bed (m}^3\text{)}} \quad (\text{-}) \qquad (6.31)$$

- the specific surface of the bed material:

$$a = \frac{\text{Surface of the particles (m}^2\text{)}}{\text{Volume of the bed (m}^3\text{)}} \quad (\text{m}^{-1}) \qquad (6.32)$$

According to the equation of Fanning, the following is valid for the pressure drop Δp over a straight tube with (hydraulic) diameter d_h and length L:

$$\Delta p = 4f\frac{L}{d_h}\left(\frac{1}{2}\rho < v >^2\right) \qquad (6.33)$$

It will be clear that equation (6.33) is not applicable as it is for the description of the pressure drop Δp over a packed bed, as the hydraulic diameter and the length of the "tubes" are basically still unknown. It is valid for the hydraulic diameter d_h that:

$$d_h = 4 \frac{\text{area of all tubes through which the fluid flows}}{\text{wetted circumference of all tubes}} \tag{6.34}$$

If we multiply the numerator and denominator in (6.34) by the average length of the tubes L_b, we get:

$$d_h = 4 \frac{\text{streamed through volume of all tubes}}{\text{wetted surface of all tubes}} = 4 \frac{\varepsilon}{a} \tag{6.35}$$

In equation (6.33), the pressure drop is expressed in terms of the average velocity <v>. For packed beds, however, one preferably uses the superficial velocity v_0, which is related to <v> as follows:

$$v_0 = \varepsilon < v > \tag{6.36}$$

The superficial velocity v_0 equals the quotient of the volume debit Φ_v, supplied to the bed and the total surface A of the tube in which the bed is located and through which the fluid flows ($v_0=\Phi_v/A$). The superficial velocity v_0 is actually the average flow velocity of the empty tube and is therefore also called the "empty tube velocity". Combination of (6.35) and (6.36) with (6.33) gives the following expression for the pressure drop Δp:

$$\Delta p = f \frac{aL_b}{\varepsilon^3} \frac{1}{2} \rho v_0^2 \tag{6.37}$$

where L is substituted by L_b. In equation (6.37), L_b represents the average length of the tubes, which is naturally bigger than the length L of the packed bed. In relation to practical considerations, the length of the packed bed is taken for L_b (L_b=L), which in fact leads to a correction of the friction coefficient (f). As f should be obtained empirically, the relevant correction factor can be accommodated in f. Analogous to the flow through a tube, the friction coefficient for the packed bed is dependent on the flow regime, which we will now consider more closely.

A) Laminar flow:

For laminar flow conditions, f will be inversely proportional to the Re-number:

$$f \approx \frac{1}{\mathrm{Re}} = \frac{\nu}{< v > d_h} = \frac{\nu}{\frac{v_0}{\varepsilon} 4 \frac{\varepsilon}{a}} = \frac{\nu a}{4 v_0} \tag{6.38}$$

Substitution of this proportion relation for f into equation (6.37) then gives the following for the pressure drop Δp in the laminar flow regime:

$$\Delta p = C_{la\min ar} \frac{a^2}{\varepsilon^3} \eta v_0 L \tag{6.39}$$

with $C_{laminar}$ being a proportion constant that should be determined empirically. On the basis of analysis of a great number of measurements, it seemed that the value $C_{laminar} \approx 25/6$ best corresponds with experimental data.

B) Turbulent flow

For turbulent flow conditions, f is independent of the Re-number, so that it is valid for the pressure drop Δp in the turbulent flow regime that:

$$\Delta p = C_{turbulent} \frac{aL}{\varepsilon^3} \rho v_0^2 \tag{6.40}$$

with $C_{turbulent}$ a proportion constant to be determined empirically. Here the value $C_{turbulent} \approx 7/24$ corresponds best with experimental data.

The equation that describes the pressure drop of a packed bed in both the laminar and turbulent flow regimes, is now simply obtained by adding (6.39) and (6.40) together:

$$\Delta p = \frac{25}{6} \frac{a^2}{\varepsilon^3} \eta v_0 L + \frac{7}{24} \frac{aL}{\varepsilon^3} \rho v_0^2 \tag{6.41}$$

The resulting equation is called the Ergun equation, which is of great importance for the pressure drop calculation for packed beds. In this equation, the specific particle surface a can also be expressed in a number of quantities that can be determined experimentally. For the situation where the bed consists of spherical particles with a uniform particle diameter d_p, we will calculate it more closely. In this situation it is valid that:

$$n\left(\frac{1}{6}\pi d_p^3\right) = 1 - \varepsilon \tag{6.42a}$$

$$n\left(\pi d_p^2\right) = a \tag{6.42b}$$

with n the number of particles per volume unit (“particle concentration”). Elimination of n from (6.42a) and (6.42b) gives the following expression for the specific surface a:

$$a = \frac{6(1-\varepsilon)}{d_p} \tag{6.43}$$

Substitution of (6.43) into (6.41) gives the following alternative expression for the Ergun equation, which gives the pressure drop per length unit.

$$\frac{\Delta p}{L} = 150\frac{(1-\varepsilon)^2}{\varepsilon^3}\frac{\eta v_0}{d_p^2} + 1.75\frac{(1-\varepsilon)}{\varepsilon^3}\frac{\rho v_0^2}{d_p} \tag{6.44}$$

The first term in equation (6.44) represents the laminar friction factor, which is dominant at low flow velocities and/or for small bed particles. If the first term in (6.44) completely dominates, the Ergun equation reduces to the Blake-Kozeny equation:

$$\frac{\Delta p}{L} = 150\frac{(1-\varepsilon)^2}{\varepsilon^3}\frac{\eta v_0}{d_p^2} \tag{6.45}$$

which is valid in the laminar flow regime, i.e. if $(G_0 d_p/\eta)(1/(1-\varepsilon))<10$. The quantity G_0 is the mass flux for the empty tube: G_0=⍰v_0 with dimension kg/(m^2.s).

The second term in equation (6.44) represents the turbulent friction factor, which is dominant at high flow velocities and/or for large bed particles. If the second term in (6.44) completely dominates, the Ergun equation reduces to the Burke-Plummer equation:

$$\frac{\Delta P}{L} = 1.75\frac{(1-\varepsilon)}{\varepsilon^3}\frac{\rho v_0^2}{d_p} \tag{6.46}$$

which is valid in the turbulent flow regime, i.e. if $(G_0 d_p/\eta)(1/(1-\varepsilon))>1000$.

As stated, the Ergun equation is valid for both the laminar and turbulent flow regimes. The Ergun equation can also be written in the following dimensionless form, which is given together with the dimensionless Blake-Kozeny and Burke-Plummer in Fig. 6.8.:

$$\frac{(\Delta p)\rho}{G_0^2}\left(\frac{d_p}{L}\right)\left(\frac{\varepsilon^3}{1-\varepsilon}\right) = 150\frac{(1-\varepsilon)}{(G_0 d_p/\eta)} + 1.75 \tag{6.47}$$

If the Ergun equation is applied for gases, the density ρ should be evaluated at $(p_0+p_L)/2$, where p_0 and p_L are the pressures at the entrance and exit of the packed bed, respectively. If the pressure drop $\Delta p=p_0-p_L$ is large, one should work with the differential form of (6.44), whereby the pressure drop per length is substituted by (-dp/dz), where z is the main flow direction through the bed:

$$\left(-\frac{dp}{dz}\right) = 150\frac{(1-\varepsilon)^2}{\varepsilon^3}\frac{\eta}{d_p^2}\frac{G_0}{\rho} + 1.75\frac{(1-\varepsilon)}{\varepsilon^3}\frac{1}{d_p}\frac{G_0^2}{\rho} \tag{6.48}$$

At the same time, the superficial velocity v_0 is expressed here in the mass flux G_0 and the density ρ.

On the basis of the law of conservation of mass, G_0 is constant in the steady-state condition (and thus independent of z). The density ρ of the gas is (via the equation of state), however, a (known) function of the pressure. Substitution of the equation of state into (6.48) then gives a (non-linear) first order differential equation, which describes the pressure as a function of z.

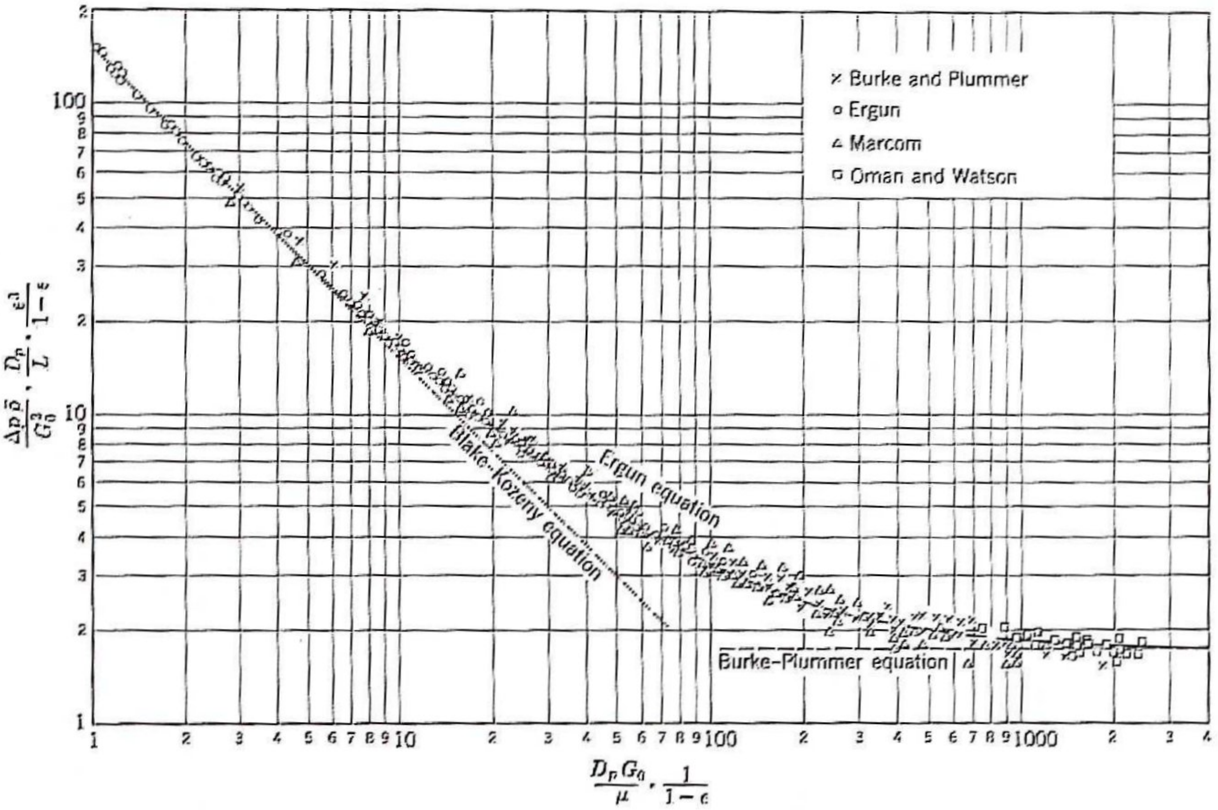

Fig. 6.8. Representation of the dimensionless form of the Ergun equation (6.47). The dimensionless equations of Blake-Kozeny and Burke-Plummer, as well as the experimental data, are also given.

7 Molecular energy transport

In physical and chemical engineering often processes occur in which, next to momentum transport, heat transport and/or (coupled) mass transport takes place. The heat and mass transport on the one hand and momentum transport on the other hand can strongly influence one another. For the description and design of chemical engineering processes, the rate at which heat and mass transport (possibly in interaction with momentum transport) takes place, plays a crucial role. In this and the following chapters the transport phenomena involved in heat transfer will be discussed. Also, important concepts generally applied in chemical engineering, such as setting up macro- and microbalances, comparing transfer resistances and using dimensionless numbers, are introduced along the way and are applied.

In this chapter, molecular heat transport in a stagnant object or fluid is studied. First, the steady state temperature profiles and the associated heat fluxes (steady conduction) are derived for three different geometries: infinite flat plates, cylinders and spheres. Subsequently, the theory is extended to instationary conduction in semi-infinite and finite objects. In this course, we will derive the equations only for purely one-dimensional molecular heat transport. Although analytical expressions could be derived for specific higher dimensional cases, often engineers resort to an approximation introduced by Newman, which is described at the end of the chapter. The chapter concludes with an elaboration on internal and external heat transfer resistances.

7.1 Fourier's law

The molecular heat transport is described with Fourier's law, given by:

$$\bar{\Phi}_h'' = -\lambda \nabla T \tag{7.1}$$

Or, in one-dimensional form:

$$\Phi_h'' = -\lambda \frac{dT}{dx} \tag{7.2}$$

Here, λ is the thermal conductivity of the material. For various materials values can be found in literature. It is often considered a constant, but in principle it is not:

- The thermal conductivity of gases and liquids typically depends on the local temperature, pressure and composition.
- Generally, the thermal conductivity is independent of the direction in the material in which the conduction takes place. That is, most materials are *isotropic*. However, for some materials, the thermal conductivity is different in different directions. Examples include wood or polymers, where the thermal conductivity depends on the orientation of the grains in the wood, or the polymer chains. These non-isotropic materials are left out of consideration in this course.

Also, often in literature for composite materials the assumption of a pseudo-homogeneous medium is made. In such cases a single (lumped) thermal conductivity is used and the medium, such as for example a packed bed, consisting of particles with a fluid (gas or liquid) in the interstitial space between the particles, is described as if it were homogeneous. This approach is typically applicable if the inhomogeneity of the material is found at a much smaller scale than that at which the conduction process takes place and this inhomogeneity is uniformly distributed within the medium. The effective thermal conductivity of such a medium depends on the thermal conductivity coefficients of the individual phases, the volume fractions of the phases and the geometry of the dispersed elements. Although the assumption of a pseudo-homogeneous medium is quite common, one should always verify the validity of this assumption.

7.2 Stationary conduction

7.2.1 Stationary conduction in a flat plate

The first situation that is studied is stationary one-dimensional molecular heat transport in a (homogeneous) flat plate with a thickness d (see Figure 1.1). The dimensions of the plate in the directions perpendicular to the *x*-direction are very large compared with the thickness of the plate, so that for this example only transport in the *x*-direction needs to be considered. The left side of the plate is kept at a constant temperature T_1, while the right side of the plate is kept constant at a lower temperature $T_2 < T_1$. As a result of the temperature difference there will be a temperature gradient in the plate, so that in accordance with Fourier's law, there will be molecular heat transport through the plate. The questions to be answered are: how does the temperature profile look like and what is the heat flux through the plate? These questions can be answered by setting up a microscopic stationary thermal energy balance and combine this with Fourier's law for the molecular heat flux.

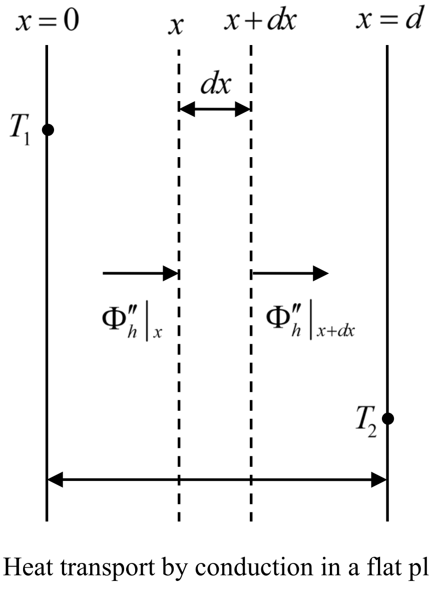

Figure 7.1: Heat transport by conduction in a flat plate with thickness *d*

For the analysis of this heat transport problem, we formulate a differential thermal energy balance over a infinitesimally small control volume, $dV = Adx$ in which A is the cross-sectional area of the plate perpendicular to the *x*-direction. In words, the balance reads:

Accumulation of thermal energy in the control volume per unit of time **=**
ingoing amount of thermal energy per unit of time
– outgoing amount of thermal energy per unit of time
+ amount of energy **produced** within the control volume per unit of time

In the stationary situation, there is no heat accumulation and in this problem there is also no heat production. The differential heat balance reduces to:

$$0 = \Phi''_h A\Big|_x - \Phi''_h A\Big|_{x+dx} \tag{7.3}$$

Dividing by the control volume *Adx* and taking the limit of *dx* $\rightarrow$ 0:

$$0 = -\lim_{dx\to 0} \frac{\Phi''_h\big|_{x+dx} A - \Phi''_h\big|_x A}{Adx} = -\lim_{dx\to 0} \frac{\Phi''_h\big|_{x+dx} - \Phi''_h\big|_x}{dx} = -\frac{d}{dx}\left(\Phi''_h\right) \tag{7.4}$$

having used the definition of the (partial) differential. Combining the differential energy balance with Fourier's law yields:

$$\frac{d}{dx}\left(\lambda \frac{dT}{dx}\right) = 0 \tag{7.5}$$

When the thermal conductivity λ is constant, it can be taken out of the differential operator. By subsequently dividing by λ, the equation reduces to:

$$\frac{d^2T}{dx^2} = 0 \tag{7.6}$$

From the above equation it can be deducted that for steady conduction in a flat plate with constant thermal conductivity, a linear temperature profile results. Integrating equation (7.6) twice with respect to *x* and subsequently substituting the boundary conditions of constant temperatures at both sides of the plate, gives finally the following expression for the temperature profile $T(x)$ in the plate:

$$\frac{T(x) - T_1}{T_2 - T_1} = \frac{x}{d} \tag{7.7}$$

Now that the temperature profile has been derived, the heat *flux* Φ''_h is obtained using Fourier's law:

$$\Phi_h'' = -\lambda \frac{dT}{dx} = \frac{\lambda}{d}\left(T_1 - T_2\right) \tag{7.8}$$

Note that the heat flux for this case is independent on the position with respect to the surfaces of the plate. The heat *flow* Φ_h is obtained by multiplication of the heat flux Φ_h'' with the cross-sectional area *A*:

$$\Phi_h = \Phi_h'' A = A\frac{\lambda}{d}\left(T_1 - T_2\right) \tag{7.9}$$

Heat transfer resistances

The equation (7.9) can be rewritten in the standard form “driving force = resistance × flow” as follows:

$$\Delta T = \frac{d}{A\lambda}\Phi_h = \frac{d}{\lambda}\Phi_h'' \tag{7.10}$$

This expression for the heat flow is analogous to Ohm’s law. According to Ohm’s law, the following applies for the relation between the electrical potential difference ΔU, the electrical resistance R and the current intensity I:

$$\Delta U = R \cdot I = \rho \frac{d}{A} I = \rho \cdot d \cdot J \tag{7.11}$$

In this equation ρ is the specific electrical resistance of the material, d is the thickness or the length of the material, A is the area perpendicular to the direction of the electrical current and J is the electrical current density. Evidently, the reciprocal thermal conductivity $1/\lambda$ corresponds to the specific electrical resistance ρ. This analogy can be used when considering parallel or serial connections of heat transfer resistances, because the same rules apply as to Ohmic resistances. By comparing heat transfer resistances one can quickly find out which resistances are determining the overall heat flux.

For parallel connections:

$$\frac{1}{R_{total}} = \sum_{i=1}^{N} \frac{1}{R_i} \tag{7.12}$$

For serial connections:

$$R_{total} = \sum_{i=1}^{N} R_i \tag{7.13}$$

In these equations, R_{total} is the total resistance, N is the number of parallel or serial resistances and R_i is the i^{th} resistance.

As an example, the qualitative temperature profile is sketched for stationary heat conduction in a composite material in Figure 7.2. The different layers in this composite material each can have a different thermal conductivity λ_i and different thickness d_i. Possible heat losses between the layers are ignored. In this situation there is a serial connection of three heat transfer resistances, where the total driving force ΔT and the heat flow Φ_h are related via:

$$\Delta T = T_1 - T_4 = \frac{\Phi_h}{A}\sum_{i=1}^{N}\frac{d_i}{\lambda_i} = \frac{\Phi_h}{A}\left(\frac{d_1}{\lambda_1}+\frac{d_2}{\lambda_2}+\frac{d_3}{\lambda_3}\right) = \Phi_h^{"}\left(\frac{d_1}{\lambda_1}+\frac{d_2}{\lambda_2}+\frac{d_3}{\lambda_3}\right) \qquad (7.14)$$

Or:

$$\Delta T = T_1 - T_4 = \Phi_h''\left(\frac{x_2 - x_1}{\lambda_1}+\frac{x_3 - x_2}{\lambda_2}+\frac{x_4 - x_3}{\lambda_3}\right) \qquad (7.15)$$

Use of the correspondence with electrical resistances has allowed us to directly and quickly find the overall heat transfer resistance. Alternatively, the heat flow through the three layers of the composite material could have been derived independently as a function of the both sides of the layers, i.e. T_1, T_2, T_3 and T_4. Two of these equations can be used to eliminate the variables T_2 and T_3, which yields after substitution in the remaining equation, and after much more work, the above equation.

<u>Question:</u> Which layer in the composite material, for which the temperature profile is given in Figure 7.2, has the largest heat transfer resistance?

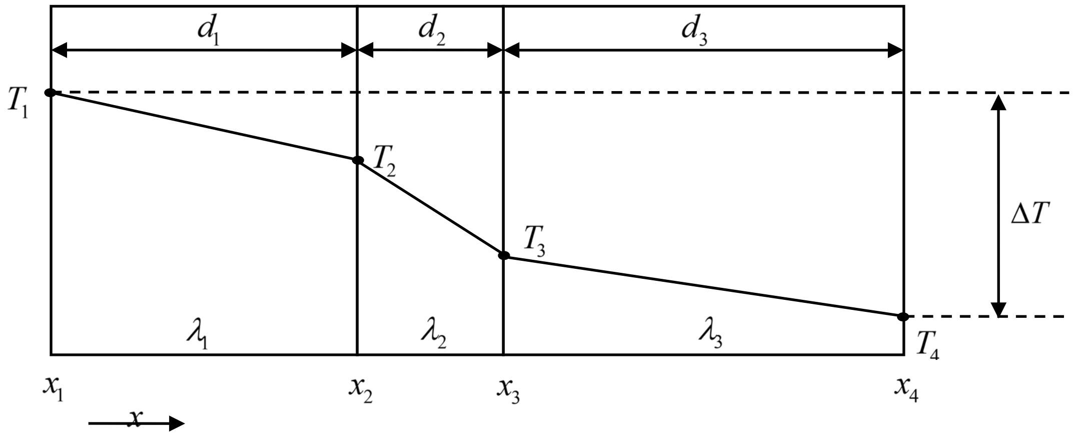

Figure 7.2: Heat conduction in a composite material in which the layers have different thickness and thermal conductivity.

7.2.2 Stationary conduction in a cylinder

As a second case, we study stationary conduction in cylindrical coordinates. Consider the radial heat transport in the insulation material around a tube (see Figure 7.3). Denote the outer radius of the tube with $r = R_1$. The cylindrical insulation jacket has a uniform thickness $\delta = R_2 - R_1$, where R_2 is the outer radius of the insulation jacket. The temperatures at the inside and the outside of the jacket are T_1 and T_2, respectively, with $T_1 > T_2$. Due to the temperature difference $\Delta T = T_1 - T_2$, there will be a temperature gradient in the radial direction, hence molecular heat transport in the radial direction will take place (according to Fourier's law).

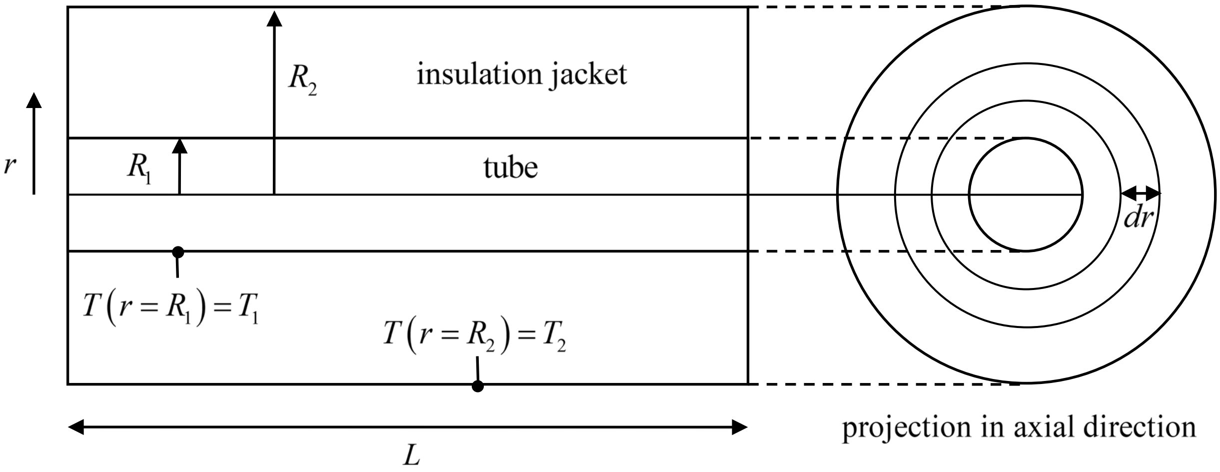

Figure 7.3 Radial heat transport in an insulation jacket around a tube with thickness $\delta = R_2 - R_1$

For the analysis of the heat transport problem, we set up a differential thermal energy balance over an infinitesimally small control volume $dV = 2\pi r dr dz$. Again, in this problem there is no heat accumulation (steady state) and no heat production, so that the differential thermal energy balance reads:

$$0 = \Phi''_h\Big|_r 2\pi r dz - \Phi''_h\Big|_{r+dr} 2\pi\left(r + dr\right) dz \tag{7.16}$$

which states that the heat flow in the radial direction has to be constant. From this equation, the differential form is easily derived by dividing by dV and taking the limit of $dr \to 0$:

$$\frac{d}{dr}\left(r\Phi''_h\right) = 0 \tag{7.17}$$

According to Fourier's law, for the heat flux Φ''_h the following applies:

$$\Phi_h'' = -\lambda \frac{dT}{dr} \tag{7.18}$$

Combination of the differential thermal energy balance (7.17) with Fourier's law (7.18) yields:

$$\frac{d}{dr}\left(r\lambda \frac{dT}{dr} \right) = 0 \tag{7.19}$$

When the thermal conductivity λ is constant, it can be taken outside of the differential operator and equation (7.19) reduces to:

$$\frac{d}{dr}\left(r \frac{dT}{dr} \right) = 0 \tag{7.20}$$

From this equation it can be seen that the radial temperature profile as a function of the radial coordinate in the insulation jacket (for constant λ) is not linear for steady conduction in a cylindrical material. Solving (7.20) with the appropriate boundary conditions, given by

Boundary conditions: $T = T_1 \quad \text{for} \quad r = R_1$

$T = T_2 \quad \text{for} \quad r = R_2$

gives an equation for the radial temperature profile $T(r)$ in the insulation jacket (Try to derive this equation yourself!):

$$\frac{T(r) - T_2}{T_1 - T_2} = \frac{\ln(r/R_2)}{\ln(R_1/R_2)} \tag{7.21}$$

For the heat flux Φ_h'' the following applies according to Fourier's law:

$$\Phi_h'' = -\lambda \frac{dT}{dr} = \frac{\lambda}{r}\left(\frac{T_1 - T_2}{\ln(R_2/R_1)} \right) \tag{7.22}$$

The local heat flow Φ_h follows from the product of the heat flux Φ_h'' and the area $2\pi rL$, in which L is the length of the tube:

$$\Phi_h = \Phi_h'' 2\pi rL = \frac{2\pi\lambda L}{\ln(R_2/R_1)}(T_1 - T_2) \tag{7.23}$$

From equation (7.22) follows that the heat flux in the insulation jacket is inversely proportional with the radial coordinate r, whereas for a plate the heat flux is constant for the stationary situation. This difference is caused by the increasing surface area through which heat is transported with increasing radius. However, similar to the case of the flat plate, the heat flow through the isolation mantle is independent on the radial position, as can be seen from equation (7.23). When (7.23) is rewritten in the form "driving force = resistance × flow", the following holds for the heat transfer resistance of the insulation jacket:

$$R_i = \frac{\ln\left(R_2/R_1\right)}{2\pi\lambda L} \tag{7.24}$$

Using this equation for the heat resistances in cylindrical geometries, we can quickly estimate the overall heat loss from a cylindrical tube when it is insulated with a composite material.

7.2.3 Stationary conduction around a sphere

The last case of stationary conduction discussed here concerns stationary conduction of energy from a sphere with radius R to a surrounding stagnant medium. The temperature of the sphere is uniform and constant at T_1 while the temperature of the stagnant medium at large distance of the sphere is T_∞, (see Figure 7.4). $T_1 > T_\infty$. The strategy is again to solve the temperature profile and subsequently apply Fourier's law to find the heat flow away from the sphere.

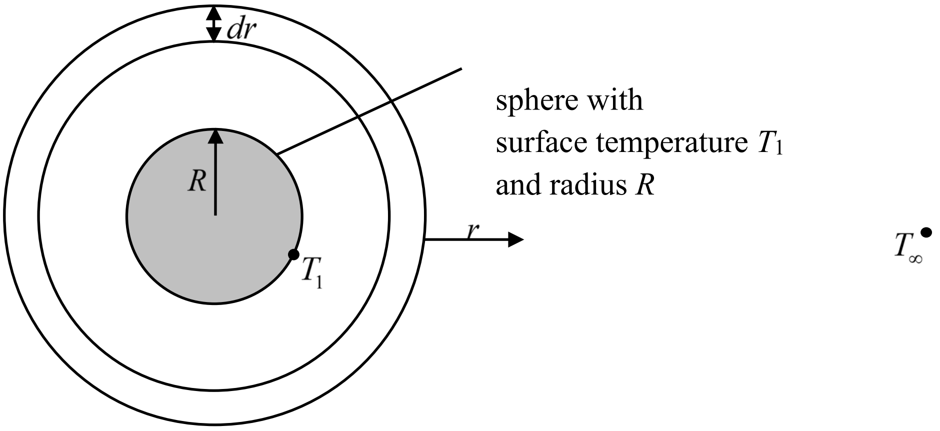

Figure 7.4: Heat transfer from a sphere with radius R and temperature T_1 to a stagnant medium with temperature T_∞ at very large distance from the sphere.

For the analysis of this heat transport problem a stationary differential thermal energy balance over a spherical layer of air surrounding the sphere with thickness dr and control volume $dV = 4\pi r^2 dr$ is formulated:

$$0 = \Phi_h''\big|_r 4\pi r^2 - \Phi_h''\big|_{r+dr} 4\pi\left(r + dr\right)^2 \tag{7.25}$$

Dividing by the control volume and taking the limit $dr \to 0$, equation (7.25) reduces to the following differential equation after substitution of Fourier's law:

$$\frac{d}{dr}\left(r^2\lambda\frac{dT}{dr}\right) = 0 \tag{7.26}$$

For a constant thermal conductivity λ, equation (7.26) reduces to a 2nd order differential equation:

$$\frac{d}{dr}\left(r^2\frac{dT}{dr}\right) = 0 \tag{7.27}$$

Integration of equation (7.27) with the appropriate boundary conditions gives the following expression for the radial temperature profile in the stagnant medium around the sphere:

$$\frac{T(r) - T_\infty}{T_1 - T_\infty} = \frac{R}{r} \tag{7.28}$$

According to Fourier's law, the heat flux Φ_h'' is given by:

$$\Phi_h'' = -\lambda\frac{dT}{dr} = \lambda\frac{R}{r^2}\left(T_1 - T_\infty\right) \tag{7.29}$$

The local heat flow Φ_h follows from the product of the heat flux Φ_h'' and the area $4\pi r^2$:

$$\Phi_h = \Phi_h'' 4\pi r^2 = 4\pi\lambda R\left(T_1 - T_\infty\right) \tag{7.30}$$

Analogous to the situation with the insulation jacket, again the heat flux is not constant, while the heat flow is. The physical explanation for this is the same as for the insulation jacket, but in this case the area increases quadratically with the radial coordinate r.

7.2.4 Newton's law of cooling and the Nusselt number

Newton formulated a "Law of Cooling", to describe the rate of cooling of a body by stating that the heat flow Φ_h is proportional to the heat exchange area A and the temperature difference between the outer surface of the body and the environment $\left(T_1 - T_\infty\right)$. The proportionality constant is called the (external) heat transfer coefficient α $[W/m^2K]$. This purely phenomenological quantity accounts for all (unknown) information about the heat transfer process. According to Newton's law of cooling:

$$\Phi_h = \alpha A\left(T_1 - T_\infty\right) \tag{7.31}$$

Nusselt correlation for stationary conduction around a sphere in a stagnant medium

For the case of heat transfer from a sphere to a surrounding stagnant medium, we can derive – by comparing equations (7.30) and (7.31) – for the heat transfer coefficient α:

$$\alpha = \frac{\lambda}{R} \tag{7.32}$$

Generally (for example for the case of a flow past a sphere) the heat transfer coefficient needs to be determined empirically. Here one uses correlations where the heat transfer coefficient α is represented in dimensionless form using the Nusselt number *Nu*, defined as:

$$Nu = \frac{\alpha L}{\lambda} \tag{7.33}$$

where *L* represents a characteristic length. In fact, the Nusselt number is the ratio of two heat transfer resistances:

$$Nu = \frac{d/\lambda}{1/\alpha} = \frac{\text{conduction resistance of a stagnant flat plate with thickness } d}{\text{resistance to heat transport}} \tag{7.34}$$

For example, a Nusselt number of 5 indicates that the heat transfer for the case under consideration is 5 times faster compared to heat conduction through a flat plate of characteristic thickness *d*.

For the case of heat transfer around a sphere, the characteristic length is the diameter of the sphere, so that the Nusselt-correlation for heat transfer around a sphere in a stagnant medium is:

$$Nu = \frac{\alpha d}{\lambda} = \frac{\frac{\lambda}{R} d}{\lambda} = 2 \tag{7.35}$$

Note that λ is the thermal conductivity of the surrounding medium and *not* the thermal conductivity of the sphere, since we are describing the heat transfer in the surrounding medium.

7.2.5 Stationary conduction: general energy balance

Summarizing the results of this section, the general differential energy balance for a stagnant medium with one-directional molecular heat transport in the steady state is given by:

$$0 = \frac{1}{r^n} \frac{\partial}{\partial r} \left(r^n \lambda \frac{\partial T}{\partial r} \right) + q \tag{7.36}$$

Here q denotes the volumetric heat production $\left[W/m^3 \right]$. The value of n depends on the coordinate system employed, i.e. n = 0 for a Cartesian, n = 1 for a cylindrical (with transport in the radial direction) and n = 2 for spherical coordinate systems. The geometric scale factors r^n corrects for varying surface area as a function of the radial coordinate.

7.3 Instationary conduction

Now, we will consider unsteady molecular heat transport in one-dimension. First, we will derive Fourier's differential equation. The solution of this partial differential equation[2] will be given for two different, often occurring, geometries, namely heat penetration in a "semi-infinite" body and heat penetration in a finite body.

1. *Semi-infinite heat penetration:* In this case, the time span in which the heat transport occurs is so short that the heat penetration occurring at one side of the body is not or barely noticeable at the other side of the body. For the mathematical description we can then assume one-sided penetration in a "semi-infinite" body, while the body in fact has a finite size in the direction of the heat transport.

2. *Finite heat penetration:* In this case, the time span in which the heat penetration occurs is large enough for the heat penetration to be felt everywhere in the body. In this situation we can no longer assume that the body is "semi-infinite", since the body is heated everywhere inside the body.

Note that the differences between these two cases is only related to differences in the boundary conditions, while for both cases the unsteady thermal energy balance (Fourier's differential equation) is the exactly same. For the sake of simplicity, in this course we will only consider the flat plate geometry (see Figure 7.1) when deriving the equations. For other geometries, solutions have been formulated, which are given here in graphical form. However, very often (at least in many engineering cases) the boundary curvature can be neglected and the solutions for a flat plate geometry can be used as a good approximation. In the following discussion, for simplicity in the discussion, we will assume that $T_1 > T_0$ (that is, the body is heated), however, the results are equally valid for $T_1 < T_0$ (cooling of the body).

7.3.1 Derivation of Fourier's differential equation for a flat plate

The starting point for the derivation of Fourier's differential equation is the differential thermal energy balance, which is formulated in words in section 7.2.1. In the case of instationary heat conduction, the amount of heat in the control volume $dV = Adx$ changes in time. The instationary heat balance reads:

$$\rho C_p \left(T\big|_{t+dt} - T\big|_t \right) dV = \Phi_h''\big|_x A dt - \Phi_h''\big|_{x+dx} A dt \tag{7.37}$$

---

[2] For additional information on the analytical solution techniques for the (heat) diffusion equation one is referred to the excellent book named "Conduction of Heat in Solids" by H.S. Carslaw and J.C. Jaeger

The left side of equation (7.37) states the change of the amount of heat in the control volume $dV = Adx$ occurring in a period of time dt, while the right side of equation (7.39) shows the net ("in" – "out") heat flow by conduction in the same period of time dt. Check for yourself that the dimension of this balance is $[J]$.

Dividing by the control volume and the time duration (i.e. $Adxdt$) and taking the limit of *dx* $\rightarrow$ 0 and *dt* $\rightarrow$ 0, yields

$$\rho C_p \lim_{dt\to 0} \frac{T\big|_{t+dt} - T\big|_t}{dt} = -\lim_{dx\to 0} \frac{\Phi''_h\big|_{x+dx} - \Phi''_h\big|_x}{dx} \tag{7.38}$$

$$\rho C_p \frac{dT}{dt} = -\frac{d}{dx}\left(\Phi''_h\right) \tag{7.39}$$

Substituting Fourier's law for the heat flux, the following partial differential equation is obtained, which describes the temperature in the plate as a function of the *x*-coordinate and time t:

$$\rho C_p \frac{\partial T}{\partial t} = \frac{\partial}{\partial x}\left(\lambda \frac{\partial T}{\partial x}\right) \tag{7.40}$$

When the thermal conductivity λ is constant, it can be taken outside of the differential operator and equation (7.40) reduces to *Fourier's differential equation*:

$$\frac{\partial T}{\partial t} = a \frac{\partial^2 T}{\partial x^2} \tag{7.41}$$

where a, the *thermal diffusivity* of the material with dimension $[m^2/s]$ has been introduced:

$$a = \frac{\lambda}{\rho C_p} \tag{7.42}$$

To solve the temperature profile described by equation (7.41), one initial condition and two boundary conditions need to be specified. The initial condition describes the temperature distribution at a certain time, e.g. in the case of a uniform initial temperature:

$$T(x) = T_0 \quad \text{for} \quad t = 0$$

The two boundary conditions describe the temperature and/or temperature gradient at the two boundaries of the body, e.g.:

$$T = T_1 \quad \text{for} \quad x = 0$$

$$\frac{\partial T}{\partial x} = 0 \quad \text{for} \quad x = d$$

In other words, at $x = 0$ the temperature is fixed at T_1. At $x = d$ the temperature gradient (and so the heat flux) is fixed at 0. It is evident that the solution of equation (7.41) will depend on the boundary conditions that are applied. For example, it would be possible to impose a heat flux on the boundary by setting the derivative $\frac{dT}{dx}$ on the wall to a non-zero value, according to Fourier's law. Fourier's differential equation is now solved for two different cases, namely i) heat penetration in a semi-infinite object and ii) heat penetration in a finite object.

7.3.2 Heat penetration in a semi-infinite body (Penetration theory)

Derivation of the temperature profile

Fourier's differential equation will first be solved for a body of which the initial temperature is T_0 throughout. At time $t = 0$, the temperature at the interface $x = 0$ is suddenly increased to a constant temperature $T_1 > T_0$ (see Figure 7.5). As a consequence of this (stepwise) applied temperature change at $x = 0$, heat will penetrate the body from $x = 0$.

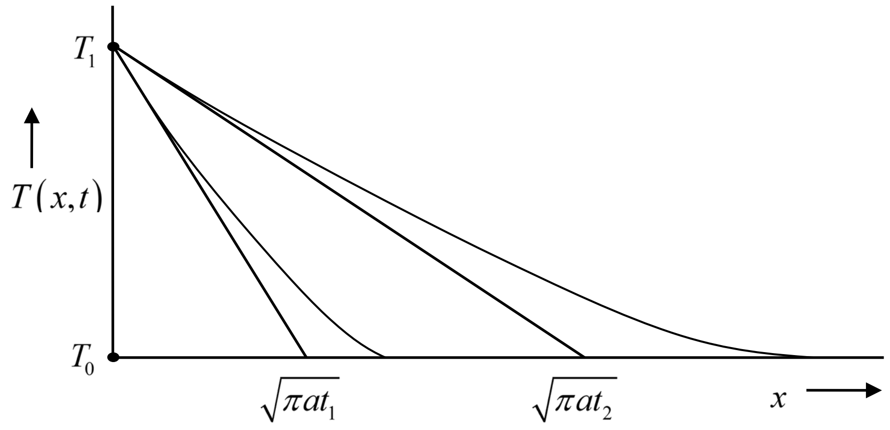

Figure 7.5 Heat penetration in a "semi-infinite" body. T_0 is the initial temperature, T_1 is the applied temperature at $x = 0$

The initial and boundary conditions for the solution of Fourier's differential equation for this problem are:

$$T = T_0 \quad \text{for} \quad t = 0 \quad \text{and} \quad 0 \le x \le \infty \tag{7.43}$$

$$T = T_1 \quad \text{for} \quad t > 0 \quad \text{and} \quad x = 0 \tag{7.44}$$

$$T = T_0 \quad \text{for} \quad t > 0 \quad \text{and} \quad x = \infty \tag{7.45}$$

Equation (7.39) can be solved with these conditions using the method of combination of independent variables and the solution is given by:

$$T(x,t) = (T_0 - T_1) \cdot \operatorname{erf}\left(\frac{x}{\sqrt{4at}}\right) + T_1 \tag{7.46}$$

In dimensionless form this is:

$$Y(x,t) = \frac{T_1 - T(x,t)}{T_1 - T_0} = \operatorname{erf}\left(\frac{x}{\sqrt{4at}}\right) \tag{7.47}$$

where the dimensionless temperature $Y(x,t)$ is introduced, which represents the present (at time t) and local (at position x) *relative* driving force:

$$Y(x,t) = \frac{T_1 - T(x,t)}{T_1 - T_0} = \frac{\text{present local driving force}}{\text{maximal driving force}} \tag{7.48}$$

In the solution, 'erf' represents the so-called error function, which is defined as:

$$\operatorname{erf}(z) = \frac{2}{\sqrt{\pi}} \int_0^z e^{-\beta^2} d\beta \tag{7.49}$$

The error function is of great importance to physics. Since there is no analytical solution for this integral, tables are available in which the value of $\operatorname{erf}(z)$ is given as a function of z (see e.g. Table 7.1). For the sake of clarity, the error function is also graphically represented in Figure 7.6. The resulting (qualitative) temperature profiles were already shown in Figure 7.5.

Table 7.1: **Values for the error function** $\operatorname{erf}(z)$

$\frac{x}{\sqrt{4at}}$	$\operatorname{erf}\left(\frac{x}{\sqrt{4at}}\right)$	$\frac{x}{\sqrt{4at}}$	$\operatorname{erf}\left(\frac{x}{\sqrt{4at}}\right)$
0.00	0.0000	1.10	0.8802
0.05	0.0564	1.20	0.9103
0.10	0.1125	1.30	0.9340
0.15	0.1680	1.40	0.9523
0.20	0.2227	1.50	0.9661
0.25	0.2763	1.60	0.9763
0.30	0.3286	1.70	0.9838
0.35	0.3794	1.80	0.9890
0.40	0.4284	1.90	0.9928
0.45	0.4755	2.00	0.9953
0.50	0.5205	2.10	0.9976
0.55	0.5633	2.20	0.9981
0.60	0.6039	2.30	0.9989
0.65	0.6420	2.40	0.9993
0.70	0.6778	2.50	0.9996
0.75	0.7112	2.60	0.9998
0.80	0.7421	2.70	0.9999
0.85	0.7707	2.80	0.9999
0.90	0.7969	2.90	0.9999
0.95	0.8209	3.00	0.9999
1.00	0.8427		

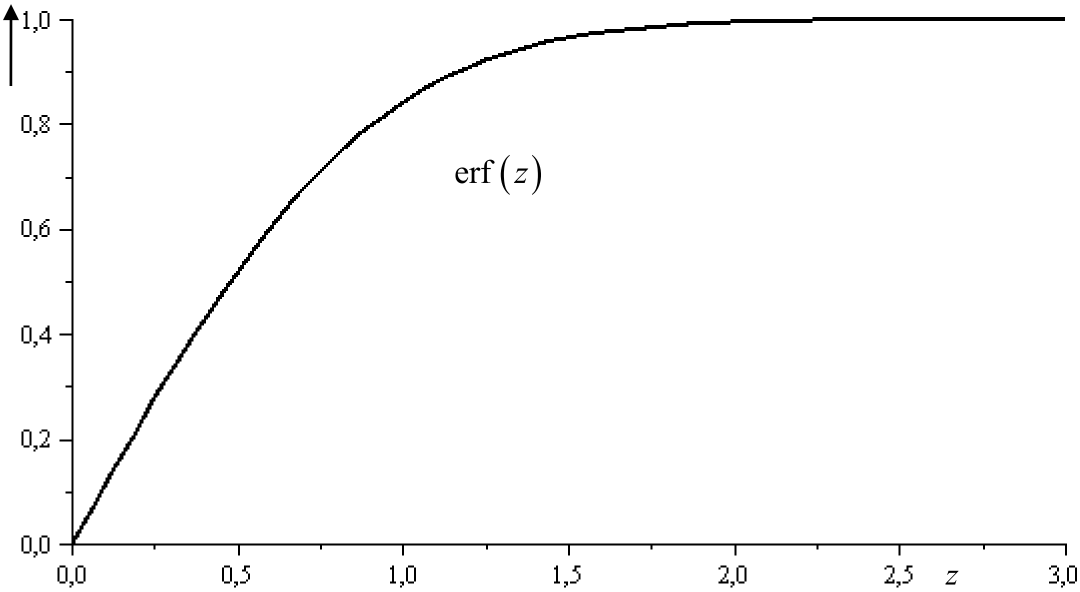

Figure 7.6 The error function $\operatorname{erf}(z)$ as a function of z

Present and time-averaged heat flux

Often one is not so much interested in the temperature profile, but rather in the amount of energy transferred through the boundary *x* = 0 into the object. The expression for the present heat flux at $x = 0$, $\Phi''_h\big|_{x=0}$, can be derived with Fourier’s law, with the following result:

$$\Phi''_h\big|_{x=0} = -\lambda \frac{\partial T}{\partial x}\big|_{x=0} = \left(\frac{\lambda}{\sqrt{\pi a t}}\right)\left(T_1 - T_0\right) \quad (>0) \qquad (7.50)$$

From equation (7.50) follows that the heat flux at $x = 0$ is positive, which is expected because of the assumption $\left(T_1 > T_0\right)$. With use of the definition of the thermal diffusivity (equation (7.42)), equation (7.50) can also be written as:

$$\Phi''_h\big|_{x=0} = \Phi''_{h,w} = \sqrt{\frac{\lambda \rho C_p}{\pi t}}\left(T_1 - T_0\right) \qquad (7.51)$$

Note that the heat flux decreases with the square-root of time, related to the decreasing temperature gradients at the boundary *x* = 0 due to the heating of the object.

Next to the present heat flux $\Phi''_{h,w}$ often the (time-)averaged heat flux $\left\langle \Phi''_{h,w} \right\rangle$ is relevant, for example for calculating the total amount of heat transferred. It is measured over a certain time t_e (measured from $t = 0$):

$$\left\langle \Phi''_{h,w} \right\rangle = \frac{\int_0^{t_e} \Phi''_{h,w}\, dt}{\int_0^{t_e} dt} = \frac{1}{t_e}\int_0^{t_e} \left\{ \sqrt{\frac{\lambda \rho C_p}{\pi t}}\left(T_1 - T_0\right) \right\} dt \qquad (7.52)$$

Elaborating the above integral yields

$$\left\langle \Phi''_{h,w} \right\rangle = 2\sqrt{\frac{\lambda \rho C_p}{\pi t}}\left(T_1 - T_0\right) \qquad (7.53)$$

expressing that the time-averaged heat flux is exactly equal to twice the instantaneous heat flux at the end of the period *t* = *t*t_e.

Present and time-averaged heat transfer coefficients

Recall Newton's law of cooling and the definition of the heat transfer coefficient α, defined as the heat flux Φ_h'' per unit of driving force ΔT:

$$\alpha = \frac{\Phi_h''}{\Delta T} \tag{7.54}$$

In general, for the driving force ΔT, the difference between the applied temperature T_1 and the *volume average* temperature of the body $\langle T \rangle$ is taken. When the penetration theory can be applied (i.e. conditions (7.59) or (7.60) are fulfilled), a good approximation is to assume that the average temperature of the body $\langle T \rangle$ is still approximately equal to T_0, which means that the driving force ΔT is equal to $\left(T_1 - T_0\right)$. When the equations (7.52) and (7.53) are divided by $\left(T_1 - T_0\right)$, we get the following expressions for the present and time averaged heat transfer coefficients, respectively:

$$\alpha = \sqrt{\frac{\lambda \rho C_p}{\pi t}} \tag{7.55}$$

$$\langle \alpha \rangle = 2\sqrt{\frac{\lambda \rho C_p}{\pi t_e}} \tag{7.56}$$

Note that the time average heat transfer coefficient $\langle \alpha \rangle$, which occurs in the time interval $\left[0, t_e\right]$ is exactly twice as large as the present heat transfer coefficient at $t = t_e$. Check for yourself that the heat transfer coefficients α and $\langle \alpha \rangle$ have the dimension $[W/\left(m^2 K\right)]$.

Penetration depth

One needs a quick estimate whether the penetration theory can be applied or not. From equation (7.50) it follows directly that the tangent line to the temperature profile at $x = 0$ will, independently of the exact value of the (non-zero) temperature difference of $\left(T_1 - T_2\right)$, cut off a distance δ_* at the *x*-axis given by:

$$\delta_* = \sqrt{\pi a t} \tag{7.57}$$

In Figure 7.7, this result is represented in dimensionless form (also see Figure 7.5). From this figure and Table 7.1 we can read that for $z = z_* \approx 0.886$, which corresponds to δ_*, the actual relative driving force Y amounts to about 0.79. For $z = 2z_* \approx 1.772$, the relative driving force is about 0.99, at $z = 2\delta_*$. That is, a change in relative driving force of only $1 - 0.99 = 0.01$ is to be found beyond $z = 2\delta_*$. This means that the principal temperature change is situated in a layer of thickness $2\delta_*$. In other words, the heat penetration depth, δ_h, is now defined as:

$$\delta_h = 2\sqrt{\pi a t} \tag{7.58}$$

From this equation follows that the heat penetration depth δ_h increases with the root of time t. The heat penetration depth plays an important role in determining the validity of application of the penetration theory for the description of instationary molecular heat transport, analogous to the momentum penetration depth. A criterion for checking the validity of the penetration theory is described in the next paragraph.

Validity of the penetration theory and the Fourier number

When the heat penetration depth δ_h is smaller than or equal to the characteristic size L of the body, the penetration theory can be applied:

$$\frac{\delta_h}{L} = \frac{2\sqrt{\pi a t}}{L} \leq 1 : \quad \text{penetration theory applicable} \tag{7.59}$$

For one-sided heat penetration the characteristic length *L* equals the total thickness d of the material, while in the case of two-sided heat penetration (as sketched in Figure 7.8) the characteristic length L equals half of the thickness, $d/2$, of the material. Note that for a heat penetration in an (infinitely long) cylinder (in the radial direction) and in a sphere, the *characteristic* length *L* equals the radius *R* (assuming that $\delta_h/R << 1$). Referring to Figure 7.8, the results of the penetration theory is applicable for $t<t_2$. For $t>t_2$ the temperature at the centre of the object starts to increase, so that boundary condition (7.45) and hence the solutions of the penetration theory are no longer applicable.

Equivalently, the condition can also be rewritten in the dimensionless form:

$$Fo = \frac{at}{L^2} \leq \frac{1}{4\pi} \approx 0.08 \tag{7.60}$$

Here, Fo is the (dimensionless) Fourier number. This number represents the ratio of process time t and the characteristic process time L^2/a for heat conduction. For a cylinder and a sphere the penetration theory can be applied with good accuracy for *Fo* numbers smaller than 0.04 and 0.018 respectively (due to curvature effects).

The advantage of using the dimensionless time Fo is that the temperature profiles put in a dimensionless form for different objects (for which, in this case, the penetration theory applies) corresponds for the same dimensionless time Fo. This allows deriving general correlations for heat transfer.

The following Nusselt relations, for example, are derived by rewriting the derived heat transfer relations for the penetration theory (equations (7.55) and (7.56)) in dimensionless form:

$$Nu = \frac{\alpha L}{\lambda} = \frac{1}{\sqrt{\pi}}\left(\frac{at}{L^2}\right)^{-\frac{1}{2}} = \frac{1}{\sqrt{\pi}}\left(Fo\right)^{-\frac{1}{2}} \tag{7.61}$$

$$\langle Nu \rangle = \frac{\langle \alpha \rangle L}{\lambda} = \frac{2}{\sqrt{\pi}}\left(\frac{at_e}{L^2}\right)^{-\frac{1}{2}} = \frac{2}{\sqrt{\pi}}\left(Fo_e\right)^{-\frac{1}{2}} \tag{7.62}$$

As mentioned before, the Nusselt number represents the ratio of two heat transfer resistances. The Nusselt number in equation (7.61) gives the ratio of the stationary conduction resistance $\left(L/\lambda\right)$ and the instationary conduction resistance $\left(1/\alpha\right)$. The Nusselt number is also used to characterize convective heat transport, as we will see in the next chapter.

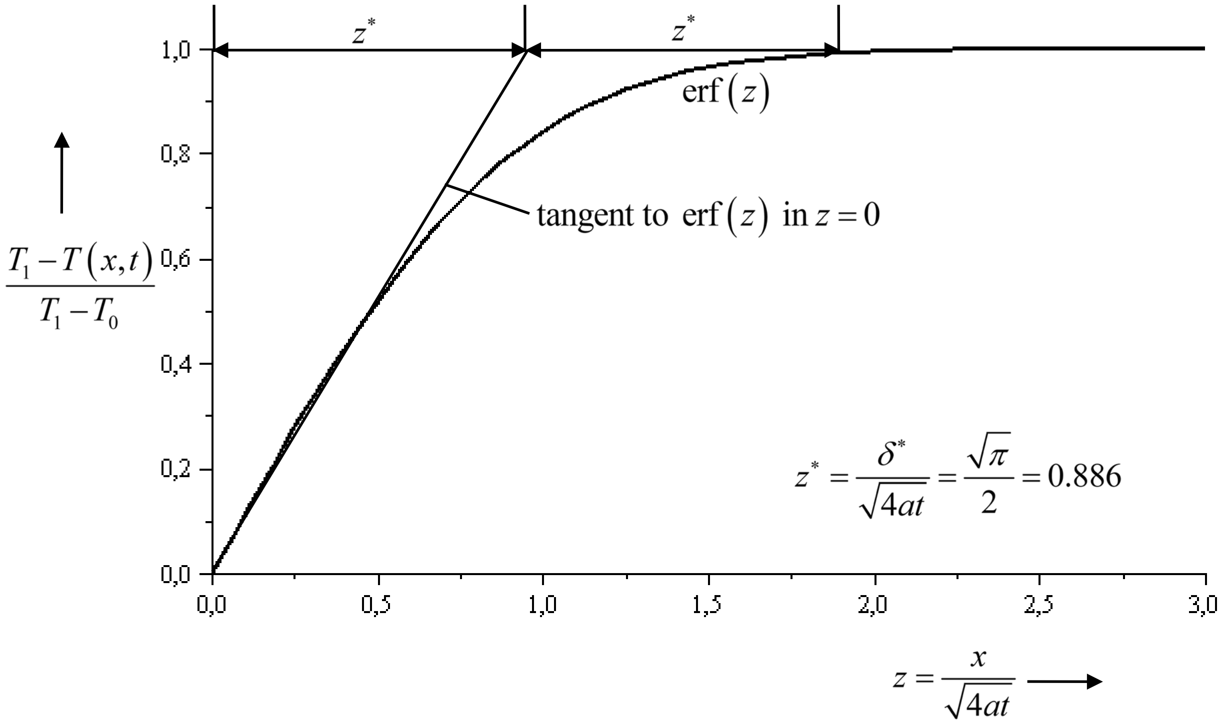

Figure 7.7 Meaning of δ_* defined in equation (7.57)

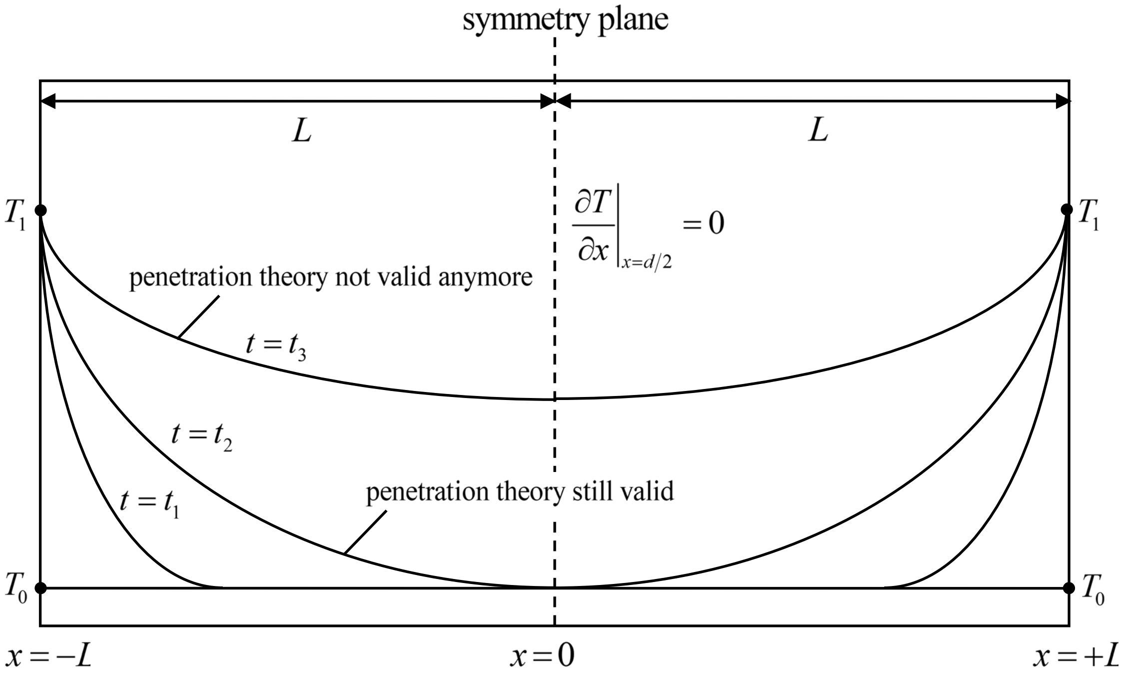

Figure 7.8 Two-sided heat penetration in a flat plate with initial temperature T_0 and applied temperature T_1 at the two walls ($x = -L$ and $x = +L$). ($t_3 > t_2 > t_1$)

7.3.3 Heat penetration in a finite body (Fourier solution)

In this section, Fourier's differential equation will be solved for the situation where also the core of the body is heated (i.e. $t > t_2$, referring to Figure 7.8). We will assume two-sided heat penetration in a flat body, similar to the geometry depicted in Figure 7.8. The initial temperature of the body is again uniform and equal to T_0. At time $t = 0$ the temperature of the wall of the body (at $x = -L$ and $x = +L$) is instantaneously raised to $T_1 > T_0$. Note that in this case $x = 0$ is at the center of the body, where the temperature gradient is zero (because of symmetry), i.e.

$$\left. \frac{dT}{dx} \right|_{x=0} = 0 \tag{7.63}$$

This implies that there is no conduction of heat through the centre of the body. Thus, the equations derived below are also applicable for the case of one-sided penetration into a finite flat plate where the back-side of the plate is kept at adiabatic conditions (i.e. no heat losses).

Short derivation using dimensionless numbers

Fourier's differential equation (7.41) and the initial condition (7.43) remain valid (but in this case: $-L \le x \le L$). The boundary conditions (7.44) and (7.45) are replaced by the following (symmetrical) boundary conditions:

$$T = T_1 \quad \text{for} \quad t > 0 \quad \text{and} \quad x = -L \tag{7.64}$$

$$T = T_1 \quad \text{for} \quad t > 0 \quad \text{and} \quad x = +L \tag{7.65}$$

In order to solve equation (7.41) with initial condition (7.43) and boundary conditions (7.64) and (7.65) it is beneficial to introduce the following dimensionless variables:

Dimensionless length ϕ:

$$\phi = \frac{x}{L} \tag{7.66}$$

Dimensionless time Fo:

$$Fo = \frac{at}{L^2} \tag{7.67}$$

Dimensionless temperature $Y = Y(\phi, Fo)$:

$$Y = Y(\phi, Fo) = \frac{T_1 - T(\phi, Fo)}{T_1 - T_0} \tag{7.68}$$

With these dimensionless variables, Fourier's differential equation is rewritten in dimensionless form as:

$$\frac{\partial Y}{\partial Fo}=\frac{\partial^2 Y}{\partial \phi^2} \tag{7.69}$$

With the following corresponding initial condition and boundary conditions:

$$Y=1 \quad \text{for} \quad \text{Fo}=0 \quad \text{and} \quad -1\le\phi\le 1 \tag{7.70}$$

$$Y=0 \quad \text{for} \quad \text{Fo}>0 \quad \text{and} \quad \phi=-1 \tag{7.71}$$

$$Y=0 \quad \text{for} \quad \text{Fo}>0 \quad \text{and} \quad \phi=+1 \tag{7.72}$$

The solution of (7.69) with the initial and boundary conditions (7.70), (7.71), (7.72) can be determined with the method of "separation of variables" and the solution is given in the form of a Fourier series:

$$Y\left(\phi,Fo\right)=2\sum_{n=0}^{\infty}\left\{\frac{\left(-1\right)^n}{\left(n+\frac{1}{2}\right)\pi}e^{-\left(n+\frac{1}{2}\right)^2\pi^2 Fo}\right\}\cos\left(\left(n+\tfrac{1}{2}\right)\pi\phi\right) \tag{7.73}$$

With equation (7.73) all the important variables for the heat penetration process can be derived and the results are summarized in Table 7.2.

Graphical representation of the Fourier solutions for heat penetration in a finite object

For the series shown above, there are graphs available in which the average (dimensionless) temperature Y_G, the (dimensionless) heart temperature Y_M or the (present) heat flux through the wall $\Phi''_{h,w}$ are plotted as a function of the dimensionless time Fo. In Figure 7.9, an example of such a graph is shown. In this figure, Y_G and Y_M are plotted as a function of the dimensionless time Fo. Note that in Figure 7.9, the vertical axis is logarithmic. In this figure also the result for an infinitely long cylinder (with radius R) and a sphere (with radius R) are shown. In literature, graphs are also available for the present and time-averaged heat fluxes. The most important aspects of the solutions depicted in Figure 7.9 are discussed in Table 7.3

Table 7.2 Fourier solutions for the heat penetration process in a finite object

The average (dimensionless) temperature Y_G (term-wise integration to ϕ):	$Y_G = \frac{\int_{-1}^{1} Y\left(\phi, Fo\right) d\phi}{\int_{-1}^{1} d\phi} = 2\sum_{n=0}^{\infty}\left\{\frac{1}{\left(\left(n+\frac{1}{2}\right)\pi\right)^2} e^{-\left(n+\frac{1}{2}\right)^2 \pi^2 Fo}\right\}$	(7.74)
The (dimensionless) temperature in the centre of the body Y_M	$Y_M = 2\sum_{n=0}^{\infty}\left\{\frac{\left(-1\right)^n}{\left(n+\frac{1}{2}\right)\pi} e^{-\left(n+\frac{1}{2}\right)^2 \pi^2 Fo}\right\}$	(7.75)
The present heat flux through the wall $\Phi''_{h,w}$ (term-wise differentiation to ϕ)	$x = -L \quad \left(\phi = -1\right):$ $\Phi''_{h,w} = +\frac{\lambda}{L}\left(T_1 - T_0\right) 2\sum_{n=0}^{\infty}\left\{e^{-\left(n+\frac{1}{2}\right)^2 \pi^2 Fo}\right\}$	(7.76)
	$x = +L \quad \left(\phi = +1\right):$ $\Phi''_{h,w} = -\frac{\lambda}{L}\left(T_1 - T_0\right) 2\sum_{n=0}^{\infty}\left\{e^{-\left(n+\frac{1}{2}\right)^2 \pi^2 Fo}\right\}$	(7.77)
The average heat flux through the left wall $\left(x = -L\right)$ and through the right wall $\left(x = +L\right)$ can be derived from equations (7.76) and (7.77), respectively, analogous to the derivation of the expression for Y_G. Note that, as one would expect, the (present) heat flux at $x = -L$ is positive (i.e. directed in the positive *x*-direction), while the heat flux at $x = +L$ is negative (i.e. directed in the negative *x*-direction).		

The solutions provided by the Fourier series solution for penetration in a finite body basically also include the solution for the limiting case described by penetration theory. However, evaluating the Fourier series, is computationally more expensive, whereas the penetration theory within its region of validity can be readily applied to obtain derived quantities such as the time-averaged heat flux. Additionally, the results provided by penetration theory lend themselves better for interpretation. Thus, when the penetration theory is valid, those results should be used.

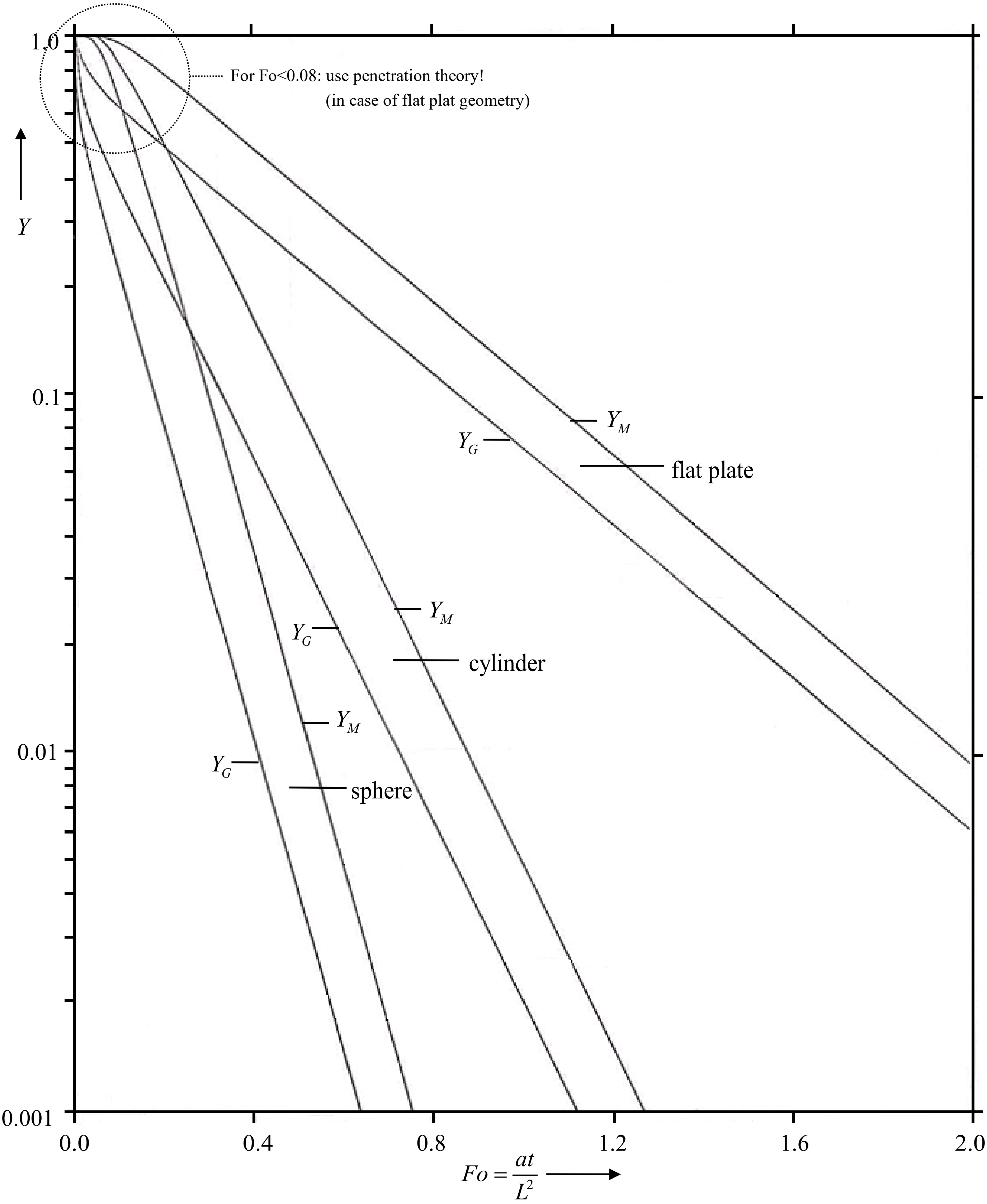

Figure 7.9: The dimensionless temperatures Y_G and Y_M as a function of Fo for one-dimensional instationary heat transport in a sphere, an infinitely long cylinder and an infinitely stretched flat plate.

Table 7.3 Important observations for instationary heat conduction

Observation	**Interpretation**
$\left(Y_G\right)_{sphere} < \left(Y_G\right)_{cylinder} < \left(Y_G\right)_{plate}$ (7.78)	This implies that the sphere heats the quickest, followed by the infinitely long cylinder and the infinitely stretched flat plate. This behavior is caused by the fact that the sphere has the highest ratio of area A (through which heat is delivered) to volume V (which is heated). $\left(\frac{A}{V}\right)_{sphere} > \left(\frac{A}{V}\right)_{cylinder} > \left(\frac{A}{V}\right)_{plate}$
For all geometries and all values of Fo: $Y_G < Y_M$ (7.79)	This implies that the average driving force Y_G is smaller than the driving force in the centre of the body, Y_M. This is to be expected, because the instantaneous increase in temperature of the surface (from T_0 to T_1) is noticeable latest in the centre of the body.
For large values of Fo, Y_G for a flat plate approaches on the logarithmic scale a straight line according to: $\ln\left(Y_G\right) = \ln\left(\frac{8}{\pi^2}\right) - \left(\frac{\pi^2}{4}Fo\right)$ (7.80)	Because of the exponential term, for sufficiently large values of Fo, the first term of the Fourier series (that is, for $n = 0$) dominates. For the temperature in the center of the body Y_M a similar situation occurs. Please note that in the graph not the natural logarithm but instead the $^{10}\log$ is used.

7.3.4 Multi-dimensional transport (Newman's rule)

Strictly speaking, the solutions illustrated in Figure 7.9 are only valid for purely one-dimensional heat transport. In practice, however, often systems are investigated where heat transport takes place in more than one direction simultaneously.

For finite systems, we can use the solutions in Figure 7.9 (in good approximation) by using Newman's rules. The basic principle of Newman's rule is, that the *N*-dimensional heat conduction problem is split into *N* one-dimensional heat conduction problems. In order to determine the value of Y_M or Y_G for a certain time t, the following approach is used:

1. Determine per coordinate direction the value of the Fourier number and read the values of Y_G or Y_M from Figure 7.9.

2. The value of Y_G or Y_M for the *N*-dimensional problem follows via multiplication of the *N* separately determined values of Y_G or Y_M.

These rules are summarized in Figure 7.10. The subscript "s" (with $s = x, y, z$ for rectangular shapes and $s = r, z$ for finite cylindrical shapes) stands for the resulting Y value if only the heat transport in the s-direction is considered. It is clear that $Y_s = 1$ if there is no heat transport in the s-direction, as e.g. for a finite cylinder this situation arises when e.g. the jacket of the cylinder is perfectly insulated ('adiabatic wall'), in which case $Y_r = 1$.

geometry	calculation rule
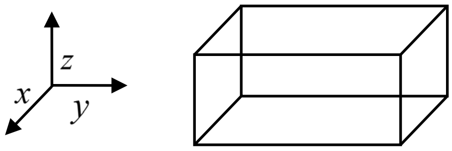	$Y = Y_x Y_y Y_z$
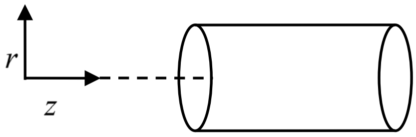	$Y = Y_r Y_z$

Figure 7.10 Newman's rules for the description of simultaneous multi-dimensional heat transport in the x-, y-, z-direction for a finite rectangular body and the r-, z-direction for a finite cylinder.

Example using Newman's rules

Exercise: A can of tomato-sauce (with height $2L = 0.1\ \mathrm{m}$, radius $R = 0.05\ \mathrm{m}$ and uniform initial temperature $T_0 = 40\ ^\circ\mathrm{C}$), is suddenly (at $t = 0\ \mathrm{s}$) placed in the kitchen sink while water is flowing through (with a bulk temperature $T_1 = 5\ ^\circ\mathrm{C}$). The water flows in such a manner that the temperature of the surface of the can is always equal to the bulk temperature of the water. The heat transfer resistance of the metal can be neglected. Note that in this example $T_1 < T_0$, i.e. the can is cooled down. What is the temperature in the centre of the can after 2000 s?

Physical data:

thermal conductivity of the tomato-sauce: $\lambda = 0.5\ \mathrm{W/\left(m^\circ C\right)}$

volumetric heat capacity of the tomato-sauce: $\rho C_p = 1.0 \cdot 10^6\ \mathrm{J/\left(m^3\,{}^\circ C\right)}$.

Solution: In this situation, both radial and axial heat transport are significant and need to be taken into account. For the radial transport, $r = 0$ is a symmetry-line, while for the axial transport, $z = 0$ is the symmetry-plane (see Figure 7.11). This means that the characteristic length to be used in the Fourier number for the radial and axial heat transport are equal to R and L, respectively.

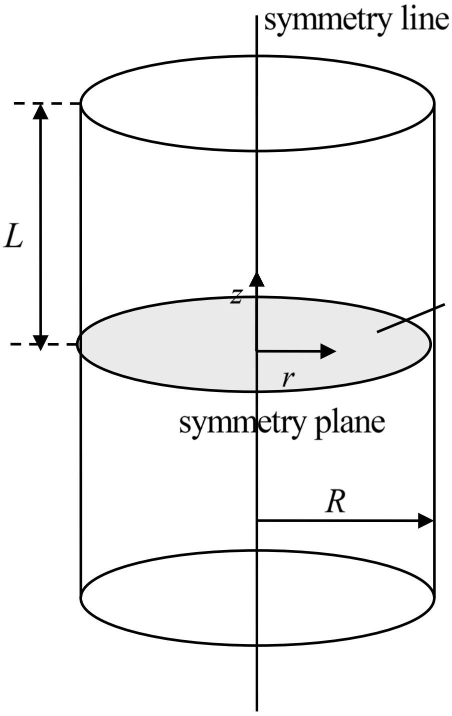

Figure 7.11 Characteristic distances for the two-dimensional heat transport

First, the Fourier number for the radial direction is calculated, using $a = \frac{\lambda}{\rho C_p} = \frac{0.5}{1 \cdot 10^6} = 5.0 \cdot 10^{-7} \frac{\text{m}^2}{\text{s}}$:

$$Fo = \frac{at}{R^2} = \frac{5.0 \cdot 10^{-7} \cdot 2000}{0.05^2} = 0.40 \tag{7.81}$$

Now, using this Fourier number, from Figure 7.9, Y_M can be determined (taking the line for a cylinder):

$$\left(Y_M\right)_{cylinder} \approx 0.16 \tag{7.82}$$

Calculation of the Fourier number for axial heat transport:

$$Fo = \frac{at}{L^2} = \frac{5 \cdot 10^{-7} \cdot 2000}{0.05^2} = 0.4 \tag{7.83}$$

With Figure 7.9 now Y_M for the axial direction can be determined (taking the line for a plate):

$$\left(Y_M\right)_{plate} \approx 0.5 \tag{7.84}$$

The Y -value for the centre of the can $\left(Y_M\right)_{can}$ follows from Newman's rules:

$$\left(Y_M\right)_{can} = \left(Y_M\right)_{cylinder} \left(Y_M\right)_{plate} = 0.16 \cdot 0.5 = 0.08 \tag{7.85}$$

The temperature in the centre of the can may now be calculated using (7.68): $T = 7.8$ °C

7.3.5 External heat transfer limitation

For the discussion of instationary molecular heat transport, it has been assumed that at the surface of the body, there is a constant imposed temperature T_1. Referring to the above example, it was assumed that energy from the outside wall of the can could be transferred *infinitely fast* towards the bulk of the flowing water, i.e. the resistance to heat transport is situated fully inside the tomato-sauce in the can (neglecting the heat resistance of the wall of the can). Another limiting case presents itself when the resistance to heat transport lies fully outside of the can. In this situation, there are no temperature differences within the body and there is one uniform body temperature T.

This limiting case will now be analyzed for an arbitrary body with a heat-exchanging area A and volume V, which is exchanging heat with the environment. It is assumed that the volumetric heat capacity of the body ρC_p is constant. For the description of the external heat transfer process the already introduced Newton's law of cooling is used. The instationary thermal energy balance for a body with heat-exchanging area A and volume V reads:

$$\rho C_p \frac{dT}{dt} V = \alpha \left(T_1 - T \right) A \tag{7.86}$$

Integration of equation (7.86) with boundary condition $T = T_0$ at $t = 0$ gives:

$$\frac{T_1 - T(t)}{T_1 - T_0} \equiv Y(t) = \exp\left(-\frac{\alpha A t}{\rho C_p V} \right) \tag{7.87}$$

The ratios of heat-exchanging area A to volume V for different geometries are given in Table 7.4.

Table 7.4 Ratio of heat-exchanging area to volume (A/V) for different geometries

Geometry	A/V
Two sided heat penetration in infinitely stretched flat plate of thickness d	$\frac{2}{d}$
Infinitely long cylinder	$\frac{2}{R}$
Sphere	$\frac{3}{R}$

8 Energy transport by forced convection

In the previous chapter we focused on the analysis of stationary and instationary molecular heat transport. We assumed that the heat transport took place in stagnant media, i.e. media in which convective (heat-) transport does not play a role. However, we often deal with flowing media where there is heat exchange with a fixed system wall, caused by a temperature difference between the wall and the flowing medium. In this chapter we will restrict ourselves to heat transport by forced convection. Heat transport by free convection will be treated in the next chapter.

In this chapter we will consider two types of geometries: i) forced convective heat transport in tubes, as for example encountered in heat exchangers, and ii) forced convective heat transport in flows past objects, as for example relevant to describe the heat exchange between a catalytic particle and the surrounding reaction mixture. First, the general problem is described and the heat transfer coefficient and mixing cup temperature are defined for heat transfer to a fluid flowing through a tube.

8.1 Newton's cooling law applied to forced convection

We would like to be able to predict the amount of energy per unit of time exchanged between a flowing fluid and a wall or an object in the flow. Here we will restrict ourselves to the case where the wall or object has a constant uniform temperature. For ease of discussion, we will again assume that the fluid is heated, but the results are also applicable for the case the fluid is cooled. Consider now the case shown in Figure 8.1, which depicts a control volume, showing thermal energy entering and leaving the control volume by convective transport and heat exchange with the wall.

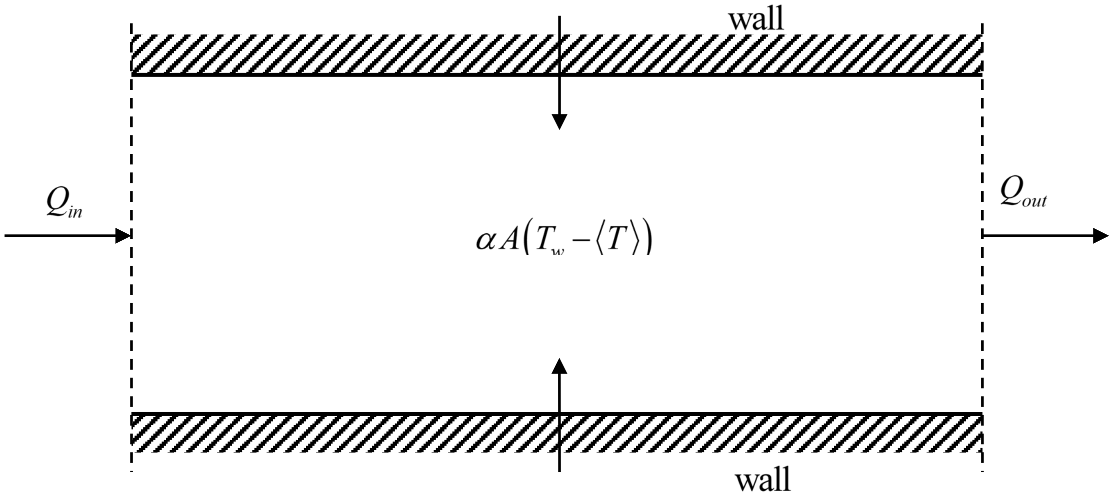

Figure 8.1 A system with ingoing $\left(Q_{in}\right)$ and outgoing $\left(Q_{out}\right)$ heat flows in which $\alpha A\left(T_w - \langle T\rangle\right)$ $[J/s]$ is transferred from the wall (with temperature T_w) to the flowing medium (average temperature: $\langle T\rangle$).

Applying Newton's law of cooling, the amount of thermal energy exchanged between the wall and the fluid per unit time is given by

$$\Phi_h = \alpha A \left| T_w - \langle T \rangle \right| \tag{8.1}$$

where A denotes the heat exchanging area, T_w the wall temperature and $< T >$ the average temperature of the flowing fluid. In this equation the heat transfer coefficient α has been defined, which represents the amount of heat exchanged per unit of time, per unit of heat-exchanging area and per unit of average driving force. Often one uses dimensionless heat transfer coefficients in the form of the already introduced Nusselt number:

$$Nu = \frac{\alpha L}{\lambda} = \frac{\frac{L}{\lambda}}{\frac{1}{\alpha}} = \frac{\text{conduction resistance for medium of thickness } L}{\text{convective heat transfer resistance}} \tag{8.2}$$

where L is a characteristic length of the considered system.

In the definition of the heat transfer coefficient, the average driving force is the difference between the (constant) wall temperature and the average temperature $\langle T \rangle$ of the flowing fluid. Taking into account that there can be radial profiles of the temperature and axial velocity, the average temperature we are after, is the temperature of the fluid that we would measure when we would collect the fluid in a cup and stir the fluid ideally (without any heat losses). This is referred to as the *'flow-averaged'* or '*mixing cup temperature*', for flow through a cylindrical tube defined as:

$$\langle T \rangle (z) = \frac{\int_0^R T(r,z) v_z(r) 2\pi r dr}{\int_0^R v_z(r) 2\pi r dr} \tag{8.3}$$

With the help of an example, we will show the importance of heat transfer coefficients to quantify heat transfer processes. Often we want to calculate the flow-averaged outlet temperature of a fluid, when knowing the inlet temperature $\langle T \rangle_{in}$, volumetric flow rate Φ_v and heat exchanging area A (see also Figure 8.1). If the fluid is ideally mixed within the vessel, the flow-averaged outlet temperature $\langle T \rangle_{out}$ can be found by setting up a macroscopic thermal energy balance (assuming constant volumetric heat capacity ρC_p):

$$0 = Q_{in} - Q_{out} + \langle \alpha \rangle A \left(T_w - \langle T \rangle \right) \tag{8.4}$$

where the convective energy flows are given by

$$Q_{in} = \Phi_v \rho C_p \langle T \rangle_{in} \tag{8.5}$$

$$Q_{out} = \Phi_v \rho C_p \langle T \rangle_{out} \tag{8.6}$$

Thus, the mixing-cup outlet temperature can be calculated, once quantitative information on the average heat transfer coefficient $\langle\alpha\rangle$ is available. The heat transfer coefficient generally depends on

- The surface properties of the heat exchanging area;
- The physical properties of the flowing medium;
- The hydrodynamics of the flow (laminar or turbulent).

For certain cases, analytical equations can be derived for the heat transfer coefficient, while in most cases we have to resort to semi-empirical correlations. These correlations (typically in the form of dimensionless Nusselt numbers) and the necessary background will be discussed in the next sections.

However, looking back at the previous example, the driving force for the heat exchange is the temperature difference between the wall and flowing fluid. If the fluid is ideally mixed, the bulk temperature of the flowing fluid equals the mixing-cup temperature of the outgoing fluid, i.e. $\langle T\rangle = \langle T\rangle_{out}$ and a macroscopic energy balance suffices. However, in case of plug flow of a fluidum through a tube, the flow-averaged bulk temperature of the fluid is changing along the axial coordinate of the tube, thus also changing the local driving force for heat exchange with the wall. In this case we need to set up a differential thermal energy balance (assuming a cylindrical tube with diameter *D*):

$$0 = \Phi_v \rho C_p \langle T\rangle\big|_z - \Phi_v \rho C_p \langle T\rangle\big|_{z+dz} + \alpha\pi D dz\left(T_w - \langle T\rangle\right) \tag{8.7}$$

Dividing by *dz* and taking the limit of *dz* → 0, we cast the above difference equation into a differential equation:

$$0 = -\Phi_v \rho C_p \frac{d\langle T\rangle}{dz} + \alpha\pi D\left(T_w - \langle T\rangle\right) \tag{8.8}$$

Note that the heat transfer coefficient can in principle vary along the axial coordinate. With the boundary condition $\langle T\rangle = \langle T\rangle_{in}$ at $z = 0$, this equation can be integrated using the method of separation of variables:

$$\int_{\langle T\rangle_{in}}^{\langle T\rangle_{out}} \frac{d\langle T\rangle}{\left(T_w - \langle T\rangle\right)} = \frac{\pi D}{\Phi_v \rho C_p}\int_0^L \alpha(z)dz \tag{8.9}$$

which yields:

$$\ln\left(\frac{T_w - \langle T\rangle_{out}}{T_w - \langle T\rangle_{in}}\right) = -\frac{\pi D L}{\Phi_v \rho C_p}\frac{\int_0^L \alpha(z)\,dz}{L} \tag{8.10}$$

Here $\frac{1}{L}\int_0^L \alpha(z)\,dz \equiv \langle\alpha\rangle$ denotes the length-averaged heat transfer coefficient. Once information on the (average) heat transfer coefficient is available, the mixing-cup outlet temperature can be calculated. In the next sections Nusselt correlations for laminar and turbulent flow through tubes and for flow past objects will be discussed (assuming a constant wall temperature or a constant surface temperature of the object).

8.2 Convective heat transport through tubes

8.2.1 Laminar incompressible flow through tubes

Derivation of the thermal energy balance

In this section we will consider laminar convective heat transport through a cylindrical tube with only convection in the axial direction (i.e. fully developed laminar flow). First, the general microbalance for thermal energy will be derived, where we will take the following into account:

- Instationary heat transport
- Convective heat transport in the axial direction only
- Molecular heat transport in the radial and axial direction
- Heat production q $\left[W/m^3\right]$

The differential balance will be set up using cylindrical coordinates assuming rotational (azimuthal) symmetry. The control volume is a 'napkin ring' with volume $dV = 2\pi r dr dz$ (see Figure 8.2).

In words, the microbalance of thermal energy reads:

Accumulation of thermal energy in the control volume per unit of time =
ingoing amount of thermal energy by convection and conduction per unit of time
– outgoing amount of thermal energy by convection and conduction per unit of time
+ heat production in the control volume per unit of time

In Figure 8.2, the in- and outgoing convective and conductive heat flows have been indicated. Thus, the differential thermal energy balance is given by:

$$\begin{aligned}\left(\rho C_p \frac{\partial T}{\partial t}\right) 2\pi r dr dz &= \left(\rho C_p T\right) v_z\Big|_z 2\pi r dr - \left(\rho C_p T\right) v_z\Big|_{z+dz} 2\pi r dr \\ &- \left(\lambda \frac{\partial T}{\partial r}\right)\Bigg|_r 2\pi r dz + \left(\lambda \frac{\partial T}{\partial r}\right)\Bigg|_{r+dr} 2\pi\left(r+dr\right) dz \\ &- \left(\lambda \frac{\partial T}{\partial z}\right)\Bigg|_z 2\pi r dr + \left(\lambda \frac{\partial T}{\partial z}\right)\Bigg|_{z+dz} 2\pi r dr + \left(q\right) 2\pi r dr dz\end{aligned} \tag{8.11}$$

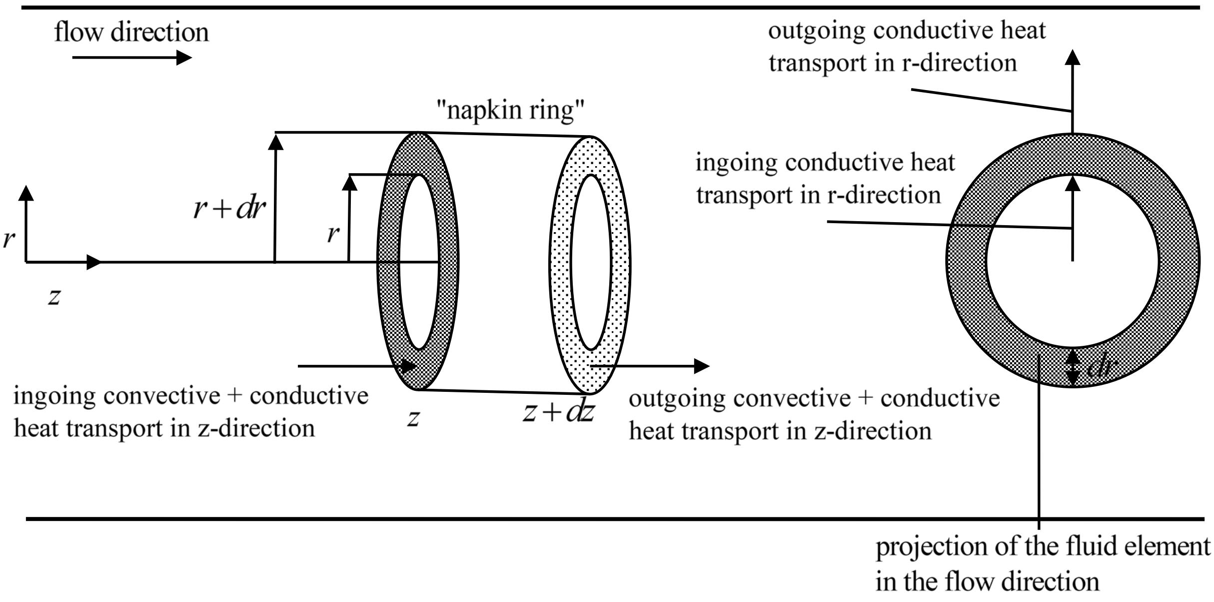

Figure 8.2 Forced convective heat transport in a round tube. The different transport terms in the microbalance of heat have been indicated.

Equation (8.11) is divided by the control volume $dV = 2\pi r dr dz$ and then in the limit of $dr \to 0$ and $dz \to 0$ the following partial differential equation is obtained:

$$\rho C_p \frac{\partial T}{\partial t} = -\rho C_p v_z \frac{\partial T}{\partial z} + \frac{1}{r}\frac{\partial}{\partial r}\left(r\lambda \frac{\partial T}{\partial r} \right) + \frac{\partial}{\partial z}\left(\lambda \frac{\partial T}{\partial z} \right) + q \tag{8.12}$$

The left hand side of equation (8.12) represents the increase in the amount of thermal energy per unit of volume and time. The first term on the right hand side represents the net increase of heat per unit of volume and time resulting from axial convection, and the second and third term represent the net conductive radial and axial heat transport, respectively, per unit of volume and time, q represents the volumetric heat production with units $\left[W/m^3 \right]$.

This general equation is now further simplified by assuming the following:

- The system is stationary
- The contribution by axial conduction is negligible in comparison with axial convection
- The thermal conductivity is constant
- The axial velocity is independent of the axial coordinate (i.e. fully developed flow)
- There is no internal heat production

The simplified thermal energy microbalance then reads:

$$v_z\left(r \right) \frac{\partial T}{\partial z} = a \frac{1}{r}\frac{\partial}{\partial r}\left(r \frac{\partial T}{\partial r} \right) \tag{8.13}$$

To solve equation (8.13) we need:

- an expression for the radial velocity profile $v_z(r)$;
- one boundary condition which describes the radial temperature distribution at the beginning of the tube (at $z = 0$);
- two boundary conditions which (for $z > 0$) describe the temperature and/or radial gradient of the temperature at $r = 0$ and/or $r = R$.

Here, the following boundary conditions are considered:

$$T = T_0 \quad \text{for} \quad z = 0 \quad \text{and} \quad 0 \le r \le L \tag{8.14}$$

$$\frac{\partial T}{\partial r} = 0 \quad \text{for} \quad r = 0 \quad \text{and} \quad 0 < z \le L \tag{8.15}$$

$$T = T_1 \quad \text{for} \quad r = R \quad \text{and} \quad 0 < z \le L \tag{8.16}$$

where L is the length of the tube. Note that T_0 denotes the uniform inlet temperature and T_1 denotes the constant imposed wall temperature. With respect to the expression for the radial velocity profile $v_z(r)$ for laminar flow we will distinguish the following two limiting cases:

- Uniform velocity profile (Plug flow):

$$v_z(r) = \langle v \rangle \tag{8.17}$$

- Parabolic velocity profile (Hagen-Poiseuille flow):

$$v_z(r) = 2\langle v \rangle \left(1 - \left(\frac{r}{R} \right)^2 \right) \tag{8.18}$$

where $\langle v \rangle$ is the average flow velocity in the tube. Please note that the plug flow case here refers to the case of laminar flow with a uniform velocity profile, such as for example encountered in the case of a liquid jet flowing downwards through a gas, not to be confused with turbulent plug flow.

The Greatz number

To solve equation (8.13) with boundary conditions (8.14), (8.15) and (8.16), we introduce the following dimensionless variables:

- Dimensionless radial coordinate ω:

$$\omega = \frac{r}{d} \tag{8.19}$$

Note that the tube diameter instead of the tube radius is selected as characteristic length for the radial direction! This is the convention for tube flow.

- Dimensionless axial coordinate ϕ:

$$\phi = \frac{z}{L} \tag{8.20}$$

- Dimensionless temperature Y :

$$Y = Y(\omega,\phi) = \frac{T_1 - T(\omega,\phi)}{T_1 - T_0} \tag{8.21}$$

When the dimensionless variables are introduced in equation (8.13), the result is shown in equation (8.22):

$$\frac{v_z(\omega)}{\langle v\rangle}\frac{\partial Y}{\partial\phi} = \left(\frac{aL}{\langle v\rangle d^2}\right)\frac{1}{\omega}\frac{\partial}{\partial\omega}\left(\omega\frac{\partial Y}{\partial\omega}\right) \tag{8.22}$$

where the dimensionless Graetz number, Gz, appears, which is defined as:

$$Gz = \left(\frac{aL}{\langle v\rangle d^2}\right) \tag{8.23}$$

The Graetz number represents the ratio between the rate of heat transport as a result of *radial conduction* and the heat transport as a result of *axial convection*.

The boundary conditions, in dimensionless form, are given by:

$$Y = 1 \quad \text{for} \quad \phi = 0 \quad \text{and} \quad 0 \le \omega \le \tfrac{1}{2} \tag{8.24}$$

$$\frac{\partial Y}{\partial\omega} = 0 \quad \text{for} \quad \omega = 0 \quad \text{and} \quad 0 < \phi \le 1 \tag{8.25}$$

$$Y = 0 \quad \text{for} \quad \omega = \tfrac{1}{2} \quad \text{and} \quad 0 < \phi \le 1 \tag{8.26}$$

with the dimensionless velocity profiles for laminar uniform and parabolic velocity profile, resp.:

- Uniform velocity profile (plug flow):

$$\frac{v_z(\omega)}{\langle v\rangle} = 1 \tag{8.27}$$

- Parabolic velocity profile (Hagen-Poiseuille flow):

$$\frac{v_z(\omega)}{\langle v\rangle} = 2\left(1 - 4\omega^2\right) \tag{8.28}$$

The solution of equation (8.22) with boundary conditions (8.24), (8.25) and (8.26) can be obtained analytically for laminar flow with a uniform and a parabolic velocity profile and gives the dimensionless temperature Y as a function of ω, ϕ and the Graetz number Gz: $Y = Y(\omega,\phi,Gz)$. With this dimensionless temperature profile we can derive the following important quantities:

- Mixing cup dimensionless temperature at the outlet $\langle Y \rangle$:

$$\langle Y \rangle = \frac{\int_0^{\frac{1}{2}} Y(\omega, 1, Gz) v_z(\omega) 2\pi\omega d\omega}{\int_0^{\frac{1}{2}} v_z(\omega) 2\pi\omega d\omega} \tag{8.29}$$

which is simply the dimensionless form of equation (8.3).

- Local dimensionless heat transfer coefficient *Nu*:

$$Nu = \frac{\alpha d}{\lambda} = -\frac{1}{\langle Y \rangle} \frac{\partial Y}{\partial \omega}\bigg|_{\omega=\frac{1}{2}} \tag{8.30}$$

which is easily understood when recalling the definition of the heat transfer coefficient:

$$\alpha = \frac{\Phi_h''}{T_1 - \langle T \rangle} = \frac{-\lambda \left.\dfrac{\partial T}{\partial r}\right|_{r=R}}{T_1 - \langle T \rangle} \tag{8.31}$$

Note that in the definition of the *Nu* number for flow through tubes, the tube diameter has been chosen as the characteristic length.

The important result of the above derivation is that <u>for laminar flow</u> the dimensionless mixing cup temperature $\langle Y \rangle$ is only a function of the *Gz* number! Thus, laminar flow of two different fluids with different physical properties flowing through a round tube with different diameters will actually achieve the same dimensionless mixing cup temperature if they the cases have the same *Gz* number.

Secondly, it can be easily seen from equation (8.30) that the *Nu* number, i.e. the dimensionless heat transfer coefficient, for laminar flow depends on the axial coordinate. Therefore, a local *Gz* number is defined, where the length *L* is replaced with local axial coordinate *z*.

$$Gz\,\phi = \frac{aL}{\langle v \rangle d^2} \frac{z}{L} = \frac{az}{\langle v \rangle d^2} \tag{8.32}$$

Next, the solutions of equation (8.22) for the two different velocity profiles will be examined. In Figure 8.3 the local Nu value is plotted as a function of the local number $Gz\,\phi$ for both a uniform and a parabolic velocity profile, and in Figure 8.4 the dimensionless flow average temperature $\langle Y \rangle$ is plotted as a function of Gz, again for both velocity profiles. Note that $\langle Y \rangle$ is solely dependent on the overall Graetz number Gz, while the Nusselt number Nu also depends on the local Graetz number $Gz\,\phi$, i.e. the (dimensionless) axial position.

Two limiting situations are distinguished:

1. Thermally *developing* flow: In this region, the local Nusselt number is a function of $Gz\,\phi$
2. Thermally *developed* flow: In this region, the local Nusselt number is constant.

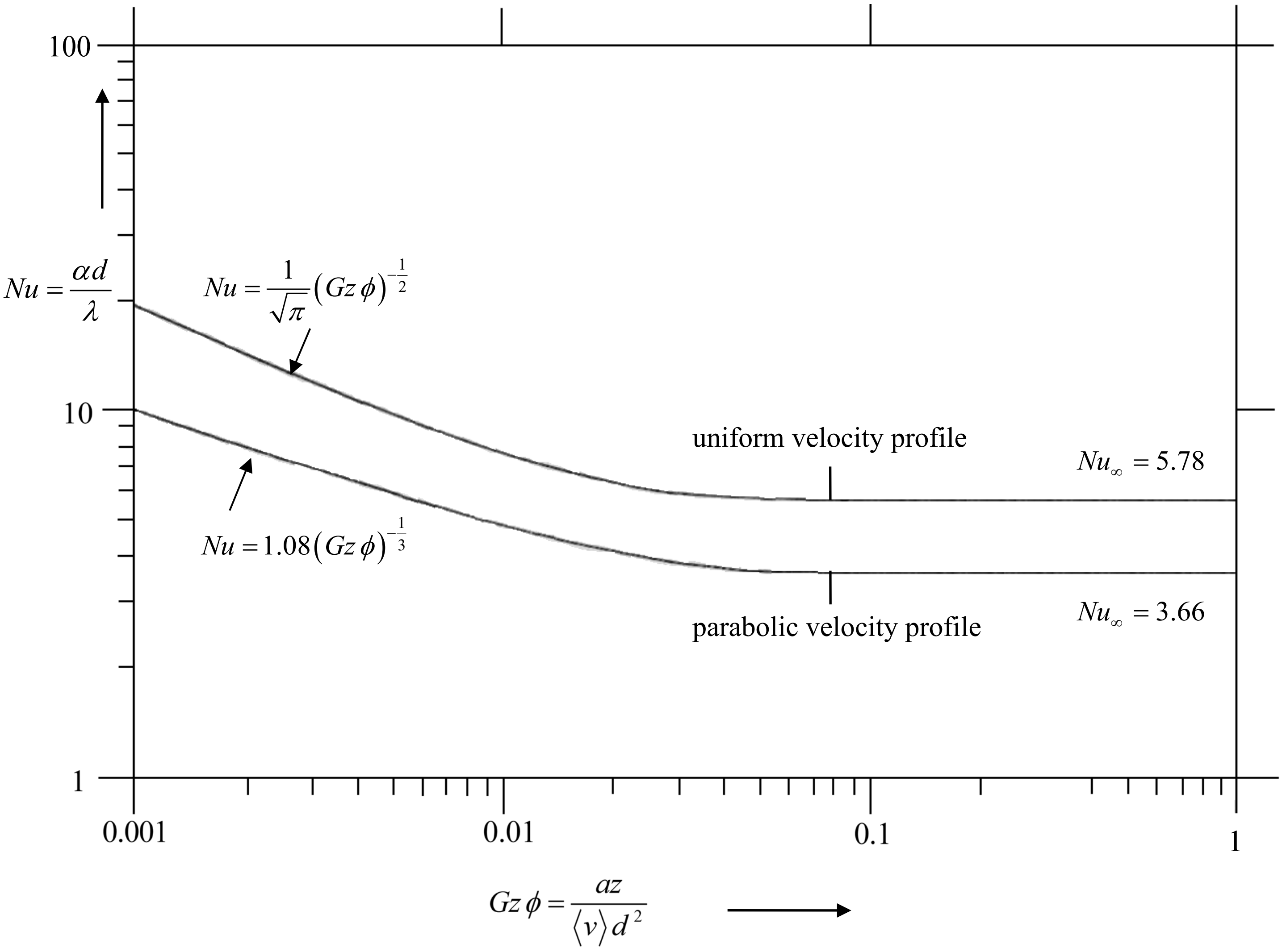

Figure 8.3 The local value of the Nusselt number as a function of the local Graetz number defined by equation (8.32) for a uniform and parabolic velocity profile (both laminar flow) in a cylindrical tube

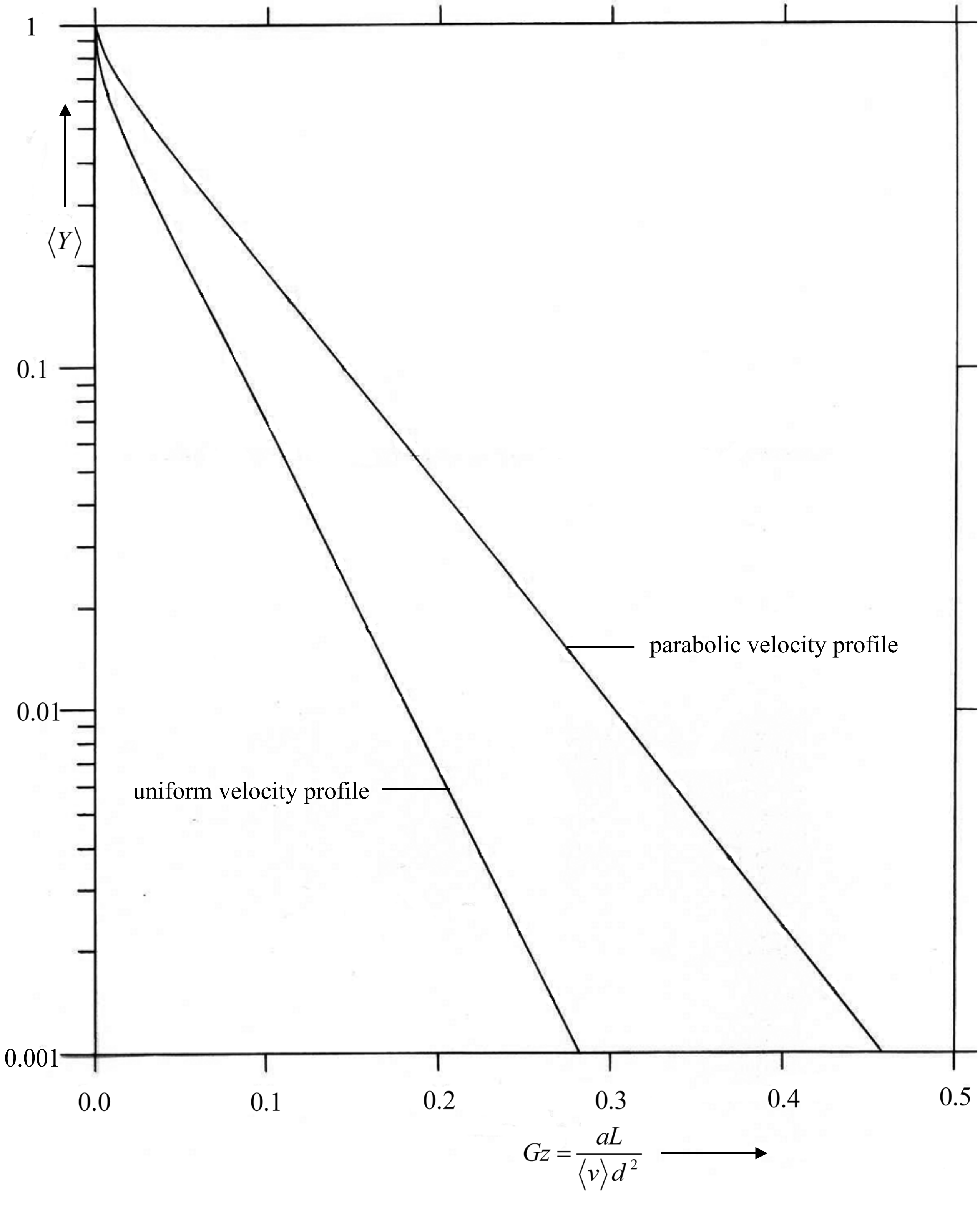

Figure 8.4 The dimensionless flow average temperature $\langle Y \rangle$ as a function of the Graetz number Gz for a uniform and parabolic velocity profile (both laminar flow) in a cylindrical tube

Uniform velocity profile (laminar plug flow)

For the case of a uniform velocity profile, all equations (thermal energy balance and boundary conditions) are basically the same as the equations we had derived before for instationary heat conduction in an infinitely long cylinder, compare e.g. the following equations:

Steady laminar convective flow through a tube with a uniform velocity profile with heat penetration via the walls:

$$\langle v \rangle \frac{\partial T}{\partial z} = a \frac{1}{r} \frac{\partial}{\partial r}\left(r \frac{\partial T}{\partial r} \right) \tag{8.33}$$

Instationary molecular transport into a cylinder:

$$\frac{\partial T}{\partial t} = a \frac{1}{r} \frac{\partial}{\partial r}\left(r \frac{\partial T}{\partial r} \right) \tag{8.34}$$

It can be seen that when selecting $t = \frac{z}{\langle v \rangle}$, which represents the travelling time of the medium through the tube, both equations become identical (which is allowed only because $\langle v \rangle$ is a constant, i.e. for uniform velocity profile!). Physically, this means the following. When looking at the heat transport process from a stationary coordinate system, fluid is flowing through the tube and a steady state profile of the mixing-cup temperature as a function of the axial coordinate is observed. However, imagine we would be able to miniaturize ourselves and be able to travel along with the fluid on its path through the tube. In this case, we would actually see the temperature profile in the radial direction evolving without any convective contribution, since the fluid flows as a plug through the tube (i.e. no radial velocity differences). It is stressed here, that the analogy is only valid for the case of a uniform velocity profile. Thus, the case of steady convective transport with radial conduction with a uniform velocity profile corresponds with the case of instationary radial conduction, simply by changing over to the local residence time. Therefore, all the solutions discussed in the previous chapter (e.g. graphical solution given in section 0) are equally valid for this case of laminar plug flow through a tube.

Thus, the local Greatz number is related to the Fourier number. When the time t from the Fourier number Fo is replaced by the travelling time $z/\langle v \rangle$ of the medium in the tube, the following is obtained:

$$Fo = 4Gz\,\phi \tag{8.35}$$

This can be seen very clearly by slightly rewriting the dimensionless numbers for the case of a cylinder:

$$Gz\phi = \frac{a}{d^2} \frac{z}{\langle v \rangle} = \frac{1}{4} \frac{a}{R^2} \frac{z}{\langle v \rangle} \tag{8.36}$$

and:

$$Fo = \frac{a}{R^2} t \tag{8.37}$$

The local Greatz and Fourier numbers differ by a factor 4, which is caused by choice of different definitions of the characteristic length for a cylinder between these dimensionless variables, namely the radius *R* for the *Fo* number and the diameter *d* for the *Gz* number.

Thermally developing flow

In analogy with instationary heat conduction in an infinitely long bar, using the results of the penetration theory, the following holds for the local Nu for laminar plug flow:

$$Nu = \frac{\alpha d}{\lambda} = \frac{1}{\sqrt{\pi}}\left(\frac{az}{\langle v\rangle d^2}\right)^{-\frac{1}{2}} = \frac{1}{\sqrt{\pi}}\left(Gz\,\phi\right)^{-\frac{1}{2}} \tag{8.38}$$

when the condition $Gz\,\phi < 0.01$ is fulfilled. For the length-averaged Nu-value $\langle Nu\rangle$ the following applies:

$$\langle Nu\rangle = \frac{\langle\alpha\rangle d}{\lambda} = \frac{2}{\sqrt{\pi}}\left(\frac{aL}{\langle v\rangle d^2}\right)^{-\frac{1}{2}} = \frac{2}{\sqrt{\pi}}\left(Gz\right)^{-\frac{1}{2}} \tag{8.39}$$

when the condition $Gz < 0.01$ is satisfied. Note the slightly more stringent restriction compared to the penetration theory for a flat plate, because of the cylindrical geometry.

Equations (8.38) and (8.39) can easily be obtained from (7.61) and (7.62) by taking the tube diameter d as the characteristic length in the Nusselt number instead of the radius R. Note that the radius of curvature of the cylinder is neglected (compared to the heat penetration depth) and that the driving force is calculated with the inlet temperature T_0 instead of the flow average temperature $\langle T\rangle$. In the thermally developing regime these approximations can be justified because there is only a small amount of heat-transfer realized.

The equations show that the dimensionless heat transfer coefficient *Nu* is decreasing with square-root of the local *Gz* number, which is related to the fact that the dimensionless temperature gradient *at* the wall is decreasing along the axial coordinate. In Figure 8.3 the *Nu* number is plotted as a function of the local *Gz* number.

Thermally developed flow

As can be seen from Figure 8.3, for $Gz\,\phi < 0.1$ the Nu number decreases continuously for increasing values of $Gz\,\phi$, however, for $Gz\,\phi > 0.1$ the local dimensionless heat exchange coefficient becomes constant and approaches the asymptotic value for an infinitely long tube. This is referred to as the regime of thermally fully developed flow. In the thermally developed regime, the shape of the radial temperature profile no longer changes, so that the dimensionless temperature gradient at the wall, and hence the dimensionless heat transfer coefficient, becomes constant (obviously the mixing-cup temperature is still changing!).

The Nu -values reach an asymptotic value for an infinitely long tube when $Gz\,\phi > 0.1$.

$$Nu_\infty = \frac{\alpha_\infty d}{\lambda} = 5.78 \quad \text{(uniform velocity profile)} \tag{8.40}$$

It is stressed here that this is a *local* Nusselt number. For $Gz >> 0.1$, the length-averaged $\langle Nu \rangle$ will converge towards Nu_∞. For practical applications, however, in general the influence of the heat transfer in the region for $Gz \cdot \phi \le 0.1$ on $\langle Nu \rangle$ is significant, so that for these cases $\langle Nu \rangle > Nu_\infty$.

The thermally fully developed heat transfer regime is of little practical importance, because for $Gz.\phi > 0.1$ the heat transfer (due to the small driving force) is relatively little effective. The regime with thermally developing flow (i.e. with a non-constant (local) heat transfer coefficient) however, is of great practical importance and occurs at relatively low $Gz.\phi$ values (in practice, at the beginning of the tube).

Parabolic velocity profile (Hagen-Poiseuille flow)

Thermally developing flow:
For a parabolic velocity profile (the usual case of laminar flow through a tube), given by equation (8.28), the following result can be derived by solving equation (8.22) with boundary conditions (8.24), (8.25) and (8.26):

$$Nu = \frac{\alpha d}{\lambda} = 1.08\left(\frac{az}{\langle v \rangle d^2}\right)^{-\frac{1}{3}} = 1.08\left(Gz\,\phi\right)^{-\frac{1}{3}} \tag{8.41}$$

when the condition $Gz.\phi < 0.01$ is satisfied. For the *Nu* value averaged over the tube length L , $\langle Nu \rangle$, can be derived (check yourself!):

$$\langle Nu \rangle = \frac{\langle \alpha \rangle d}{\lambda} = 1.62\left(\frac{aL}{\langle v \rangle d^2}\right)^{-\frac{1}{3}} = 1.62\left(Gz\right)^{-\frac{1}{3}} \tag{8.42}$$

if $Gz < 0.01$.
Substituting equation (8.41) in the differential thermal energy balance given by equation (8.10), the following expression for the (dimensionless) flow averaged temperature can be derived (check this yourself!):

$$\ln\left(\frac{T_1 - \langle T \rangle}{T_1 - T_0}\right) = \ln\left(\langle Y \rangle\right) = -6.48\left(\frac{aL}{\langle v \rangle d^2}\right)^{\frac{2}{3}} = -6.48\left(Gz\right)^{\frac{2}{3}} \tag{8.43}$$

Again, in the thermally developing regime with a parabolic velocity profile, the dimensionless heat transfer coefficient decreases with increasing local *Gz* number, however, now with the power -1/3 (instead of -1/2 for the case of a uniform velocity profile).

Thermally developed flow

As can be discerned from Figure 8.3, also for the case of a parabolic velocity profile, the *Nu* number approaches a constant value when $Gz\,\phi > 0.1$:

$$Nu_{\infty} = \frac{\alpha_{\infty} d}{\lambda} = 3.66 \quad \text{(parabolic velocity profile)} \tag{8.44}$$

The asymptotic value in case of a parabolic velocity profile is lower than the asymptotic value in case of a uniform velocity profile (see also Figure 8.3, showing that the Nu -curve for the uniform velocity profile lies above the Nu -curve for the parabolic velocity profile). This is caused by the larger fluid velocity (and thus a larger thermal loading capacity) near the heat-exchanging fixed wall in case of plug flow.

With respect to the presented results it should be noted that two important assumptions were made:

a) The physical properties of the flowing medium are independent of the temperature.
b) The flow is hydrodynamically fully developed.

The implications of deviations from these assumptions are discussed below.

Temperature dependent viscosity

When the physical properties of the flowing medium (like density ρ and viscosity η) are constant, the (parabolic) laminar velocity distribution is not influenced by the prevailing temperature gradients. However, the viscosity of a fluid is (strongly) dependent on the temperature and therefore the velocity profile will not be parabolic, which of course has consequences for the heat transfer. It has been empirically determined that for heat transfer in laminar tubular flow, the following modified form of equation (8.42) gives a satisfactory representation of the experimental results:

$$\langle Nu \rangle = 1.86 (Gz)^{-\frac{1}{3}} \left(\frac{\eta_g}{\eta_w} \right)^{\frac{1}{7}} \tag{8.45}$$

where η_g and η_w are the viscosities at the flow-averaged temperature $\langle T \rangle$ and the wall temperature T_1, respectively. Because the viscosity of a liquid decreases with increasing temperature (note: for a gas it is the other way around!), from equation (8.45) (variable viscosity) and equation (8.42) (constant viscosity) it can be concluded that the heat transfer is improved when a flowing liquid is heated, while the opposite is true when the liquid is cooled. This behavior is explained by the change in shape of the radial velocity profile due to the temperature gradients and is illustrated in a qualitative way in Figure 8.5. When interpreting this figure, we compare cases with the same average fluid velocity $\langle v \rangle$. In case of heating of a liquid in a tube, the viscosity near the tube wall is lower than that in the centre of the tube, causing the velocity profile to become more flattened near the wall compared to the isothermal case with a parabolic velocity profile. The higher liquid velocities near the wall induce a higher 'refresh-rate' near the wall, increasing the heat transfer exchange of the liquid with the wall. In the case of cooling of a liquid in a tube, the viscosity near the tube wall is higher than in the centre of the tube and the velocity profile is elongated in the centre when compared to isothermal flow, resulting in a decrease of the heat exchange rate with the wall.

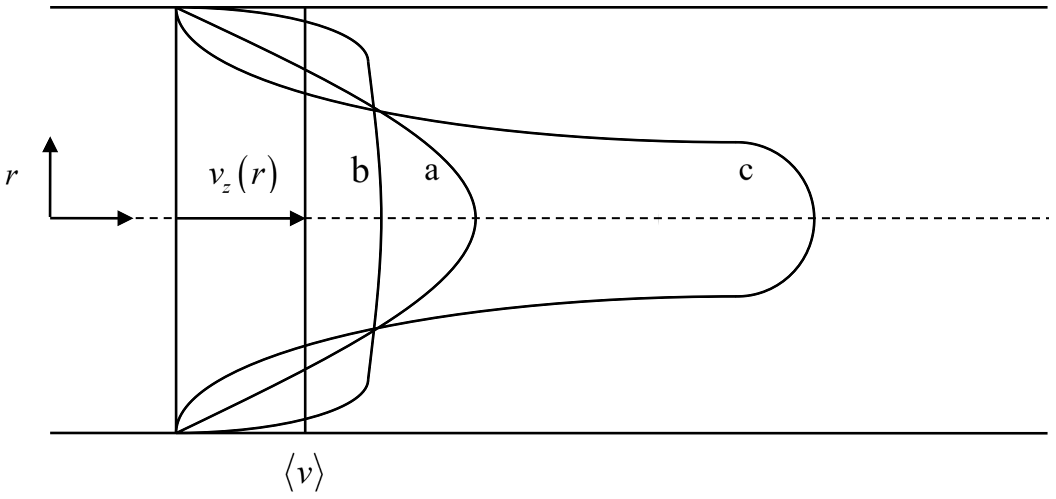

Figure 8.5 Velocity profiles in laminar tubular flow (a: isothermal flow, b: heated tube wall, c: cooled tube wall). The average flow velocity $\langle v\rangle$ is kept constant.

Hydrodynamically developing flow

In the derivations described before, it has always been assumed that the flow was hydrodynamically fully developed (i.e. the velocity profile is no longer changing as a function of the axial position), already at the beginning of the tube. However, there are practical situations in which the flow is hydrodynamically still developing, so the temperature profile and the velocity profile develop simultaneously. A well-known example is the case of heat exchangers where the heat-exchanging medium flows from a distributing part to a large number of parallel tubes, where the heat exchange occurs. At the beginning of these tubes, the velocity profile will be flat and with increasing axial position in the tubes, the velocity profile will develop gradually. In this situation, the ratio of two physical variables which determine the (radial) molecular transport of momentum and thermal energy plays an important role. These variables are the kinematic viscosity ν and the thermal diffusivity a, respectively. The ratio of these variables is called the Prandtl number, Pr, which is defined as:

$$Pr = \frac{\nu}{a} = \frac{\eta C_p}{\lambda} \tag{8.46}$$

In the hydrodynamically developing regime, the Prandtl number appears as an independent dimensionless group and for the local value of the Nusselt number in laminar tubular flow, the following approximation could be used:

$$Nu = \frac{\alpha d}{\lambda} = 0.332\left(Re\frac{d}{z}\right)^{\frac{1}{2}}\left(Pr\right)^{\frac{1}{3}} \tag{8.47}$$

This expression was obtained from the Nusselt correlation for flow past a flat plate (see paragraph 8.3) by multiplying both sides with d/z and replacing the flow velocity v_∞ by $\langle v \rangle$. From expression (8.47) follows that for hydrodynamically developing flow, the exponents of the Reynolds number Re and the Prandtl number Pr are different, while for hydrodynamically developed flow (equation (8.41)) these exponents have the same value, because $Gz\,\phi$ can be rewritten as:

$$Gz\,\phi = \frac{az}{\langle v \rangle d^2} = \frac{\nu}{\langle v \rangle d}\frac{a}{\nu}\frac{z}{d} = \frac{1}{Re\,Pr}\frac{z}{d} \tag{8.48}$$

Taking the flat plate analog a step further, a rough estimate for the region in which the flow is still hydrodynamically developing may be obtained from the penetration depth of the laminar velocity profile for a flat plate:

$$1 \geq \frac{4.64}{R}\sqrt{\frac{\nu z}{\langle v \rangle}} \tag{8.49}$$

This allows for a rough estimate of the influence of the local Nusselt values in the hydrodynamically developing region on the length-averaged Nusselt number. In the remainder of this course, it is assumed that the flow is always hydrodynamically fully developed already from the inlet of the tube.

8.2.2 Turbulent flow through tubes

In process equipment we are often confronted with situations in which a turbulent flowing medium exchanges heat with a wall. This type of heat transfer cannot be described analytically, so we have to resort to an empirical approach. Dimensionless groups are used to allow for a compact description of the experimental results. For laminar flow, the heat transfer could be described with $Nu = f\left(Gz\right)$, for turbulent flow this can be done with a relation of the form $Nu = f\left(Re, Pr\right)$. For heat transfer between a turbulent flowing medium and a fixed wall, the Nusselt correlations have the following general form:

$$Nu = C_1 + C_2\left(Re\right)^m\left(Pr\right)^n \tag{8.50}$$

Here the constants C_1, C_2, m and n have to be determined experimentally. In situations in which there is transfer between a turbulent flowing medium and a *fixed* wall (i.e. a wall where the "no-slip" condition applies), a theoretical foundation can be laid using the film theory, while for situations in which there is transfer between a turbulent flowing medium and a *freely moving* wall (i.e. a wall where the "free-slip" condition holds), a theoretical foundation can be laid using the penetration theory. This difference in wall types, and corresponding boundary condition for momentum transfer with the wall, results in a difference in the exponent n of Pr in equation (8.50). For heat exchange with fixed walls, the exponent of Pr has typically the value of $1/3$, while for heat exchange with freely moving walls (interfaces), the exponent has the value of $1/2$. Since heat transfer at freely moving walls occurs in practice less frequent than heat transfer at fixed walls, in the next paragraph the theoretical foundations of equation (8.50) are given using the film theory. In mass transport, the situation is actually the other way around and the theoretical foundations can in principle be based on the penetration theory.

For heat transfer in turbulent flow through a tube, there are many practical correlations available, of which the most well-known is given by:

$$Nu = 0.023\left(Re\right)^{0.8}\left(Pr\right)^{0.33} \tag{8.51}$$

which can be used under the following conditions: $0.5 < Pr < 100$, $10^4 < Re < 10^5$ and $L/d > 60$ (with L is the length of the tube). This empirical correlation has a remarkably good correspondence with the result that we will derive with film theory in the next paragraph. Note that this local Nusselt number is independent of the axial position, contrary to the case for laminar flow in the thermally developing regime. Finally, it is noted that this equation is often also used to find a quick *estimate* of the heat transfer coefficient for turbulent flow through channels with a non-circular cross-section. In this case, the tube diameter d needs to be replaced by the hydraulic diameter d_h in the equations for Re and Nu.

Theoretical background

In Figure 8.6, a qualitative picture of the radial profiles of the time-averaged axial velocity and temperature are shown for heat transfer in turbulent flow through a tube. In turbulent flow, for both profiles an (almost) flat profile is observed in the center of the tube, while in the (very) thin fluid layers near the tube wall (the hydrodynamic and thermal boundary layer, respectively), strong velocity and temperature gradients are observed. The film theory schematizes this as shown in Figure 8.6.

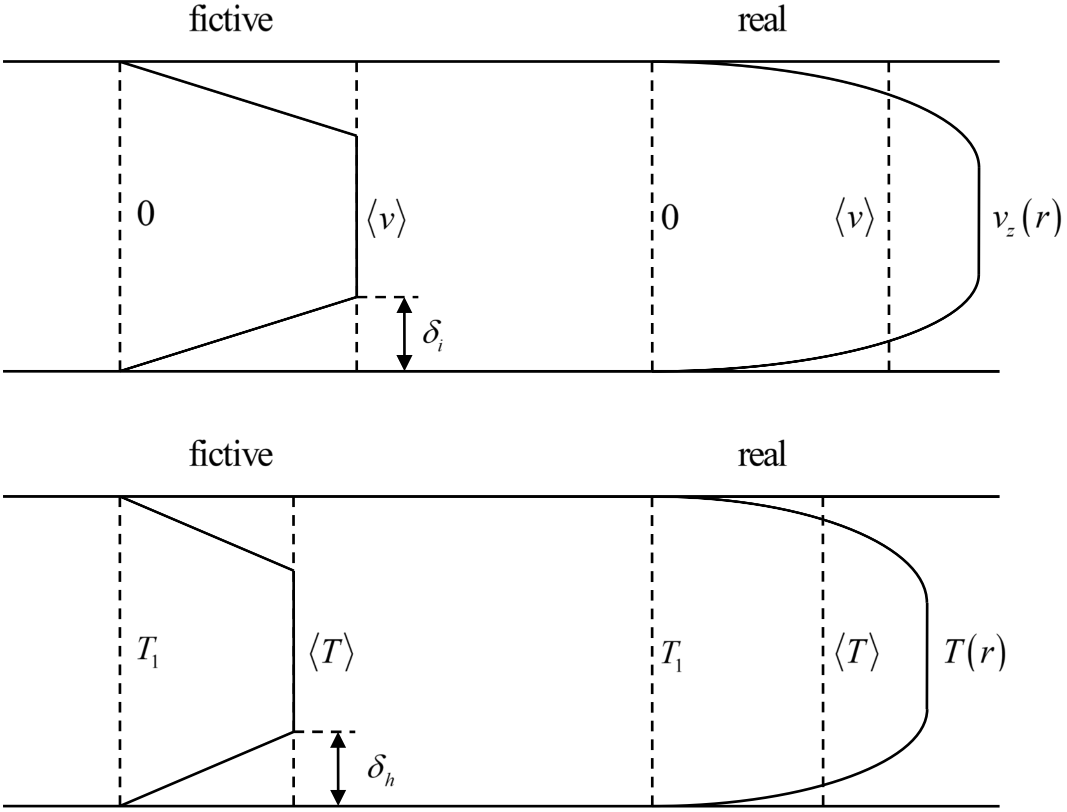

Figure 8.6 Schematized radial velocity and temperature profiles in terms of the film theory for heat transfer in turbulent flow through a tube.

The (radial) velocity profile is approximated by a trapezoid, so that the flow is approximated as core-annulus flow. The core moves with a uniform velocity $\langle v \rangle$, while in the annulus region close to the wall with a thickness δ_i the velocity reduces linearly from $\langle v \rangle$ to 0 at the tube wall. In the core, there is a very strong radial exchange of momentum by the vortices (resulting in a uniform velocity profile in the core), while in the hydrodynamic boundary layer, according to the assumption of the film theory, the radial momentum transport is dominated by molecular transport. It will be clear that this strict spatial distinction between the mechanisms of radial impulse transport is fictitious. In reality, there will be a gradual transition. However, the approximation shows a larger resemblance to physical reality for higher Re values, i.e. when the flow through the tube is more turbulent. For the radial temperature profile, an analogous approximation is made, where the thickness of the wall zone is denoted by δ_h.

Starting with a macroscopic momentum balance:

$$0 = \sum F = p_0 S - p_L S - \tau_w ZL = \left(\Delta p\right) S - \tau_w ZL \tag{8.52}$$

and the Fanning friction equation (basically the definition equation of the friction coefficient *f*):

$$\Delta p = f\left(\frac{ZL}{S}\right)\left(\frac{1}{2}\rho\left\langle v\right\rangle^2\right) = 4f\left(\frac{ZL}{4S}\right)\left(\frac{1}{2}\rho\left\langle v\right\rangle^2\right) \tag{8.53}$$

the following can be derived for the average shear stress on the wall τ_w in turbulent flow:

$$\tau_w = \frac{f}{2}\left(\rho\left\langle v\right\rangle^2\right) \tag{8.54}$$

According to the film theory, the following approximation for the velocity gradient is used:

$$\tau_w = -\eta\left.\frac{dv_z}{dr}\right|_{r=R} = -\eta\frac{\left\langle v\right\rangle - 0}{\left(R-\delta_i\right)-R} = \eta\frac{\left\langle v\right\rangle}{\delta_i} \tag{8.55}$$

and from equations (8.54) and (8.55) follows:

$$\frac{d}{\delta_i} = \frac{f}{2}Re \tag{8.56}$$

Completely analogously for the heat transfer exchange between the fluid and the wall, using Newton's law of cooling (using T_1 to denote the wall temperature):

$$\Phi_h'' = \alpha\left(\left\langle T\right\rangle - T_1\right) \tag{8.57}$$

and the approximation based on the film theory:

$$\Phi_h'' = -\lambda\left.\frac{\partial T}{\partial r}\right|_{r=R} = -\lambda\frac{\left\langle T\right\rangle - T_1}{\left(R-\delta_h\right)-R} = \lambda\frac{\left(\left\langle T\right\rangle - T_1\right)}{\delta_h} \tag{8.58}$$

so that

$$\alpha\left(\left\langle T\right\rangle - T_1\right) = \lambda\frac{\left(\left\langle T\right\rangle - T_1\right)}{\delta_h} \tag{8.59}$$

From equation (8.59) follows after substitution of (8.56) for the Nu-number:

$$Nu = \frac{\alpha d}{\lambda} = \frac{d}{\delta_h} = \frac{d}{\delta_i}\frac{\delta_i}{\delta_h} = \frac{f}{2}Re\frac{\delta_i}{\delta_h} \tag{8.60}$$

For the ratio of the hydrodynamic and thermal boundary layer thickness holds for $Pr >> 1$ (which is often valid for fluids):

$$\frac{\delta_i}{\delta_h} = \left(\frac{\nu}{a}\right)^{\frac{1}{3}} = \left(Pr\right)^{\frac{1}{3}} \tag{8.61}$$

The friction coefficient f in equation (8.60) depends on Re. For smooth tubes in the range $4 \cdot 10^3 < Re < 10^5$, f is well described by Blasius's relation:

$$4f = 0.316\ (Re)^{-0.25} \tag{8.62}$$

Substitution of equations (8.61) and (8.62) into equation (8.60) yields the following expression for the Nu-number:

$$Nu = 0.0395\left(Re\right)^{0.75}\left(Pr\right)^{0.33} \tag{8.63}$$

Note that the same dependency of Nu on the Pr number is found as was derived before for laminar flow. Despite the fact that the film theory is based on a strong simplification of physical reality, the agreement between equation (8.63) and experimental results, fitted in equation (8.51), is quite reasonable. For actual calculations, of course equation (8.51) should be used. When using empirical correlations, one needs to realize that these are representations of a collection of measuring points in a mathematical form. This means, that one always needs to carefully check the range of validity (geometry, Re-range, Pr-range, etc.) of the correlation and how the different physical variables are defined. In literature, for a specific situation, not always the same type of Nu-correlation is used and/or the exponents of Re and Pr can differ. In addition, often there are additional correction factors to account for e.g.:

a) The temperature dependency of the viscosity;
b) Development of the thermal boundary layer in the (turbulent) flow.

Temperature dependency of the viscosity

The effect of variable viscosity on heat transfer is taken into account for turbulent flow, analogous to the situation for laminar tubular flow, by multiplying the right hand side of equation (8.51) with $\left(\eta_g / \eta_W\right)^{1/7}$. This is referred to as the Sieder-Tate correction. Here, η_g is the viscosity corresponding to the flow-averaged temperature and η_w is the viscosity at the wall temperature T_1.

Thermally developing turbulent flow

Also in the case of turbulent flow, there is a region where the flow is not yet thermally developed, and where the local heat transfer coefficient is higher than in the remainder of the tube. However, this region is much smaller for turbulent flow than in the case of laminar flow and can often be neglected for sufficiently long and/or thin tubes. Often the effect of the development of the development of the thermal boundary layer is taken into account by multiplying the right hand side of equation (8.51) with a correction factor $\left(1 + d/L\right)^{2/3}$.

In practice, often charts with empirical data are used for the description of heat transfer to a (turbulent) flowing medium. In these charts, both the obtained empirical Nusselt correlation and the primary measurement data are shown. In this way, one can quickly see how accurately the obtained empirical correlation describes the experimental data. In Figure 8.7 an example is shown in which the dimensionless quantity $\left(Nu/Pr^{0.42}\right) / \left(\eta_g / \eta_W\right)^{1/7}$ is plotted as a function of Re, for heat transfer in tubular flow. In the turbulent regime ($Re > 2200$) the following relation can be extracted from the figure:

$$Nu = 0.015\left(Re\right)^{0.83}\left(Pr\right)^{0.42}\left(\frac{\eta_g}{\eta_W}\right)^{1/7} \tag{8.64}$$

while for the laminar regime ($Re < 2000$) the following applies:

$$Nu = 1.86\left(Re\frac{d}{L}\right)^{1/3}\left(Pr\right)^{0.42}\left(\frac{\eta_g}{\eta_W}\right)^{1/7} \tag{8.65}$$

Equations (8.64) and (8.65) show small discrepancies compared to the earlier presented correlations for heat transfer in turbulent and laminar tubular flow. The most important cause for this is the difference in primary experimental data, from which the empirical correlation is determined. The relations presented earlier are used as a basis for this course. The twist in Figure 8.7 relates to the transition from laminar to turbulent tubular flow, which occurs around $Re \approx 2200$.

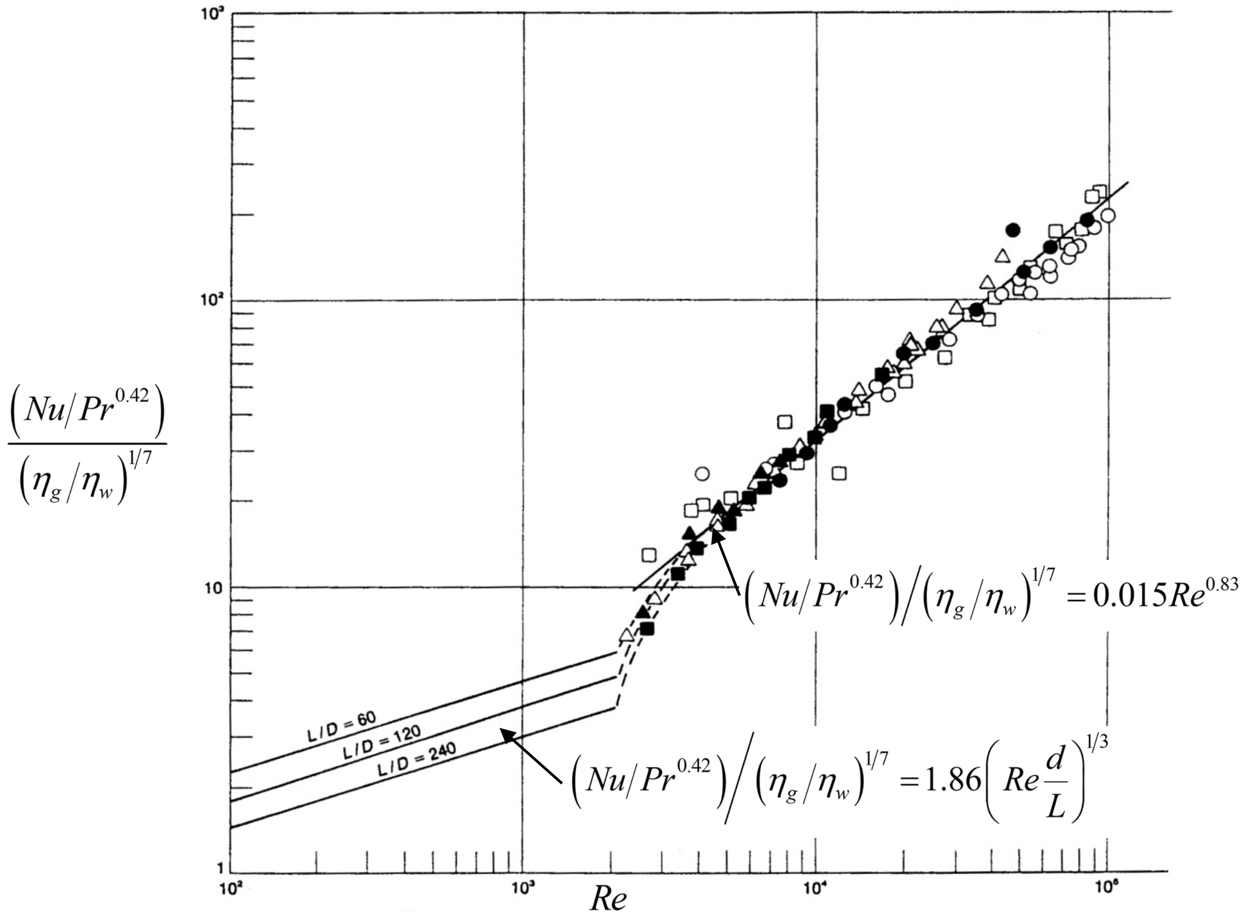

Heat transfer to fluids in turbulent flow in tubes.
○ Lawrence and Sherwood, heating water, $L/D = 59$. △ Morris and Whitman, heating and cooling oil, $L/D = 196$. □ Sherwood and Petrie, heating acetone, $L/D = 96$. ● Deissler and Eian, heating air, $L/D = 100$. ▲ Colburn and Coghlan, heating hydrogen–nitrogen mixtures, $L/D = 97$. ■ Friend and Metzner, heating corn syrup, $L/D = 161$.

Figure 8.7 The dimensionless variable $\left(Nu/Pr^{0.42}\right)/\left(\eta_g/\eta_w\right)^{1/7}$ as a function of the Reynolds number Re for heat transfer in tubular flow. (at $Re \approx 2200$ a transition of laminar to turbulent flow occurs).

8.2.3 Overall heat transfer coefficient

In practice, we often encounter situations where there are several heat transfer processes occurring in series, as e.g. encountered in the description of heat exchange between two or more phases in a heat exchanger. In addition to the partial local heat transfer coefficients α, which are given in dimensionless form in equations (8.64) and (8.65) for turbulent and laminar tubular flow conditions respecively, we make use of an overall heat transfer coefficient U. We will elucidate how to derive the overall heat transfer coefficient for a series connection of heat transfer resistances for the simple case of a flat plate geometry (or the limiting case of a thin-walled tube), which is easily extended to cylindrical geometries where the curvature of the tube cannot be neglected.

As an example, we consider heat exchange between two flowing phases "1" and "2" (with bulk mixing-cup temperatures $\left\langle T^{(1)}\right\rangle$ and $\left\langle T^{(2)}\right\rangle$), which are separated by a metal wall (with thickness d_m and thermal conductivity λ_m), as schematically depicted in Figure 8.8. On the metal wall in contact with phase "2", a thin layer of dirt has precipitated, with a thickness d_d and thermal conductivity λ_d. The (partial) heat transfer of the flowing phases "1" and "2" to the walls is described with the respective (partial) convective heat transfer coefficients α_1 and α_2. An expression for the stationary heat flux between phases "1" and "2" needs to be obtained in terms of the bulk mixing-cup temperatures of the two phases.

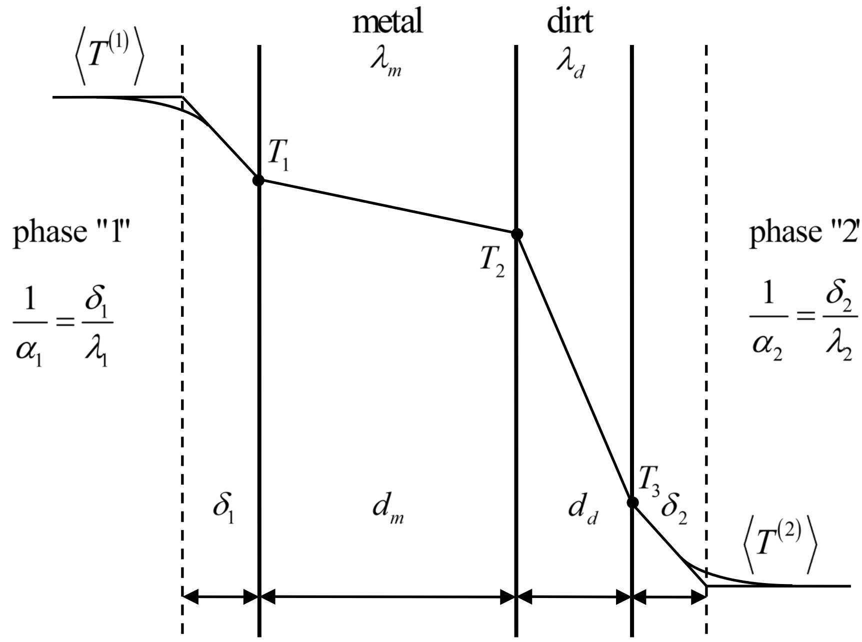

Figure 8.8 Qualitative description of temperature profiles in two heat-exchanging phases "1" and "2", which are separated by a (thin) metal wall. The idealization of the temperature profiles according to the film theory is also illustrated (δ_1 and δ_2 represent the thickness of the thermal boundary layers).

In this situation we face a problem with a serial connection of heat resistances, where the heat flux is constant (in the steady state). The heat transport from phase “1” to phase “2” consists of the following four partial heat transfer steps, with their expressions for the heat flux given by:

1. Heat transport from phase “1” to the metal wall:

$$\Phi_h'' = \alpha_1 \left(\left\langle T^{(1)} \right\rangle - T_1 \right) \tag{8.66}$$

2. Heat transport in the metal wall:

$$\Phi_h'' = \frac{\lambda_m}{d_m} \left(T_1 - T_2 \right) \tag{8.67}$$

3. Heat transport in the dirt layer:

$$\Phi_h'' = \frac{\lambda_d}{d_d} \left(T_2 - T_3 \right) \tag{8.68}$$

4. Heat transport from the dirt layer to phase “2”:

$$\Phi_h'' = \alpha_2 \left(T_3 - \left\langle T^{(2)} \right\rangle \right) \tag{8.69}$$

Elimination of the temperatures T_1, T_2 and T_3 yields the following relation between the heat flux and the overall driving force ($\left\langle T^{(1)} \right\rangle - \left\langle T^{(2)} \right\rangle$):

$$\Phi_h'' = \frac{\left\langle T^{(1)} \right\rangle - \left\langle T^{(2)} \right\rangle}{\dfrac{1}{\alpha_1} + \dfrac{d_m}{\lambda_m} + \dfrac{d_d}{\lambda_d} + \dfrac{1}{\alpha_2}} \tag{8.70}$$

The heat flux between phases “1” and “2” can be defined in terms of the overall heat transfer coefficient U:

$$\Phi_h'' = U \left(\left\langle T^{(1)} \right\rangle - \left\langle T^{(2)} \right\rangle \right) \tag{8.71}$$

so that from equations (8.70) and (8.71) the following expression for the overall heat transfer coefficient U is obtained:

$$\frac{1}{U} = \frac{1}{\alpha_1} + \frac{d_m}{\lambda_m} + \frac{d_d}{\lambda_d} + \frac{1}{\alpha_2} \tag{8.72}$$

Inspection of equation (8.72) learns that the total heat resistance $1/U$ consists of the sum of two convective heat resistances ($1/\alpha_1$ and $1/\alpha_2$) and two conductive heat resistances (d_m/λ_m and d_d/λ_d).

If the thickness of the tube wall is not negligible with respect to the tube diameter, but the thickness of the dirt layer still is, the relation for the overall heat transfer coefficient takes the following form:

$$\frac{1}{U_o}=\frac{1}{\alpha_1}+\frac{d_o\ln\left(\frac{R_{m,o}}{R_{m,i}}\right)}{2\lambda_m}+\frac{R_{m,o}}{R_{m,i}}\cdot\frac{d_d}{\lambda_d}+\frac{R_{m,o}}{R_{m,i}}\cdot\frac{1}{\alpha_2} \tag{8.73}$$

where $R_{m,o}$ and $R_{m,i}$ are the outer and inner radius of the metal tube, respectively. It is easily verified that that for the limit $d_m = R_{m,o} - R_{m,i} \to 0$, this approaches the case described above for the thin-walled tube.

To conclude this section, in Table 8.1 an overview is given of typical values of the heat transfer coefficients for a number of different heat transfer processes. When using values from this table, realize that only the order of magnitude of U is given.

Table 8.1 Typical values for heat transfer coefficients (in $W/\left(m^2\,°C\right)$) for a number of heat transfer processes.

Heat flow	Gas (free) $\alpha = 5-15$	Gas (flow) $\alpha = 10-100$	Fluid (free) $\alpha = 50-1000$	Fluid (flow) Water: $\alpha = 3000-10000$ Other fluids: $\alpha = 500-2000$	Boiling fluid Water: $\alpha = 3500-60000$ Other fluids: $\alpha = 1000-20000$
Gas (free) $\alpha = 5-15$	room-outside through glass $U = 1-2$	Overheaters $U = 3-10$		Furnace $U = 10-40$ + Radiation	Steam kettle $U = 10-40$ + Radiation
Gas (flow) $\alpha = 10-100$		Heat exchangers for gasses $U = 10-30$	Gas kettle $U = 10-50$		
Fluid (free) $\alpha = 50-1000$	Radiator central heating $U = 5-15$		Oil bath for heating $U = 25-500$	Cooling spiral $U = 500-1500$ When stirred	
Fluid (flow) Water: $\alpha = 3000-10000$ Other fluids: $\alpha = 500-3000$		Gas coolers $U = 10-50$	Heating spiral in vessel Water-water: No stirring: $U = 50-250$ With stirring: $U = 500-2000$	Heat exchangers Water-water: $U = 900-2500$ Water-other: $U = 200-1000$	Evaporators of cooling aggregates, brine coolers $U = 300-1000$
Condensing vapor Water: $\alpha = 5000-30000$ Other fluids: $\alpha = 1000-4000$	Steam radiators $U = 5-20$	Air heaters $U = 10-50$	Steam mantles around vessels with stirrers, Water: $U = 300-1000$ Other fluids: $U = 150-50$	Condensors Steam-water: $U = 1000-4000$ Other vapor-water: $U = 300-1000$	Evaporators Steam-water: $U = 1500-6000$ Steam-other: $U = 300-2000$

8.3 Heat transport in flow past objects

In the case of heat transfer for flow past objects, the flow conditions always correspond with simultaneously hydrodynamically and thermally developing flow. The general form of the Nusselt correlations is given in equation (8.50). For fixed objects, the exponent of the Prandtl number is in principle equal to $1/3$, while for not too high Reynolds numbers, the exponent of the Reynolds number can, as a rule of thumb, be taken equal to $1/2$. For a number of frequently encountered geometries, the appropriate Nusselt correlations will be shortly discussed and graphically depicted.

8.3.1 Flow past a flat plate

For the laminar part of (axial) flow past a flat plate at a uniform temperature, the following is valid for the local Nusselt number Nu_x:

$$Nu_x = \frac{\alpha x}{\lambda} = 0.332\left(Re_x\right)^{0.5}\left(Pr\right)^{0.33} = 0.332\left(\frac{\rho v_\infty x}{\eta}\right)^{0.5}\left(\frac{\nu}{a}\right)^{0.33} \tag{8.74}$$

provided that $Re_x < 3.2\cdot 10^5$ and $0.6 < Pr < 10$, where v_∞ is the (undisturbed) flow velocity and x is the main flow direction. Note that equation (8.74) gives an expression for the local heat transfer coefficient α. For the average heat transfer coefficient over the entire length L of the plate, the following Nusselt correlation is easily derived

$$\langle Nu\rangle = \frac{\langle\alpha\rangle L}{\lambda} = 0.664\left(Re_L\right)^{0.5}\left(Pr\right)^{0.33} = 0.664\left(\frac{\rho v_\infty L}{\eta}\right)^{0.5}\left(\frac{\nu}{a}\right)^{0.33} \tag{8.75}$$

again provided that $Re_L < 3.2\cdot 10^5$ and $0.6 < Pr < 10$. Equation (8.75) is derived from (8.74) by integration over x and subsequently dividing by L (try this yourself!). Both equations are valid for the laminar flow regime, thus at the beginning of the plate.

For sufficiently long plates, a turbulent flow region will develop in the region behind the laminar region. This gives rise to two areas with different flow- and heat transfer characteristics. For $x < x_c$, there is laminar flow, while for $x > x_c$ there is turbulent flow, where x_c represents the x-coordinate at which the change in flow regime occurs (x_c corresponds to the critical Reynolds number $Re_c = \rho v_\infty x_c/\eta$). In the area with turbulent flow, the following empirical Nusselt correlation can be used to describe the local heat transfer coefficient:

$$Nu_x = \frac{\alpha x}{\lambda} = 0.029\left(Re_x\right)^{0.8}\left(Pr\right)^{0.43} = 0.029\left(\frac{\rho v_\infty x}{\eta}\right)^{0.8}\left(\frac{\nu}{a}\right)^{0.43} \tag{8.76}$$

This correlation is valid when: $3.2\cdot 10^5 < Re_x < 5\cdot 10^6$.

For the calculation of the average heat transfer coefficient $\langle\alpha\rangle$ in the case of flow past a flat plate, a distinction is made between two situations:

1. There is turbulent flow over practically the entire plate. For the average heat transfer coefficient $\langle\alpha\rangle$, the following Nusselt correlation is used (via integration of equation (8.76) over *x* and dividing by *L*):

$$\langle Nu\rangle = \frac{\langle\alpha\rangle L}{\lambda} = 0.036\left(Re_L\right)^{0.8}\left(Pr\right)^{0.43} = 0.036\left(\frac{\rho v_\infty L}{\eta}\right)^{0.8}\left(\frac{\nu}{a}\right)^{0.43} \qquad (8.77)$$

2. There is laminar flow at the beginning of the plate (*x*<*x_c*) and turbulent flow at the rest of the plate (*x*>*x_c*). Then, the average heat transfer coefficient $\langle\alpha\rangle$ can be found via:

$$\langle\alpha\rangle = \frac{1}{L}\left\{\int_0^{x_c}\alpha_{\text{laminar}}dx + \int_{x_c}^{L}\alpha_{\text{turbulent}}dx\right\} \qquad (8.78)$$

Substitution of equation (8.74) for α_{laminar} and (8.76) for $\alpha_{\text{turbulent}}$ yields the following Nusselt correlation (check this yourself!):

$$\langle Nu\rangle = 0.036\left[\left(Re_L\right)^{0.8} - \left(Re_c\right)^{0.8}\right]\left(Pr\right)^{0.43} + 0.664\left(Re_c\right)^{0.5}\left(Pr\right)^{0.33} \qquad (8.79)$$

Note that (8.79) reduces to (8.77) when the critical Reynolds number Re_c is much smaller than the Reynolds number over the total plate length Re_L. In this situation, $x_c/L << 1$ and the laminar flow region (that in principle is always present) is of minor importance.

In
Figure 8.9 , the Nusselt correlation for heat transfer for axial flow past a flat plate is illustrated. In this figure, the dimensionless quantity $\left(\langle Nu\rangle/\left(Pr\right)^{0.43}\right)/\left(\eta_\infty/\eta_W\right)^{1/4}$ is shown as a function of the Reynolds number Re. A correction factor for variable viscosity (due to temperature differences) appears, where η_∞ corresponds to the viscosity for the flow conditions in front of the plate. In this figure, also the measuring points, forming the basis of the Nusselt correlation, are shown. The figure shows two curves. The differences between these curves are related to the earlier or later occurrence of the transition to turbulent flow (i.e. for lower or higher Re values). The continuous curve is valid for $Re_c < 10^5$, while for the dashed curve $Re_c \approx 2\cdot 10^5$. Differences in Re_c are caused by differences in the experimental conditions, e.g. the turbulence-intensity of the undisturbed flow.

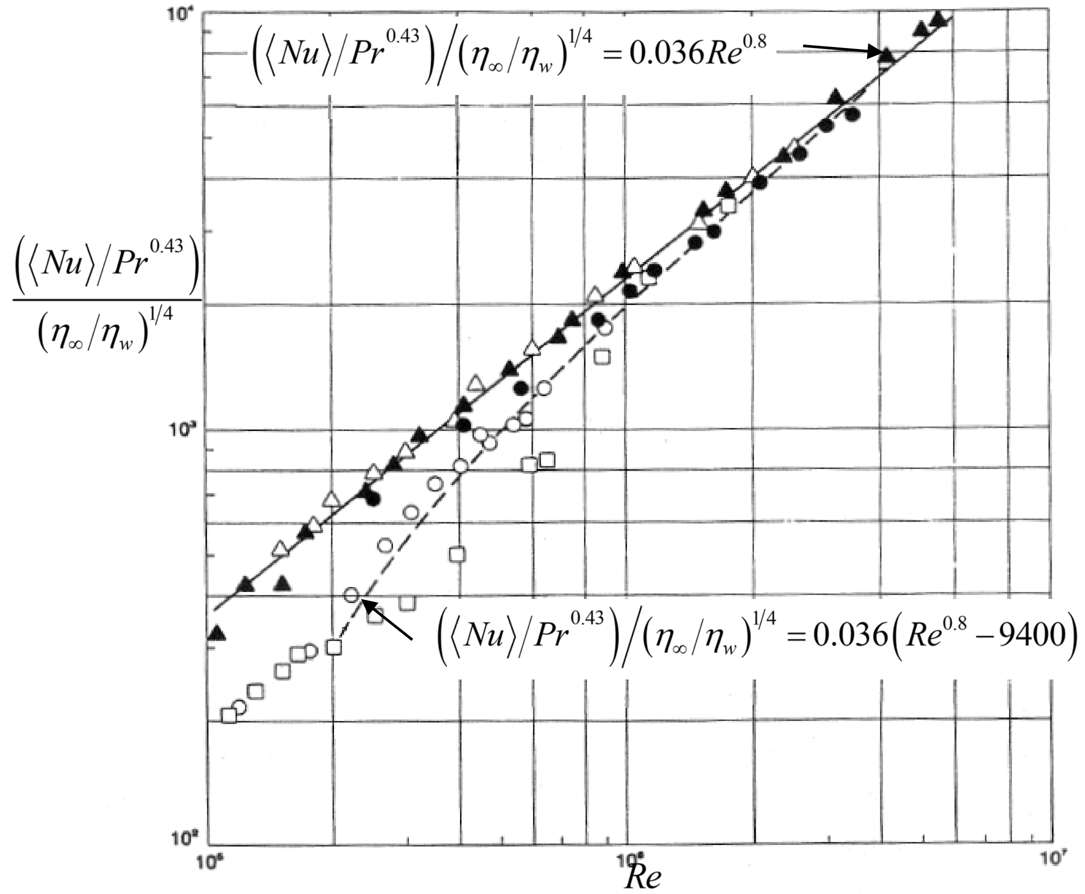

Heat transfer to fluids flowing past a thin, flat plate.
○ Parmalee and Huebscher, heating air, unspecified free stream turbulence. □ Edwards and Furber. heating air, negligible free stream turbulence. △ Edwards and Furber, heating air, 5% free stream turbulence. ● Reynolds, Kays, and Kline, heating air, unspecified free stream turbulence. ▲ Zhukauskas and Ambrazyavichyus, heating and cooling air, water, and oil, unspecified free stream turbulence.

Figure 8.9 The dimensionless variable $\left(\langle Nu\rangle / (Pr)^{0.43}\right) / \left(\eta_\infty / \eta_W\right)^{1/4}$ as a function of the Reynolds number Re for heat transfer in (axial) flow past a flat plate.

8.3.2 Flow past a sphere

For flow past a sphere, the following Nusselt correlation has been determined for the average heat transfer coefficient (averaged over the entire surface of the sphere), which is also known in the literature as the Ranz-Marshall correlation:

$$\langle Nu\rangle = \frac{\langle\alpha\rangle d}{\lambda} = 2.0 + 0.6(Re)^{0.5}(Pr)^{0.33} = 2.0 + 0.6\left(\frac{\rho v_\infty d}{\eta_\infty}\right)^{0.5}\left(\frac{\nu}{a}\right)^{0.33} \qquad (8.80)$$

The Ranz-Marshall correlation is valid when: $1 < Re < 7\cdot 10^4$ and $0.6 < Pr < 400$ and is shown graphically in Figure 8.10. Note that for $Re = 0$, equation (8.80) reduces to $\langle Nu\rangle = 2$, which is consistent with equation (7.35) derived in paragraph 7.2.4.

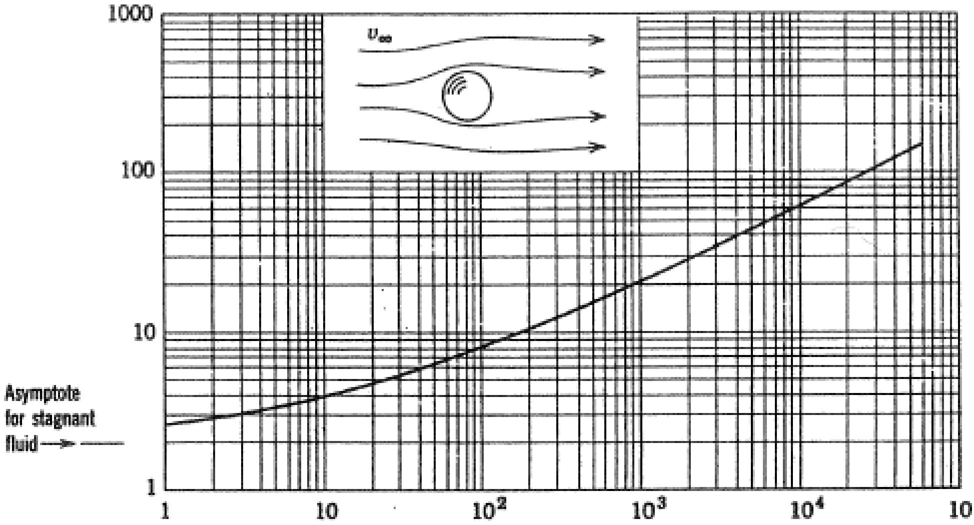

Figure 8.10 The Nusselt number $\langle Nu \rangle$ as a function of the Reynolds number Re, according to the Ranz-Marshall correlation (equation (8.80), for flow past a sphere.

8.3.3 Flow past a cylinder

For an infinitely long cylinder (with diameter d), of which the central axis is perpendicular to the main flow direction, the following Nusselt correlation is given for the average heat transfer coefficient (averaged over the cylinder surface):

$$\langle Nu \rangle = \frac{\langle \alpha \rangle d}{\lambda} = 0.42(Pr)^{0.2} + 0.57(Re)^{0.5}(Pr)^{0.33} \tag{8.81}$$

This correlation is valid for: $1 < Re < 10^4$. For this geometry, also other Nusselt correlations are available, of which Figure 8.11 gives an example. In this figure, the dimensionless quantity $\left(\langle Nu \rangle / (Pr)^{0.4}\right) / (\eta_\infty / \eta_W)$ is given as a function of the Reynolds number Re. The line represents the following Nusselt correlation, which describes the experimental data satisfactory for $10 < Re < 10^5$:

$$\langle Nu \rangle = \frac{\langle \alpha \rangle d}{\lambda} = \left(0.4(Re)^{0.5} + 0.06(Re)^{0.67}\right)(Pr)^{0.4}\left(\frac{\eta_\infty}{\eta_w}\right)^{0.25} \tag{8.82}$$

Note that in this correlation, the exponents of Re and Pr deviate from those in equation (8.81), which is caused by differences in experimental data. For perpendicular flow past tubes of all kinds of shapes other than circular, a large number of correlations is available in literature. This also holds for flow past bundles of tubes, as encountered in e.g. shell-and-tube heat exchangers.

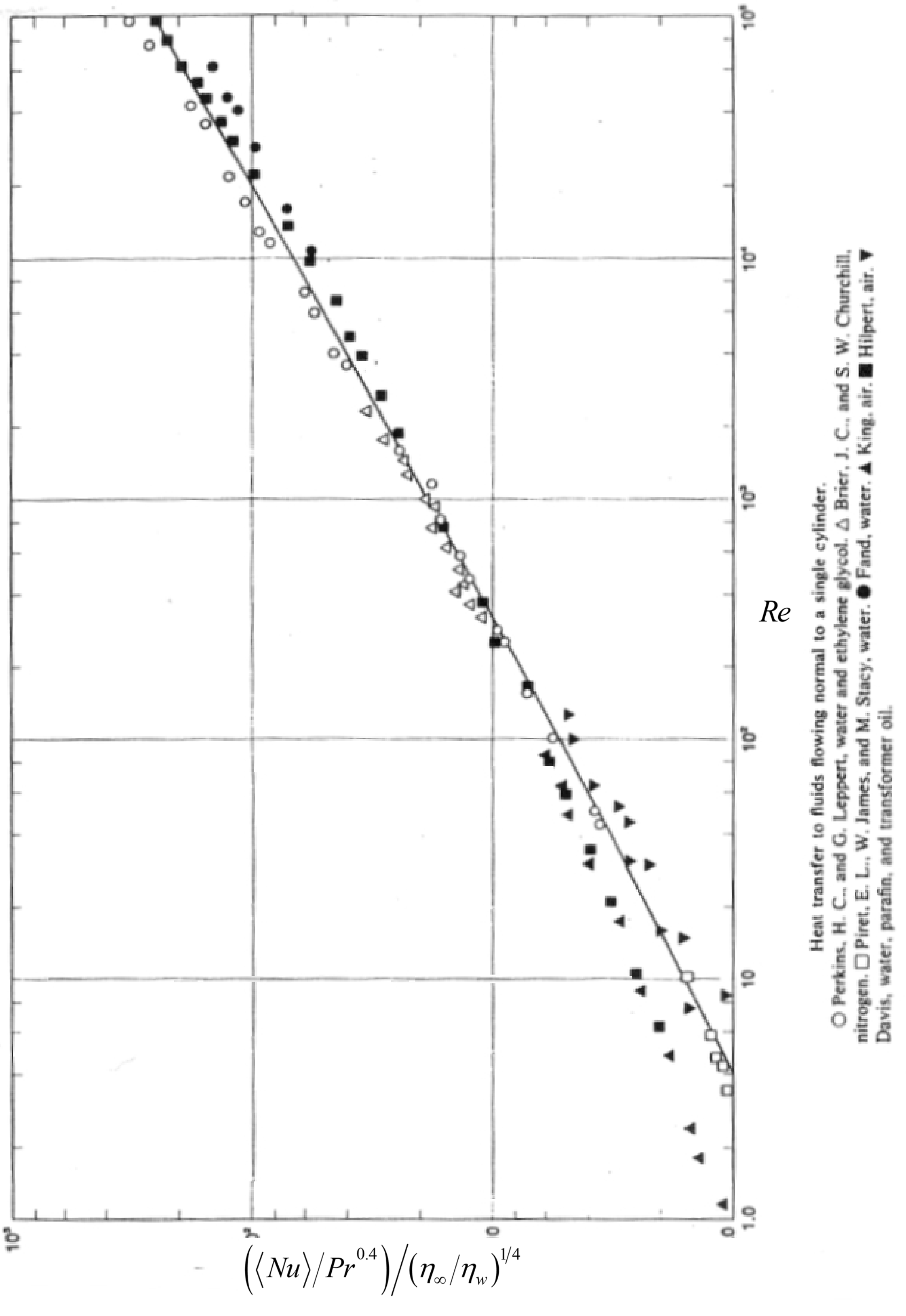

Figure 8.11 The dimensionless quantity $\left(\langle Nu\rangle/(Pr)^{0.4}\right)/\left(\eta_\infty/\eta_w\right)$ as a function of the Reynolds number Re for heat transfer in perpendicular flow past an infinitely long cylinder.

9 Energy transport by free convection

9.1 Introduction

In the discussion of forced convective heat transport in the previous chapter, we have seen that the heat exchange with walls or objects in the presence of a forced convective flow is *influenced* by the heat transport. Due to the temperature gradients perpendicular to the wall/surface of the object, the local velocity profile is affected, which affects the heat exchange rate, which was into account in the form of an empirical correction term for the temperature dependence of the viscosity (Sieder-Tate correction). In the case of free convection, also referred to as natural convection, the interaction between the flow field and the heat transfer is much more intimate: in free convection the convection (i.e. macroscopic movement of the fluid) is not caused by an external force like the pressure gradient or gravity, but is actually *caused* by the heat transport.

Heat transport due to free convection occurs if a fluid (a gas or a liquid), in absence of forced convection, exchanges heat with a fixed body. Because the density of gasses and (to a lesser extent) liquids is dependent on the temperature, density changes prevail due to the heat exchange, which induces free convective flow in the fluid due to the created buoyancy forces, provided that the internal friction (viscous) forces can be overcome. In the case of forced convective heat transport, free convection is in principle always present as an additional heat transport mechanism, but because the heat transfer coefficient for free convection is very much smaller than that for forced convection, free convection is often of minor importance ($\alpha_{\text{free convection}} << \alpha_{\text{forced convection}}$). However, in the absence of forced convection, heat exchange by free convection can play an important role in addition to heat exchange via radiation (discussed in the next chapter), for example when studying heat losses from an insulated reactor to the surroundings.

Free convection can in principle occur if:

- there is a temperature difference ΔT between the fluid and the wall,
- the density ρ of the fluid is temperature dependent,
- the stabilizing viscous forces are small (i.e. low viscosity η).

Free convection is strongest with large temperature differences, large variation of the density ρ with temperature T, low viscosity η (gasses) and a large value of the gravitational acceleration. Density differences can also be caused by differences in the concentration of solutes in liquids, so that free convection can also play a role in mass transport processes.

In Figure 9.1, the qualitative development of the (stationary) temperature- and velocity profiles for free convection to a vertical plate with a uniform wall temperature T_1 is depicted. At a large distance of the plate, the fluid (in rest) has a temperature T_∞. Fluid elements in the direct vicinity of the wall will expand due to heating and will therefore experience a lower gravitational force per unit volume than their less heated neighboring fluid elements and will therefore rise because of the upward force (buoyancy).

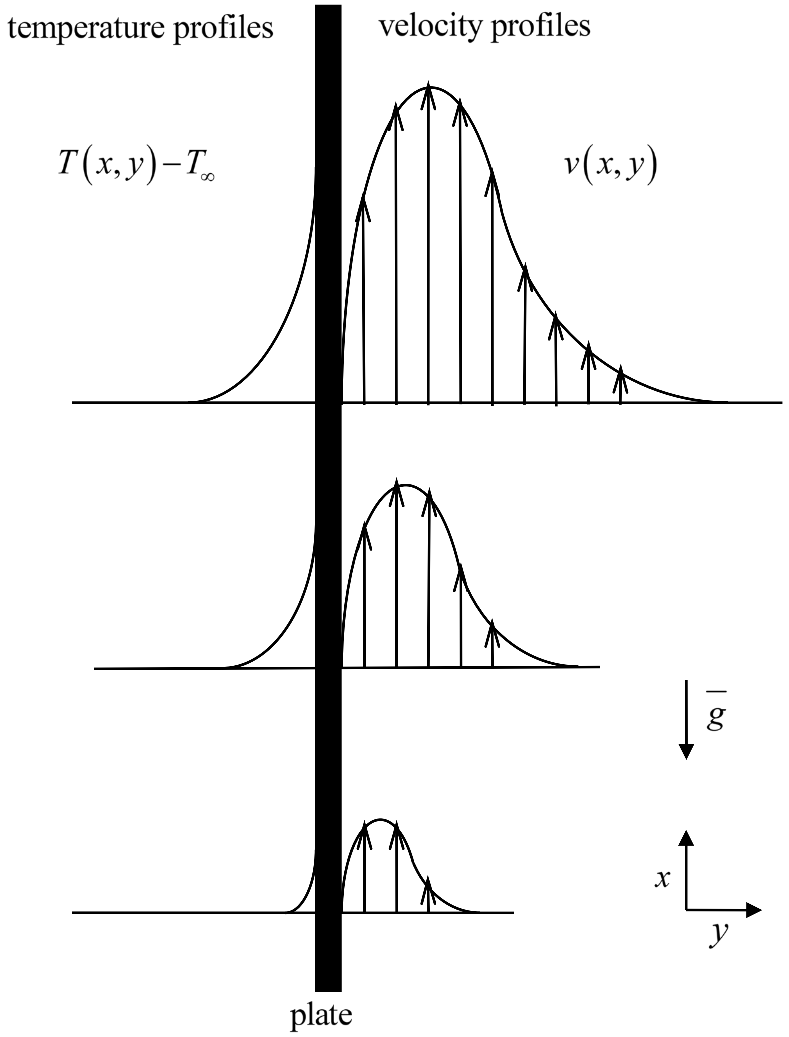

Figure 9.1 Qualitative development of the (stationary) temperature- and velocity profiles for free convection to a vertical plate with a uniform wall temperature T_1.

(T_∞ is the bulk temperature of the fluid at a large distance of the plate).

Because the heating process progresses with increasing height x along the wall, a velocity distribution develops in the fluid where the maximum velocity increases with increasing x. The thickness of the area in which the principal velocity gradients are located (referred to as the boundary layer thickness $\delta(x)$) increases due to the increasing extent of heating with increasing x. In the stationary situation, a height- and x-dependent velocity distribution $v_x(x,y)$ is established, which is, among other things, determined by the heat-flux from the wall to the fluid. This heat flux is in its turn dependent on the velocity distribution. Therefore, the microbalances for momentum (i.e. the Navier-Stokes equations) and thermal energy need to be solved simultaneously to get a quantitative description. This solution can in principle be obtained analytically for geometrically simple systems with laminar free convection.

9.2 Empirical relations

For the local heat transfer coefficient α for free convection, it turns out that the following general form is obtained (for a general derivation see paragraph 9.3):

$$Nu_x = \frac{\alpha x}{\lambda} = f\left(\frac{gx^3}{a\nu}\beta\left|T_1 - T_\infty\right|\right) \tag{9.1}$$

In this equation, x is the coordinate direction in which free convection takes place. The physical transport properties λ, a and ν generally need to be evaluated at the average temperature of the boundary layer. In equation (9.1), β is the relative cubic expansion coefficient, defined by:

$$\beta = -\frac{1}{\rho}\left(\frac{\partial\rho}{\partial T}\right)_p \tag{9.2}$$

For gasses and liquids, β needs to be evaluated at the bulk temperature and the average film temperature, respectively. The relative cubic expansion coefficient β can be calculated when an equation of state is available which describes the density ρ of the fluid as a function of the temperature T. With help of the ideal gas law and the definition of β, for gasses, the following can be easily derived (check this yourself!):

$$\beta_\infty = \frac{1}{T_\infty} \tag{9.3}$$

For fluids, tables are used in which the relative cubic expansion coefficient β is given as a function of temperature. The average heat transfer coefficient $\langle\alpha\rangle$ which occurs over a certain length L, has a form that resembles equation (9.1), but where the local x-coordinate is replaced by the length L:

$$\langle Nu\rangle = \frac{\langle\alpha\rangle L}{\lambda} = F\left(\frac{gL^3}{a\nu}\beta\left|T_1 - T_\infty\right|\right) \tag{9.4}$$

For the local and average heat transfer coefficient, the driving force is the difference between the wall temperature T_1 and the bulk temperature of the fluid T_∞. As can be seen in equation (9.4), the heat transport is determined by the dimensionless number $\left(gL^3/a\nu\right)\beta\left|T_1 - T_\infty\right|$. This is called the Rayleigh number for length L:

$$Ra_L = \frac{gL^3}{a\nu}\beta\left|T_1 - T_\infty\right| \tag{9.5}$$

The Rayleigh number Ra_L can be written as the product of the Grashof number for length L, Gr_L, and the Prandtl number Pr:

$$Ra_L = \frac{gL^3}{\nu^2}\beta\left|T_1 - T_\infty\right|\frac{\nu}{a} = Gr_L\,Pr \tag{9.6}$$

From equation (9.6) follows that the Grashof number for length L, Gr_L, is defined as:

$$Gr_L = \frac{gL^3}{\nu^2}\beta\left|T_1 - T_\infty\right| \tag{9.7}$$

The Grashof number plays an important role in the description of free convection and this dimensionless number takes over the role that the Reynolds number Re plays in forced convection.

9.2.1 Free convection past a vertical flat plate

Completely analogous to the case of forced convection, also in free convection past a flat plate, there is laminar region at the beginning of the plate and at a certain critical distance from the beginning of the plate a transition to turbulent free convection sets in. For a vertically positioned flat plate, this is schematically shown in Figure 9.2.

For laminar free convection along vertical surfaces it has been determined (via theoretical and experimental routes), that the following equation describes the average heat transfer coefficient:

$$\langle Nu\rangle = \frac{\langle\alpha\rangle L}{\lambda} = 0.55\left(Ra_L\right)^{1/4} = 0.55\left(Gr_L\cdot Pr\right)^{1/4} \tag{9.8}$$

This equation is valid for $10^4 < Ra_L < 10^9$. When $Ra_L > 10^9$, a transition from laminar to turbulent free convection takes place. For turbulent free convection past a vertical plate, it has been empirically determined that the average heat transfer coefficient can be calculated with:

$$\langle Nu\rangle = \frac{\langle\alpha\rangle L}{\lambda} = 0.13\left(Ra_L\right)^{1/3} = 0.13\left(Gr_L\cdot Pr\right)^{1/3} \tag{9.9}$$

This equation is valid for $10^9 < Ra_L < 10^{12}$. Note that $\langle\alpha\rangle$ in the turbulent regime is independent of the length L of the (vertical) plate.

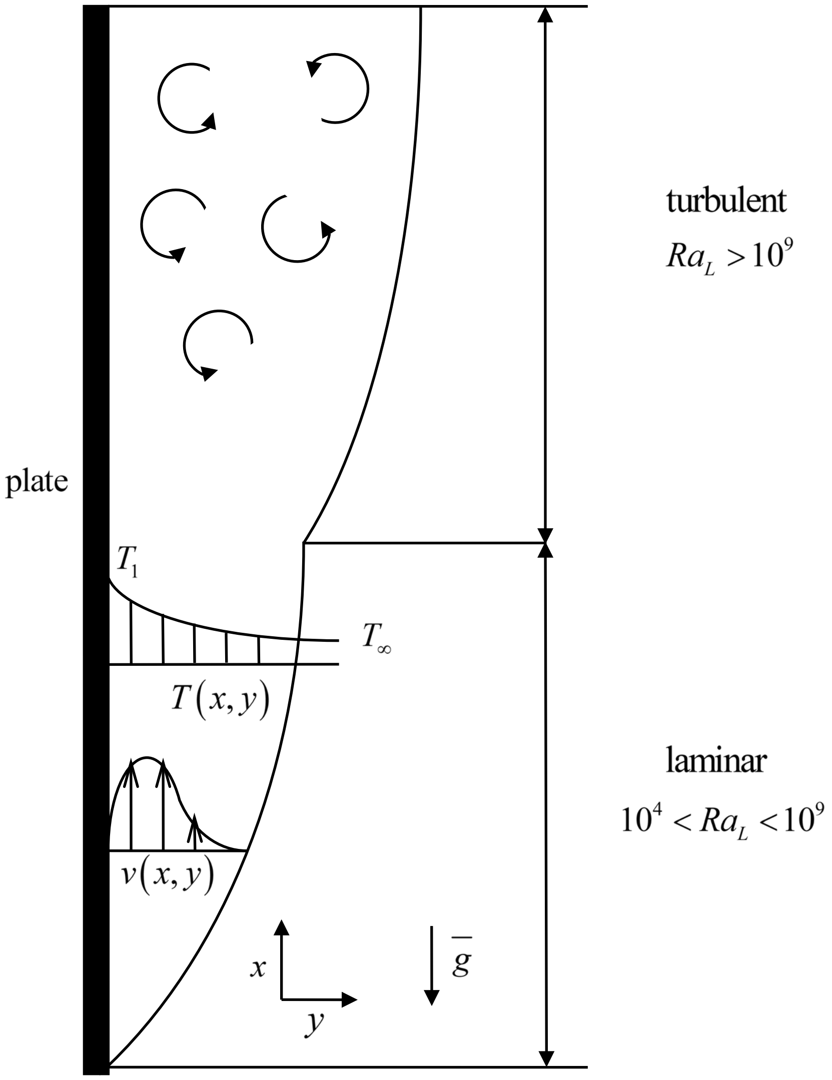

Figure 9.2 Transition from laminar to turbulent free convection for a vertical flat plate. The transition occurs when $Ra_L > 10^9$.

The above Nusselt correlations for free convection along a vertical flat plate can also be used in good approximation to *estimate* the heat transport rate due to free convection for the following geometries:

- Spheres with diameter *L*
- Vertical cylinders with height *L*
- Horizontal cylinders with diameter *L*
- Cubes with edge *L*

9.2.2 Free convection past a horizontal flat plate

The heat exchange due to free convection between a horizontally positioned flat plate (with uniform wall temperature T_1) and a fluid (with bulk temperature T_∞) can be described with a Nusselt correlation of the following general form:

$$\langle Nu \rangle = \frac{\langle \alpha \rangle L}{\lambda} = c\left(\frac{gL^3}{\nu^2} \beta \left| T_1 - T_\infty \right| \cdot \frac{\nu}{a} \right)^n = c\left(Gr_L \cdot Pr \right)^n \tag{9.10}$$

The values of the constant c and exponent n are dependent of the orientation of the plate (see Table 9.1). The quantities a, ν, λ and β are defined in the same way as for the vertical flat plate. As can be seen in Table 9.1, in situations where the hot wall is at the lower side of the plate or the cold wall is on the upper side of the plate, the system is relatively stable, because the regime with laminar free convection exists up to very high values of $Ra_L = Gr_L\, Pr \approx 3 \cdot 10^{10}$.

For the characteristic length L, depending on the geometry, is taken:

- The length of an edge for a square plate
- The average of the lengths of the edges for a rectangular plate
- $0.9D$ for a round disc with diameter D

Table 9.1 Values of the constant c and the exponent n in equation (9.10). for free convection from a horizontally positioned flat plate.

Orientation of the plate	$Gr_L \cdot Pr$	c	n	Regime
Hot wall on the upper side or cold wall on the lower side	10^5 to $2 \cdot 10^7$	0.54	1/4	Laminar
Hot wall on the upper side or cold wall on the lower side	$2 \cdot 10^7$ to $3 \cdot 10^{10}$	0.14	1/3	Turbulent
Hot wall on the lower side or cold wall on the upper side	$3 \cdot 10^5$ to $3 \cdot 10^{10}$	0.27	1/4	Laminar

9.3 Theoretical background

At the end of this chapter we will give a derivation to show that the Nusselt correlations for free convection will take the general form described with equation (9.4). The starting point is given by the (stationary) microbalances for mass, momentum and thermal energy, which describe the velocity profiles $v_x\left(x,y\right)$ and $v_y\left(x,y\right)$ and the temperature profile $T\left(x,y\right)$ in the boundary layer. For the formulation and simplification of these equations, we will assume the geometry sketched in Figure 9.1 (vertical flat plate).

Microbalance for mass (continuity equation):

$$\frac{\partial v_x}{\partial x}+\frac{\partial v_y}{\partial y}=0 \tag{9.11}$$

Microbalance for x-momentum (Navier-Stokes equation for a Newtonian fluid):

$$\rho\left(v_x\frac{\partial v_x}{\partial x}+v_y\frac{\partial v_x}{\partial y}\right)=-\frac{\partial p}{\partial x}+\eta\left(\frac{\partial^2 v_x}{\partial x^2}+\frac{\partial^2 v_x}{\partial y^2}\right)+\rho g_x \tag{9.12}$$

Microbalance for thermal energy:

$$v_x\frac{\partial T}{\partial x}+v_y\frac{\partial T}{\partial y}=a\left(\frac{\partial^2 T}{\partial x^2}+\frac{\partial^2 T}{\partial y^2}\right) \tag{9.13}$$

These equations are principally valid for a fluid with constant density (incompressible fluid), so strictly speaking, they are not applicable for the analysis of free convection in the boundary layer. However, this simplification will not influence the result of our analysis.

The microbalance for x-momentum (9.12) can be further simplified by means of the following assumptions/simplifications:

1. The momentum transport in the x-direction is dominated by convection:

$$\left|\eta\frac{\partial^2 v_x}{\partial x^2}\right|<<\left|\rho v_x\frac{\partial v_x}{\partial x}\right| \tag{9.14}$$

2. The pressure gradient in the developed boundary layer is equal to the pressure gradient in the stagnant medium:

$$\frac{\partial p}{\partial x}=\left(\frac{dp}{dx}\right)_\infty=\rho_\infty g_x \tag{9.15}$$

With these assumptions, the following simplified form of the microbalance for x-momentum is obtained (with $g_x=-g$):

$$v_x \frac{\partial v_x}{\partial x} + v_y \frac{\partial v_x}{\partial y} = \nu \frac{\partial^2 v_x}{\partial y^2} + \left(\frac{\rho_\infty - \rho}{\rho} \right) g \tag{9.16}$$

In the microbalance for thermal energy, the molecular heat transport in the x-direction is neglected compared to the convective heat transport in the x-direction, so (9.13) reduces to:

$$v_x \frac{\partial T}{\partial x} + v_y \frac{\partial T}{\partial y} = a \frac{\partial^2 T}{\partial y^2} \tag{9.17}$$

Equations (9.16) and (9.17) are coupled via the temperature dependent density ρ. For gasses, according to the ideal gas law and the definition of the relative cubic expansion coefficient β, the following holds for the term $(\rho_\infty - \rho)/\rho$:

$$\frac{\rho_\infty - \rho}{\rho} = \frac{\frac{1}{T_\infty} - \frac{1}{T}}{\frac{1}{T}} = \frac{T - T_\infty}{T_\infty} = \beta_\infty (T - T_\infty) \tag{9.18}$$

For liquids, there is generally no equation of state which explicitly defines the density ρ as a function of the temperature T. Therefore, using a Taylor series expansion, ρ and ρ_∞ are expressed in a reference density ρ_r, which is the density of the liquid at temperature T_r. Generally the average temperature of the heat transfer film is taken as T_r. On basis of these Taylor series expansions, we can deduce the following for the density difference $(\rho_\infty - \rho)$:

$$\rho_\infty - \rho = \left(\frac{\partial \rho}{\partial T} \right)_r (T_\infty - T) \tag{9.19}$$

When equation (9.19) is divided by ρ_r, the following can be stated using the definition of the relative cubic expansion coefficient β:

$$\frac{\rho_\infty - \rho}{\rho_r} = \frac{1}{\rho_r} \left(\frac{\partial \rho}{\partial T} \right)_r (T_\infty - T) = \beta_r (T - T_\infty) \tag{9.20}$$

Because changes in density are generally very small for liquids, the term $(\rho_\infty - \rho)/\rho$ at the right hand side of equation (9.16) can in good approximation be replaced by $(\rho_\infty - \rho)/\rho_r$. After combination with equation (9.20) the following is obtained:

$$\frac{\rho_\infty - \rho}{\rho} \approx \frac{\rho_\infty - \rho}{\rho_r} = \beta_r (T - T_\infty) \tag{9.21}$$

So the term $\left(\rho_\infty - \rho\right)/\rho$ at the right hand side of equation (9.16) can for both gasses and liquids be written as the product of a relative cubic expansion coefficient β and a (local) temperature difference $\left(T - T_\infty\right)$, so that the following alternative form of the microbalance for x-momentum can be obtained:

$$v_x \frac{\partial v_x}{\partial x} + v_y \frac{\partial v_x}{\partial y} = \nu \frac{\partial^2 v_x}{\partial y^2} + \beta\left(T - T_\infty\right) g \tag{9.22}$$

Equations (9.11), (9.17) and (9.22) are rewritten in dimensionless form by introducing:

The dimensionless x- and y- coordinates:

$$x^* = \frac{x}{L} \quad \text{and} \quad y^* = \frac{y}{L} \tag{9.23}$$

The dimensionless velocity components:

$$v_x^* = \frac{L v_x}{\nu} \quad \text{and} \quad v_y^* = \frac{L v_y}{\nu} \tag{9.24}$$

The dimensionless temperature:

$$T^* = \frac{T - T_\infty}{\left|T_1 - T_\infty\right|} \tag{9.25}$$

After substitution of these dimensionless variables (9.23), (9.24) and (9.25) in (9.11), (9.17) and (9.22), the following dimensionless transport equations are obtained:

The dimensionless microbalance for mass:

$$\frac{\partial v_x^*}{\partial x^*} + \frac{\partial v_y^*}{\partial y^*} = 0 \tag{9.26}$$

The dimensionless microbalance for x-momentum:

$$v_x^* \frac{\partial v_x^*}{\partial x^*} + v_y^* \frac{\partial v_x^*}{\partial y^*} = \frac{\partial^2 v_x^*}{\partial y^{*2}} + \left(\frac{gL^3}{\nu^2} \beta \left|T_1 - T_\infty\right|\right) T^* \tag{9.27}$$

The dimensionless microbalance for thermal energy:

$$v_x^* \frac{\partial T^*}{\partial x^*} + v_y^* \frac{\partial T^*}{\partial y^*} = \frac{a}{\nu} \frac{\partial^2 T^*}{\partial y^{*2}} \qquad (9.28)$$

In these dimensionless transport equations, the Grashof number Gr_L and the Prandtl number Pr appear as dimensionless variables. When the transport equations (9.26), (9.27) and (9.28) are solved with suitable boundary conditions, among other things the dimensionless temperature T^* is obtained, which is a function only of x^*, y^*, Gr_L and Pr:

$$T^* = T^*\left(x^*, y^*, Gr_L, Pr\right) \qquad (9.29)$$

From equation (9.29) follows that the average dimensionless heat transfer coefficient $\langle Nu \rangle$ is a function only of the dimensionless variables Gr_L and Pr, as expressed in equation (9.10). For laminar and turbulent free convection it turns out that the exponents Gr_L and Pr are often the same, so that the Grashof and Prandtl numbers can be combined into a new dimensionless number, namely the Rayleigh number Ra_L. This is completely analogous to case of laminar forced convection where the Graetz number *Gz* appeared as the combination of the Reynolds number *Re* and the Prandtl number *Pr*.

10 Energy transport by radiation

10.1 Introduction

The exchange of thermal energy from the sun to the earth is the most well-known example of energy transport by radiation. However, also in process equipment radiative energy transport can play an important role, in addition to other transport mechanisms, e.g. in ovens or high temperature reactors. The energy transport by radiation differs fundamentally from the other transport mechanisms (conduction and convection), the most salient discrepancy being that radiation is brought about via electromagnetic waves and does not require an intervening medium, so that radiative energy transport becomes dominant in vacuum or low pressure systems. Moreover, the driving force and hence the temperature dependency of energy transport by radiation is fundamentally different in comparison to other transport mechanisms. For objects at room temperature, the energy exchange between the object and its surroundings due to radiation is generally in the same order of magnitude as that caused by free convection, but much lower than that by forced convection. However, the importance of radiative energy transport increases very strongly with increasing temperatures. Finally, there is no analog of radiation in mass transport.

All physical objects above the absolute zero temperature emit radiation, caused by the transition of the atoms/molecules in an object between different energy levels, which is accompanied by the absorption or emission of a photon, thus bringing about energy exchange via electromagnetic waves. Since these electromagnetic waves are the result of a multitude in possible changes in electronical, vibrational and rotational energy, the emitted radiation spans a certain range of wavelengths. In engineering applications the most important spectrum is the wavelength range between 10^{-7} and 10^{-4} m, often referred to as thermal radiation. Radiation in the visible part of the spectrum constitutes only a narrow range of wavelengths, which are typically only significantly emitted by objects at very high temperature. Heat transport due to radiation for objects at ambient conditions typically occurs at wavelengths in the (far) infrared region.

For radiative energy transport, in principle no intermediate medium is required. However, liquids typically absorb all the radiative energy in a very small layer, while most gasses do hardly absorb the radiation at all, referred to as *non-participating* media (where CO_2 and H_2O are the most famous exceptions). A non-participating medium surrounding two objects does not absorb any radiation emitted from the objects and hence does not influence the radiative energy exchange between the two objects. In this case, convective and radiative energy transport takes place independently and in parallel (although indirectly coupled via the temperature of the surfaces of the objects).

Moreover, objects can be *transparent* or *opaque* for radiation (which can actually be different at different temperatures or for different wavelengths). From a transparent object, such as glass, salt crystals, high temperature gasses, the radiation emitted via the surface of the object results from emissions from throughout the entire object. In this case, emission of radiation is a bulk or volumetric phenomenon. On the other hand, radiation emitted from within an opaque object, such as metals, brick and wood, cannot reach the surface and only radiation emitted from material in the direct vicinity of (typically within 1 μm from) the external surface will be emitted from the object. In this case, emission of radiation is a surface phenomenon. Note that whether an object is transparent or opaque for radiation in principle also depends on the temperature.

The mathematical description of radiation differs strongly from that for convection and the equations involved (stemming from quantum mechanics) are often very difficult to solve (integro-partial differential equations), especially in cases where participating media and transparent objects with difficult geometrical shapes are involved. Fortunately, simplified limiting cases can be identified which for many engineering applications can give a first quick estimate of the importance of radiative heat transport. Therefore, in this chapter we will focus on the radiative energy exchange between two opaque objects in a non-participating medium. First, we start with some general theoretical background on emission and absorption of radiation and subsequently we will study the radiative energy exchange for two limiting geometrical cases:

1. Two infinitely long flat plates;
2. One object enclosed within another one.

10.2 Emission and absorption of radiation

10.2.1 Black bodies

An ideal '*black*' body absorbs all incident radiation (i.e. no reflection of radiation). Note that here the term black does not refer to the color of the object, since the human eye can detect radiation only in very limited range of wavelengths. A black body also emits radiation in a range of wavelengths, where the intensity of radiation $\Phi''_{b,e,\lambda}$ (in W/m^2) emitted by a black body at a certain wavelength λ is a function of the temperature of the object, is given by Planck's law:

$$\Phi''_{b,e,\lambda} = \frac{2\pi c^2 h}{\lambda^5} \cdot \frac{1}{\exp\left(\frac{hc}{\lambda kT}\right) - 1} \tag{10.1}$$

where h is Planck's constant (h = 6.6256·10^{-34} J·s), k is Boltzmann's constant (k = 1.38054·10^{-23} J·K), c is the speed of light (c = 2.9979·10^8 m/s).
The maximum intensity of the spectrum of wavelengths emitted by a black body shifts towards smaller wavelengths with increasing temperature according to Wien's law.

$$\lambda_{\max} T = 2880 \ \mu\text{m} \cdot \text{K} \tag{10.2}$$

For our sun $\lambda_{\max} \approx 0.5 \ \mu\text{m}$, so that the surface temperature of the sun can be estimated at 5760 K.

When integrating over all wavelengths, the total heat flux due to radiation emitted by a black body can be found, referred to as Stefan-Boltzmann's law:

$$\Phi''_{b,e} = \int_0^\infty \Phi''_{b,e,\lambda}(\lambda)\,d\lambda = \left(\frac{2}{15}\frac{\pi^5 k^4}{c^2 h^3}\right) T^4 = \sigma T^4 \tag{10.3}$$

Here, the Stefan-Boltzmann constant σ is defined with $\sigma = 5.67 \cdot 10^{-8}$ W/(m^{2}K^4).

10.2.2 Real bodies

Emissivity

Real bodies do not absorb all incident radiation, but they reflect and possibly transmit part of the radiation. In this course we will only consider opaque bodies, i.e. emission and absorption only takes place at the surface of the body.

The ratio of the radiation emitted by a real object and the radiation emitted by an ideal black radiator at the same temperature, both for a single given wavelength, is defined as the monochromatic hemispherical emission coefficient e_λ. This coefficient depends on the wavelength of the emitted radiation and the temperature of the object. For a black body, e_λ is equal to one by definition. The term "hemispherical" refers to the hemisphere that encloses the area from which the radiation emerges. Integration over all directions, on which the emissivity can also be dependent, has already been performed.

$$e_\lambda = \frac{\Phi''_{r,e,\lambda}}{\Phi''_{r,b,e,\lambda}} \tag{10.4}$$

The integral emission coefficient *e* is defined as the ratio of the (total) radiation emitted by a real object compared to that which would be emitted by a black body at the same temperature:

$$e = \frac{\Phi''_{r,e}}{\Phi''_{r,b,e}} = \frac{\int_0^\infty e_\lambda(\lambda)\Phi''_{b,e,\lambda}\,d\lambda}{\int_0^\infty \Phi''_{b,e,\lambda}\,d\lambda} = \frac{\int_0^\infty e_\lambda(\lambda)\Phi''_{b,e,\lambda}\,d\lambda}{\sigma T^4} \tag{10.5}$$

The radiation emitted by a black body presents the upper limit, so that $0 \le e \le 1$.

In engineering applications, detailed information on the emissivity as a function of wavelength is unfortunately often not available. However, for many materials, the monochromatic hemispherical emission coefficient e_λ can be assumed (more or less) independent of the wavelength. Surfaces for which e_λ is independent of the wavelength λ are known as *gray* surfaces. The emitted heat flux from a gray surface is then given by:

$$\Phi''_{r,e} = e\sigma T^4 \tag{10.6}$$

Absorptivity

The fraction of the incident radiative energy that is absorbed by a real object, both at a certain wavelength, is defined as the monochromatic absorption coefficient a_λ:

$$a_\lambda = \frac{\Phi''_{r,a,\lambda}}{\Phi''_{r,i,\lambda}} \tag{10.7}$$

Note that for a black body $a_\lambda = 1$. Integrated over all wavelengths, the integral absorption coefficient *a* is defined as:

$$a = \frac{\Phi''_{r,a}}{\Phi''_{r,i}} \tag{10.8}$$

Kirchhoff's law (for a gray body)

If the intensity of the emitted radiation is independent on the direction with respect to the surface, the surface is called *diffuse*. For diffuse gray surfaces, Kirchhoff's law states that:

$$e = a \tag{10.9}$$

That is, the absorption coefficient is equal to the emission coefficient for these surfaces. Finally, some typical values of emission (or absorption) coefficients are shown in Figure 10.1. Note that metals generally have a low emission coefficient. Also note that for example paint, having generally a low absorption in the visible spectrum, has actually a high absorption coefficient. This originates from the dependency on the wavelength of the absorption coefficient.

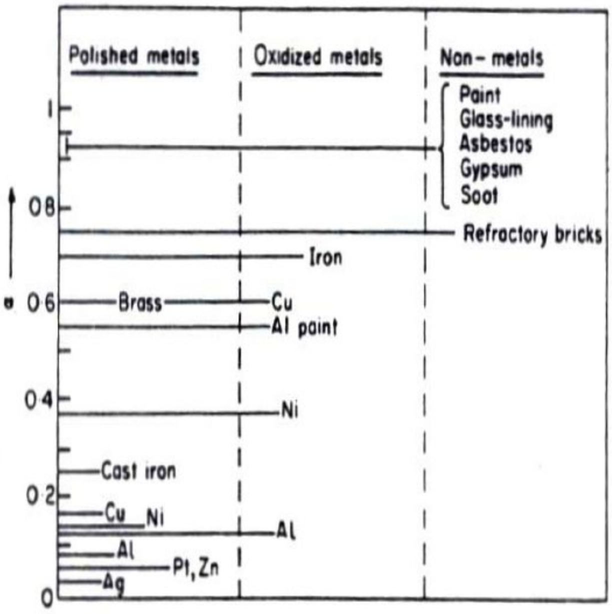

Figure 10.1: Emission coefficients of some commonly used materials

10.3 Radiative energy exchange between two opaque gray bodies

The emitted energy flux due to radiation from an object is, in itself, independent of the surroundings. However, the energy exchange between two bodies depends on their temperatures and the geometric arrangement. Consider for example Figure 10.2, clearly showing that not all radiation originating from the first object impinges on the second. In literature (e.g. Perry's 'Handbook for Chemical Engineers' or the excellent book 'Radiant Heat Transmission' by H.C. Hottel), for various geometries so-called "view factors" (or "angle factors") are published. The view factor F_{ij} is defined as the fraction of the total radiation originating from object i that reaches object j. Note the difference between F_{ij} and F_{ji}, so that generally $F_{ij} \neq F_{ji}$, but $F_{ij}A_i = F_{ji}A_j$, where A_i is the surface area of object *i*.

The view factors are calculated by considering the surfaces of both objects to be built up from infinitesimally small sub-surfaces. The view factors are related to the fractions of the hemispheres surrounding these emitting sub-surfaces of object *i* that are directed towards those of object *j*. The mathematical treatment of view factors is left out of consideration in this introductory course. Here, two limiting cases that can often be usefully applied are considered, where the view factors are trivial from the geometrical arrangement.

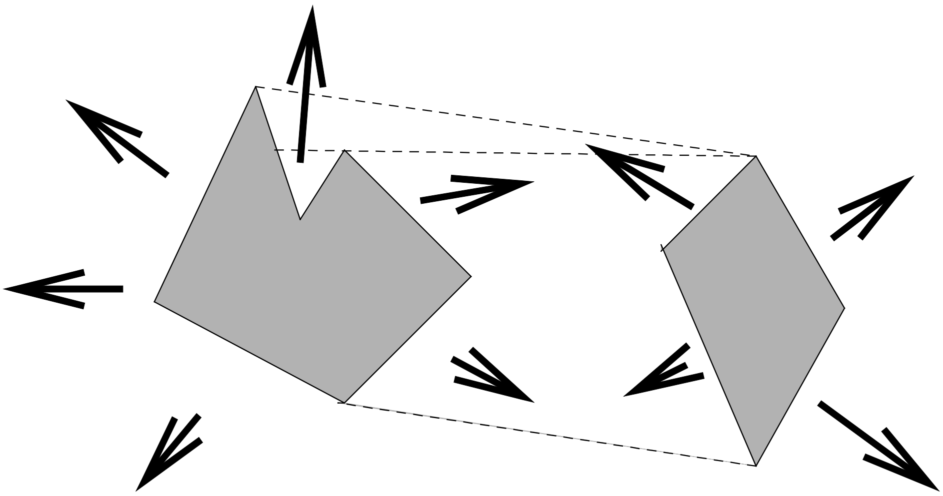

Figure 10.2: Schematical representation of heat transfer by radiation between two bodies

Exchange between two opaque black bodies:

Consider now the net radiative energy exchange between two opaque black bodies, with a temperature T_1 and T_2 respectively, in a non-participating medium. Since black bodies absorb all the incident radiation (no reflection), all the radiative energy emitted by object 2 that reaches object 1 is absorbed by object 1 and vice versa, in the steady state.

$$\begin{aligned} \Phi_{a,1} &= \Phi''_{b,e,2} A_2 F_{21} \\ \Phi_{a,2} &= \Phi''_{b,e,1} A_1 F_{12} \end{aligned} \tag{10.10}$$

The net radiative energy exchanged per unit of time between the two objects is then

$$\begin{aligned} \Phi_{r,1\rightarrow 2} &= \Phi''_{b,e,1} A_1 F_{12} - \Phi_{a,1} \\ \Phi_{r,2\rightarrow 1} &= \Phi''_{b,e,2} A_2 F_{21} - \Phi_{a,2} \end{aligned} \tag{10.11}$$

Substitution of equations (10.10) yield for the net radiative energy flux:

$$\Phi_{r,1\to 2} = -\Phi_{r,2\to 1} = \Phi''_{b,e,1}A_1F_{12} - \Phi''_{b,e,2}A_2F_{21} \tag{10.12}$$

Subsituting Stefan-Boltzmann's law for the radiative energy flux for black radiators and using $F_{12}A_1 = F_{21}A_2$, the following can be derived for the net rate of energy exchange per unit of time by radiation from object 1 to object 2:

$$\Phi_{r,1\to 2} = \sigma\left(T_1^4 - T_2^4\right)A_1F_{12} \tag{10.13}$$

Exchange between two opaque gray bodies:

In the case of radiative energy exchange between gray bodies, the total radiated energy flux, referred to as radiosity *J*, equals the sum of the emitted radiative flux from the body itself ($e\Phi''_{r,e}$) and the part of the total incident flux *G* that is being reflected ($\left(1-a\right)G$):

$$J = e\Phi''_{b,e} + \left(1-a\right)G \tag{10.14}$$

The net radiative energy flux leaving object 1 (Φ''_r) is equal to the total emitted flux ($e\Phi''_{b,e}$) minus the absorbed flux (aG), which equals the total radiated energy flux minus the total incident radiative energy flux (substitute equation (10.14)):

$$\Phi''_r = e\Phi''_{b,e} - aG = J - G \tag{10.15}$$

Thus $G = J - \Phi''_r$ and substitution in equation (10.14) yields (making use of Kirchhoff's law stating that *a* = *e*):

$$J = e\Phi''_{b,e} + \left(1-e\right)\left(J - \Phi''_r\right) \tag{10.16}$$

so that net radiative energy flux is given by

$$\Phi''_r = \frac{\Phi''_{b,e} - J}{\dfrac{\left(1-e\right)}{e}} \tag{10.17}$$

or equivalently for the net radiative energy flow:

$$\Phi_r = \Phi''_r A = \frac{\Phi''_{b,e} - J}{\dfrac{\left(1-e\right)}{eA}} \tag{10.18}$$

This equation can be interpreted in terms of Ohm's law, where the driving force $\Phi''_{b,e} - J$ equals flow Φ_r times resistance $\dfrac{\left(1-e\right)}{eA}$, which allows an easy derivation of the total resistance in networks of objects (e.g. several parallel radiation sheets). Now the net energy exchange between two opaque gray bodies is derived for two geometrically simple (but practically important) cases.

10.3.1 Radiation between two gray infinitely long parallel flat plates

Consider the case of two infinitely large parallel plates of gray, diffuse material, where we assume that both plates individually have a uniform temperature T_1 and T_2 respectively (see Figure 10.3). Only the surfaces facing each other are considered. For infinitely long plates, only an infinitesimally small fraction of the radiation coming from the first plate will not reach the second plate, and vice versa, i.e. the view factors $F_{12} = F_{21} \approx 1$. Then, it can be assumed that *all* radiation received by a plate is coming from the other, and that all radiation emitted by a plate is received by the other and that there are no losses in radiative heat transfer.

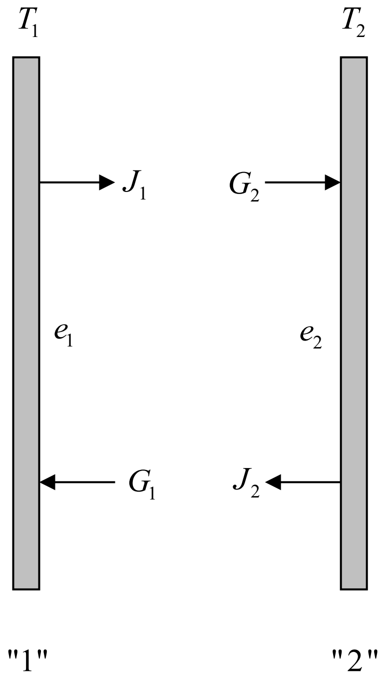

Figure 10.3: Radiative energy exchange between two parallel infinitely long flat plates

Since the surface area of both plates are identical ($A_1 = A_2 = A$), this can be expressed as:

$$\begin{aligned} G_1 &= J_2 \\ G_2 &= J_1 \end{aligned} \tag{10.19}$$

and

$$\begin{aligned} \Phi_{r,1} &\equiv \left(J_1 - G_1\right) A = \left(J_1 - J_2\right) A \\ \Phi_{r,2} &\equiv \left(J_2 - G_2\right) A = \left(J_2 - J_1\right) A \end{aligned} \tag{10.20}$$

so that

$$\Phi_{r,1} = -\Phi_{r,2} \tag{10.21}$$

Using equation (10.18):

$$\begin{aligned} \Phi_{r,1} &= \frac{\Phi''_{b,e,1} - J_1}{\dfrac{\left(1-e_1\right)}{e_1 A}} \\ \Phi_{r,2} &= \frac{\Phi''_{b,e,2} - J_2}{\dfrac{\left(1-e_2\right)}{e_2 A}} \end{aligned} \tag{10.22}$$

Rewriting using equation (10.21) yields:

$$\begin{aligned} J_1 &= \Phi''_{b,e,1} - \frac{(1-e_1)}{e_1 A}\Phi_{r,1} \\ J_2 &= \Phi''_{b,e,2} + \frac{(1-e_2)}{e_2 A}\Phi_{r,1} \end{aligned} \tag{10.23}$$

After subtraction of these equations:

$$J_1 - J_2 = \Phi''_{b,e,1} - \Phi''_{b,e,2} - \left[\frac{(1-e_1)}{e_1 A} + \frac{(1-e_2)}{e_2 A}\right]\Phi_{r,1} \tag{10.24}$$

and upon substitution in equation (10.20):

$$\frac{1}{A}\Phi_{r,1} = \Phi''_{b,e,1} - \Phi''_{b,e,2} - \left[\frac{(1-e_1)}{e_1 A} + \frac{(1-e_2)}{e_2 A}\right]\Phi_{r,1} \tag{10.25}$$

$$\left[\frac{1}{A} + \frac{(1-e_1)}{e_1 A} + \frac{(1-e_2)}{e_2 A}\right]\Phi_{r,1} = \Phi''_{b,e,1} - \Phi''_{b,e,2} \tag{10.26}$$

so that finally for the net radiative energy exchange rate between two gray, opaque, infinitely long parallel plates is found:

$$\Phi_{r,1\to 2} = \Phi_{r,1} = \frac{\sigma\left(T_1^4 - T_2^4\right)}{\frac{1}{A} + \frac{(1-e_1)}{e_1 A} + \frac{(1-e_2)}{e_2 A}} \tag{10.27}$$

Note that this equation indeed reduces to equation (10.13) for radiative energy exchange between black bodies for the case of $e_1 = e_2 = 1$ (since F_{12}=1).

10.3.2 Radiative energy exchange with an enclosed gray object

Consider the case of a gray object, “1”, that is fully enclosed by another gray object, “2” (see Figure 10.4). This could for example be a tank “1” in a concrete shed “2” or two concentric tubes or spheres. In this situation, all radiation emitted by object “1” is received by object “2”. Object “2” may be emitting to its own surroundings too, but here we only consider the net radiative energy exchange with object “1”.

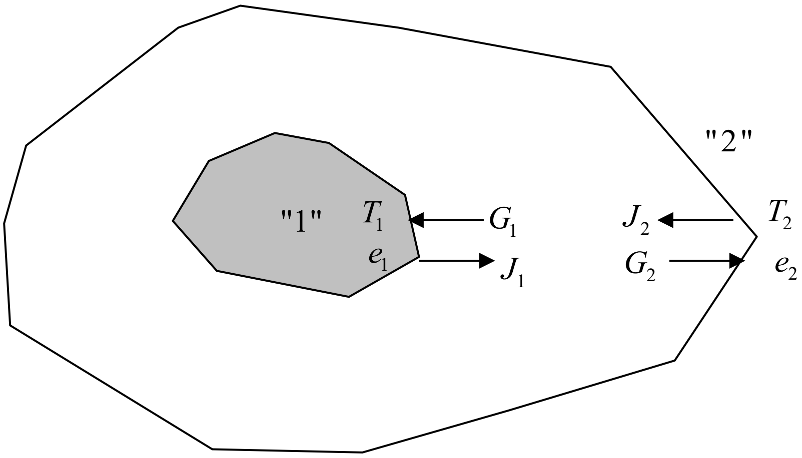

Figure 10.4:
Graphical representation of radiative heat exchange between an enclosed (“1”) and an enclosing (“2”) object.

For this geometry holds:

$$F_{12} = 1 \tag{10.28}$$

$$\begin{aligned} G_1 &= J_2 \\ G_2 &= J_1 \end{aligned} \tag{10.29}$$

so that again

$$\Phi_{r,1\rightarrow 2} = \Phi_{r,1} = -\Phi_{r,2} \tag{10.30}$$

For this geometry the net radiative energy exchange from the enclosed object is:

$$\Phi_{r,1\rightarrow 2} = \left(J_1 - G_1\right) A_1 F_{12} = \left(J_1 - J_2\right) A_1 \tag{10.31}$$

Similar to before, use equation (10.18):

$$\begin{aligned} \Phi_{r,1} &= \frac{\Phi''_{b,e,1} - J_1}{\dfrac{\left(1-e_1\right)}{e_1 A_1}} \\ \Phi_{r,2} &= \frac{\Phi''_{b,e,2} - J_2}{\dfrac{\left(1-e_2\right)}{e_2 A_2}} \end{aligned} \tag{10.32}$$

and rewrite using equation (10.30) to obtain:

$$\begin{aligned} J_1 &= \Phi''_{b,e,1} - \frac{\left(1-e_1\right)}{e_1 A_1} \Phi_{r,1} \\ J_2 &= \Phi''_{b,e,2} + \frac{\left(1-e_2\right)}{e_2 A_2} \Phi_{r,1} \end{aligned} \tag{10.33}$$

After subtraction of these equations:

$$J_1 - J_2 = \Phi''_{b,e,1} - \Phi''_{b,e,2} - \left[\frac{\left(1-e_1\right)}{e_1 A_1} + \frac{\left(1-e_2\right)}{e_2 A_2} \right] \Phi_{r,1} \tag{10.34}$$

and upon substitution in equation (10.31):

$$\frac{1}{A_1} \Phi_{r,1} = \Phi''_{b,e,1} - \Phi''_{b,e,2} - \left[\frac{\left(1-e_1\right)}{e_1 A_1} + \frac{\left(1-e_2\right)}{e_2 A_1} \right] \Phi_{r,1} \tag{10.35}$$

$$\left[\frac{1}{A_1} + \frac{\left(1-e_1\right)}{e_1 A_1} + \frac{\left(1-e_2\right)}{e_2 A_2} \right] \Phi_{r,1} = \Phi''_{b,e,1} - \Phi''_{b,e,2} \tag{10.36}$$

so that finally for the net radiative energy exchange rate between two gray, opaque, infinitely long parallel plates is found:

$$\Phi_{r,1\to 2} = \Phi_{r,1} = \frac{\sigma\left(T_1^4 - T_2^4\right)}{\frac{1}{A_1} + \frac{\left(1-e_1\right)}{e_1 A_1} + \frac{\left(1-e_2\right)}{e_2 A_2}} \qquad (10.37)$$

In many cases the surface area of object "1" is much smaller than that of object "2", i.e. $A_1 << A_2$, so that equation (10.37) reduces to

$$\Phi_{r,1\to 2} = e_1 \sigma\left(T_1^4 - T_2^4\right) A_1 \qquad (10.38)$$

10.3.3 Radiative heat transfer coefficient

In many cases, for example in comparing the relative importance transport due to radiation and free convection, it is handy to define a (fictitious) heat transfer coefficient due to radiation according to:

$$\alpha_r \equiv \frac{\Phi''_{r,1\to 2}}{\left(T_1 - T_2\right)} = \frac{e_{ov}\sigma\left(T_1^4 - T_2^4\right)}{\left(T_1 - T_2\right)} \qquad (10.39)$$

with

$$e_{ov} = \frac{1}{1 + \frac{\left(1-e_1\right)}{e_1} + \frac{\left(1-e_2\right)}{e_2}} \quad \text{(infinitely long parallel flat plates)}$$

$$e_{ov} = \frac{1}{1 + \frac{\left(1-e_1\right)}{e_1} + \frac{A_1}{A_2}\frac{\left(1-e_2\right)}{e_2}} \quad \text{(object "1" enclosed in object "2")} \qquad (10.40)$$

For radiative heat exchange between objects with temperatures around room temperature and having typical values for the emission coefficient, a typical value of α_r of about 6 W/(m^{2}K) is found, which is quite comparable with heat exchange coefficients found for free convection. However, α_r increases strongly with increasing temperatures.

11 Molecular mass transport

11.1 Introduction

There is a very strong analogy between mass and heat transfer processes, both for molecular and convective transport processes, so that the mathematical description for these processes is very similar and many results already discussed for heat transfer processes in the previous chapters can be easily 'translated' and used to describe mass transfer processes. In this chapter molecular mass transport, or diffusion, is studied. The combination of mass transfer processes in combination with chemical reactions is outside the scope of this course. The extension to chemically reactive systems is treated in the course 'Chemical Reaction Engineering'. In this chapter, first the similarities between molecular heat and mass transfer processes are indicated. The analogy holds for diluted one-phase systems. For two-phase systems one has to take the effect of the distribution coefficient (i.e. different solubility in different phases) into account and for undiluted systems drift-fluxes may become important. This is discussed in the second part of this chapter.

Molecular mass transport, or diffusion, is caused by differences in composition, i.e. mole or mass fraction gradients, and is related to the mobility of molecules. More fundamentally, the driving force for molecular mass transport is the difference in chemical potential of a component. However, for ideal systems the gradient in chemical potential is linearly related to the gradient in the mole fraction, and when a constant total concentration can be assumed, also linearly related to the gradient in the concentration of the component to be transferred, as described by Fick's law (equation (11.1)). This mobility of a component differs strongly between gasses, fluids and solids, which results in large differences in their respective diffusion coefficients (see Table 11.1). For gasses, the diffusion coefficients are in the same order of magnitude as thermal diffusivity coefficients, while for fluids and solids the diffusion coefficients are in general much smaller than the thermal diffusivities. Therefore, in liquids, convective transport dominates molecular transport earlier (i.e. at lower fluid velocity) in mass transport than in heat transport.

Table 11.1 Typical values for diffusion coefficients (D).

Medium	Typical values
Gasses	$D \approx 10^{-5}\ m^2/s$
Fluids	$D \approx 10^{-9}\ m^2/s$
Solids	$D \approx 10^{-10}$ to $10^{-15}\ m^2/s$

A major difference between molecular mass transport and molecular transport of thermal energy, is that in the case of mass transport in two-phase systems, there is generally a concentration jump at the interface of two media, due to differences in solubility of the solute in different solvents The ratio of concentrations at the interface is defined as the distribution coefficient K_d, and will play an important role in mass transfer between two phases, as will be discussed in the second part of this chapter.

Finally, next to the effect of the distribution coefficient K_d, there is an additional discrepancy in the description of heat and mass transfer processes for undiluted systems. Fick's law (given by equation (11.1)), is strictly speaking only valid for situations in which there is no net transport through the considered surface. In practice, however, we are often confronted with systems in which this condition is not met. For example, in (selective) absorption and extraction, and distillation, the net transport of one of the components of a mixture is always principally unequal to zero. Also in heterogeneously catalyzed reactions, the mole fluxes of the reactants and products are generally unequal. When describing mass transport in these systems, the dragging of mass by a drift flux needs to be taken into account. The drift flux is caused by the mass transport itself. This dragging of mass in the drift flux must not be confused with convective mass transport as a consequence of (for example) an externally applied pressure gradient, because the drift flux is internally generated. The discussion of this phenomenon will in this course be restricted to binary systems. It will be shown that the effects of drift-fluxes are only important in undiluted systems.

11.2 Molecular transport in one-phase diluted systems

11.2.1 Stationary diffusion

For equimolar diffusion or diffusion in diluted systems (i.e. low mole fractions), molecular mass transport can be described with Fick's law, which gives a relation between the mole flux $\Phi''_{mole,i}$ of a component i and the concentration gradient dc_i/dx of this component:

$$\Phi''_{mole,i} = -D_i \frac{dc_i}{dx} \quad \left[kmol/m^2 s\right] \tag{11.1}$$

Fick's law is in fact fully analogous to Fourier's law, which gives a relation between the heat flux Φ''_h and the temperature gradient dT/dx:

$$\Phi''_h = -\lambda \frac{dT}{dx} \quad \left[W/m^2\right] \tag{11.2}$$

For constant ρC_p, Fourier's law can be written in a form which more clearly shows the analogy:

$$\Phi''_h = -\frac{\lambda}{\rho C_p}\frac{d}{dx}\left(\rho C_p T\right) = -a\frac{d}{dx}\left(\rho C_p T\right) \tag{11.3}$$

In Table 11.2, the rules of correspondence for molecular mass transport (Fick's law) and molecular heat transport (Fourier's law) are summarized. Note that $\rho C_p T$ represents a kind of energy concentration (J/m^3).

Table 11.2 Rules of correspondence for molecular mass and energy transport in one-phase diluted systems

Mass transport	Energy transport
$\Phi''_{mole,i}$	Φ''_h
c_i	$\rho C_p T$
D_i	a

The examples of stationary heat conduction, discussed in paragraph 0, can be directly "translated" to the corresponding stationary diffusion problem, using the correspondence rules stated in Table 11.2. For example, the steady mole flow permeated through a cylindrical dense membrane can be easily derived from equation (7.24) to be

$$\Phi_{mole,i} = \frac{2\pi D_i L}{\ln\left(\dfrac{R_2}{R_1}\right)}\left(c_{i,1} - c_{i,2}\right) \tag{11.4}$$

upon substitution of the correspondence rules given in Table 11.2.

11.2.2 Instationary diffusion

The results that are obtained in paragraph 7.2.5 for instationary one-dimensional heat transport can, using the same rules of correspondence as listed in Table 11.2, be applied for the discussion of instationary one-dimensional mass transport, provided that the concentration of the transported component is small. For instationary one-dimensional mass transport in diluted systems, the second law of Fick holds:

$$\frac{\partial c_i}{\partial t} = D_i \frac{\partial^2 c_i}{\partial x^2} \tag{11.5}$$

Fick's second law is completely analogous to Fourier's differential equation (equation (7.41)) as can be easily seen when using the rules of correspondence from Table 11.2. Alternatively, equation (11.5) can be derived based on an instationary mass balance for component i. To solve equation (11.5), appropriate boundary conditions (i.e. one initial and two boundary conditions) need to be specified. Analogous to the situation of instationary heat conduction, a distinction is made between mass penetration in a "semi-infinite" body and in a finite body, which is reflected in the difference in boundary conditions.

Mass penetration in a 'semi-infinite' body

The solution of (11.5) with the appropriate boundary conditions for penetration in a 'semi-infinite' object completely analogous to (7.43)-(7.45) is given by:

$$Y(x,t) = \frac{c_{i,1} - c_i(x,t)}{c_{i,1} - c_{i,0}} = \operatorname{erf}\left(\frac{x}{\sqrt{4D_i t}}\right) \tag{11.6}$$

In this equation, $c_{i,0}$ is the initial concentration of i in the regarded material and $c_{i,1}$ is the applied concentration on $x=0$ in the same material. Note that $c_{i,0}$ and $c_{i,1}$ correspond to T_0 and T_1, respectively. The expression for the momentary mole flux at $x=0$, $\Phi''_{mole,i}\big|_{x=0}$, can be derived using Fick's law, resulting in:

$$\Phi''_{mole,i}\big|_{x=0} = -D_i \left.\frac{\partial c_i}{\partial x}\right|_{x=0} = \sqrt{\frac{D_i}{\pi t}}\left(c_{i,1} - c_{i,0}\right) \tag{11.7}$$

The (time-)average mole flux $\left\langle \Phi''_{mole,i} \right\rangle$, which occurs over a certain time t_e (from $t=0$), can be then be found from the momentary mole flux by integration over time:

$$\left\langle \Phi''_{mole,i} \right\rangle = \frac{1}{t_e}\int_0^{t_e}\left\{\sqrt{\frac{D_i}{\pi t}}\left(c_{i,1} - c_{i,0}\right)\right\}dt = 2\sqrt{\frac{D_i}{\pi t_e}}\left(c_{i,1} - c_{i,0}\right) \tag{11.8}$$

and the expression for the mass penetration depth δ_m is given by:

$$\delta_m = 2\sqrt{\pi D_i t} \tag{11.9}$$

The mass penetration depth δ_m plays an important role in determining the boundary of the applicability of the penetration theory for the description of instationary molecular mass transport. When the mass penetration depth δ_m is smaller than (or equal to) the characteristic size L of the body, the penetration theory may be applied:

$$\frac{\delta_m}{L} = \frac{2\sqrt{\pi D_i t}}{L} \le 1 : \quad \text{penetration theory is applicable} \tag{11.10}$$

In the case of single-sided mass penetration, L equals the total thickness d of the material, while in two-sided mass penetration, L equals half of the thickness $d/2$ of the material.

Condition (11.10) can also be expressed in dimensionless form using the Fourier number:

$$Fo = \frac{D_i t}{L^2} \leq \frac{1}{4\pi} \approx 0.08 \tag{11.11}$$

Note that here the Fourier number is defined differently (but fully analogous) to the case of heat transfer. The Fourier number here represents the ratio between the process time t and the characteristic time for diffusion L^2/D_i. In liquids and solids, diffusion coefficients are generally much smaller than the thermal diffusivity, so that the penetration theory for mass transport is applicable for longer process times than for heat transport.

Analogous to heat transport, the momentary and time-average mole fluxes can also be expressed with a mass transfer coefficient k. This variable represents the mole flux $\Phi''_{mole,i}$ per unit driving force Δc_i:

$$k = \frac{\Phi''_{mole,i}}{\Delta c_i} \tag{11.12}$$

For the driving force Δc_i, generally the difference between the applied concentration $c_{i,1}$ and the average concentration of the body $\langle c_i \rangle$ is taken. Because both concentrations are based on the same phase, the distribution coefficient K_d does not appear in the expression for the driving force. Under the conditions in which the penetration theory is valid, the driving force can be approximated by $\left(c_{i,1} - c_{i,0}\right)$ so that for the momentary and time-average mass transfer coefficients follows:

$$k = \sqrt{\frac{D_i}{\pi t}} \quad \left[m/s\right] \tag{11.13}$$

$$\langle k \rangle = 2\sqrt{\frac{D_i}{\pi t}} \quad \left[m/s\right] \tag{11.14}$$

The expressions for the momentary and time-average mass transfer coefficients can also be expressed in dimensionless form, introducing the Sherwood number Sh:

$$Sh = \frac{kL}{D_i} = \frac{1}{\sqrt{\pi}}\left(\frac{D_i t}{L^2}\right)^{-\frac{1}{2}} = \frac{1}{\sqrt{\pi}}\left(Fo\right)^{-\frac{1}{2}} \tag{11.15}$$

$$\langle Sh \rangle = \frac{\langle k \rangle L}{D_i} = \frac{2}{\sqrt{\pi}}\left(\frac{D_i t_e}{L^2}\right)^{-\frac{1}{2}} = \frac{2}{\sqrt{\pi}}\left(Fo_e\right)^{-\frac{1}{2}} \tag{11.16}$$

The Sherwood number Sh in equation (11.15) corresponds to the Nusselt number Nu and gives here the ratio of the stationary diffusion resistance ($= L/D_i$) and the instationary diffusion resistance ($1/k$). Comparing (11.15) and (11.16) to (7.61) and (7.62) learns (with: $\left(\lambda/\left(\rho C_p\right)=a\right)\leftrightarrow D_i$) that the mass transfer coefficients k and $\langle k\rangle$ correspond to $\alpha/\left(\rho C_p\right)$ and $\langle\alpha\rangle/\left(\rho C_p\right)$, respectively.

11.2.2.1 Mass penetration in a finite medium

For the description of mass transport in a finite body in which the boundary conditions are analogous to (7.64) and (7.65), all analytical and graphical results that are obtained for heat penetration in a finite body can be used, taking the rules of correspondence of Table 11.3 into account. Newman's rules can also be applied for systems in which there is simultaneous mass transport in several directions. Note that the rules of correspondence do not imply that the value of *Sh* and *Nu* are necessarily identical!

Table 11.3 Rules of correspondence

Mass transport	Heat transport
$\Phi''_{mole,i}$ or $\Phi''_{mass,i}$	Φ''_h
c_i or ρ_i	$\rho C_p T$
D_i	a
k	$\alpha/\left(\rho C_p\right)$
Sh	Nu
Sc	Pr

11.2.2.2 Example of instationary mass transport in a very long cylinder:

Question:

A very long porous cylinder with radius $R=0.05\ m$ is drenched with a saline solution (initial salt concentration $c_{z,0}=1.0\ kmol/m^3$). At time $t=0$, the cylinder is placed in flowing "clean" water. The water flows around the cylinder in such a way that the concentration of the dissolved salt is negligible at the surface of the cylinder. The diffusion coefficient of salt in water is $10^{-9}\ m^2/s$

a) Calculate the mass transfer coefficient for the mass transport from the cylinder to the surrounding water, 15 minutes after bringing the cylinder in contact with the water.

b) How much time does it take to remove 99% of the initially present salt?

Solution:

In this case, the mass transfer from the cylinder to the surrounding water is completely determined by the diffusion inside the cylinder, because the concentration at the cylinder surface was given to be equal to the bulk concentration (≈ 0) of the water. Inside the cylinder, there will in principle be molecular mass transport both in the radial direction and in the axial direction. However, for a very long cylinder, the radial mass transport will dominate. For the radial mass transport $r = 0$ is the "natural" symmetry line, so that the radius R is the characteristic length in Fourier's number:

$$Fo = \frac{D_i t}{R^2} = \frac{10^{-9} \cdot 900}{\left(0.05\right)^2} = 3.6 \cdot 10^{-4} << 0.04 \tag{11.17}$$

This Fo -value is low enough to allow application of the penetration theory for the calculation of the desired (momentary) mass transfer coefficient k :

$$k = \sqrt{\frac{D_i}{\pi t}} = \sqrt{\frac{10^{-9}}{\pi \cdot 900}} = 5.95 \cdot 10^{-7} \;\; m/s \tag{11.18}$$

When 99% is to be removed, the penetration theory will no longer be applicable. First, the Y -value (dimensionless driving force) is calculated which corresponds to a degree of removal of 99%. The degree of removal can be associated with Y_G :

$$Y_G = \frac{c_{i,1} - \left(c_i\right)_G}{c_{i,1} - c_{i,0}} = \frac{0 - 0.01}{0 - 1.0} = 0.01 \tag{11.19}$$

In which $c_{i,0}$ is the initial salt concentration in the cylinder, $c_{i,1}$ is the imposed concentration and is in this exercise equal to the bulk concentration of the salt in the surrounding water and $\left(c_i\right)_G$ is the average concentration of the salt in the cylinder. Using Figure 7.9, the Fo number can be determined (take the Y_G line for a cylinder):

$$Fo = \frac{D_i t}{R^2} = 0.73 \tag{11.20}$$

From this Fo number follows a time of $t = 1.83 \cdot 10^6 \; s \approx 21 \text{ days}$. This high value for the process time is quite characteristic for diffusion phenomena and is related to the extremely low value of the diffusion coefficient. Finally, note that the maximum mole fraction of the salt in the solution below 2%, so that a Fickian description of the mass transport is allowed (see also paragraph 11.4).

$$x_{i,\max} = \frac{c_{i,0}}{c_L} = \frac{c_{i,0}}{\dfrac{\rho_L}{M_L}} = \frac{1000}{\dfrac{1000}{18.02 \cdot 10^{-3}}} = 0.018 << 1 \tag{11.21}$$

11.3 Two phase systems: the effect of the distribution coefficient

The system displayed in Figure 7.2, showing conductive heat transport in a composite material (i.e. different layers with different thermal conductivities) *cannot* be directly 'translated' to the mass transfer analogy of molecular mass transport between different phases using the rules of correspondence listed in Table 11.3, because the diffusing component generally has different solubilities in the different layers. This difference in solubility in different phases, described with the distribution coefficient K_d, results in a concentration jump at the boundaries between the two layers. Obviously in conductive heat transport in a composite material, the temperature profile is continuous across the interface.

To study the effect of the distribution coefficient K_d on the overall mass transfer rate, we study the stationary diffusion of component A in a composite material that is composed of layer "1" and layer "2" (see Figure 11.1). The solubilities of component A are different for layer "1" and layer "2" and are related by the distribution coefficient (sometimes also referred to as the partition coefficient) K_d:

$$K_d = \frac{\left(c_{A,2}\right)_{\text{equilibrium}}}{\left(c_{A,1}\right)_{\text{equilibrium}}} \tag{11.22}$$

Note that for heat transfer holds: $K_d = 1$ (no temperature jump at boundaries between two phases). Using stationary differential mass balances we can deduce, fully analogously to stationary heat conduction in a flat plate, that the mole flux of A in both layers should be constant:

$$\Phi''_{mole,A,1} = C_1 \qquad \text{and:} \qquad \Phi''_{mole,A,2} = C_2 \tag{11.23}$$

No mass can disappear during the transport from layer $"1"$ to layer $"2"$ (also no accumulation at the interface in the steady state), hence the constants C_1 and C_2 are equal: $C_1 = C_2 = C$, or: $\Phi''_{mole,A,1} = \Phi''_{mole,A,2} = \Phi''_{mole,A} = C$.

Based on Fick's law, it can be concluded that the concentration profile in both layers is linear. Using Figure 11.1, the following expressions for the mole fluxes are obtained:

$$\Phi''_{mole,A,1} = \frac{D_{A,1}}{d_1}\left(c_{A,1} - c^i_{A,1}\right) \tag{11.24}$$

And:

$$\Phi''_{mole,A,2} = \frac{D_{A,2}}{d_2}\left(c^i_{A,2} - c_{A,2}\right) \tag{11.24}$$

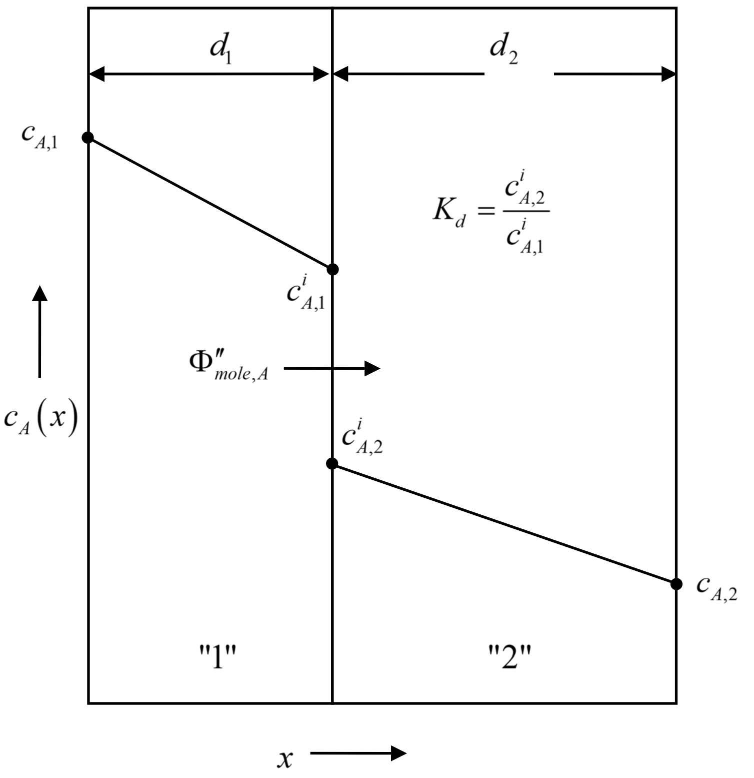

Figure 11.1 Diffusion in a composite material in which the thickness and the diffusion coefficient of A differs per layer. Additionally, A has a different solubility in layers "1" and "2".

If equilibrium is reached at the interface between the two layers, which is generally assumed, the following expression can be derived for the (overall) mole flux of A (try this for yourself!):

$$\Phi''_{mole,A} = \frac{c_{A,1} - \frac{c_{A,2}}{K_d}}{\frac{d_1}{D_{A,1}} + \frac{d_2}{K_d D_{A,2}}} = K_1\left(c_{A.1} - c^*_{A,1}\right) \tag{11.26}$$

where K_1 is the overall mass transfer coefficient related to layer "1":

$$\frac{1}{K_1} = \frac{d_1}{D_{A,1}} + \frac{d_2}{K_d D_{A,2}} \tag{11.27}$$

And $c^*_{A,1}$ is a fictitious concentration related to layer "1" which is in equilibrium with the actual concentration in layer "2", $c_{A,2}$:

$$c^*_{A,1} = \frac{c_{A,2}}{K_d} \tag{11.28}$$

Analogously, equation (11.26) can also be written in a completely equivalent following form, using the concentrations and the overall mass transfer coefficient related to layer "2" :

$$\Phi''_{mole,A} = \frac{K_d c_{A,1} - c_{A,2}}{\dfrac{K_d d_1}{D_{A,1}} + \dfrac{d_2}{D_{A,2}}} = K_2\left(c^*_{A,2} - c_{A,2}\right) \tag{11.29}$$

Here K_2 is the overall mass transfer coefficient related to layer "2" :

$$\frac{1}{K_2} = \frac{K_d d_1}{D_{A,1}} + \frac{d_2}{D_{A,2}} \tag{11.30}$$

And $c^*_{A,2}$ is a (fictitious) concentration related to layer "2" which is in equilibrium with the actual concentration in layer "1", $c_{A,1}$:

$$c^*_{A,2} = K_d c_{A,1} \tag{11.31}$$

Equations (11.26) and (11.29) can be interpreted in terms of Ohm's law: the mole flux of A is the ratio of a driving force $\left(c_{A,1} - c^*_{A,1}\right)$ or $\left(c_{A,2} - c^*_{A,2}\right)$ and an overall mass transfer resistance $\left(1/K_1\right)$ or $\left(1/K_2\right)$. Note that the driving force is not simply the concentration difference between the two layers, but an altered expression taking into account the differences in solubility. That this is required can easily be understood when considering the mass transfer of a component from one phase to another, where the solubility of the component in the first phase is very low and in the second phase very high (i.e. K_d is very large): without properly accounting for the effect of the distribution coefficient on the driving force, one could easily predict mass transfer in the wrong direction once the concentration of the component in the second phase starts building up. In this case there is mass transfer from a phase with low concentration to a phase with a high concentration (due to the much higher solubility)! The total mass transfer resistance (with the dimension $[s/m]$) is equal to the sum of the partial mass transfer resistances $\left(d_1/D_{A,1}\right)$ for layer "1" and $\left(d_2/D_{A,2}\right)$ for layer "2", with a correction for the difference in solubility. Note that the effect of the distribution coefficient K_d on the overall mass transfer resistance is such, that the mass transfer resistance shifts to the phase in which A has the lowest solubility:

$$\frac{\text{partial mass transfer resistance layer "1"}}{\text{partial mass transfer resistance layer "2"}} = \frac{d_1}{d_2}\frac{D_{A,2}}{D_{A,1}} K_d \tag{11.32}$$

Check for yourself that this outcome is independent of taking equation (11.27) or (11.30) as the starting point. Finally it is noted, that the results discussed in this paragraph can be generalized from stationary diffusion resistances to other mass transfer resistances (*viz.* instationary diffusion, free or forced convection) by changing $\left(d_1/D_{A,1}\right)$ to $\left(1/k_1\right)$ and $\left(d_2/D_{A,2}\right)$ to $\left(1/k_2\right)$.

11.4 Undiluted systems: the effect of drift fluxes

In addition to the effect of the distribution coefficient K_d, there is an additional discrepancy in the description of heat and mass transfer processes for undiluted systems. Due to a net transport of one of the components of a mixture (e.g. from one phase to another or to and from a catalytic surface), the total mole flux is unequal to zero, which necessitates the extension of Fick's law to account for these drift-fluxes.

In the following sections we will make a distinction between diffusion in liquids and solids on the one hand and diffusion in gasses on the other hand. This distinction is not fundamental, but has to do with the choice of the measure of concentration with which the diffusion is usually described: in liquids and solids, the density ρ_i is often used as a measure of concentration of component i (ρ_i is the amount of *i* in kg per unit volume of the mixture), while in gasses the concentration c_i (c_i is the number of $kmole\ i$ per unit volume of the mixture) is often used or the partial pressure P_i.

11.4.1 Diffusion in liquids and solids

For diffusion in a liquid which consists of two components A and B, the following expressions are valid for the mass fluxes of A and B:

$$\Phi''_{mass,A} = -\overline{D}_{AB}\frac{d\rho_A}{dx} + \frac{\rho_A}{\rho}\left(\Phi''_{mass,A} + \Phi''_{mass,B}\right) \quad \left[kg/\left(m^2 s\right)\right] \tag{11.33}$$

$$\Phi''_{mass,B} = -\overline{D}_{BA}\frac{d\rho_B}{dx} + \frac{\rho_B}{\rho}\left(\Phi''_{mass,A} + \Phi''_{mass,B}\right) \quad \left[kg/\left(m^2 s\right)\right] \tag{11.34}$$

Here ρ is the total density $(\rho = \rho_A + \rho_B)$, which has been assumed constant, and $\overline{D}_{AB}$ and $\overline{D}_{BA}$ are the binary diffusion coefficients of A and B in the mixture, respectively. The first terms on the right hand side of (11.33) and (11.34) describe the molecular transport due to the density gradients of A and B, while the second terms in these equations describe the molecular transport as a consequence of the so-called drift fluxes. When the sum of the mass fluxes is equal to zero, equations (11.33) and (11.34) reduce to Fick's law and the system. Note that for diffusion in diluted systems ($\rho_A/\rho << 1$ or $\rho_B/\rho << 1$), the mass transport can also be described by Fick's law. It can be proven that the binary diffusion coefficients $\overline{D}_{AB}$ and $\overline{D}_{BA}$ are equal to each other:

$$\overline{D}_{AB} = \overline{D}_{BA} = \overline{D} \tag{11.35}$$

11.4.2 Diffusion in gases

For diffusion in a gas which consists of two components A and B, the following expressions are valid for the mole fluxes of A and B:

$$\Phi''_{mole,A} = -D_{AB}\frac{dc_A}{dx} + \frac{c_A}{c}\left(\Phi''_{mole,A} + \Phi''_{mole,B}\right) \quad \left[kmole/\left(m^2 s\right)\right] \tag{11.36}$$

$$\Phi''_{mole,B} = -D_{BA}\frac{dc_B}{dx} + \frac{c_B}{c}\left(\Phi''_{mole,A} + \Phi''_{mole,B}\right) \quad \left[kmole/\left(m^2 s\right)\right] \tag{11.37}$$

where c, the total concentration $\left(c = c_A + c_B\right)$ has been assumed constant, and D_{AB} and D_{BA} are the binary diffusion coefficients of A and B in the mixture, respectively. The first terms of the right hand side of (11.36) and (11.37) describe again the molecular transport resulting from the concentration gradients of A and B, while the second terms in these equations describe the molecular transport as a consequence of dragging (the so-called drift fluxes). When the sum of the mole fluxes is equal to zero, (11.36) and (11.37) reduce to Fick’s law and this case is reffered to “equimolar diffusion”, which will be investigated in the next section. Note that for diffusion in diluted systems ($c_A/c << 1$ or $c_B/c << 1$), the mass transport can also be described by Fick’s law. Again the binary diffusion coefficients D_{AB} and D_{BA} are equal:

$$D_{AB} = D_{BA} = D \tag{11.38}$$

For an ideal gas, the total concentration c is proportional to the total pressure p and because pressure balancing in gasses is very fast with respect to (molecular) mass transport, the assumption of a constant total concentration c can often be justified. Using the example of binary gas diffusion, the cases of equimolar and non-equimolar diffusion will now be compared.

11.4.3 Example of equimolar diffusion

Two vessels $"1"$ and $"2"$ contain a mixture of two ideal gases *A* and *B*. The total pressure p and the temperature *T* are equal in both vessels, the partial pressures of *A* and *B* (indicated with p_A and p_B) are kept constant in both vessels, see Figure 11.2. Vessel $"1"$ contains a relatively high amount of *A* ($p_{A,1} > p_{B,1}$), while vessel $"2"$ contains a relatively high amount of *B* ($p_{B,2} > p_{A,2}$). Both vessels are free of concentration gradients due to good mixing. The two vessels are connected through a tube with a constant diameter. Because of the differences in partial pressure (concentration gradients) there is transport of A (from $"1"$ to $"2"$) and B (from $"2"$ to $"1"$), while the total pressure p is constant.

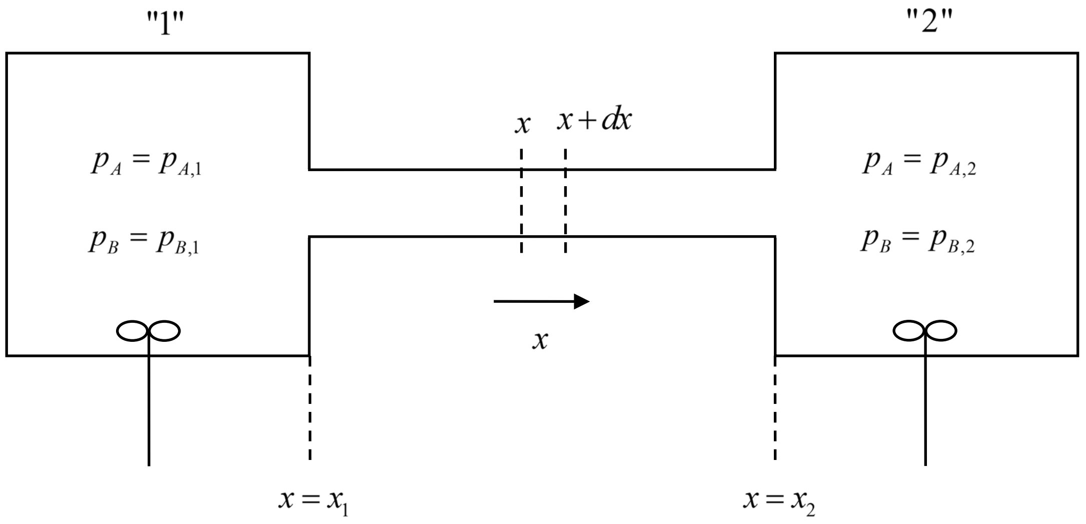

Figure 11.2 Diffusion in a binary system at constant pressure and temperature.

Because $c_A = p_A/RT$ and $c_B = p_B/RT$, in this system an equal amount of A molecules has to be transported from "1" to "2" as B molecules from "2" to "1" (otherwise the total pressure would not be constant), i.e.:

$$\Phi''_{mole,A} + \Phi''_{mole,B} = 0 \tag{11.39}$$

This means that equations (11.36) and (11.37), because of the equimolar diffusion in this situation, reduce to:

$$\Phi''_{mole,A} = -D\frac{dc_A}{dx} = -\frac{D}{RT}\frac{dp_A}{dx} \tag{11.40}$$

And:

$$\Phi''_{mole,B} = -D\frac{dc_B}{dx} = -\frac{D}{RT}\frac{dp_B}{dx} \tag{11.41}$$

Having used $D_{AB} = D_{BA} = D$. When expressions (11.40) and (11.41) are combined with the respective stationary differential component balances (constant mole fluxes of A and B inside the connection tube), the following differential equations are obtained for the partial pressures of A and B in the tube:

$$\frac{d^2 p_A}{dx^2} = 0 \quad \text{and:} \quad \frac{d^2 p_B}{dx^2} = 0 \tag{11.42}$$

With boundary conditions:

$$x = x_1: \; p_A = p_{A,1} \quad p_B = p_{B,1} \tag{11.43}$$

$$x = x_2: \; p_A = p_{A,2} \quad p_B = p_{B,2} \tag{11.44}$$

From equation (11.42) follows that the profiles of the partial pressures of A and B in the tube are linear. From the solution of equation (11.42) with boundary conditions (11.43) and (11.44), the following expressions for the mole fluxes of A and B in the tube can be obtained (check this yourself!):

$$\Phi''_{mole,A} = -\frac{D}{RT}\frac{p_{A,2}-p_{A,1}}{x_2-x_1} \quad (>0) \tag{11.45}$$

$$\Phi''_{mole,B} = -\frac{D}{RT}\frac{p_{B,2}-p_{B,1}}{x_2-x_1} \quad (<0) \tag{11.46}$$

11.4.4 Example of non-equimolar diffusion

The phenomenon of non-equimolar diffusion is discussed using the example of the evaporation of a volatile component A into an inert gas B. The set-up as shown in Figure 11.2 is adjusted so that the tube before $x = x_1$ is in contact with pure liquid A, while the tube before $x = x_2$ is in contact with a mixture of A and B. The total pressure p and the temperature T are both constant (i.e. independent of x). At $x = x_1$, the partial pressure of A is equal to the saturation pressure of A at the prevailing temperature ($p_A = p_{A,1}$, $p_B = p - p_{A,1} = p_{B,1}$), while at $x = x_2$, the partial pressure of A is smaller than the saturation pressure ($p_A = p_{A,2} < p_{A,1}$, $p_B = p - p_{A,2} = p_{B,2}$). In Figure 11.3, the adjusted set-up is shown. The volatile component, which is at the bottom of a vertical tube, evaporates at the interface at $x = x_1$, diffuses due to the partial pressure gradient perpendicularly to the interface and is taken up by a gas flow of constant composition at $x = x_2$.

For the stationary situation we can easily derive again that the mole fluxes of A and B in the tube are constant:

$$\frac{d}{dx}\left(\Phi''_{mole,A}\right) = 0 \tag{11.47}$$

$$\frac{d}{dx}\left(\Phi''_{mole,B}\right) = 0 \tag{11.48}$$

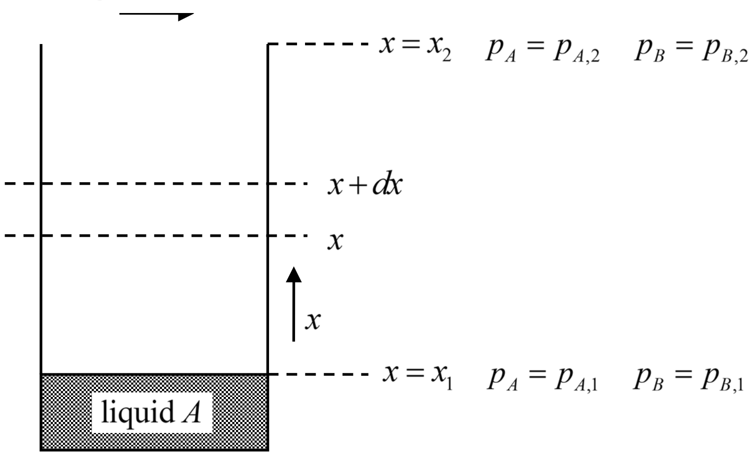

Figure 11.3 Evaporation of a volatile component A in a vertical tube.

Because the interface $x = x_1$ is impenetrable to B (i.e. *B* does not dissolve in liquid *A*), the mole flux of B must be equal to zero because of equation (11.48): $\Phi''_{mole,B} = 0$. This means that equations (11.36) and (11.37), because of the non-equimolar diffusion in this situation, reduce to:

$$\Phi''_{mole,A} = -D\frac{dc_A}{dx} + \frac{c_A}{c}\left(\Phi''_{mole,A}\right) = -\frac{D}{RT}\frac{dp_A}{dx} + \frac{p_A}{p}\left(\Phi''_{mole,A}\right) \tag{11.49}$$

$$0 = -D\frac{dc_B}{dx} + \frac{c_B}{c}\left(\Phi''_{mole,A}\right) = -\frac{D}{RT}\frac{dp_B}{dx} + \frac{p_B}{p}\left(\Phi''_{mole,A}\right) \tag{11.50}$$

From equation (11.49) it follows that the transport of A is partly due to molecular transport because of a concentration gradient of A and partly due to drift-fluxes. Although also for component B molecular transport occurs due to a concentration gradient of B, this transport is canceled out by the molecular transport of B due to the drift-fluxes in the opposite direction.

Rewriting equation (11.49) to obtain for the mole flux of A:

$$\Phi''_{mole,A} = -\frac{D}{RT}\frac{p}{p - p_A}\frac{dp_A}{dx} \tag{11.51}$$

Combining equation (11.49) with the stationary differential component balance of A yields upon integration the following expression for the partial pressure profile of A in the tube:

$$\frac{p - p_A(x)}{p - p_{A,1}} = \left(\frac{p - p_{A,2}}{p - p_{A,1}}\right)^{\frac{x - x_1}{x_2 - x_1}} \tag{11.52}$$

Using $p_B = p - p_A$, from (11.52) the profile of the partial pressure of B in the tube can be derived:

$$\frac{p_B(x)}{p_{B,1}} = \left(\frac{p_{B,2}}{p_{B,1}}\right)^{\frac{x - x_1}{x_2 - x_1}} \tag{11.53}$$

From equations (11.52) and (11.53) follows, contrary to the situation of equimolar diffusion, that the partial pressure profiles $p_A(x)$ and $p_B(x)$ are non-linear for the systems with non-equimolar diffusion. In Figure 11.4, the partial profile pressures are illustrated for both equimolar and non-equimolar diffusion.

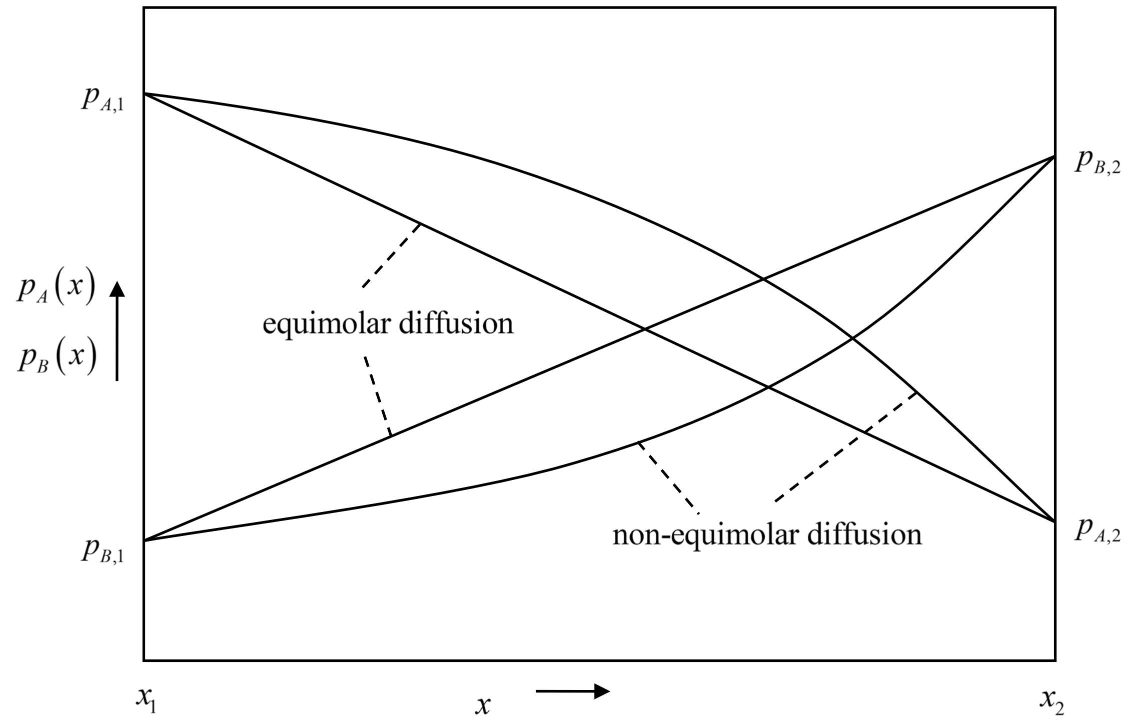

Figure 11.4 Partial pressure profiles for equimolar and non-equimolar diffusion in a binary system composed of components A and B.

Using equations (11.51) and (11.52), the following expression for the mole flux of the evaporating component A can be obtained:

$$\Phi''_{mole,A} = \frac{D}{RT}\frac{p}{x_2 - x_1}\ln\left(\frac{p - p_{A,2}}{p - p_{A,1}}\right) \tag{11.54}$$

For equimolar diffusion we had already found:

$$\Phi''_{mole,A} = -\frac{D}{RT}\frac{p_{A,2} - p_{A,1}}{x_2 - x_1} \tag{11.55}$$

To get insight into the extent to which the mole flux for non-equimolar diffusion differs from the mole flux for equimolar diffusion, the Stefan-factor f_d is introduced and is defined as:

$$f_d = \frac{\text{mole flux of } A \text{ for non-equimolar diffusion}}{\text{mole flux of } A \text{ for equimolar diffusion}} \tag{11.56}$$

Substituting equations (11.54) and (11.55) into the definition equation (11.56) gives:

$$f_d = \frac{p}{p_{A,1} - p_{A,2}} \ln\left(\frac{p - p_{A,2}}{p - p_{A,1}}\right) = 1 + \frac{1}{2}\frac{p \cdot (p_1 + p_2)}{(p - p_1)^2} - \frac{p_1^2}{(p - p_1)^2} + \frac{1}{3}\left(\frac{(p_1 - p_2)}{(p - p_1)}\right)^3 = 1 + \ldots \qquad (11.57)$$

For the Stefan-factor f_d holds: $f_d > 1$, so that the mole flux of A for non-equimolar diffusion is always larger than the mole flux for equimolar diffusion. This can be easily understood, because in the situation of non-equimolar diffusion, additional transport occurs as a consequence of the drift flux. From (11.57) follows that for relatively low partial pressures of A (with respect to the total pressure p), i.e. diluted systems, the Stefan-factor f_d is practically equal to 1, which means that the diffusion process can be described by Fick's law with good accuracy.

11.4.5 Maxwell-Stefan equations

One often has to deal with multi-component systems in which the components are divided over one or more phases and in which transport occurs under instationary conditions and possibly together with other transport mechanisms (e.g. convection) and/or in interaction with other transport phenomena (e.g. heat transport). For the description of (non-ideal) multi-component systems one principally uses the generalized form of the flux equations (11.33)-(11.34) and (11.36)-(11.37), which are known as the Maxwell-Stefan equations. These flux equations need to be solved simultaneously with the component balances (and possibly the heat balances). A detailed discussion on the Maxwell-Stefan equations is outside the scope of this course.

12 Convective mass transport

12.1 Mass transfer analogy of Newton's cooling law

In process equipment often situations occur in which there is mass exchange with a fixed or movable system wall (boundaries). Well known practical examples of mass exchange through boundaries are distillation, absorption and extraction. The absolute amount of mass which is exchanged per unit time is defined analogous to the description of heat transport through system walls in terms of an average mass transfer coefficient k, the mass-exchanging area A and the (absolute) average driving force, which can be based on density gradients (number of kg component i per m^3) $\left|\rho_{i,w}-\langle\rho_i\rangle\right|$ or concentration gradients (number of $kmole$ of component i per m^3) $\left|c_{i,w}-\langle c_i\rangle\right|$:

$$\Phi_{mass,i}=kA\left|\rho_{i,w}-\langle\rho_i\rangle\right| \quad [kg/s] \tag{12.1}$$

$$\Phi_{mole,i}=kA\left|c_{i,w}-\langle c_i\rangle\right| \quad [kmole/s] \tag{12.2}$$

In these equations, $\rho_{i,w}$ and $c_{i,w}$ are the wall (or interface) concentrations of the transported component i and $\langle\rho_i\rangle$ and $\langle c_i\rangle$ are the average concentrations of this component in the flowing medium. Equations (12.1) and (12.2) can also be expressed in terms of a mass flux or a mole flux:

$$\Phi''_{mass,i}=k\left|\rho_{i,w}-\langle\rho_i\rangle\right| \quad \left[kg/\left(m^2s\right)\right] \tag{12.3}$$

$$\Phi''_{mole,i}=k\left|c_{i,w}-\langle c_i\rangle\right| \quad \left[kmole/\left(m^2s\right)\right] \tag{12.4}$$

Often, the mass transfer coefficients are used in dimensionless form using the already introduced Sherwood number Sh:

$$Sh=\frac{kL}{D_i}=\frac{\frac{L}{D_i}}{\frac{1}{k}}=\frac{\text{diffusion resistance of medium of thickness } L}{\text{convective mass transfer resistance}} \tag{12.5}$$

12.2 Analogy between mass and heat transfer

For convective mass transport, the analogy between heat and mass transfer processes, i.e. the rules of correspondence in Table 11.3, can be fully exploited, so that for all the basic principles we simply refer the reader the description of forced and free convective heat transfer (Chapters 8 and 9).

Thus, when for a certain geometry the rate of heat transport can be described with a dimensionless correlation of the form:

$$Nu = \frac{\alpha L}{\lambda} = f_1\left(Re, Pr, \frac{x}{L} \right) = f_1\left(\frac{\rho \langle v \rangle L}{\eta}, \frac{\nu}{a}, \frac{x}{L} \right) \tag{12.6}$$

then, based on the rules of correspondence in Table 11.3, it can be concluded that the mass transfer rate, for the same geometry and boundary conditions, can be described with a dimensionless correlation of the form:

$$Sh = \frac{kL}{D_i} = f_2\left(Re, Sc, \frac{x}{L} \right) = f_2\left(\frac{\rho \langle v \rangle L}{\eta}, \frac{\nu}{D_i}, \frac{x}{L} \right) \tag{12.7}$$

Here the Schmidt number, $Sc = \nu / D_i$, the ratio of molecular momentum transport rate to the molecular mass transport rate, takes over the role that the Prandtl number, $Pr = \nu / a$, plays in heat transport. The Schmidt number Sc is typically approximately 1 for gases, while Sc is between 100 and 1000 for normal liquids.

The function f_1 for heat transport can be used for the description of mass transport f_2, provided that the mass transfer process is indeed completely analogous to the heat transfer processes, in which case $f_1 = f_2$. This is valid if the following conditions are met:

- There are no chemical reactions.
- The flow regimes are identical.
- There is no significant transport by radiation.
- The transport is in only one phase (K_d effect)
- The relative concentrations of the diffusing components are small (i.e. Fick's law applies).
- The transfer must involve the same wall-type (fixed/moving).
- The Prandtl number Pr and the Schmidt number Sc have the same order of magnitude.
- The dependence on temperature or composition of the transport variables for heat transport and mass transport, respectively, should not differ too much.

12.2.1 The Chilton-Colburn analogy

The analogy between heat and mass transport is especially useful when e.g. mass transfer coefficients *k* can be calculated from theoretical (i.e. in the form of correlations or graphs) or experimental data on heat transfer coefficients α and vice versa. In the discussion of convective heat transport it was already found that Nu-correlations have the following general form:

$$Nu = C_1 + C_2 \left(Re\right)^m \left(Pr\right)^n \tag{12.8}$$

When the abovementioned conditions are satisfied, the correlation for the analogous mass transport process the following relation will have the following form:

$$Sh = C_1 + C_2 \left(Re\right)^m \left(Sc\right)^n \tag{12.9}$$

The value for the exponent n is in principle $1/3$ for fixed walls and $1/2$ for moving walls. Equations (12.8) and (12.9) are used for a further consideration of the analogy between heat and mass transport which was first proposed by Chilton and Colburn.

When dividing equation (12.8) by equation (12.9) we obtain

$$\frac{Nu}{Sh} = \frac{C_1 + C_2 \left(Re\right)^m \left(Pr\right)^n}{C_1 + C_2 \left(Re\right)^m \left(Sc\right)^n} \tag{12.10}$$

In the Chilton-Colburn analogy it is assumed that:

1. The transport occurs at fixed walls (exponent $n = 1/3$)
2. The constant C_1 in (12.8) and (12.9) is either absent or negligible with respect to the second (convective) term (i.e. sufficiently large Re-numbers).

Then equation (12.10) reduces to

$$\frac{Nu}{Sh} = \frac{\left(Pr\right)^{\frac{1}{3}}}{\left(Sc\right)^{\frac{1}{3}}} = \left(\frac{D_i}{a}\right)^{\frac{1}{3}} \tag{12.11}$$

Substituting the definitions for *Nu* and *Sh*, we can finally derive the following correlation between the heat transfer coefficient α and the mass transfer coefficient k (check this!):

$$\frac{\dfrac{\alpha}{\rho C_p}}{k} = \left(\frac{a}{D_i}\right)^{\frac{2}{3}} = \left(Le\right)^{\frac{2}{3}} \tag{12.12}$$

where the dimensionless *Lewis* number, $Le = a/D_i$, has been introduced. Interestingly, equation (12.12) shows that the ratio of heat and mass transfer coefficients only depends on material properties. Of course, the Chilton-Colburn analogy can be extended to other correlations with a different exponent *n* for the Prandtl and Schmidt numbers, resulting in a similar correlation to relate the heat and mass transfer coefficients as equation (12.12), however, where the power 2/3 of the Lewis number is replaced by (1-*n*).

With regard to the Chilton-Colburn analogy, it is noted that the analogy is applicable for both laminar and turbulent flows. Only when using the analogy for laminar flows one needs to take into consideration that the length required to have thermally fully developed flow could be different from the length required to have mass-transfer fully developed flow, and that the analogy only holds if the flow regime is completely identical. For example, for the description of mass transport in laminar flow through a tube, a needs to be replaced by D_i in the Graetz-number. Because for liquids $D << a$, the local Sh-number will become constant "later", i.e. for a larger z. For gases, $D_i \approx a$, so there is no difference with regard to position at which the Sherwood resp. Nusselt number become constant.

The analogy between heat and mass transport is also valid for free convection. In free convection due to mass transport, density gradients are due to concentration gradients. In principle, the Nu-correlations given in Chapter 9 can also be used for the description of mass transport, given that, in the case the free convection is driven by differences in overall density due to concentration differences, the Grashof number Gr_L needs to be defined as:

$$Gr_L = \frac{gL^3}{\nu^2} \frac{\left|\rho_1 - \rho_\infty\right|}{\rho_\infty} \tag{12.13}$$

In this equation, ρ_1 and ρ_∞ are the density at the mass transferring wall and the density at large distance of the mass transferring wall/interface, respectively. When applying the Chilton-Colburn analogy for these systems, take the different values for the power n of the Prandtl number into account. In systems in which coupled heat and mass transfer occurs (see Chapter 13) the density gradient is caused by both temperature and concentration gradients and the presented form of the Chilton-Colburn analogy is not readily applicable.

13 Coupled heat and mass transport

The transport of mass from one phase to the other is principally coupled with a heat effect. Examples are evaporation, sublimation or dissolving a gas or a solid in a liquid. In these types of processes, the occurring heat and mass fluxes through the boundaries are coupled by the heat of evaporation, heat of sublimation and heat of dissolution, respectively. The temperature at the interface adjusts to a value that depends on the rate of heat removal (in the case of a positive heat effect, i.e. an exothermic process: $\Delta H < 0$) or the rate of heat supply (in the case of a negative heat effect, i.e. an endothermic process: $\Delta H > 0$). Note that the abovementioned processes are caused by concentration or density gradients, and that the required heat transport is a consequence. Next to the coupling of heat and mass fluxes via the enthalpy change ΔH of the phase transition, there is a second coupling, because the saturation partial pressure / concentration at the interface depends on the temperature, given by an equilibrium relation (from thermodynamics):

- In evaporation and sublimation, the partial pressure at the interface is a function of temperature (Clausius-Clapeyron equation).
- In dissolving a gas or solid in a liquid, the concentration at the interface is a function of temperature.

The analysis of processes with coupled heat and mass transport will be carried out using the example of evaporation. As a model system we choose a spherical rain droplet falling through unsaturated humid air.

13.1 Example: Droplet evaporation

13.1.1 Qualitative description

Consider a rain droplet falling through unsaturated humid air. Initially, the falling raindrop and the surrounding air have the same temperature, T_0. At the surface of the droplet, the saturation vapor pressure will be reached, which is coupled to T_0 via the equilibrium relation. Because the surrounding air is not saturated with water, the vapor pressure (concentration) of water at the droplet surface is higher than the vapor pressure (concentration) in the bulk of the surrounding air, which induces water transport from the droplet surface to the bulk of the surrounding air. The decreasing concentration of water at the droplet surface will be counteracted by evaporation of the droplet. Heat is needed for this evaporation and because initially this heat cannot be supplied by the surrounding air, the droplet will have to supply the required heat of evaporation and its temperature will decrease slightly. Because of the developed temperature gradient, the surrounding air will start supplying heat for the evaporation. Both the droplet and the surrounding air are now supplying heat for the evaporation process, but because the droplet cools down further, the contribution of the surrounding air to the heat supply increases. When the amount of water that evaporates per unit time is assumed to be equal to the initial evaporation rate, this eventually leads to a state in which the droplet temperature has decreased so much that the surrounding air can supply all the necessary heat for evaporation. In practice, the temperature of the droplet will not have to decrease this much because of the equilibrium relation between the droplet temperature and the saturation vapor pressure. When the droplet temperature decreases, the vapor pressure of water at the droplet surface will also decrease and because of this, the driving force for the evaporation will also decrease. Because of the decreasing driving force, the evaporation rate will decrease, so that the equilibrium situation, in which the surrounding air supplies all heat for evaporation, is reached earlier.

13.1.2 Quantitative description

For a quantitative description of the coupled heat and mass transfer of an evaporating droplet, the described equilibrium situation (see Figure 13.1 with *A* = H_2O) is assumed.

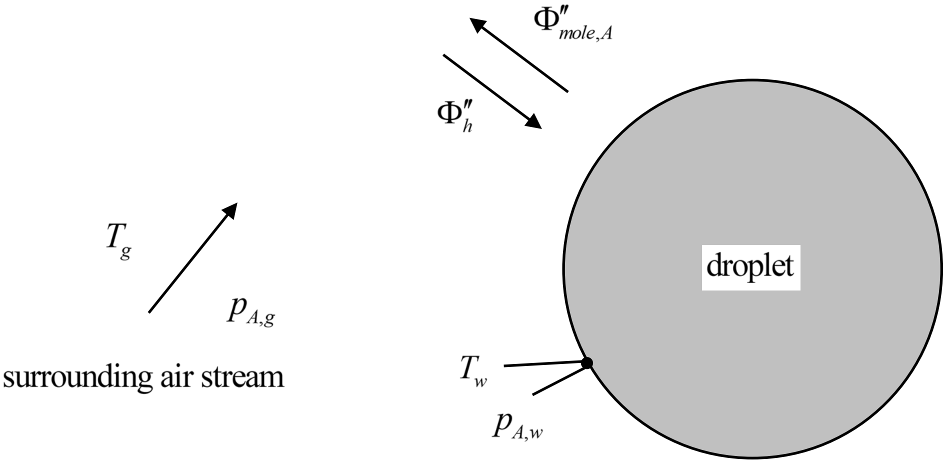

Figure 13.1 Coupled heat and mass transfer in the evaporation of a droplet

For the description we have two equations clearly showing the coupling between heat and mass transfer:

$$\Phi''_h = \Delta H_{v,A} \Phi''_{mole,A} \tag{13.1}$$

$$p_{A,w} = f\left(T_w\right) \tag{13.2}$$

Furthermore, we have expressions for the heat flux Φ''_h and the mole flux $\Phi''_{mole,A}$:

$$\Phi''_h = \alpha\left(T_g - T_w\right) \tag{13.3}$$

$$\Phi''_{mole,A} = k\left(c_{A,w} - c_{A,g}\right) = k\left(\frac{p_{A,w}}{RT_w} - \frac{p_{A,g}}{RT_g}\right) \tag{13.4}$$

In these equations, $\Delta H_{v,A}$ is the molar heat of evaporation of A at T_w, f is the equilibrium relation, α and k are the heat and mass transfer coefficients, respectively. Filling in the flux equations (13.3) and (13.4) into equation (13.1), which describes the coupling between the heat and mole fluxes, gives:

$$\frac{\dfrac{p_{A,w}}{T_w}-\dfrac{p_{A,g}}{T_g}}{T_g-T_w}=\frac{R}{\Delta H_{v,A}}\frac{\alpha}{k} \tag{13.5}$$

The partial pressure at the droplet surface $p_{A,w}$ is a function of the temperature at this surface T_w according to the equilibrium relation (13.2). When T_w and T_g do not differ too much, T_w and T_g in the numerator of the left hand side of equation (13.5) can be replaced by the linear average $\langle T\rangle$ of T_w and T_g , i.e. $\langle T\rangle=\left(T_w+T_g\right)/2$, so that this equation can be (approximately) written as:

$$\frac{p_{A,w}-p_{A,g}}{T_g-T_w}=\frac{R\langle T\rangle}{\Delta H_{v,A}}\left(\frac{\alpha}{k}\right) \tag{13.6}$$

In this equation, α and k relate to the same geometry and the same flow regime (i.e. the same Re-number). When the conditions are met to apply the Chilton-Colburn analogy, equation (12.12) holds for the relation between the heat and mass transfer coefficient. Combination of equation (12.12) and (13.6) yields:

$$\frac{p_{A,w}-p_{A,g}}{T_g-T_w}=\frac{R\langle T\rangle}{\Delta H_{v,A}}\rho C_p\left(Le\right)^{\frac{2}{3}} \tag{13.7}$$

In which Le is the Lewis number: $Le=Sc/Pr=a/D_A$. The Lewis number Le is between 0.5 and 2.0 for gases, but is much larger for liquids. Now we have two equations (equations (13.2) and (13.7)) to describe this system with four unknown variables (T_g, T_w, $p_{A,g}$ and $p_{A,w}$). This allows for elimination of one free variable, so that one of the three remaining variables can be calculated if two others are known. This is, for example, used in the measurement of the humidity of air with a psychrometer. In this device, two thermometers are used: one thermometer measures the air temperature (T_G) and the other thermometer is kept wet and this temperature (T_w) is also measured. Using T_w, a value for the vapor pressure $p_{A,w}$ can be determined, using a vapor pressure table (see Table 13.1). Using equation (13.7), the vapor pressure of A in the bulk of the air $p_{A,g}$ can be calculated. Note that the determined $p_{A,g}$ does not depend on the velocity of the air flow (Re), if the conditions for the analogy between heat and mass transport are met.

Table 13.1 Equilibrium vapor pressure of water as a function of T.
(To convert from mmHg to kPa, multiply with 0.1333224.)

$T\ [K]$	$p_{H_2O}\ [mmHg]$	$T\ [K]$	$p_{H_2O}\ [mmHg]$
273	4.58	299	25.21
275	5.29	301	28.35
277	6.10	303	31.82
279	7.01	305	35.66
281	8.05	307	39.90
283	9.21	309	44.56
285	10.52	311	49.69
287	11.99	313	55.32
289	13.63	315	61.50
291	15.48	317	68.26
293	17.54	319	75.65
295	19.83	321	83.71
297	22.38	323	92.51

Temperature T_w is called the *wet-bulb temperature*, and should not be confused with another important variable, the *adiabatic saturation temperature* T_s. This is the temperature a gas (e.g. air with a temperature T_g and water vapor pressure $p_{A,g}$) will attain when it is fully saturated with vapor and the gas itself supplies all the necessary heat of evaporation by cooling down from T_g to T_s. Based on an energy balance for the gas, the following equation for the adiabatic saturation temperature T_s (and the matching equilibrium vapor pressure $p_{A,s} = f\left(T_s\right)$) can be derived (check this yourself!):

$$\frac{\dfrac{p_{A,s}}{T_s} - \dfrac{p_{A,g}}{T_g}}{T_g - T_s} = \frac{R}{\Delta H_{v,A}} \rho C_p \tag{13.8}$$

This equation can, assuming again that T_s and T_g do not differ too much, be written in the following form:

$$\frac{p_{A,s} - p_{A,g}}{T_g - T_s} = \frac{R\langle T\rangle}{\Delta H_{v,A}} \rho C_p \tag{13.9}$$

With: $\langle T\rangle = \left(T_s + T_g\right)/2$. Except for the factor $\left(Le\right)^{2/3}$, the expression for the adiabatic saturation temperature T_s, equation (13.9), corresponds to the expression for the wet-bulb temperature T_w (and the matching $p_{A,w}$), equation (13.7). The transport coefficients a and D_A have no influence on the magnitude of T_s, but they do have an influence on the rate at which T_s is reached. For all gas mixtures, Le is close to 1, and for the system air/water vapor

$(Le)^{2/3} = 0.95$. This is the reason for the fact that sometimes there is made no distinction between T_w and T_s, although they are of a very different origin.

13.2 Humidity diagram

At the end of this chapter the so-called humidity diagram is discussed, which is often used for calculations in practice. First we introduce the following definitions:

Humidity H: the mass of water vapor per kg of dry air, so:

$$H = \frac{kg \text{ water vapor}}{kg \text{ dry air}} \tag{13.10}$$

Saturation Humidity H_s: the absolute humidity of air which is saturated with water. For the system water/air this is about 0.015 at $20°C$ and 0.086 at $50°C$. For H_s (s = saturation) holds:

$$H_s = \left(\frac{kg \text{ water vapor}}{kg \text{ dry air}} \right)_s \tag{13.11}$$

Relative Humidity RH: the pressure of water vapor in humid air, divided by the saturation pressure of water vapor at the same temperature:

$$RH = \frac{p_{H_2O}}{p_{H_2O,s}} \tag{13.12}$$

Humid Heat Θ_h: the amount of heat required to heat one kg of dry air, together with the contained water vapor, $1°C$ at constant pressure. For the system water/air holds at atmospheric pressure:

$$\Theta_h = 1 + 1.9H \quad \left[kJ/kg \text{ dry air} \cdot °C \right] \tag{13.13}$$

Dew point: the temperature at which the condensation of water vapor commences as humid air is cooled down. So the dew point is the temperature at which humid air is saturated with water vapor.

Next to the abovementioned definitions, the earlier introduced definitions for the adiabatic saturation temperature and the wet-bulb temperature, are important concepts when reading the humidity diagram for the water/air system (see Figure 13.2). We had already noted that these two variables, although principally different, have almost the same value for the water/air system. Using a number of examples, it is clarified how to read the humidity diagram.

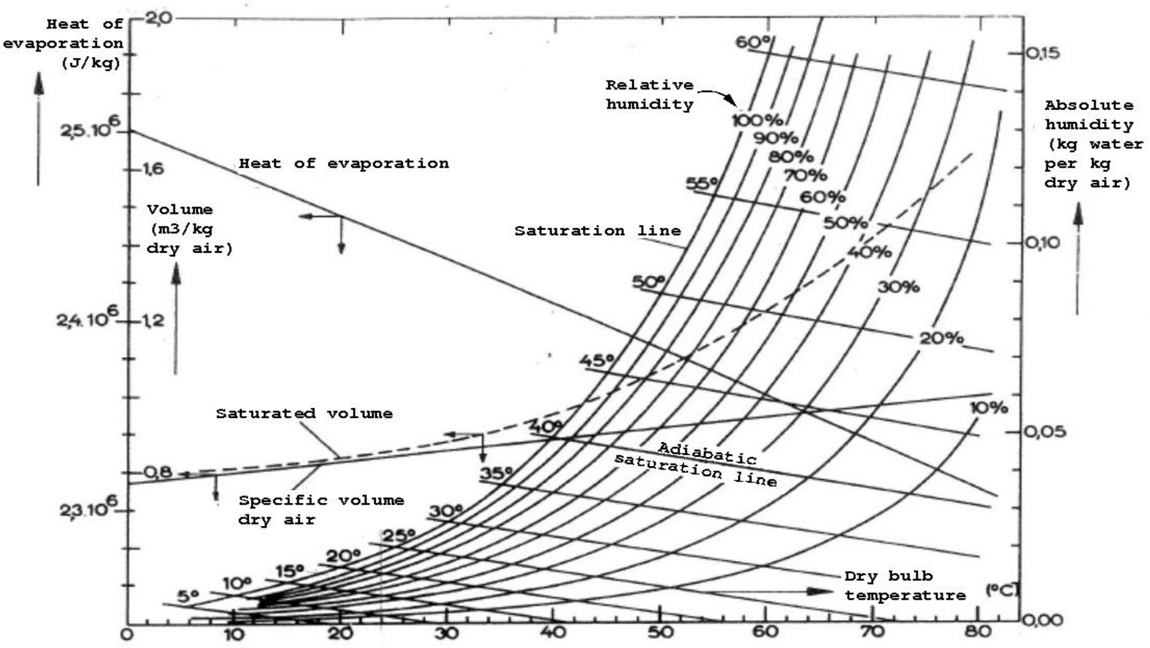

Figure 13.2 The humidity diagram for the water/air system at atmospheric pressure.

1. What are the humidity and the relative humidity of air at $70°C$*, which has a wet-bulb temperature of* $55°C$ *? What is the dew point?*

The intersection of the adiabatic saturation line of this air with the saturation line is found at the temperature of $55°C$. We follow the adiabatic saturation line to the right until the temperature of $70°C$ is reached (at the horizontal axis) and at the right vertical axis, we can read that the humidity H equals 0.105 kg water per kg dry air. From the humidity diagram follows that the relative humidity of this air is about 39%. Cooling air increases the relative humidity; the absolute humidity is not changed. The humidity diagram shows that air with an absolute humidity of 0.105 kg water per kg dry air is saturated at $53.7°C$.

2. The same air is cooled down to $30°C$*. How much water vapor will condense per* m^3 *of saturated air of* $30°C$ *?*

From the humidity diagram, we read that saturated air of $30°C$ contains about 0.027 kg water per kg dry air. So $0.105-0.027=0.078$ kg water per kg dry air is condensed. In the humidity diagram we also read that the saturated volume for air of $30°C$ is about $0.88\ m^3$ per kg dry air. So the amount of condensed vapor is:

$$\frac{0.078}{0.88}=0.089 \quad \left[\frac{kg\ \text{condensed water}}{m^3\ \text{saturated air of } 30°C}\right] \tag{13.14}$$

3. The saturated air of $30°C$ is heated at constant pressure to $70°C$. How much heat is needed to do this and what is the relative humidity and the dew point of the heated air?

During the heating of the air, the humidity H does not change. This humidity stays 0.027 kg water per kg dry air. The humid heat is equal to $1.0513\ kJ$ per kg dry air per $°C$, according to equation (13.13). The required heat is $\left(70-30\right)1.0513=42\ kJ$ per kg dry air. The dew point is of course $30°C$, because the air is saturated at $30°C$. In the humidity diagram we read a relative humidity of 10%.

14 Heat and mass exchange equipment

14.1 Introduction

The purpose of many physical and chemical engineering process steps is exchange of mass and/or energy between two (or more) different streams. Important examples: heat exchangers to heat up a stream by cooling another stream, and bubble, extraction and distillation columns and membrane contactors to transfer a component from one phase to another. The quantitative description of the occurring processes is discussed for mass exchange equipment, which can be very easily ‘translated’ back to describe equivalent heat transfer equipment.

In mass exchange equipment two (or more) phases are brought into contact with one another in order to accomplish mass transfer (often selectively of one specific component) from one phase to the other. The simplest description of mass exchange equipment is with the so-called ‘single stream exchanger’, where the concentration of the component to be transferred is constant in one of the phases. Sometimes, the description of mass exchange equipment can be simplified to the ‘single stream exchanger’, for example in extraction columns with very large solvent flows or heat exchangers with extremely large cooling water flows etc. The description of single steam exchangers is discussed first, introducing the concepts of the number and height of transfer units and the extraction factor on the way.

Contrary to the situation for a single stream exchanger, in practice we often encounter mass exchangers where the concentration of the component that is being transferred varies in all phases that are contacted as a consequence of the mass exchange. We will derive the equations to describe these two-stream contactors, however, in this course we will restrict the discussion to two much encountered types of two-stream-exchangers, which only differ with respect to the way of contacting of the two phases:

1. The co-current exchanger: both phases “1” and “2” flow in the same direction.
2. The counter-current exchanger: both phases “1” and “2” flow in the opposite direction

14.2 Single stream exchanger

The most basic example of a mass exchanger is the so-called single stream exchanger. In this type of exchanger, the concentration of the transferred component is constant (or can be approximately assumed constant) in one of the two phases. The following limiting cases can be distinguished for the single stream exchanger:

1. The phase with the constant concentration is fixed (e.g. flow through a tube with a constant concentration at the tube wall).
2. The phase with the constant concentration is moving (e.g. bubbles of a pure gas which is transferred to the liquid phase in which the bubbles are rising).

The single-stream exchanger will be discussed using an example from the first category (see Figure 14.1). A fluid (phase 1) with a volumetric flow rate Φ_v flows through a round tube with inner diameter d. The wall of the tube (phase 2) consists of a component A which is soluble in the fluid. The concentration of A in phase 2 and the concentration of A in phase 1 at the tube wall are coupled via an equilibrium relation:

$$K_d = \left(\frac{c_{A,1}}{c_{A,2}} \right)_{\text{equilibrium}} = \frac{c_{A,1,w}}{c_{A,2,w}} \tag{14.1}$$

We will assume that K_d is independent of the composition and that Fick's law can be applied (diluted systems). Moreover, we will assume that the total mole flow that is transferred is relatively small compared to the total molar flow rate of the process stream, so that the volumetric flow rate is constant along the axial coordinate. Then, the differential mass balance for the transferred component A for the single stream exchanger reads (neglecting axial diffusion/dispersion):

$$0 = \Phi_v c_{A,1} \big|_x - \Phi_v c_{A,1} \big|_{x+dx} + k \left(c_{A,1,w} - c_{A,1} \right) \pi d \, dx \tag{14.2}$$

After separation and integration (assuming constant mass transfer coefficient k), the following equation is obtained, which gives the relation between the inlet and outlet concentration:

$$\frac{c_{A,1,w} - c_{A,1}^L}{c_{A,1,w} - c_{A,1}^0} = \frac{K_d c_{A,2,w} - c_{A,1}^L}{K_d c_{A,2,w} - c_{A,1}^0} = \exp\left(-\frac{k \pi d L}{\Phi_v} \right) \tag{14.3}$$

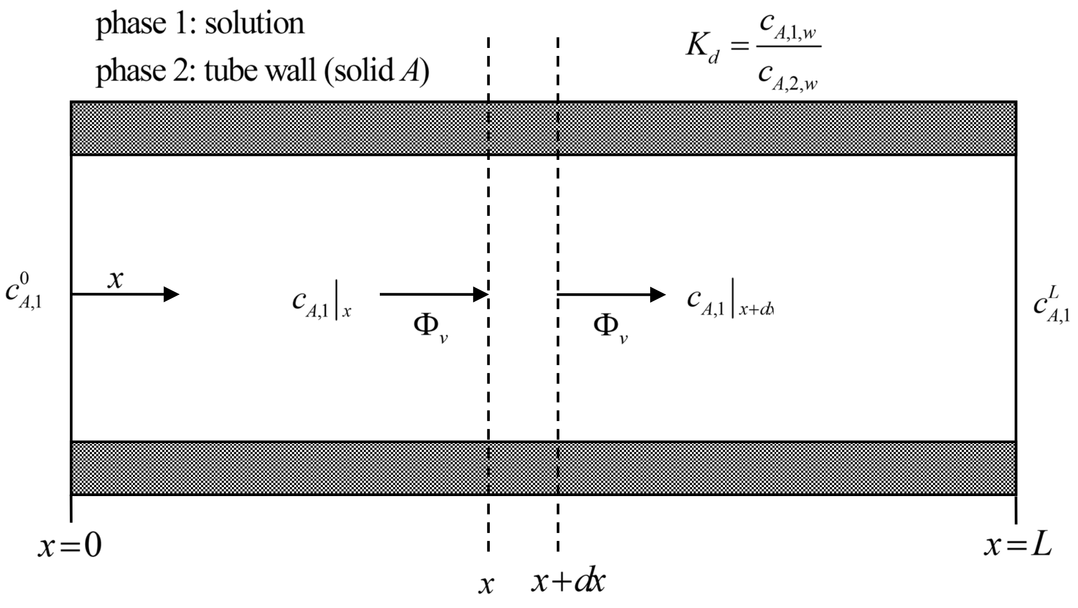

Figure 14.1 Mass exchange between a tube wall (consisting of solid A) and a solution in a single-stream exchanger.

The left hand side of equation (14.3) represents the ratio of the driving force for mass transfer at $x = L$ to the driving force for mass transfer at $x = 0$ (i.e. dimensionless driving force). In the case of mass transfer in packed beds, the term πdL (cylindrical contact area) in equation (14.3) is replaced by aAL:

$$\frac{c_{A,1,w} - c_{A,1}^{L}}{c_{A,1,w} - c_{A,1}^{0}} = \frac{K_d c_{A,2,w} - c_{A,1}^{L}}{K_d c_{A,2,w} - c_{A,1}^{0}} = \exp\left(-\frac{kaAL}{\Phi_v} \right) = \exp\left(-\frac{kaL}{v_o} \right) \qquad (14.4)$$

where a is the specific mass transfer area (amount of m^2 mass transfer area per m^3 packed bed), A is the cross-sectional area of the packed bed and v_o is the velocity in the empty tube or the *superficial velocity* ($v_o = \Phi_v / A$).

Equation (14.3) or (14.4) can also be written as:

$$\frac{c_{A,1,w} - c_{A,1}^{L}}{c_{A,1,w} - c_{A,1}^{0}} = Y = \frac{\text{driving force } x = L}{\text{driving force } x = 0} = \exp\left(-\frac{L}{HTU} \right) \qquad (14.5)$$

where HTU, the height of a transfer unit, is introduced, which represents the tube length or column height (for a packed column) over which the driving force changes with a factor e^{-1} (≈ 37%) (for a single stream exchanger). This variable is defined as:

$$HTU = \frac{\Phi_v}{kaA} = \frac{v_o}{ka} \qquad (14.6)$$

The required tube length to realize a certain relative change of the driving force (concentration change) can be expressed in this length unit as the number of HTU's, also called NTU (number of transfer units):

$$L = NTU \cdot HTU \qquad (14.7)$$

The HTU is a variable that describes the rate of the mass transfer process: a small value of the HTU corresponds to a high mass transfer rate, while a large value of the HTU corresponds to a low mass transfer rate. Note, that in case the overall mass transfer coefficient varies along the length of the apparatus, the length-averaged value should be used in the HTU. The NTU describes the extent of mass exchange realized in the mass exchanger. Finally, note that for an infinitely long tube, the exit concentration equals the equilibrium concentration which occurs in phase 1 at the wall of the tube.

14.3 Two-stream co-current exchanger

In the two-stream co-current exchanger, two phases 1 and 2 with respective volumetric flows $\Phi_{v,1}$ and $\Phi_{v,2}$ are contacted co-currently (i.e. flowing in the same direction, so the inlets of both streams are at the same side of the equipment and the outlets of both streams are at the other side of the equipment) in order to bring about mass exchange of a dissolved component A between 1 and 2 (see Figure 14.2). First, the equilibrium situation is discussed, after which the equations are derived to describe a co-current exchanger of finite size.

14.3.1 Equilibrium situation

In an infinitely long co-current mass exchanger, the outlet streams of both phases are in thermodynamic equilibrium, i.e.:

$$K_d = \frac{c_{A,1}^L}{c_{A,2}^L} \tag{14.8}$$

Combining this with the integral “overall” mass balance over the mass exchanger, given by:

$$\Phi_{v,1}c_{A,1}^0 + \Phi_{v,2}c_{A,2}^0 - \Phi_{v,1}c_{A,1}^L - \Phi_{v,2}c_{A,2}^L = 0 \tag{14.9}$$

the following two expressions can be derived for the outlet concentrations in phase 1 and phase 2, respectively:

$$c_{A,1}^L = \frac{Ec_{A,1}^0 + K_d c_{A,2}^0}{1+E} \tag{14.10}$$

And:

$$c_{A,2}^L = \frac{c_{A,2}^0 + E\dfrac{c_{A,1}^0}{K_d}}{1+E} \tag{14.11}$$

where the so-called extraction factor E has been introduced, which is defined as:

$$E = K_d\frac{\Phi_{v,1}}{\Phi_{v,2}} = \frac{\text{capacity for } A \text{ in phase 1}}{\text{capacity for } A \text{ in phase 2}} \tag{14.12}$$

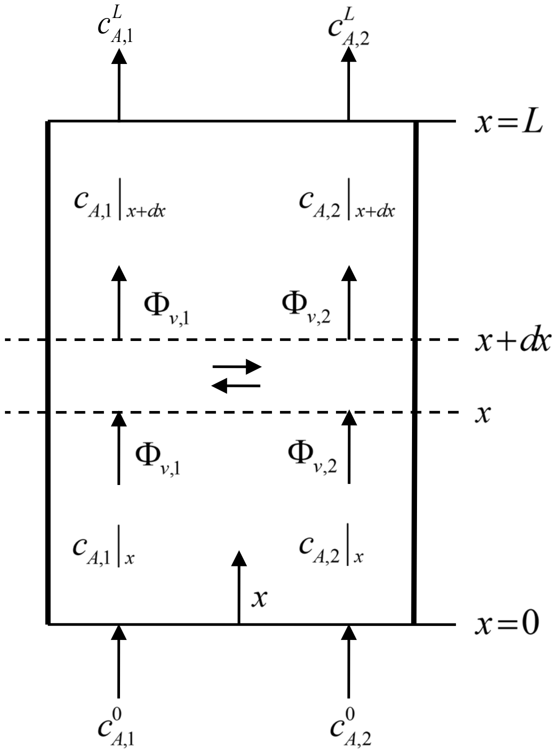

Figure 14.2 Mass exchange between two phases "1" and "2" in a co-current exchanger.

The extraction factor E is important for the choice of the type of equipment in which the mass transfer process is carried out. When component A has to be transferred from phase 2 to a "clean" phase 1, according to (14.10) the value of K_d should be high and the value of E should be low in order to reach a high outlet concentration of A in phase 1. This leads to the demand $\Phi_{v,1} << \Phi_{v,2}$ which can be satisfied by dispersing phase 1 (i.e. in the form of small droplets) in the continuous phase 2.

If, however, phase 2 should reach a high level of depletion (i.e. a low exit concentration A in phase 2), then according to (14.11) both K_d and E should have a high value, or: $\Phi_{v,1} \approx \Phi_{v,2}$. When the initial concentration of A in phase 1 is small, then K_d can be smaller, but because of the requirement for E, in that case $\Phi_{v,1} >> \Phi_{v,2}$.

14.3.2 Kinetic description

In a real device of finite length, thermodynamic equilibrium is not reached and because of this, a kinetic description has to be used for the prediction of the exit concentrations. The starting point are the differential mass balances for both phases (see Figure 14.2):

Phase 1:

$$0 = \Phi_{v,1} c_{A,1} \Big|_{x} - \Phi_{v,1} c_{A,1} \Big|_{x+dx} - \Phi''_{mole,A,1\rightarrow 2} aAdx \tag{14.13}$$

Phase 2:

$$0 = \Phi_{v,2} c_{A,2} \Big|_{x} - \Phi_{v,2} c_{A,2} \Big|_{x+dx} + \Phi''_{mole,A,1\rightarrow 2} aAdx \tag{14.14}$$

where a is the specific mass transfer area between phases 1 and 2. For the solution of the differential mass balances, the expression for the mole flux through the interface from phase 1 to phase 2 has to be developed ($\Phi''_{mole,A,1\rightarrow 2}$). Consider Figure 14.3, in which the qualitative concentration profiles in phases 1 and 2 in the direct vicinity of the interface are illustrated. In principle, in both phases 1 and 2 there could be a (partial) mass transfer resistance which depends on the respective (partial) mass transfer coefficients k_1 and k_2.

Fully analogous to the derivation of the mole flux for stationary diffusion through a composite material (see paragraph 11.3) it can easily be derived that (check this yourself!):

$$\Phi''_{mole,A,1\rightarrow 2} = \frac{c_{A,1} - K_d c_{A,2}}{\frac{1}{k_1} + \frac{K_d}{k_2}} = K_1 \left(c_{A,1} - c^*_{A,1} \right) \tag{14.15}$$

where K_1 is the overall mass transfer coefficient with respect to phase 1 and $c^*_{A,1}$, a (fictitious) concentration of A in phase 1, which is in equilibrium with the local concentration of A in phase 2. The overall mass transfer coefficient K_1 with respect to phase 1 is given by:

$$\frac{1}{K_1} = \frac{1}{k_1} + \frac{K_d}{k_2} \tag{14.16}$$

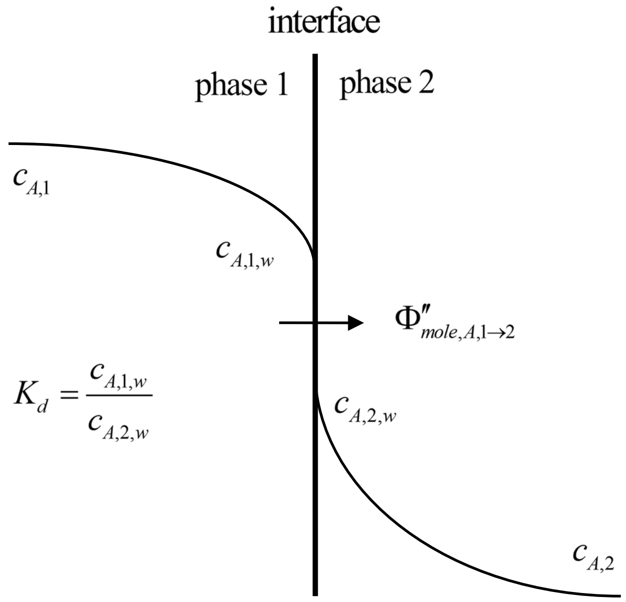

Figure 14.3 Qualitative illustration of the concentration profiles in phases 1 and 2 in the direct vicinity of the interface.

Combination of the mass balance for phase 1, equation (14.13), and the overall expression for the mole flux through the interface (14.15) yields in the limit of $dx \to 0$:

$$\Phi_{v,1} \frac{dc_{A,1}}{dx} = -K_1 \left(c_{A,1} - K_d c_{A,2} \right) aA \tag{14.17}$$

This differential equation cannot be solved in this form because both the concentrations in phase 1 and phase 2 are changing. To solve equation (14.17) the concentration change of A in phase 1 must be related to the change of the driving force $\left(c_{A,1} - K_d c_{A,2} \right)$. This relation can be obtained by adding up equations (14.13) and (14.14):

$$\Phi_{v,1} \frac{dc_{A,1}}{dx} = -\Phi_{v,2} \frac{dc_{A,2}}{dx} \tag{14.18}$$

Using the definition of the extraction factor and equation (14.18) the following can be derived:

$$\frac{d}{dx}\left(c_{A,1} - K_d c_{A,2} \right) = \frac{dc_{A,1}}{dx} - K_d \frac{dc_{A,2}}{dx} = \frac{dc_{A,1}}{dx} + K_d \frac{\Phi_{v,1}}{\Phi_{v,2}} \frac{dc_{A,1}}{dx} = \left(1 + E \right) \frac{dc_{A,1}}{dx} \tag{14.19}$$

which we can use to rewrite equation (14.17) in terms of the change of the driving force $\left(c_{A,1} - K_d c_{A,2} \right)$.

Combining equation (14.17) and (14.19) gives the following differential equation after separation:

$$\frac{d\left(c_{A,1}-K_d c_{A,2}\right)}{\left(c_{A,1}-K_d c_{A,2}\right)}=-\left(1+E\right)\frac{K_1 aA}{\Phi_{V,1}}dx \tag{14.20}$$

Integration of equation (14.20) from $x=0$ to $x=L$ gives:

$$\ln\left(\frac{c_{A,1}^L-K_d c_{A,2}^L}{c_{A,1}^0-K_d c_{A,2}^0}\right)=\ln\left(\frac{\Delta c_A^L}{\Delta c_A^0}\right)=-\left(1+E\right)\frac{K_1 aAL}{\Phi_{V,1}}=-\left(1+E\right)\frac{L}{HTU_1} \tag{14.21}$$

where HTU_1 represents the height of a transfer unit related to phase 1. Because there could be a mass transfer resistance in both phases 1 and 2, instead of the “partial” HTU there is an “overall” HTU which is related to phase 1, because the driving force in (14.21) is also related to phase 1. HTU_1 is given by:

$$HTU_1=\frac{\Phi_{v,1}}{K_1 aA} \tag{14.22}$$

When equation (14.21) for the two stream co-current exchanger is compared to equation (14.5) for the single stream exchanger, it can be seen that the difference is only the occurrence of the extraction factor E as an additional parameter in the equation for the co-current exchanger. On basis of an integral mass balance over the column, E can be expressed as a function of the inlet and outlet concentrations or equation (14.19) (check this yourself!):

$$1+E=\frac{\left(c_{A,1}^0-K_d c_{A,2}^0\right)-\left(c_{A,1}^L-K_d c_{A,2}^L\right)}{c_{A,1}^0-c_{A,1}^L}=\frac{\Delta c_A^0-\Delta c_A^L}{c_{A,1}^0-c_{A,1}^L} \tag{14.23}$$

Fully analogous to the situation for the single stream exchanger, the column length L can be expressed as the product of HTU_1 and NTU_1 so equation (14.21) can be rewritten as:

$$\ln\left(\frac{\Delta c_A^L}{\Delta c_A^0}\right)=-\left(1+E\right)\frac{L}{HTU_1}=-\left(1+E\right)NTU_1 \tag{14.24}$$

After combination with (14.23) the following equation results for the required number of transfer units NTU_1 related to phase 1:

$$NTU_1=\frac{L}{HTU_1}=\frac{1}{1+E}\ln\left(\frac{\Delta c_A^0}{\Delta c_A^L}\right)=\frac{c_{A,1}^0-c_{A,1}^L}{\Delta c_A^0-\Delta c_A^L}\ln\left(\frac{\Delta c_A^0}{\Delta c_A^L}\right) \tag{14.25}$$

Note that the number of transfer units related to phase 1 NTU_1 can be expressed in exclusively the inlet and outlet concentrations.

Before an equation is derived for the total amount that is transferred, first the counter-current-exchanger is considered in very much the same way as the co-current exchanger was discussed.

14.4 Two stream counter-current exchanger

Two phases 1 and 2 with respective volumetric flow rates $\Phi_{v,1}$ and $\Phi_{v,2}$ (both defined positive) are contacted counter-currently to bring about exchange of a dissolved component A between the streams 1 and 2 (see Figure 14.4). In the discussion of the two-stream co-current exchanger, the equilibrium situation was considered first, which will occur at the end of an infinitely long co-current exchanger, which was followed by a kinetic description. In the two-stream counter-current exchanger also a thermodynamic equilibrium will be reached, however, it is not clear beforehand where this equilibrium is reached. Therefore, for the discussion of the counter-current exchanger we will first discuss the kinetic description and followed by a discussion on the location where in a counter-current exchanger equilibrium is reached.

14.4.1 Kinetic description

The starting points for the kinetic description are the differential mass balances for both phases (see Figure 14.4):

Phase 1:

$$0 = \Phi_{v,1} c_{A,1} \Big|_{x} - \Phi_{v,1} c_{A,1} \Big|_{x+dx} - \Phi''_{mole,A,1\to 2} aAdx \tag{14.26}$$

Phase 2:

$$0 = \Phi_{v,2} c_{A,2} \Big|_{x+dx} - \Phi_{v,2} c_{A,2} \Big|_{x} + \Phi''_{mole,A,1\to 2} aAdx \tag{14.27}$$

Comparison of these balances with the corresponding mass balances for the co-current exchanger shows that the mass balance for phase 1 is unchanged, while a minus-sign appears in the mass balance for phase 2. The expression for the mole flux remains obviously unchanged.

Summing the two mass balances, equations (14.26) and (14.27), yields

$$\Phi_{v,1} \frac{dc_{A,1}}{dx} = +\Phi_{v,2} \frac{dc_{A,2}}{dx} \tag{14.28}$$

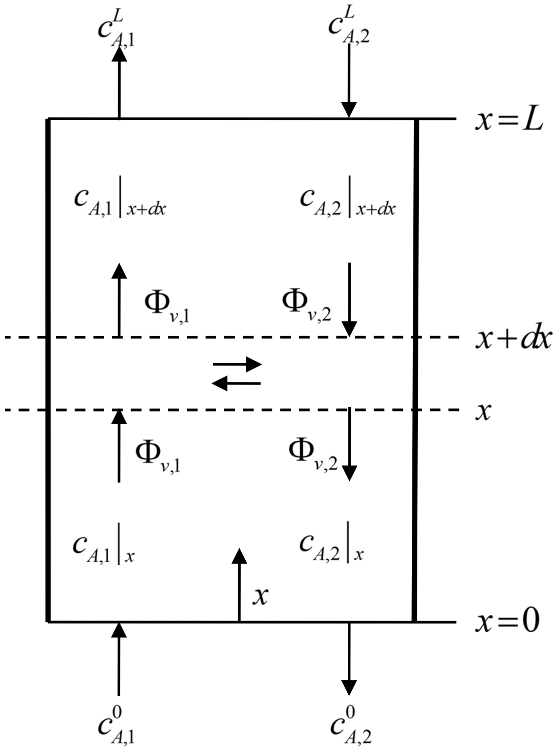

Figure 14.4 Mass transfer between two phases "1" and "2" in a counter-current exchanger.

so that with the definition of the extraction factor and equation (14.28) the following can be derived:

$$\frac{d}{dx}\left(c_{A,1}-K_d c_{A,2}\right)=\frac{dc_{A,1}}{dx}-K_d\frac{dc_{A,2}}{dx}=\frac{dc_{A,1}}{dx}-K_d\frac{\Phi_{v,1}}{\Phi_{v,2}}\frac{dc_{A,1}}{dx}=\left(1-E\right)\frac{dc_{A,1}}{dx} \qquad (14.29)$$

Note that in the special case of *E* = 1, the driving force is constant and hence also the mole flux from phase 1 to phase 2, $\Phi''_{mole,A,1\rightarrow 2}$, is constant, and equations (14.26) and (14.27) can be integrated directly.

Substitution of equation (14.29) in the differential mass balance for phase 1, equation (14.26), gives the following differential equation after separation:

$$\frac{d\left(c_{A,1}-K_d c_{A,2}\right)}{\left(c_{A,1}-K_d c_{A,2}\right)}=-\left(1-E\right)\frac{K_1 aA}{\Phi_{V,1}}dx \qquad (14.30)$$

Integration of (14.30) from $x=0$ to $x=L$ gives:

$$\ln\left(\frac{c_{A,1}^L-K_d c_{A,2}^L}{c_{A,1}^0-K_d c_{A,2}^0}\right)=\ln\left(\frac{\Delta c_A^L}{\Delta c_A^0}\right)=-\left(1-E\right)\frac{K_1 aAL}{\Phi_{V,1}}=-\left(1-E\right)\frac{L}{HTU_1} \qquad (14.31)$$

Analogous to the co-current exchanger, using the integral mass balance over the column or equation (14.30), extraction factor E can be expressed as a function of the inlet and outlet concentrations:

$$1-E=\frac{\left(c_{A,1}^{0}-K_{d}c_{A,2}^{0}\right)-\left(c_{A,1}^{L}-K_{d}c_{A,2}^{L}\right)}{c_{A,1}^{0}-c_{A,1}^{L}}=\frac{\Delta c_{A}^{0}-\Delta c_{A}^{L}}{c_{A,1}^{0}-c_{A,1}^{L}} \tag{14.32}$$

After combining (14.31) with (14.32), the following equation results for the required number of transfer units related to phase 1 NTU_1 ($L=NTU_1\cdot HTU_1$):

$$NTU_1=\frac{L}{HTU_1}=\frac{-1}{1-E}\ln\left(\frac{\Delta c_{A}^{L}}{\Delta c_{A}^{0}}\right)=\frac{c_{A,1}^{0}-c_{A,1}^{L}}{\Delta c_{A}^{0}-\Delta c_{A}^{L}}\ln\left(\frac{\Delta c_{A}^{0}}{\Delta c_{A}^{L}}\right) \tag{14.33}$$

Note that the expressions, expressed in the concentrations at both ends of the exchanger, for the number of transfer units NTU_1 are identical for the co-current exchanger (equation 14.25) and the counter-current-exchanger (equation (14.33)). The question where the equilibrium is reached in a counter-current exchanger will show the importance of the extraction factor E again. When equation (14.30) is integrated from $x=0$ to $x=x$, the following equation results (with respect to equation (14.31) every L is replaced by x):

$$\frac{c_{A,1}^{x}-K_{d}c_{A,2}^{x}}{c_{A,1}^{0}-K_{d}c_{A,2}^{0}}=\frac{\Delta c_{A}^{x}}{\Delta c_{A}^{0}}=\frac{\text{driving force at } x=x}{\text{driving force at } x=0}=\exp\left(-\left(1-E\right)\frac{x}{HTU_1}\right) \tag{14.34}$$

14.4.2 Equilibrium situation

Reaching thermodynamic equilibrium means that the local (i.e. for a certain x-value) driving force is equal to zero. From equation (14.34) follows that for $E<1$ the term in the exponent is negative, which means that the driving force decreases with increasing x; the thermodynamic equilibrium is then reached when this counter-current exchanger is extended (infinitely) upwards (in the positive x-direction). For $E>1$ the term in the exponent is positive, which means that the driving force decreases with decreasing x; the thermodynamic equilibrium is then reached when this exchanger is extended (infinitely) downwards (in the negative x-direction).

14.5 Mass transfer rate and logarithmic mean driving force

An expression for the amount of A ($\Phi_{mole,A}$) that is transferred per unit of time in the two stream co-current and counter-current exchanger is derived. For both the co-current and the counter-current exchanger, the following holds for $\Phi_{mole,A}$, using equation (14.25) and (14.33) respectively:

$$\Phi_{mole,A} = \Phi_{v,1}\left(c^0_{A,1} - c^L_{A,1}\right) = \Phi_{v,1}\frac{L}{HTU_1}\frac{\Delta c^0_A - \Delta c^L_A}{\ln\left(\dfrac{\Delta c^0_A}{\Delta c^L_A}\right)} \tag{14.35}$$

In general, the transferred amount of A per unit of time is written as the product of an overall mass transfer coefficient related to phase 1 K_1, the mass transfer area aAL and an (average) driving force $\left(\Delta c_A\right)_{lm}$ (also related to phase 1):

$$\Phi_{mole,A} = K_1 aAL\left(\Delta c_A\right)_{lm} \tag{14.36}$$

Comparing equation (14.36) (which can be viewed as the definition equation for the average driving force $\left(\Delta c_A\right)_{lm}$, with equation (14.35) after substitution of the *HTU*₁ definition equation (14.22), learns that the average driving force $\left(\Delta c_A\right)_{lm}$ is given by:

$$\left(\Delta c_A\right)_{lm} = \frac{\Delta c^0_A - \Delta c^L_A}{\ln\left(\dfrac{\Delta c^0_A}{\Delta c^L_A}\right)} \tag{14.37}$$

This so-called l̲ogarithmic m̲ean driving force $\left(\Delta c_A\right)_{lm}$ (related to phase 1) enables us to express the transfer capacity in a overall mass transfer coefficient (related to phase 1), a mass transfer area and measurable concentration differences at the inlets and outlets of the mass exchanger. The logarithmic mean driving force is an important variable in the design of the treated exchangers. You can easily find out yourself that for co-current operation the logarithmic mean driving force is smaller than that for counter-current operation, resulting in a larger required exchanger length.

14.6 Concentration profiles

In Figure 14.5 concentration profiles are shown for different configurations of exchange equipment, where $C_{A,0}$ denotes the inlet concentration of stream 1. In all cases presented here the inlet concentration of stream 2 was selected zero.

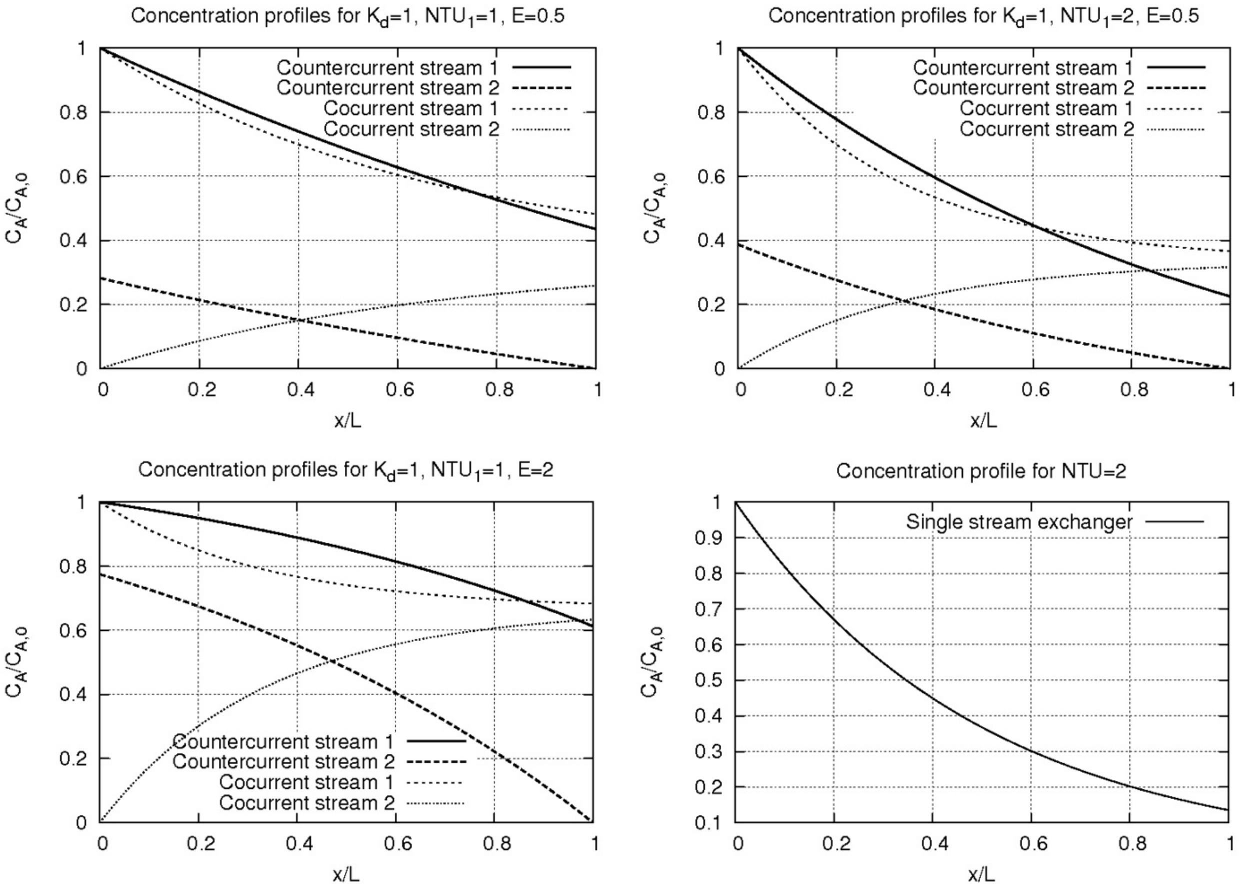

Figure 14.5 Axial relative concentration profiles for several selected cases for co- and countercurrent exchange equipment. The inlet for stream 1 is always at x/L=0.

The following can be concluded:

- The difference in concentration between stream 1 and 2 always decreases for increasing axial position for the case of co-current flow. For counter-current exchangers, it decreases with increasing position for $E < 1$, while it increases for $E > 1$.

- The amount transferred from stream 1 to stream 2 is always larger for counter-current exchangers than for co-current exchangers, due to the higher average driving force $(\Delta c_A)_{lm}$.

- The axial concentration profiles for $NTU_1 = 1$, $E = 2$ are identical to those for the case of $NTU_1 = 2$ and $E = 0.5$, if the names of stream 1 and 2 would be swapped and the meaning of the *y*-axis is read as "$1 - c_A/c_{A,0}$". For the case $E = 2$, stream 1 makes up 2/3 of the total fluid stream. In the case that E = 0.5, it makes up 1/3 of the total stream. It has decreased with a factor 2 respect to the case E = 2 and hence HTU_1 is decreased by the same factor. In order to arrive at the same length L of the equipment (and hence the same contact time), NTU_1 needs to be doubled.

- The factor by which the driving force changes as a function of NTU depends on the exact configuration for co- and countercurrent and is not as straightforward as for the case of the single stream exchanger.

Finally, for the special case that $E = 1$, a few selected cases are shown in Figure 14.6. The driving force for mass transfer is now constant for the case of counter-current contacting.

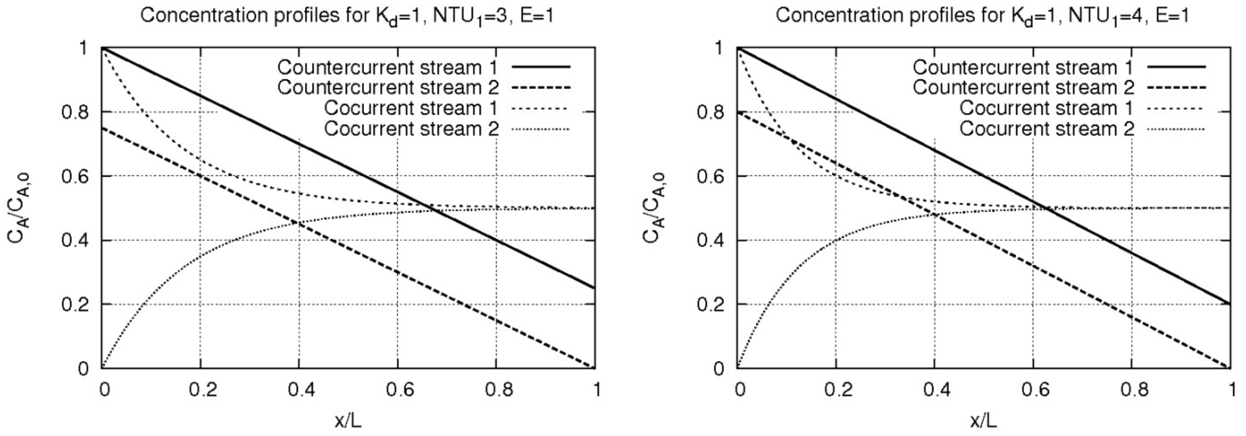

Figure 14.6 Axial relative concentration profiles for the special case of $E = 1$ for co- and countercurrent exchange equipment. The inlet for stream 1 is always at x/L=0.

14.7 Summary of exchange equipment

The equations describing single stream and two-stream co-current and counter-current mass exchange equipment have been summarized in Table 14.1.

Table 14.1 Summary of equations describing mass exchange equipment

Single stream exchanger	**Two stream exchanger** **(both co-current and counter-current)**
$L = NTU \cdot HTU$	$L = NTU_1 \cdot HTU_1$
$NTU = -\ln(Y)$	$NTU_1 = \dfrac{c_{A,1}^0 - c_{A,1}^L}{(\Delta c_A)_{lm}}$
$HTU = \dfrac{\Phi_v}{kaA} = \dfrac{v_o}{ka}$	$HTU_1 = \dfrac{\Phi_{v,1}}{K_1 aA}$ with $\dfrac{1}{K_1} = \dfrac{1}{k_1} + \dfrac{K_d}{k_2}$
$Y = \dfrac{c_{A,1,w} - c_{A,1}^L}{c_{A,1,w} - c_{A,1}^0} = \dfrac{K_d c_{A,2,w} - c_{A,1}^L}{K_d c_{A,2,w} - c_{A,1}^0}$	$(\Delta c_A)_{lm} = \dfrac{\Delta c_A^0 - \Delta c_A^L}{\ln\left(\dfrac{\Delta c_A^0}{\Delta c_A^L}\right)}$ with $\Delta c_A^x = c_{A,1}^x - K_d c_{A,2}^x$
$K_d = \left(\dfrac{c_{A,1}}{c_{A,2}}\right)_{\text{equilibrium}} = \dfrac{c_{A,1,w}}{c_{A,2,w}}$	$\Phi_{mole,A} = K_1 aAL(\Delta c_A)_{lm}$

Finally, the rules of correspondence to 'translate' the above equations for mass exchange equipment to the equations for heat exchange equipment have been listed in Table 14.2.

Table 14.2 Rules of correspondence for mass and heat exchange equipment

Mass exchange equipment	**Heat exchange equipment**
c_i	⍰$C_P T$
K_d	1
k	⍰/(⍰C_P)
⍰$_{mole}$	⍰$_h$